

UNIVERSITAT ROVIRA I VIRGILI  
COPOLIMERITZACIÓ DE DGEBA AMB ÀCID DE MELDRUM I DERIVATS  
Lidia González Búrdalo  
ISBN:978-84-691-9759-2/T-1252-2008

---

DEPARTAMENT DE QUÍMICA ANALÍTICA I QUÍMICA ORGÀNICA  
ÀREA DE QUÍMICA ORGÀNICA  
GRUP DE POLÍMERS  
UNIVERSITAT ROVIRA I VIRGILI



**COPOLIMERITZACIÓ DE DGEBA  
AMB ÀCID DE MELDRUM I DERIVATS**

---

**LÍDIA GONZÀLEZ BÚRDALO**

*Tesi presentada per optar al grau de Doctor en Química  
per la Universitat Rovira i Virgili.*

*Tarragona, Febrer del 2008*



*Ana Mantecón Arranz i Àngels Serra Albet,  
Catedràtiques d'Universitat, del Departament de Química Analítica i  
Química Orgànica de la Facultat de Química de la Universitat Rovira i  
Virgili de Tarragona fan constar:*

Que el treball "**Copolimerització de DGEBA amb àcid de Meldrum i derivats**" que ha dut a terme i que presenta Lidia González Búrdalo per l'obtenció del grau de Doctor en Química, ha estat desenvolupat sota la nostra supervisió i direcció en els laboratoris d'aquest mateix departament, i que tots els resultats obtinguts són fruit de les diferents experiències realitzades per la mencionada doctoranda.

*Tarragona, Febrer del 2008*

Ana Mantecón Arranz

Àngels Serra Albet

---



## ÍNDEX

1. INTRODUCCIÓ.....	1
2. ANTECEDENTS I OBJECTIUS.....	22
3. COPOLIMERITZACIÓ CATIÒNICA DEL DGEBA AMB ÀCID DE MELDRUM O ELS SEUS DERIVATS	
3.1. Introducció.....	26
3.2. "New Thermosets Obtained from DGEBA and Meldrum Acid with Lanthanum and Ytterbium Triflates as Cationic Initiators" .....	31
3.3. "Reduction of the Shrinkage of Thermosets by Cationic Curing of Mixtures of Diglycidyl Ether of Bisphenol A and 6,6-Dimethyl-(5,7- dioxaspiro[2.5]octane-4,8-dione)" .....	49
3.4. "The Degradation of New Thermally Degradable Thermosets Obtained by Cationic Curing of Mixtures of DGEBA and 6,6-Dimethyl-(5,7- dioxaspiro[2.5]octane-4,8-dione)" .....	62
3.5. "Kinetic Analysis by DSC of the Cationic Curing of Mixtures of DGEBA and 6,6-Dimethyl-(5,7-dioxaspiro[2.5]octane-4,8-dione)" .....	78
3.6. "Study of the Cationic Curing of DGEBA and 2,2,5,5-Tetramethyl-4,6- dioxo-1,3-dioxane and the Degradation of the Thermosets Obtained" .....	91
3.7. "New Poly(ether-ester) Thermosets Obtained by Cationic Curing of DGEBA and 7,7-Dimethyl-6,8-dioxaspiro[3.5]nonane-5,9-dione with Several Lewis Acids as Initiators" .....	106
4. COPOLIMERITZACIÓ ANIÒNICA DEL DGEBA AMB MCP o MDM	
4.1. Introducció.....	123
4.2. "Anionic Copolymerization of Diglycidyl Ether of Bisphenol A with Two Meldrum Acid Derivatives Initiated by 4-(N,N-Dimethylamino) Pyridine" .....	128

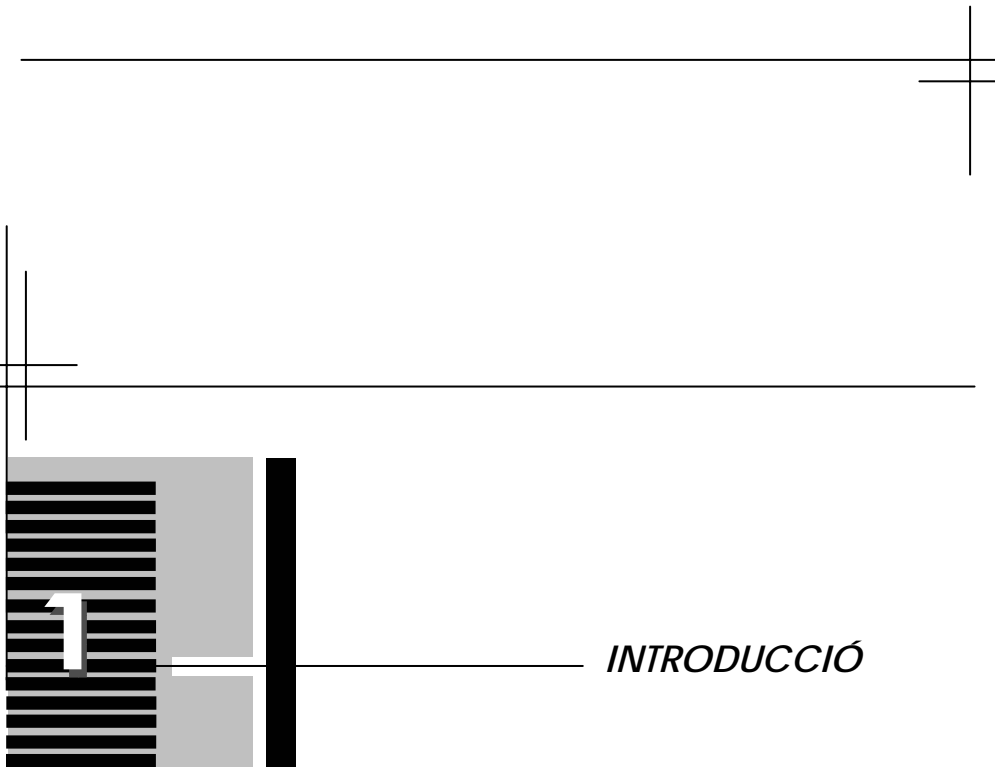


---



## ÍNDIX

<b>5. SÍNTESI D'UNA NOVA REÏNA EPOXI I COPOLIMERITZACIÓ CATIÒNICA AMB DGEBA</b>	
<b>5.1. Introducció.....</b>	<b>148</b>
<b>5.2. "Synthesis of a New Diglycidyl Meldrum Acid Derivative and Study of the Curing with Lanthanide Triflates as Initiators" .....</b>	<b>150</b>
<b>6. ESTUDI DE LES PROPIETATS MECÀNIQUES</b>	
<b>6.1. Introducció.....</b>	<b>166</b>
<b>6.2. Anàlisi termodinamomècnica (DMTA).....</b>	<b>166</b>
<b>6.3. Estudi de la microduresa.....</b>	<b>183</b>
<b>7. ESTUDI COMPARATIU ENTRE LES DIFERENTS LACTONES</b>	
<b>7.1. Introducció.....</b>	<b>191</b>
<b>7.2. Estudi per calorimetria diferencial d'escombrat (DSC).....</b>	<b>191</b>
<b>7.3. Estudi per espectroscòpia d'infraroig (ATR-FTIR).....</b>	<b>195</b>
<b>7.4. Estudi de l'estabilitat tèrmica mitjançant TGA.....</b>	<b>199</b>
<b>7.5. Estudi de la contracció.....</b>	<b>202</b>
<b>8. CONCLUSIONS.....</b>	<b>203</b>
<b>9. ANNEX I ACRÒNIMS.....</b>	<b>205</b>
<b>10. PUBLICACIONS I CONTRIBUTIONS A CONGRESSOS.....</b>	<b>215</b>



## 1. INTRODUCCIÓ

El polímers termoestables entrecruats són materials de gran interès i amb una àmplia versatilitat en el món industrial degut a les seves excel·lents propietats elèctriques, mecàniques i tèrmiques. Els termoestables són materials amb xarxes polimèriques entrecruades que es poden formar mitjançant una reacció de curat a partir de precursors de baixos pesos moleculars. Després del procés de curat, els materials són insolubles i infusibles.<sup>1</sup>

Les resines epoxi van ser introduïdes al món industrial l'any 1946 i constitueixen uns dels materials termoestables més emprats avui en dia en diferents aplicacions.<sup>2</sup> Se les utilitza per a fer recobriments tant a partir de pintures líquides com en pols. També se'ls utilitza com a adhesius, aïllaments de dispositius elèctrics i com a encapsulants de components electrònics,<sup>3</sup> evitant així que els diferents components siguin atacats per agents atmosfèrics, pols, humitat i protegint-los front el desgast mecànic.<sup>4</sup>

Al següent gràfic es representen els percentatges de les principals aplicacions de les resines epoxi als Estats Units l'any 1999.

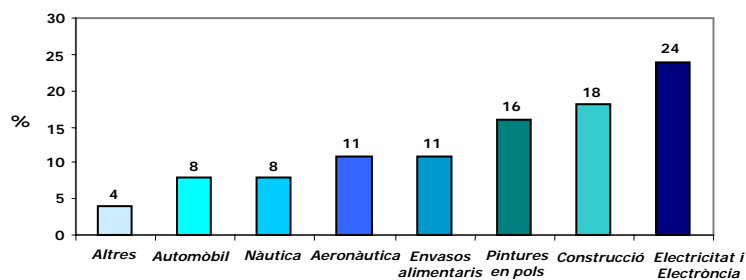
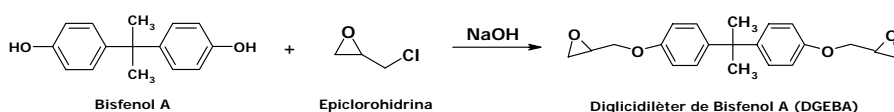


Fig.1.1. Aplicacions de les resines epoxi als EE.UU l'any 1999

<sup>1</sup> M. P. Stevens, "Polymer Chemistry. An Introduction", Oxford University Press, Oxford 1990, 2<sup>a</sup>Ed.  
<sup>2</sup> C. A. May, "Introduction to Epoxy resins" in "Epoxy Resins Chemistry and Technology", C. A. May Editor, 2nd edition, Marcel Dekker, New York, 465, 1988.  
<sup>3</sup> S. Wu, M. D. Soucek, J. Coat. Techn. **69**, 43-49 (1997).  
<sup>4</sup> D. P. Seraphim, R. Lasky, C.Y. Li, "Principes of Electronic Packaging". McGraw-Hill, New York, 1989.

La primera reïna epoxi comercial va ser el diglicidil èter de bisfenol A (DGEBA). Els primers intents comercials de producció de reïnes epoxi van tenir lloc als EE.UU l'any 1927. El mèrit de la primera síntesi d'una reïna basada en bisfenol A va ser compartit pel suís P. Castan i el nord-americà S. O. Greenlee en 1936.<sup>5</sup> El treball de P. Castan va ser recolzat per la companyia química Ciba-Geigy, la qual també era suïssa, convertint-se ràpidament en un dels tres majors fabricants mundials de reïnes epoxi. D'altra banda, el treball de S. O. Greenlee es va desenvolupar en una companyia petita, la qual més tard va ser comprada per *Shell*.

Aquesta reïna s'obté per reacció de l'epiclorohidrina amb bisfenol A en medi bàsic fort i és una de les més emprades en el món industrial (**Fig. 1.2**).



**Fig. 1.2.** Síntesi del diglicidilèter de bisfenol A

Com s'ha dit prèviament, una de les principals aplicacions de les reïnes epoxi és com a recobriments de superfícies. Aquest fet es deu a que els grups epoxi poden ser entrecruats amb un ampli ventall de compostos o agents de curat. Hi ha dos tipus generals de reïnes epoxi: *les epoxi glicidiliques i les epoxi cicloalifàtiques* (**Fig. 1.3**), les quals es diferencien per la posició de l'anell oxirànic i per la reactivitat que presenten, ja que aquesta ve determinada per la riquesa electrònica de l'oxigen oxirànic i per l'accessibilitat al grup epoxi.<sup>1</sup> El fet que aquests compostos tinguin elevada reactivitat, es deu a l'elevada tensió que pateix l'anell de tres baules del grup epoxi i a la polaritat dels enllaços èter.

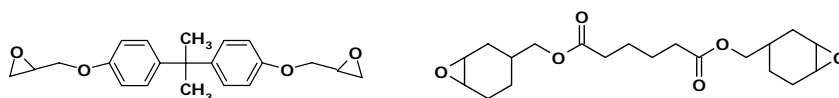


**Fig. 1.3.** Reïnes epoxi glicidiliques i epoxi cicloalifàtiques

El procés més clàssic per l'entrecruament de les reïnes epoxi es per reacció amb compostos multifuncionals, entre els que es troben les amines, els anhídrids, els diàcids, etc., els quals queden incorporats a la xarxa polimèrica, essent els més emprats les amines primàries. A la **fig. 1.4** es representa l'esquema de reacció entre un grup epoxi i una amina primària i la qual porta a materials termoestables. Les reaccions de curat epoxi-amina consten fonamentalment de dues etapes:

- 1- Reacció de l'amina primària amb un epòxid per donar lloc a una amina secundària.

<sup>5</sup> P. Castan, Swiss Pat. 211, 116 (1940).

2- Posterior reacció de l'amina secundària amb un altre epòxid per donar lloc a una amina terciària.

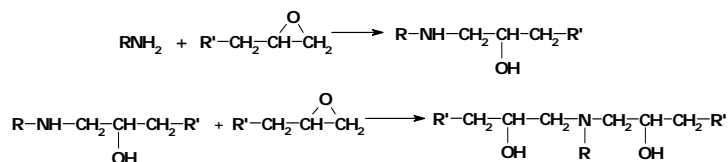


Fig.1.4. Entrecruament amb amines primàries

Una altra manera d'obtenir materials termoestables a partir de reines epoxi consisteix en la reacció d'eterificació per obertura d'anell, mitjançant mecanismes catiònic (tèrmic o fotoquímic) o aniónic. En aquest treball només ens centrarem en el curat tèrmic mitjançant mecanismes catiònics o aniónics.

- **Polimerització catiònica<sup>6</sup>**

En aquest mecanisme, l'espècie en propagació està formada per un ió oxoni, on l'electrofilia dels dos carbonis de l'anell es veu augmentada de tal forma que poden ser susceptibles de ser atacats per l'oxigen oxirànic d'una altra unitat monomèrica, tot i la seva pobra nucleofília, o pel parell d'electrons d'un oxigen d'una altra espècie present en el medi de reacció. Com a conseqüència de l'activació de l'anell del catió oxoni, l'atac nucleòfil de l'oxigen oxirànic pot realitzar-se fàcilment sobre ambdós carbonis de l'anell (obertura  $\alpha$  i  $\beta$ ). D'aquesta forma, no existeix una clara preferència per l'atac nucleòfil sobre el carboni menys substituït, degut a que en la propagació de la cadena s'estableixen de forma competitiva dos tipus de mecanisme, el  $\text{SN}_1$  i el  $\text{SN}_2$  (Fig. 1.5).

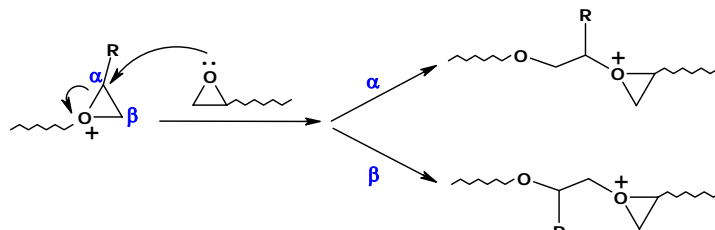


Fig.1.5. Polimerització catiònica de compostos epoxídics

La polimerització catiònica es caracteritza per generar polímers regioirregulars, les propietats físiques dels quals, sobretot les tèrmiques i mecàniques, són inferiors a les dels corresponents polímers regioirregulars. Aquest mecanisme es dona quan s'usen iniciadors amb fort caràcter d'àcid de Brønsted, l'anió dels quals no ha d'ésser bon nucleòfil, com per exemple el

<sup>6</sup> E. J. Goethals, S. Penczek, S. Slomkowski i P. Kubisa, "Comprehensive Polymer Science", G.C. Eastmond, A. Ledwith, S. Russo, P. Sigwalt. Sir. G. Allen & J.C. Bevington Eds, Pergamon Press, Oxford, Vol. 3, 711, 1989.

bisulfat, el perclorat i el bifosfat o també quan s'usen àcids de Lewis. Aquests últims poden actuar sols o conjuntament amb un compost pròtic que actui de coiniciador.<sup>7</sup>

Les sals de sulfoni, fosfoni i hidrazini han demostrat ser bons iniciadors tèrmics per la polimerització catiònica de monòmers cíclics, com els epòxids. L'ordre de reactivitat de les sals també depèn de la nucleofília del contraió ( $\text{Cl}^-$ ,  $\text{BF}_4^-$ ,  $\text{SbF}_6^-$ ,  $\text{PF}_6^-$ ) sent el més actiu aquell que l'aníó sigui menys nucleòfil. D'aquesta forma, es minimitzen o s'eliminen les reaccions de terminació de cadena per formació d'un enllaç covalent amb l'aníó.<sup>8,9</sup>

Existeix un ampli ventall d'àcids de Lewis que s'utilitzen com a iniciadors catiònics. Entre ells cal destacar:  $\text{TiCl}_4$ ,  $\text{AlCl}_3$ ,  $\text{ZnCl}_2$ ,  $\text{BCl}_3$ ,  $\text{SiCl}_4$ ,  $\text{FeCl}_3$ ,  $\text{MgCl}_2$ ,  $\text{SbCl}_5$  i els fluoroborats de molts d'aquests metalls. No obstant, un dels iniciadors més emprats avui en dia en polimeritzacions catiòniques en el camp de la tecnologia dels epòxids és el sistema  $\text{BF}_3$ /amina (amines alifàtiques o aromàtiques).<sup>10</sup> Els triflats de lantànid han demostrat ser excel·lents iniciadors catiònics en l'obertura d'anells oxirànics.<sup>11</sup>

Els àcids forts de Brønsted, com l'àcid trifluorometansulfònic (àcid triflic), també són bons candidats per polimeritzacions d'epòxids mitjançant un mecanisme catiònic.<sup>10</sup> Com a conseqüència de la pobra nucleofília de l'aníó trifluorometansulfonat (triflat), és esperable una baixa proporció de processos de terminació de cadena, produint-se així, el creixement de la cadena polimèrica. També s'han utilitzat una gran varietat de complexos metàl·lics coordinats als àcids trifluorometansulfònics.<sup>12,13</sup>

La polimerització catiònica porta a polímers de baix pes molecular degut a les possibles reaccions laterals. Entre aquestes, destaca la despolimerització o back-biting, que en sistemes entrecruats porta tan sols a modificacions estructurals de la xarxa (**Fig. 1.6**).

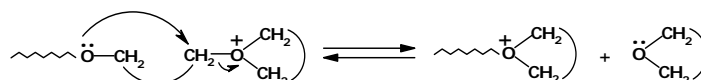


**Fig.1.6.** Mecanisme de "back-biting" que porta a la formació de cicles

<sup>7</sup> Y. Okamoto, ACS Symp. Ser., **286**, 361-372 (1985).

<sup>8</sup> T. Endo, F. Sanda, Macromol. Symp. **107**, 237-240 (1996).

<sup>9</sup> I. Ideisan, A. Abdoun, A. Ali, Eur. Polym. J. **28**, 73-78 (1992).

<sup>10</sup> Mika, T. F.; Bauer, R. S.; "Curing Agents and Modifiers" in "Epoxy Resins Chemistry and Technology", C. A. May editor, 2nd edition, Marcel Dekker, New York, 465, 1988.

<sup>11</sup> P. Castell, M. Galià, A. Serra, J. M. Salla, X. Ramis, Polymer **41**, 8465-8474 (2000).

<sup>12</sup> N. Yanagihara, S. Nakamura, M. Nakayama, Polyhedron **17**, 3625-3631 (1998).

<sup>13</sup> G. A. Molander, Chem. Rev. **92**, 29-68 (1992).

- **Polimerització aniónica**<sup>14,15</sup>

La polimerització aniónica es dóna quan intervenen iniciadors amb fort caràcter nucleofilic o amb fortes característiques bàsiques (**Fig. 1.7**).

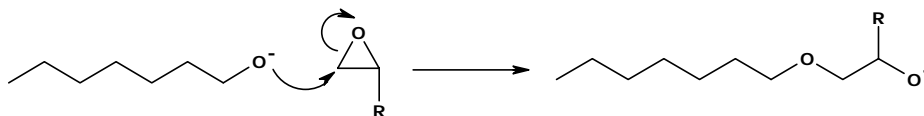


**Fig.1.7.** Polimerització aniónica de compostos epoxídics

Entre els iniciadors aniónics més emprats comercialment en el curat de les reines epoxi trobem les amines terciàries.<sup>10</sup> La piridina, el 2,4,6-tris(dimetilamino)fenol, la benzildimetilamina, la trietilamina i la 4-(N,N-dimetilamino)piridina (DMAP)<sup>16</sup> són alguns dels més emprats avui en dia.

Com que en aquest mecanisme les etapes d'iniciació i propagació són reaccions de substitució nucleòfila bimolecular (S<sub>N</sub>2), l'obertura de l'anell oxirànic es dóna en la posició menys substituïda obtenint-se així polímers regiorregulars.

L'ús de reines epoxi requereix la formació d'una estructura tridimensional entrecreuada unida mitjançant enllaços covalents i que s'origina en el procés de curat. A més, cal dir que l'estructura química, la morfologia de l'estructura tridimensional i la densitat d'entrecreuament són paràmetres que venen determinats per l'agent de curat emprat, el mecanisme d'entrecreuament i la cinètica de les reaccions.<sup>3,17,18</sup>

Degut a la interacció entre la cinètica química i els diferents canvis en les propietats físiques, el curat d'una reina resulta ser un procés complex. Els canvis més destacats són la gelificació i la vitrificació. La gelificació consisteix en la formació de la primera fracció insoluble del polímer de pes molecular infinit. El pas a l'estat en el qual el material passa a tenir característiques de vidre rep el nom de punt de vitrificació. Quan s'arriba a aquest punt el procés reactiu s'atura.

Depenent de l'aplicació dels materials curats, un dels paràmetres importants és la temperatura de transició vítria (T<sub>g</sub>). La T<sub>g</sub> augmenta des d'un valor inicial (T<sub>g0</sub>), quan el material encara no està curat, fins un valor infinit (T<sub>g∞</sub>), on el material es considera completament curat.<sup>19-22</sup>

<sup>14</sup> T. Tsuruta, Y. Kawakami, "Comprehensive Polymer Science", Vol. 3, G.C. Eastmond, A. Ledwith, S. Russo, P. Sigwalt. Ed. G. Allen i J.C. Bevington, Eds. Pergamon Press, Oxford, 457-466, 1989.

<sup>15</sup> G. Odian, "Principles of Polymerization", J. Wiley & Sons, New York, 512, 1981.

<sup>16</sup> I. E. Dell'Erba and R. J. J. Williams, Polym. Eng. Sci., **46**, 351-359 (2006).

<sup>17</sup> S. Wu, M. D. Soucek, Polymer **39**, 5747-5759 (1998).

<sup>18</sup> L. Matejka, S. Podzimek, K. Dusek, J. Polym. Sci. Part A: Polym Chem. **33**, 473-480 (1995).

<sup>19</sup> B. Ellis, "Chemistry and Technology of Epoxy Resins" Blackie Academic & Professional, New York, 1993.

<sup>20</sup> X. Ramis, J. M. Salla, J. Polym. Sci. Part B.: Polym Phys. **35**, 371-388 (1997).

Val a dir també que l'ús de les resines epoxi en algunes aplicacions, com per exemple en recobriments, es veu limitat pel fet de no posseir algunes característiques desitjables. Els tres principals inconvenients que presenten són:

- *Contracció durant el procés de curat*
- *Permanència en el medi ambient (baixa degradabilitat)*
- *Fragilitat*

El procés de curat va acompanyat generalment d'un procés d'encongiment degut a la formació d'enllaços covalents entre cadenes i, com a conseqüència, es produeix un augment de la densitat dels materials. L'encongiment genera una sèrie de deformacions en els materials degut a tensions internes, originant-se així la formació de microporus i esquerdes. Com a conseqüència es produeix una disminució, o fins i tot, una pèrdua de l'adhesió al substrat. Com a resultat final, es produeix una reducció de la durabilitat dels materials recoberts degut a la penetració d'humitat o d'agents atmosfèrics nocius.

En el camp de la microelectrònica, l'encongiment que pateix la matriu polimèrica i la diferència de coeficient d'expansió tèrmica que presenten els materials emprats en la producció de xips, fa que s'originin tensions mecàniques en el polímer, és a dir, estrès intern. Com a conseqüència d'aquest fenomen, el qual pot ser reiteratiu en el temps, es veu afectada la reina ja que pot patir fatiga mecànica i per tant produir-se una possible pèrdua de l'adhesió, desencadenant així el deteriorament del xip o dispositiu electrònic. És doncs, un dels principals inconvenients a resoldre en les aplicacions industrials dels materials polimèrics i en el camp de la ciència dels materials.<sup>23-26</sup>

Tant el tipus de mecanisme de polimerització seguit com el canvi en la distància entre àtoms abans i després del curat influeixen en l'encongiment durant el procés d'entrecruament. Les molècules es troben separades unes de les altres per una distància de Van der Waals i quan reaccionen donen lloc a un polímer, en el qual les unitats monomèriques es troben a una distància covalent.<sup>27-29</sup>

<sup>21</sup> L. Barral, J. Cano, A. J. López, P. Nogueira, C. Ramírez, J. Appl. Polym. Sci. **61**, 1553-1559 (1996).

<sup>22</sup> L. Barral, J. Cano, J. López, P. Nogueira, C. Ramírez, J. Abad, Polym. Inter. **42**, 301-306 (1997).

<sup>23</sup> R.K. Sathir, M. R. Luck, Eds. "Expanding Monomers: Synthesis, Characterization and Applications"; CRC Press: Boca Raton, FL., 1992.

<sup>24</sup> Y. Eom, L. Boogh, V. Michaud, P. Sunderland, J. A. Manson, Polym. Eng. Sci. 2001, **41**, 492-503.

<sup>25</sup> K. Chung, T. Takata, T. Endo, Macromolecules **28**, 3048-3054 (1995).

<sup>26</sup> A. M. Sikes, R. F. Brady, J. Polym. Sci.: Part A: Polym. Chem. **28**, 2533-2546 (1990).

<sup>27</sup> W. Bailey, H. Iwama, R. Tushima, J. Polym. Sci.: Polym. Symp. **56**, 117-127 (1976).

<sup>28</sup> W. Bailey, T. Endo, J. Polym. Sci. Polym. Symp. **64**, 17-26 (1978).

<sup>29</sup> H. Nishida, F. Sanda, T. Endo, T. Nakahara, T. Ogata, K. Kusumoto, J. Polym. Sci.: Part A: Polym. Chem. **37**, 4502-4509 (1999).



La contracció es relaciona amb el mecanisme de polimerització. En la polimerització per addició l'encongiment té lloc perquè es produeix un canvi de distàncies. Quan els monòmers s'uneixen per donar lloc al polímer, passen d'estar separats per distàncies de Van der Waals a distàncies covalents.<sup>23</sup> L'allargament de l'enllaç doble que passa a simple no compensa l'apropament entre monòmers (**Fig. 1.8**).

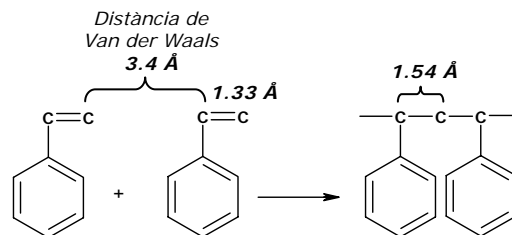


**Fig. 1.8.** Canvi en les distàncies d'enllaç en la polimerització per addició de l'estire

En la polimerització per condensació, l'encongiment és degut majoritàriament a l'eliminació de molècules petites durant la formació d'un nou enllaç i per tant serà major quan més gran sigui la molècula eliminada<sup>23</sup> (**Fig. 1.9**).

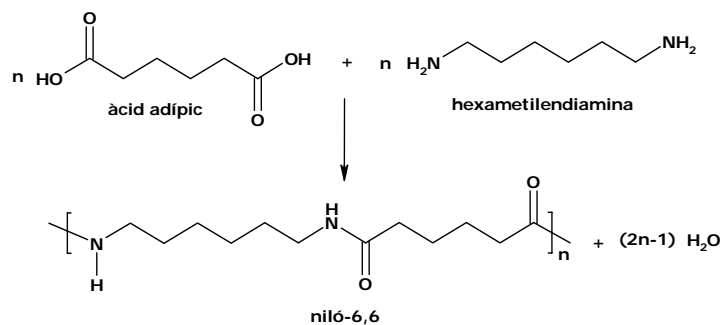


**Fig. 1.9.** Polimerització per condensació de l'àcid adípic i la hexametildiamina per donar lloc al niló-6,6

Per últim, en la polimerització per obertura d'anell, a part de no produir-se l'eliminació de cap molècula, per cada enllaç que va d'una distància de Van der Waals a una distància covalent existeix un altre enllaç que canvia des d'una distància covalent a una distància propera a la de Van der Waals<sup>23,27,30,31</sup> (**Fig. 1.10**).

<sup>30</sup> W. Bailey, J. Macromol. Sci. Chem. A9 (5), 849-865 (1975).

<sup>31</sup> F. Fukuda, M. Hirota, T. Endo, M. Okawa, W. Bailey, J. Polym. Sci.: Polym. Chem. 20, 2935-2942 (1982).

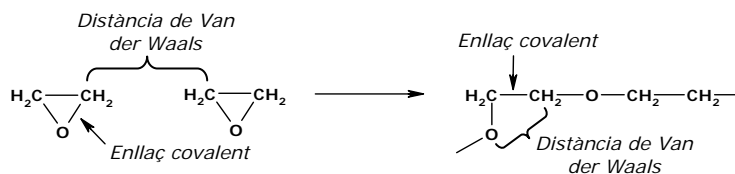


**Fig.1.10.** Variació de les distàncies d'enllaç produïdes en la polimerització per obertura d'anell de l'òxid d'etilè

A la **taula 1.1** s'exposen alguns dels valors d'encongiment produïts en el procés de polimerització de diferents compostos a través de diferents mecanismes.<sup>23,32</sup>

**Taula 1.1.** Valors d'encongiment

<b>Polimerització</b>	<b>Monòmer</b>	<b>Encongiment (%)</b>
<b>Addició</b>	Etilè	66
	Acetat de vinil	22
	Estirè	14
<b>Condensació</b>	Adipat de dioctil + hexametilendiamina	66
	Adipat de dimetil + hexametilendiamina	31
	Àcid adípic + hexametilendiamina	22
<b>Obertura d'anell</b>	Ciclopentè	15
	Ciclooctè	4.5
	5-Oxa-1,2-ditiocicloheptà	3.0
	Òxid de propilè	17
	Tetrahidrofurà	9
	Òxid d'estirè	9

Un factor a considerar en el valor d'encongiment en la polimerització per obertura d'anell és la mida de l'anell del monòmer. Quan major sigui, menor és l'encongiment que té lloc durant el procés de polimerització.

Un dels mètodes aplicats per a reduir aquest encongiment és mitjançant l'addició de càrregues inerts com per exemple la sílica, el quars, la mica, etc. o càrregues polimèriques com les escumes de poliuretà, la pols de PVC, poliestirens, etc. Tanmateix, aquestes càrregues perjudiquen en altres aspectes, ja que ocasionen un augment significatiu de la viscositat de la mescla, dificultant així el processat i per tant derivant a una difícil aplicació degut a una disminució de la fluïdesa i, a més, fent perdre la transparència del recobriments. Aquest procés condueix a l'obtenció de materials més rígids i més fràgils, incrementant-se la seva tensió interna, originant-se sistemes no homogenis i malmetent les propietats elèctriques dels materials.<sup>33</sup>

<sup>32</sup> T. Takata, T. Endo, Prog. Polym. Sci. **18**, 839-870 (1993).

<sup>33</sup> H. Lee, K. Neville, "Handbook of Epoxy Resins" McGraw-Hill, New York, 1967.

Una alternativa a l'addició de càrregues és l'ús de monòmers capaços de polimeritzar sense contracció o fins i tot amb expansió. A l'any 1973, fou introduït per primer cop el terme de monòmer expansible per William J. Bailey.<sup>34,35</sup> Aquest terme fa al·lusió a monòmers que durant la seva polimerització o procés de curat no pateixen contracció o fins i tot, condueixen a una petita expansió en el seu volum.

J. Bailey proposà una sèrie de compostos espirànics com a monòmers expansibles ja que els seus cicles s'obren amb una conversió d'enllaços covalents a distàncies de Van der Waals (**Fig. 1.11**) donant lloc a una lleugera expansió de volum.<sup>28,29,36</sup> Això implica que per cada parell d'àtoms que estan a una distància de Van der Waals i que s'uneixen a una distància covalent, com a mínim hi ha dos àtoms que van d'una distància covalent a una distància de Van der Waals, donant lloc com a resultat final aquesta lleugera expansió en el volum.

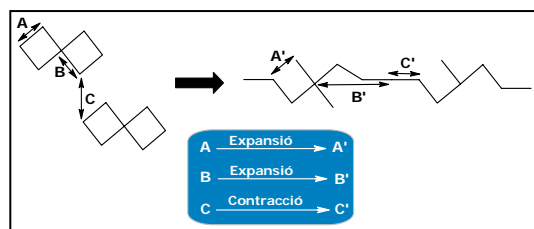


**Fig.1.11.** Esquema sobre el canvi de distàncies d'enllaç segons Bailey en monòmers expansibles

Segons el criteri de Bailey, els monòmers bicíclics han de complir els següents requisits per a poder actuar com a monòmers expansibles durant el procés de polimerització:

- *Anells fusionats*, és a dir que els anells del monòmer bicíclic han de contenir un àtom comú com a mínim.
- *Presència d'un heteroàtom* com a mínim en cada anell.
- *L'obertura dels cicles ha d'ésser asimètrica*. Això significa que per exemple, un àtom d'oxigen d'un anell pot originar un grup carbonil mentre que un àtom d'oxigen de l'altre anell pot donar lloc a un grup èter.<sup>23</sup>

<sup>34</sup> W. J. Bailey, J. Elastoplast **5**, 142-152 (1973).

<sup>35</sup> W. Bailey, R. L.-J. Sun, H. Katsuki, T. Endo, H. Iwama, R. Tushima, K. Saigou, M. M. Bitritto, "Ring-Opening Polymerization" ACS Symp. Ser. 59, T. Saegusa, E. Goethals, Eds. ACS. Washington, 1977.

<sup>36</sup> F. Sanda, M. Hitomi, T. Endo, J. Polym. Sci.: Part A: Polym. Chem. **39**, 3159-3167 (2001).

Els espiroortoesters (SOEs), els espiroortocarbonats (SOCs) i els bicicloortoesters (BOEs) són alguns dels compostos que compleixen aquests tres requisits imprescindibles per a actuar com a monòmers expansibles.<sup>23,25,37,38</sup> La polimerització dels SOEs i dels BOEs dona lloc a cadenes polimèriques que incorporen grups èter i ester, mentre que la polimerització dels SOC's dona lloc a cadenes polimèriques que contenen grups carbonat (**Fig. 1.12**). D'aquests tres monòmers, el present treball està centrat en la utilització del SOEs.

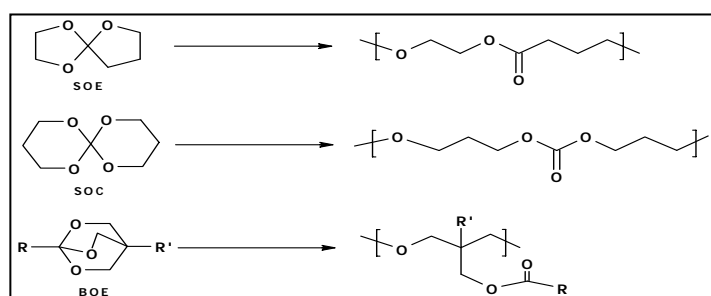


**Fig.1.12.** Monòmers bicíclics expansibles durant la polimerització

Així doncs, la polimerització per obertura d'anell d'aquests monòmers bicíclics podria ser una bona estratègia per obtenir materials amb baix encongiment aptes per a l'aplicació com a recobriments i adhesius.<sup>39</sup> No obstant, no van arribar a tenir una aplicació tecnològica degut principalment a la dificultat que presentaven per ser sintetitzats.

El mètode sintètic clàssic per l'obtenció dels SOEs és la reacció directa d'un epòxid amb una lactona en presència d'un àcid de Lewis com a catalitzador.<sup>40</sup> El primer SOE, el 1,4,6-trioxaespiro[4.4]nonà, fou sintetitzat l'any 1959 per Bodenbenner<sup>41</sup> mitjançant la reacció de condensació de l'òxid d'etilè amb la  $\gamma$ -butirolactona en presència de trifluorur de bor ( $\text{BF}_3$ ), obtenint-se un rendiment del 33% ja que en aquest medi el producte polimeritza.

Els SOEs són bastant estables en condicions alcalines però són extremadament sensibles front espècies catióniques.<sup>42</sup> La seva polimerització catiónica ve acompanyada d'un encongiment zero o d'una lleugera expansió de volum.<sup>42,43</sup> Com a exemple, per reacció del 1,4,6-trioxaespiro[4.4]nonà a la temperatura de 25°C i emprant trifluor de bor eterat ( $\text{BF}_3 \cdot \text{OEt}_2$ ) com a

<sup>37</sup> K. Saigo, W. J. Bailey, T. Endo, M. Okawa, J. Polym. Sci.: Polym. Chem. **21**, 1435 (1983).

<sup>38</sup> K. Chung, T. Takata, T. Endo, Macromolecules **28**, 1711-1713 (1995).

<sup>39</sup> F. Sanda, T. Endo, J. Polym. Sci.: Part A: Polym. Chem. **39**, 265-276 (2001).

<sup>40</sup> M. Fedtke, J. Haufe, E. Kahlert, G. Müller, Angew Makromol. Chem. **255**, 53-59 (1998).

<sup>41</sup> K. Bodenbenner, Ann. **625**, 183 (1959).

<sup>42</sup> H. Nishida, F. Sanda, T. Endo, T. Nakahara, T. Ogata, K. Kusumoto, Macromol. Chem. Phys. **200**, 745-750 (1999).

<sup>43</sup> S. Chikaoka, T. Takata, T. Endo, Macromolecules **24**, 6557-6562 (1991).

iniciador catiònic es va obtenir un poli(èter-ester) amb un 95% de rendiment i amb una expansió del 0.1%.<sup>30</sup>

Matyjaszewski<sup>44</sup> va realitzar diversos estudis sobre la polimerització catiònica dels SOEs utilitzant la tècnica espectroscòpica de RMN i va proposar que en una primera etapa ràpida es produïa l'obertura d'un dels anells, i que a continuació es produïa una reacció d'isomerització lenta per a donar lloc un poli(èter-ester) (**Fig. 1.13**). Posteriorment es realitzaren altres estudis<sup>45</sup> on es demostrà que la temperatura de polimerització era el paràmetre experimental més important a controlar ja que en funció d'aquesta es podien obtenir els dos tipus de polímer. Així doncs, a temperatures superiors als 100°C el SOE experimenta una doble obertura de l'anell, donant lloc a un poli(èter-ester), mentre que a temperatures per sota dels 40°C el SOE només experimenta l'obertura d'un sol cicle donant lloc a la formació d'un poli(cicloortoester) (**Fig. 1.13**). Cal assenyalar que aquesta última reacció únicament la donen els SOEs amb un anell d'èter de 7 membres ( $n=5$ ) i com que és una reacció d'equilibri, quan el poli(cicloortoester) es troba en presència d'àcids forts, l'equilibri es desplaça cap al monòmer de partença. El polímer es pot considerar com a reciclable ja que permet la recuperació del monòmer inicial a través d'una via de reciclatge químic.<sup>46-49</sup>

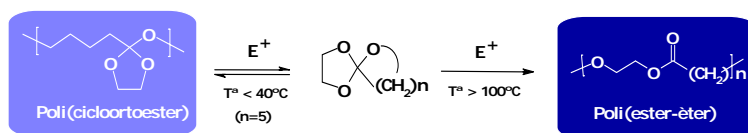


**Fig.1.13.** Evolució dels SOE en funció de la temperatura

Pascault i col.<sup>50,51</sup> van utilitzar una petita quantitat de  $\gamma$ -butirolactona com a dissolvent del  $BF_3 \cdot MEA$  en la polimerització del fenilglicidilèter (PGE) i del DGEBA i van arribar a la conclusió que es formava un espiroortoester intermedi.

Posteriorment, Fedtke i col.<sup>40</sup> van realitzar diferents estudis sobre l'efecte que tenien dos iniciadors catiònics, el trifluorur de bor/p-metoxianilina ( $BF_3 \cdot MA$ ) i el trifluorur de bor eterat ( $BF_3 \cdot Et_2O$ ) en la copolimerització del fenilglicidilèter amb la  $\gamma$ -butirolactona i la  $\epsilon$ -caprolactona. Amb ( $BF_3 \cdot MA$ ) van observar que l'epòxid reaccionava preferentment amb la lactona per donar el corresponent SOE i que aquest reaccionava a mesura que s'anava generant en el medi de reacció. D'altra banda, quan van utilitzar el ( $BF_3 \cdot Et_2O$ ) com a iniciador catiònic van observar que la reacció d'homopolimerització de l'epòxid

<sup>44</sup> K. Matyjaszewski, J. Polym. Sci. Polym. Chem. **22**, 29-40 (1984).

<sup>45</sup> S. Chikaoka, T. Takata, T. Endo, Macromolecules **25**, 625-628 (1992).

<sup>46</sup> S. Chikaoka, T. Takata, T. Endo, Macromolecules **24**, 331-332 (1991).

<sup>47</sup> M. Hitomi, F. Sanda, T. Endo, J. Polym. Sci.: Part A: Polym. Chem. **36**, 2823-2825 (1998).

<sup>48</sup> M. Hitomi, F. Sanda, T. Endo, Macromol. Chem. Phys. **200**, 1268-1273 (1999).

<sup>49</sup> T. Endo, F. Sanda, Macromol. Symp. **153**, 227-231 (2000).

<sup>50</sup> L. Matějka, P. Chabanne, L. Tighzert, J. P. Pascault, J. Polym. Sci.: Part A: Polym. Chem. **32**, 1447-1458 (1994).

<sup>51</sup> P. Chabanne, L. Tighzert, J. P. Pascault, J. Appl. Polym. Sci. **53**, 787-806 (1994).

competia fortament amb la formació del SOE, donant lloc a una mescla d'homopolimers d'epoxi i de copolímers amb baix contingut de lactona incorporada. En el cas de la  $\epsilon$ -caprolactona, a més, es van obtenir polièsters degut a l'homopolimerització de la lactona.

Tal com hem dit anteriorment, un dels inconvenients que presenten els polímers termoestables és la seva permanència en el medi una vegada finalitzada la seva vida útil, degut a que un cop aplicats no poden ser eliminats ni mitjançant l'ús de dissolvents ni per escalfament. Així doncs, són materials que presenten d'una banda l'avantatge de ser interessants en el món de la microelectrònica degut al grau de fiabilitat que presenten pel fet de donar lloc a xarxes entrecruades fortament fixades, però d'altra banda, aquesta impossibilitat de ser tractats fa que siguin desafortunadament irrecuperables o no reciclables els dispositius electrònics recoberts. S'estima que cada any queden fora de servei uns 60 milions d'ordinadors. Els processos actuals de reciclatge fan que aproximadament un 77% de circuits impresos d'ordinador no puguin ser reutilitzats a causa de no poder eliminar les reïnes termoestables que els protegeixen. Per aquesta raó, sorgeix un nou desafiament en el món dels recobriments, consistent en l'obtenció de materials termoestables que presentin una degradabilitat adequada i que alhora permeti un bon manteniment de les seves propietats i de la seva durabilitat en les condicions d'ús. El propòsit és que el recobriment es pugui eliminar per a recuperar els components electrònics o procedir a la seva reparació.

Així doncs, el que es pretén avui en dia és arribar a l'obtenció de reïnes termoestables degradables i trobar un camí que permeti trencar l'estructura de les xarxes polimèriques en petits fragments de forma acurada i controlada (**Fig. 1.14**). Degut a aquesta fragmentació es produeix una disminució de la densitat d'entrecruament i de la temperatura de transició vítria del material.

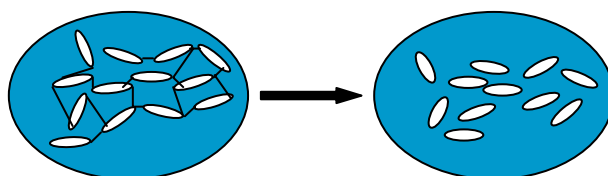


**Fig. 1.14.** Degradació d'un material termoestable

Donat que el reciclatge d'aquests materials polimèrics és encara difícil de realitzar, el que es pretén és una degradació controlada de tal forma que posteriorment es pugui eliminar el recobriment del material electrònic mitjançant l'ús de dissolvents o a través de fricció mecànica.

A la dècada dels 90 es van desenvolupar materials termoestables amb capacitat de ser degradats mitjançant diversos mètodes. Tesoro i col.<sup>52,53</sup> van sintetitzar materials termoestables que contenien enllaços disulfur, de tal manera que aquests podien ser fragmentats mitjançant una reducció química a grups tiol. Buchwalter i col.<sup>54,55</sup> van incorporar enllaços cetall i acetal en monòmers diepoxídics cicloalifàtics per obtenir xarxes que fossin fàcilment degradables mitjançant tractament amb dissolucions àcides.

Actualment un dels mètodes més rellevants per tal de degradar materials termoestables es basa en els estudis realitzats per Ober i col.<sup>56-58</sup> on van dissenyar reïnes epoxi cicloalifàtiques que contenen grups ester primaris, secundaris i terciaris, (**Fig. 1.15**) permetent així que les xarxes termoestables poguessin ser trencades a temperatures entre els 200°C i els 300°C.

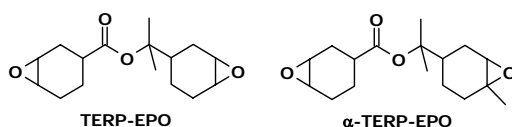


**Fig.1.15.** Estructures químiques d'epòxids cicloalifàtics

Els grups esters terciaris làbils es degraden tèrmicament de forma controlada mitjançant un mecanisme d'eliminació pirolítica. (**Fig. 1.16**)

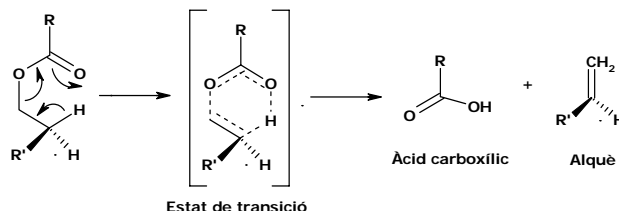


**Fig.1.16.** Mecanisme d'eliminació pirolítica d'esters

<sup>52</sup> V. R. Sastri, G. C. Tesoro, J. Appl. Polym. Sci. **39**, 1439-1457 (1990).

<sup>53</sup> G. C. Tesoro, V. R. Sastri, J. Appl. Polym. Sci. **39**, 1425-1437 (1990).

<sup>54</sup> S. L. Buchwalter, L. L. Kosbar, J. Polym. Sci.: Part A: Polym. Chem. **34**, 249-260 (1996).

<sup>55</sup> S. L. Buchwalter, L. L. Kosbar, J. Polym. Sci.: Part A: Polym. Chem. **34**, 1439-1441 (1996).

<sup>56</sup> S. Yang, J. S. Chen, H. Körner, T. Breiner, C. K. Ober, Chem. Mater. **10**, 1475-1482 (1998).

<sup>57</sup> J. S. Chen, C. K. Ober, M. D. Poliks, Polymer **43**, 131-139 (2002).

<sup>58</sup> J. S. Chen, C. K. Ober, M. D. Poliks, Y. Zhang, U. Wiesner, C. Cohen, Polymer **45**, 1939-1950 (2004).

La piròlisi dels grups esters incorporats a la xarxa produeix una disminució de la densitat d'entrecuament i per tant la possibilitat d'obtenir materials que puguin ser solubilitzats mitjançant l'ús de dissolvents o eliminats per fricció.

Els grups de Ober<sup>59</sup> i Wong<sup>60</sup> van estudiar el curat de reines cicloalifàtiques utilitzant anhídrids com agents entrecuants en presència d'amines terciàries. Ober i col.<sup>59</sup> van curar la reina cicloalifàtica  $\alpha$ -TERP-EPO de la **fig. 1.15** utilitzant com a agent de curat l'anhídrid 4-metil-1,2-ciclohexandicarboxílic, l'1,4-butanodiol com a font de protons i com a catalitzador la N,N-dimetilbenzilamina, obtenint així xarxes amb l'estructura representada a la **fig. 1.17**. En aquesta figura també es pot observar alguns dels fragments que es poden obtenir en la degradació tèrmica.

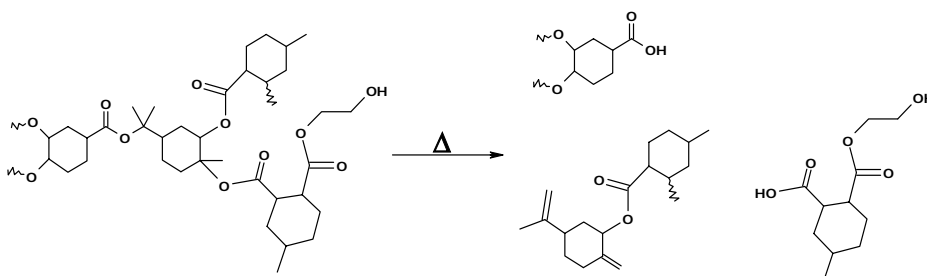


**Fig.1.17.** Degradació de la reina cicloalifàtica  $\alpha$ -TERP-EPO prèviament curada

Cal assenyalar que, en el mecanisme de descomposició d'aquests sistemes, també pot donar-se la reacció entre fragments que continguin grups d'àcid carboxílic (**Fig. 1.18**), obtenint-se així compostos que incorporen grups anhídrid que poden ser hidrolitzats posteriorment.

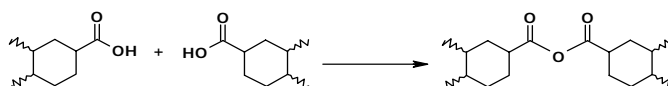


**Fig.1.18.** Reacció entre àcids carboxílics per donar lloc a un anhídrid

Existeixen algunes reines cicloalifàtiques comercials que poden ser degradades un cop finalitzada la seva vida útil<sup>61</sup>, la qual cosa permet eliminar els recobriments termoestables mitjançant l'escalfament del material electrònic per tal que es produeixi la degradació del recobriment. El principal inconvenient que presenten aquestes reines és la poca versatilitat en la selecció de les propietats mecàniques del material. Les reines de partença

<sup>59</sup> K. Ogino, J.S. Chen, C. K. Ober, Chem. Mater. **10**, 3833-3838 (1998).

<sup>60</sup> H. Li, L. Wang, K. Jacob, C. P. Wong, J. Polym. Sci.: Part A: Polym. Chem. **40**, 1796-1807 (2002).

<sup>61</sup> Henkel (<http://www.henkel.com>), Loctite (<http://www.loctite.es>).



tenen un pes molecular definit i els agents de curat aplicables són molt restringits.

Recentment, Okamura i col.<sup>62</sup> van sintetitzar noves reïnes epoxi difuncionals i trifuncionals (**Fig. 1.19**) amb unions ester terciari.

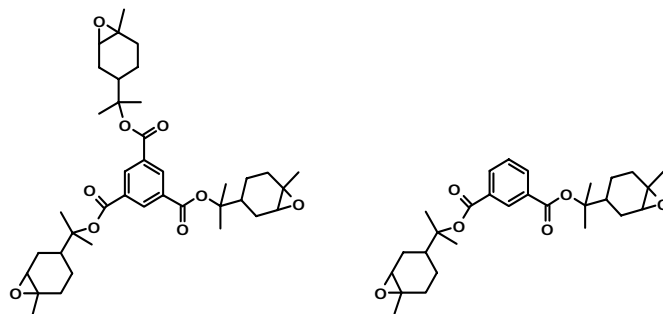


**Fig. 1.19.** Noves reïnes epoxi cicloalifàtiques que incorporen esters terciaris

Aquestes reïnes van ser aplicades com agent de curat a un sistema amb propietats fotocurables perquè poguessin desentrecreuar-se posteriorment mitjançant tractament tèrmic (**Fig. 1.20**).

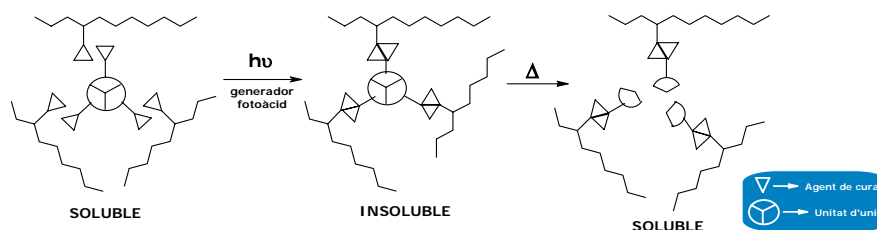


**Fig. 1.20.** Entrecruament fotoquímic i degradació tèrmica de la xarxa polimèrica

Aquest sistema està format per una mescla de poli(vinil-fenol) (PVP) o un copolímer d'àcid metacrílic i metacrilat d'etil (MAA-EMA), l'agent de curat i un generador fotoàcid (**Fig. 1.21**). La formació de la xarxa polimèrica transcorre mitjançant la reacció entre els grups epoxi de l'agent de curat i el PVP i està catalitzada pel generador fotoàcid. El posterior tractament tèrmic del polímer entrecruuat porta a la ruptura de les unions d'ester terciari, ja que aquestes al ser escalfades, descomponen produint àcids carboxílics i alguns a una temperatura inferior a la que descomponen els esters primaris i

<sup>62</sup> H. Okamura, K. Shin, M. Tsunooka, M. Shirai, J. Polym. Sci.: Part A: Polym. Chem., **42**, 3685-3696 (2004).

secundaris.<sup>63</sup> La temperatura de ruptura dels esters terciaris es menor en presència d'àcids forts.<sup>63</sup>

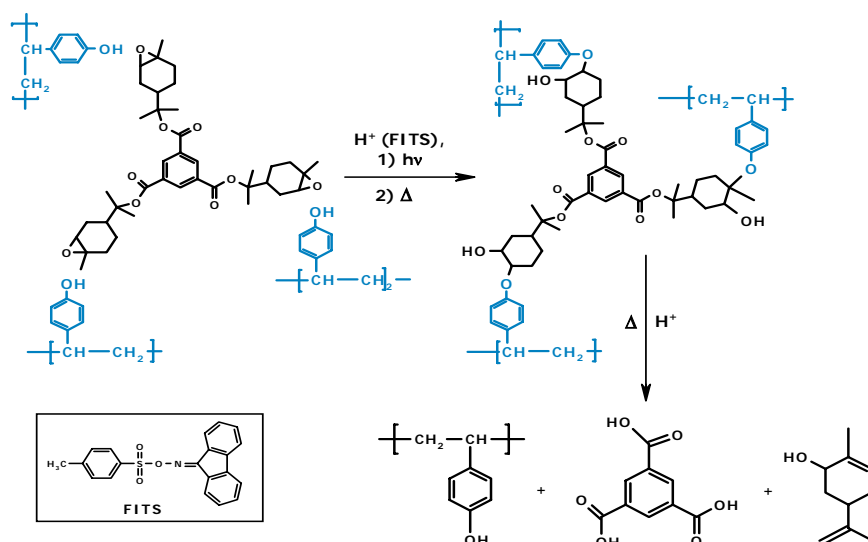


**Fig.1.21.** Entrecreuament i degradació tèrmica de la xarxa polimèrica en presència d'un generador fotoàcid (FITS)

Okamura i col.<sup>64</sup> també han desenvolupat una altra estratègia per obtenir materials termoestables degradables, utilitzant agents d'entrecreuament que incorporen grups sulfonat, els quals són tèrmicament làbils i que al mateix temps permeten un procés d'entrecreuament entre polímers com el poli(p-hidroxiestirè) o metacrilats modificats amb grup epòxid cicloalifàtics.

L'últim inconvenient esmentat que presenten les resines epoxi és la seva fragilitat. L'origen es la baixa mobilitat que presenten les cadenes polimèriques per la seva estructura entrecreuada. La solució més utilitzada tecnològicament, és la mescla amb additius plastificants. No obstant, això comporta una difícil separació en el seu reciclatge, i porta sovint a sistemes no homogenis.<sup>65</sup> La introducció d'estructures flexibles a la xarxa polimèrica i l'augment de la distància entre punts d'entrecreuament és una altra estratègia interessant per a disminuir la fragilitat, tot i que produeix una disminució del valor de la temperatura de transició vítria (Tg), el que pot limitar la temperatura d'ús del polímer.

<sup>63</sup> H. Ito, M. Uoeda, *Macromolecules*, **21**, 1475-1482 (1988).

<sup>64</sup> Y. D. Shin, A. Kawaue, H. Okamura, M. Shirai, *Polym. Degrad. Stab.* **86**, 153-158 (2004).

<sup>65</sup> F. Constantin, F. Fenouillot, J. L. Guillaume, R. Koenig, J. P. Pascault, *Macromol. Symp.* **198**, 335-344 (2003).

Un aspecte important a tenir en compte en l'obtenció de materials termoestables, que es reflecteix en el procés de curat i en les propietats finals del polímer, és el tipus d'iniciador emprat en l'obertura d'anell de les reines epoxi. A més d'iniciar el mecanisme de polimerització també poden catalitzar i accelerar la reacció global.

La polimerització catiònica per obertura d'anell la presenten aquells monòmer cíclics que poden obrir-se degut a l'acció d'un reactiu o catalitzador àcid. Dins d'aquest grup trobem els èters cíclics, com els epòxids, i les lactones. Aquesta polimerització transcorre per un mecanisme amb tres etapes: iniciació, propagació i terminació.

Penczek i Kubisa<sup>66</sup> van trobar que la polimerització catiònica per obertura d'anell pot seguir fonamentalment dos mecanismes de propagació, coneguts com AM (monòmer actiu) (**Fig. 1.22**) o ACE (final cadena actiu) (**Fig. 1.23**). A les dues figures es poden observar els dos mecanismes esmentats anteriorment, pel cas específic de la polimerització catiònica del grups epoxi.

- **Mecanisme AM (monòmer actiu):**

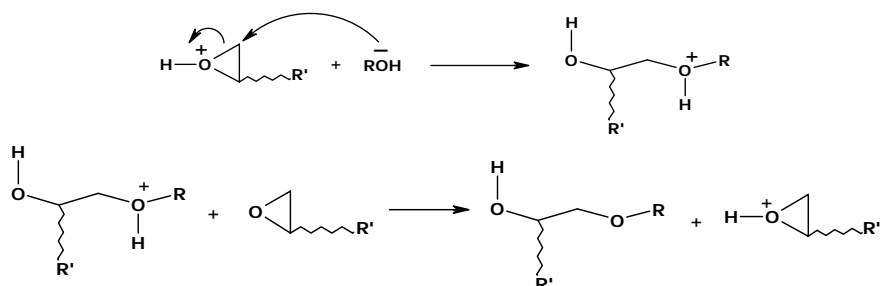


**Fig. 1.22.** Esquema del mecanisme AM

Com es pot observar a la **fig. 1.22**, el mecanisme AM consta de diferents etapes. En primer lloc el monòmer activat reacciona amb un alcohol donant lloc a un catió oxoni secundari amb un hidrogen actiu i un alcohol. Posteriorment aquest catió transfereix un protó a un monòmer donant lloc a un altre monòmer actiu, produint-se una transferència de cadena. El procés pot continuar per reacció del monòmer activat donant lloc al creixement d'una nova cadena polimèrica.

<sup>66</sup> P. Kubisa, S. Penczek, Prog. Polym. Sci. **24**, 1409-1437 (1999).

• **Mecanisme ACE (final cadena actiu):**

El mecanisme ACE, com es pot observar a la **fig. 1.23**, té lloc en absència de grups hidroxil. En primer lloc es produeix l'activació del monòmer per l'iniciador. A l'etapa de propagació un nou monòmer ataca l'epòxid activat, obre l'anell i forma un nou final actiu de cadena, allargant-se així en una unitat la cadena polimèrica.

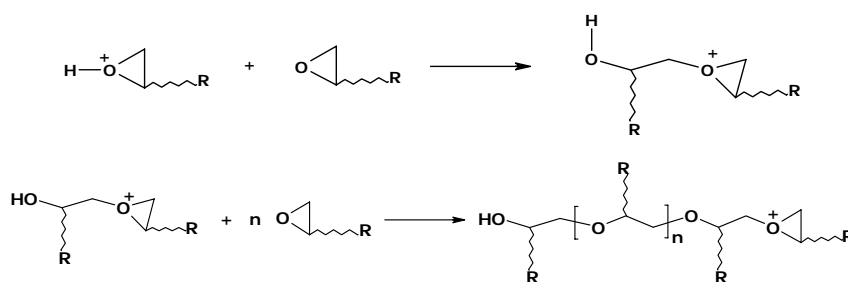


**Fig. 1.23.** Esquema del mecanisme ACE

En un sistema reactiu determinat, aquests dos mecanismes no són excloents i competeixen mútuament. El fet que un mecanisme pugui predominar vers l'altre dependrà, entre d'altres factors, de la relació en la quantitat de grups epoxi i grups hidroxil. Els grups hidroxil són més nucleòfils que els grups epoxi i, per tant, en presència de grups hidroxil, el mecanisme predominant serà el AM.

Cal afegir que en el mecanisme AM es forma un catió oxoni secundari, mentre que en el mecanisme ACE es forma un catió oxoni terciari. La detecció de l'existència d'aquestes espècies serà la que indiqui quin mecanisme de polimerització és el predominant.

Avui en dia, és de gran interès disminuir i optimitzar el temps de les reaccions de polimerització i la temperatura a la qual es dona el procés de curat per tal de poder aconseguir així un estalvi energètic. Alguns estudis realitzats per Pascault i col.<sup>67</sup> han demostrat que la polimerització catiónica és una bona estratègia en els processos industrials. No obstant, presenta un inconvenient i és que poden existir processos paral·lels com reaccions de transferència de cadena o despolimerització per "back-biting" (**Fig. 1.6**). Quan aquest procés és intramolecular genera macrocicles,<sup>68</sup> però si el procés és intermolecular, en un material termoestable, les transferències de cadena no són un greu problema ja que només donen lloc a canvis estructurals.

<sup>67</sup> P. Chabanne, L. Tighzert, J. P. Pascault, J. Appl. Polym. Sci. **53**, 769-785 (1994).

<sup>68</sup> D. J. Brunelle, "Ring Opening Polymerization" Hanser Publisher, Passau, 1993.

Un dels iniciadors més emprats en polimeritzacions catióniques en el camp de la tecnologia d'epòxids és el sistema  $\text{BF}_3$ /amina. L'inconvenient que presenten aquests sistemes és que són altament higroscòpics i a més, front la humitat i temperatures elevades, es produeix un deteriorament de les propietats elèctriques de les resines curades.<sup>69</sup> També cal afegir que els materials obtinguts presenten una alta fragilitat.

Tighzert i col.<sup>70,71</sup> van realitzar diferents estudis sobre la influència de complexos de  $\text{BF}_3$  amb amines en el curat de prepolímers epoxi i van observar que el complex  $\text{BF}_3$ /amina es dissociava en funció de la temperatura. No obstant, no van poder determinar quina era la temperatura de dissociació experimental. Ghaemy i col.<sup>72</sup> van arribar a la conclusió que l'espècie responsable del mecanisme d'iniciació de la polimerització és un protó tal i com es pot observar en el següent esquema (**Fig. 1.24**):

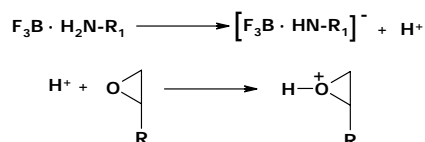


**Fig. 1.24.** Mecanisme d'iniciació amb  $\text{BF}_3$ /amina

A més, van observar que la fortalesa de la base tenia un paper important en la dissociació del complex, produint-se un augment de la reactivitat quan disminuïa la basicitat de l'amina.<sup>72</sup>

Els triflats de terres rares  $\text{RE}(\text{OTf})_3$ , incloent els triflats de lantànid han estat descrits com àcids de Lewis estables a l'aigua i capaços de catalitzar diverses transformacions orgàniques en medis pròtics.<sup>73,74</sup> Els triflats de terres rares es preparen per reacció dels seus corresponents òxids ( $\text{RE}_2\text{O}_3$ ) amb àcid trifluorometansulfònic ( $\text{TfOH}$ ) en solució aquosa. Tenen l'avantatge que en presència d'humitat o fins i tot en aigua no perden la seva activitat i poden utilitzar-se en solució aquosa ja que la seva hidròlisi és molt lenta. En 1991, Kobayashi va demostrar el notable efecte catalític dels  $\text{RE}(\text{OTf})_3$  en solució aquosa,<sup>75-77</sup> que es caracteritzen perquè són àcids de Lewis forts. L'elevada acidesa de Lewis és veu augmentada pel caràcter electroattractor

<sup>69</sup> M. Tozikawa, H. Okada, N. Wakabayashi, J. Appl. Polym. Sci. **50**, 875-884 (1993).

<sup>70</sup> N. Bouillon, J. P. Pascault, L. Tighzert, Makromol. Chem. **191**, 1403-1416 (1990).

<sup>71</sup> P. Chabanne, L. Tighzert, J. P. Pascault, B. Bonnetot, J. Appl. Polym. Sci. **49**, 685-689 (1993).

<sup>72</sup> M. Ghaemy, M. H. Khandani, J. Eur. Polym. J., **34**, 477-486 (1998).

<sup>73</sup> S. Luo, L. Zhu, A. Talukdar, G. Zhang, X. Mi, J. P. Cheng, P. G. Wang, Mini-Reviews in Organic Chemistry, **2**, 546-564, 2005.

<sup>74</sup> W. H. Xie, L. B. Yu, J. Ramírez, G. P. Wang, "Lanthanide-catalyzed organic synthesis in protic solvents. In Green chemistry". Anastas, P. T.; T. Williamson, Eds.; Oxford University Press: Cary, NC, 129-149, 1998.

<sup>75</sup> S. Kobayashi, Chem. Lett., **20**, 2187-2190 (1991).

<sup>76</sup> S. Kobayashi, T. Wakabayashi, S. Nagayama, H. Oyamada, Tetrahedron Lett. **38**, 4559-4562 (1997).

<sup>77</sup> S. Kobayashi, "Lanthanides: Chemistry and Use in Organic Synthesis" Springer, Berlin, 1999.

del grup trifluorometansulfonyl (OTf).<sup>78</sup> Els cations metàl·lics són durs segons la terminologia de Pearson<sup>79</sup>, tenen una elevada capacitat de coordinació<sup>80,81</sup> i una gran afinitat cap a l'oxigen del grup epòxid, de tal manera que debiliten l'enllaç C-O de l'anell oxirànic<sup>78,82,83</sup> afavorint així el mecanisme d'obertura de l'anell. La duresa del catió ve determinada per factors com l'electronegativitat, l'oxofília i el radi iònic del metall. A la **fig. 1.25** es mostren representats els paràmetres que afecten a l'acidesa de Lewis dels cations dels diferents triflats de terres rares emprats en aquest treball. Quant menor sigui el radi iònic i l'electronegativitat i major sigui l'oxofília, major caràcter d'àcid de Lewis presentarà la sal.

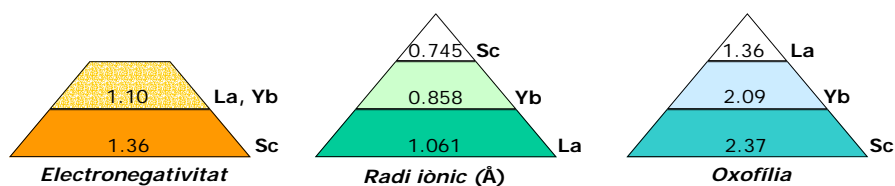


Fig. 1.25. Paràmetres que afecten a l'acidesa d'un àcid de Lewis

També podem dir que cal esperar una baixa proporció de processos de terminació de cadena degut a la baixa basicitat, pobra nucleofília i baixa capacitat de coordinació de l'anió triflat.<sup>84</sup>

El nostre grup de recerca, ha realitzat diversos estudis sobre el procés de curat de la reïna epoxi de diglicidilèter de bisfenol A (DGEBA) emprant triflats de lantànid com a iniciadors<sup>11</sup> i va demostrar la seva bona capacitat d'entrecruar reïnes epoxi a temperatures moderades, obtenint-se materials amb bones propietats mecàniques. En altres estudis, també realitzats en el nostre grup de recerca, es va demostrar que aquests iniciadors presentaven una elevada eficàcia en l'entrecruament de reïnes epoxi cicloalifàtiques, donant lloc a materials amb millors propietats mecàniques que les aconseguides amb BF<sub>3</sub>·MEA.<sup>85</sup>

<sup>78</sup> V. K. Aggarwal, G. P. Vennall, *Tetrahedron Lett.* **37**, 3745-3746 (1996).

<sup>79</sup> R. G. Pearson, *J. Am. Chem. Soc.*, **85**, 3533-3539 (1963).

<sup>80</sup> N. Iranpoor, M. Shekarriz, F. Shiriny, *Synth. Commun.* **28**, 347-366 (1998).

<sup>81</sup> S. Kobayashi, I. Hachiya, *J. Org. Chem.* **59**, 3590-3596 (1994).

<sup>82</sup> S. Kobayashi, *Synlett*, 689-701 (1994).

<sup>83</sup> T. Imamoto, "Lanthanides in Organic Synthesis" Academic Press, London, 1994.

<sup>84</sup> H. C. Aspinall, J. L. Dwyer, N. Greeves, E. G. McIver, J. C. Wooley, *Organometallics* **17**, 1884-1888 (1998).

<sup>85</sup> C. Mas, A. Serra, A. Mantecón, J. M. Salla, X. Ramis, *Macromol. Chem. Phys.* **202**, 2554-2564 (2001).

Els triflats de lantànid també han estat emprats com a excel·lents catalitzadors en l'obertura d'anells oxirànics mitjançant agents nucleòfils com amines<sup>86</sup>, indoles<sup>87</sup> o alcohols.<sup>88</sup>

També existeixen diferents publicacions on se'ls utilitza en polimeritzacions del p-metoxiestirè,<sup>89-91</sup> ciclosiloxans<sup>92</sup> i vinilèters.<sup>93</sup>

Com a resum, els triflats de lantànid presenten les següents avantatges front àcids de Lewis tradicionals com el  $\text{AlCl}_3$ ,  $\text{BF}_3$ ,  $\text{SnCl}_4$  i  $\text{TiCl}_4$ :

- *Tolerància front l'aigua.* Els triflats de lantànid es poden usar en medis aquosos, mentre que els àcids de Lewis tradicionals en presència d'aigua reaccionen amb aquesta, es dissocien i s'inactiven.<sup>76,82,89,90</sup>
- *Estabilitat a temperatura ambient.*
- *No necessiten emmagatzematge en atmosfera inert.*<sup>83</sup>
- *Bona solubilitat en compostos orgànics.* Aquest paràmetre és molt important per tal que la mescla entre la reïna epoxi i l'iniciador sigui homogènia.
- *Baixa toxicitat.* Presenten una toxicitat semblant a la dels metalls alcalins i inferior a la dels metalls de transició.<sup>83</sup>
- *Comercialment assequibles.*

<sup>86</sup> M. Chini, P. Crotti, L. Favero, F. Macchia, M. Pineschi, Tetrahedron Lett. **35**, 433-436 (1994).

<sup>87</sup> H. Kotsuki, M. Teraguchi, N. Shimomoto, M. Ochi, Tetrahedron Lett. **37**, 3727-3730 (1996).

<sup>88</sup> N. Iranpoor, M. Shekarriz, F. Shiriny, Synth. Commun. **28**, 347-366 (1998).

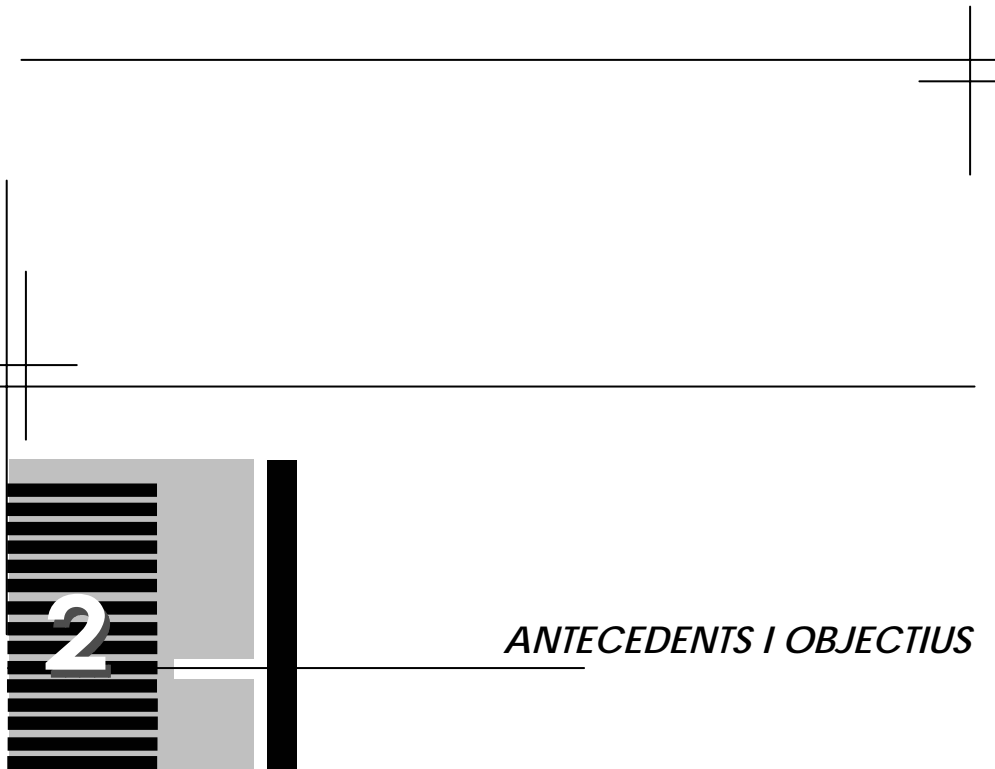
<sup>89</sup> K. Satoh, M. Kamigaito, M. Sawamoto, Macromolecules **32**, 3827-3832 (1999).

<sup>90</sup> K. Satoh, M. Kamigaito, M. Sawamoto, Macromolecules **33**, 4660-4672 (2000).

<sup>91</sup> K. Satoh, M. Kamigaito, M. Sawamoto, Macromolecules **33**, 5836-5840 (2000).

<sup>92</sup> G. Richard, A. F. Mongotaud, D. Cardinaud, A. Soum, Polym. Bull. **39**, 581-588 (1997).

<sup>93</sup> K. Satoh, H. Katayama, M. Kamigaito, M. Sawamoto, "Cationic Polymerization" ACS. Symp. Ser **665**, 106 (1997).





## 2. ANTECEDENTS I OBJECTIUS

Una de les tesis doctorals "**Modificació química de reïnes epoxi amb lactones**"<sup>94</sup> realitzada en el nostre grup de recerca, va tractar sobre l'obtenció i estudi de materials termoestables amb baix encongiment mitjançant reacció directa entre epòxids i lactones passant per la formació d'espироortoesters intermedis que poden polimeritzar en el mateix medi catiònic. La incorporació de grups esters a la xarxa polimèrica tridimensional permetia una degradació controlada, ja fos tèrmica o químicament. Per a l'obtenció d'aquests materials termoestables, l'autora de la tesi seguí les següents alternatives:

- Curat de mescles de reina glicidilica (DGEBA) o cicloalifàtica (ECH) amb la  $\gamma$ -butirolactona ( $\gamma$ -BL).
- Curat de mescles de reina glicidilica (DGEBA) amb ftalida (FT) o diftalida (DFT).

En tots els casos es van emprar els triflats de lantànid com a iniciadors i mitjançant la copolimerització catiònica es va poder arribar a reduir de forma notable l'encongiment després del punt de gelificació. No obstant, no s'observà una millora en la contracció global amb aquestes lactones de cinc baules. A més, l'addició de la lactona va comportar una acceleració del procés de curat, permetent així una disminució de la temperatura de curat i/o un escurçament del temps d'escalfament i per tant un estalvi energètic notori en les possibles aplicacions tecnològiques. Tanmateix, es va trobar que la degradació no es veia incrementada de forma notable, excepte quan es partia de la reina cicloalifàtica que ja incorporava grups ester a la seva estructura.

Una altra tesi doctoral "**Obtenció de xarxes entrecreuades a partir de reïnes epoxi modificades amb grups carbonat**"<sup>95</sup> realitzada també en el nostre grup de recerca, es centrà en l'obtenció de nous materials termoestables derivats del diglicidilèter de bisfenol A (DGEBA) per

<sup>94</sup> C. Mas, "Modificació química de reïnes epoxi amb lactones", Tesis Doctoral, Dept. Q.A i Q.O, Universitat Rovira i Virgili, Tarragona (2004).

<sup>95</sup> R. Cervellera, "Obtenció de xarxes entrecreuades a partir de reïnes epoxi modificades amb grups carbonat", Tesis Doctoral, Dept. Q.A i Q.O, Universitat Rovira i Virgili, Tarragona (2005).

copolimerització amb monòmers que permetien la introducció de grups carbonat i cadenes alifàtiques a la xarxa polimèrica.

Per a l'obtenció d'aquests nous materials termoestables, l'autora de la tesi seguí les següents estratègies:

- *Copolimerització catiònica o aniónica de la reina glicidílica de DGEBA amb carbonats cíclics de cinc o sis baules.*
- *Copolimerització catiònica de la reina glicidílica de DGEBA amb un espiroortocarbonat amb dos anells de sis baules.*

En tots els casos s'empraren els triflats de lantànid com a iniciadors catiònics i com a iniciador aniónic s'utilitzà una amina terciària, la 4-(N,N-dimetilamino)piridina (DMAP). A arrel d'aquests estudis, es va observar que els carbonats de sis baules conduïen a una major incorporació de grups carbonat a la xarxa polimèrica. A més, es va observar que la introducció d'aquests grups reduïa la temperatura d'inici de pèrdua de pes.

La copolimerització catiònica amb l'espiroortocarbonat prèviament sintetitzat sí va permetre reduir la contracció de forma notable i inclòs es va obtenir expansió. No obstant, el material curat posseïa un Tg baixa.

Davant dels resultats obtinguts en les dues tesis esmentades es considerà important continuar amb la reducció del encongiment global i després de la gelificació per reduir la generació de tensions internes a la xarxa polimèrica. La permanència en el medi es podria reduir introduint grups ester terciaris, més làbils i que permetessin la degradació tèrmica del termoestable una vegada ha finalitzat la seva vida útil. Les propietats mecàniques es podrien millorar mitjançant la introducció de cadenes alifàtiques que flexibilitzessin i reduïssin la fragilitat dels materials.

Així, l'objectiu del present treball consisteix en l'obtenció de nous materials termoestables, degradables i amb baixa contracció durant el curat amb bones característiques mecàniques. Aquest objectiu es pretén aconseguir mitjançant la modificació de reïnes epoxi per copolimerització per obertura d'anell amb lactones de sis baules. S'ha utilitzat una reïna comercial, el diglicidil èter del bisfenol A (DGEBA) i com a lactones el 2,2-dimetil-4,6-dioxo-1,3-dioxà o àcid de Meldrum (**MA**) i tres dels seus derivats: el 2,2,5,5-tetrametil-4,6-dioxo-1,3-dioxà (**MDM**), la 6,6-dimetil-5,7-dioxaspiro[2.5]octan-4,8-diona (**MCP**) i la 7,7-dimetil-6,8-dioxaspiro[3.5]nonan-5,9-diona el (**MCB**) (**Fig.2.1**).

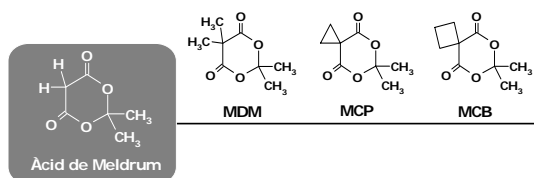


**Fig.2.1.** Lactones copolimeritzades amb la reina epoxi de DGEBA

L'àcid de Meldrum permet introduir a la xarxa polimèrica esters terciaris, més làbils que els emprats en els treballs anteriors, i és d'esperar que, degut a la seva mida de cicle, conduirà a una menor contracció durant el procés de curat en comparació amb les lactones de cinc baules. A més, l'acidesa del grup metilènic permet l'obtenció dels diferents derivats que possibilitaran l'obtenció de materials entrecruats amb diferents propietats.

A més, s'ha sintetitzat una nova reina epoxi: el 5,5-bis(2,3-epoxipropil)-2,2-dimetil-4,6-dioxo-1,3-dioxà (**DGMA**) (**Fig.2.2**), on es conjuga en un mateix compost l'anell de lactona i els grups glicidílics per a homopolimeritzar-la i copolimeritzar-la posteriorment amb la reina epoxi de diglicidil èter de bisfenol A (DGEBA).

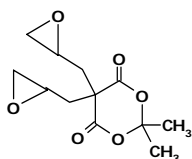


**Fig.2.2.** 5,5-(2,3-epoxipropil)-2,2-dimetil-4,6-dioxo-1,3-dioxà (DGMA)

Els processos de curat escollits han sigut catiónics o aniónics. Les copolimeritzacions catióniques s'han portat a terme utilitzant tres triflats de terres rares:  $\text{Sc}(\text{OTf})_3$ ,  $\text{Yb}(\text{OTf})_3$  i  $\text{La}(\text{OTf})_3$  i s'han comparat amb el sistema  $\text{BF}_3 \cdot \text{MEA}$ , normalment utilitzat en els processos convencionals. Les copolimeritzacions anióniques s'han dut a terme emprant una amina terciària, la 4-(N,N-dimetilamino)piridina (DMAP).

El present treball s'ha estructurat en els següents capítols:

1. *Introducció.*
2. *Antecedents i objectius.*
3. *Copolimerització catiónica de la reina epoxi de DGEBA amb àcid de Meldrum (MA) i amb alguns dels seus derivats: MCP, MDM i MCB.*
4. *Copolimerització aniónica de la reina epoxi de DGEBA amb MCP o MDM.*
5. *Síntesi d'una nova reina epoxi: el 5,5-(2,3-epoxipropil)-2,2-dimetil-4,6-dioxo-1,3-dioxà (DGMA) i posterior copolimerització catiónica amb la reina epoxi de DGEBA.*
6. *Estudi de les propietats mecàniques.*
7. *Estudi comparatiu entre les diferents lactones.*
8. *Conclusions.*

En relació a la caracterització experimental:

S'han realitzat estudis cinètics mitjançant calorimetria diferencial d'escombrat (**DSC**) i s'han aplicat mètodes isoconversionals per estudiar el comportament dels diferents sistemes i poder determinar així les constants cinètiques.

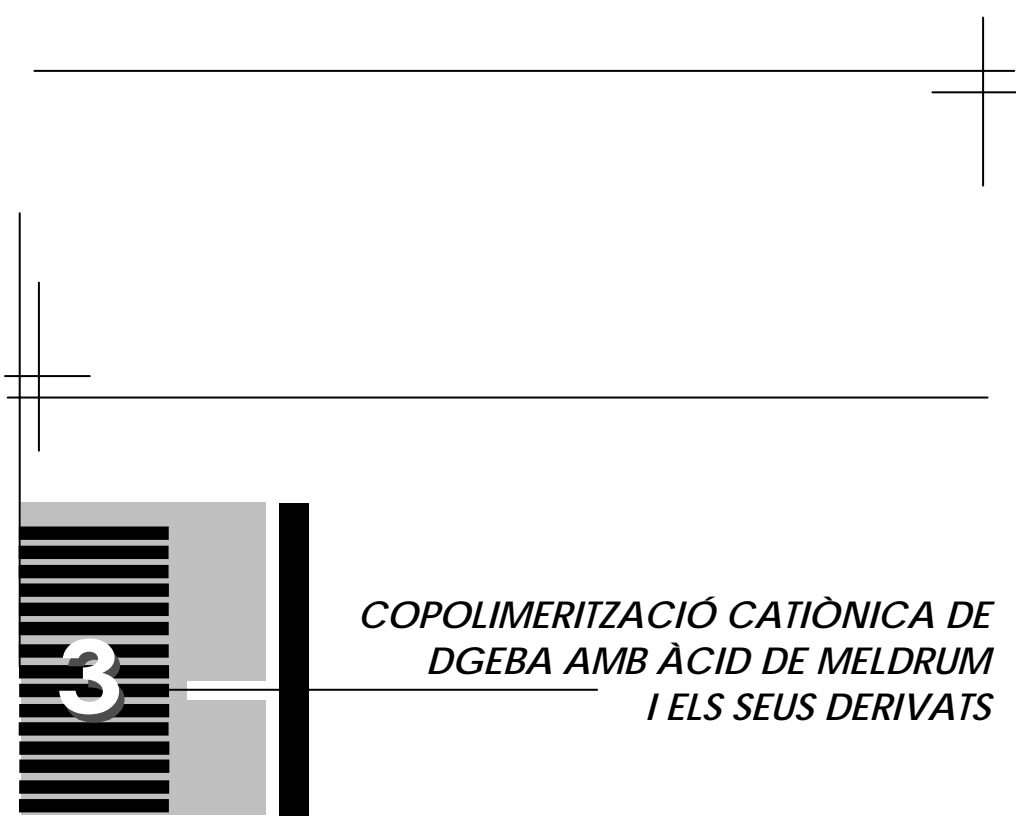
El seguiment de les reaccions de copolimerització dels diferents sistemes formats per reïna/comonòmer/iniciador es va realitzar per espectroscòpia d'infraroig a temps real (**FTIR-ATR**) a una temperatura determinada.

Mitjançant l'anàlisi termogravimètrica (**TGA**), es va realitzar l'estudi de l'estabilitat tèrmica dels diferents materials obtinguts, avaluant la influència de l'estructura del comonòmer, la seva proporció i el tipus d'iniciador emprat en el curat.

L'anàlisi termodinamomecànica (**DMTA**) va permetre determinar els mòduls d'emmagatzematge ( $E'$ ) i les tangents de pèrdues ( $\tan \delta$ ) dels diferents materials termoestables obtinguts.

L'encongiment dels diferents materials va ser determinat a partir de les mesures de les densitats de les mescles inicials abans de ser curades i dels materials un cop curats mitjançant un picnòmetre d'heli.

S'ha estudiat la microduresa dels materials termoestables obtinguts mitjançant un microindentador.



*COPOLIMERITZACIÓ CATIÒNICA DE  
DGEBA AMB ÀCID DE MELDRUM  
I ELS SEUS DERIVATS*



3.1.



*INTRODUCCIÓ*

### 3. COPOLIMERITZACIÓ CATIÒNICA DEL DGEBA AMB ÀCID DE MELDRUM I ELS SEUS DERIVATS

#### 3.1. Introducció

Com s'ha comentat anteriorment, en un dels treballs de Pascault i col.<sup>51</sup> es va estudiar la influència de la  $\gamma$ -butirolactona ( $\gamma$ -BL) com a dissolvent de complexos de  $\text{BF}_3$ /amina en la polimerització d'un monoepòxid, el fenilglicidilèter (PGE), degut a que aquesta lactona es un bon dissolvent i no pot homopolimeritzar per raons termodinàmiques. Posteriorment es realitzà el mateix estudi però emprant un diepòxid de partida, el diglicidil èter de bisfenol A (DGEBA).<sup>50</sup> De l'estudi realitzat, es va poder concloure que en la polimerització de l'epòxid en presència de la  $\gamma$ -BL no només tenia lloc la reacció d'homopolimerització de l'epòxid sinó que, a més, la lactona s'incorporava al polímer mitjançant la formació d'un espiroortoester intermedi.

En base als diferents precedents que es tenen, el present treball està enfocat globalment a l'obtenció de nous materials termoestables que incorporin diverses unitats repetitives de poli(èter-ester) per copolimerització de la reina epoxi de diglicidil èter de bisfenol A (DGEBA) i d'una lactona de sis baules, l'àcid de Meldrum (**MA**) (**Fig.3.1**) o diferents derivats d'aquest compost. Tots aquests compostos permeten l'incorporació de grups esters terciaris a la xarxa polimèrica tridimensional, el que pot permetre una millor degradació tèrmica dels materials resultants un cop la seva vida útil ha finalitzat.

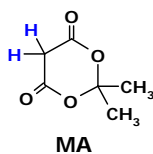


**Fig.3.1.** Àcid de Meldrum

Des del punt de vista estructural, l'àcid de Meldrum és un compost químicament interessant. A més, el fet que sigui un producte comercial i amb un preu bastant assequible fa que pugui ser de gran interès tecnològic en el

món de la indústria, podent-se obtenir materials amb un cost relativament baix.

Al 1908, A.N. Meldrum va postular que la reacció de condensació entre l'àcid malònic i l'acetona en presència d'anhidrid acètic com a dissolvent i àcid sulfúric en quantitats catalítiques donava lloc a un sòlid blanc i cristal·lí amb fórmula molecular  $C_6H_8O_4$ . Aquest es caracteritzà com a àcid monobàsic i a més perdia diòxid de carboni per escalfament.<sup>96</sup> Tot i no tenir la suficient certesa, va postular que es tractava d'un àcid carboxílic, l'àcid 2,2-dimetil-3-oxa-4-oxociclobutancarboxílic (**1**). Van ser necessaris 40 anys per demostrar que l'estructura no corresponia a la d'aquest àcid i Davidson i Bernhard<sup>97</sup> van assignar correctament l'estructura de "l'àcid de Meldrum" ja que les seves propietats estaven relacionades a les d'altres 1,3-diones cícliques com la 5,5-dimetil-1,3-diona (**2**) i l'àcid barbitúric (**3**) (**Fig.3.2**).

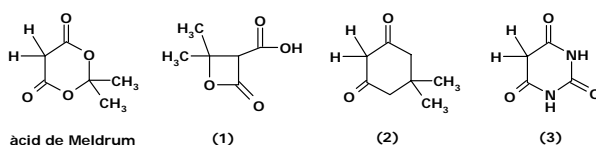


**Fig. 3.2.** Estructures de diferents 1,3-diones cícliques

Per poder tenir una idea de com pot reaccionar l'àcid de Meldrum en la copolimerització amb el DGEBA cal conèixer quines propietats físiques i químiques presenta. L'àcid de Meldrum té un  $pK_a=4.83$  en medi aquós<sup>98</sup> i de 7.3 en DMSO a 25°C.<sup>99</sup> Presenta una acidesa comparable a la de l'àcid acètic ( $pK_a=4.76$ ) i una acidesa aproximadament d'uns vuit ordres de magnitud superior a la dels malonats acíclics. L'explicació d'aquesta forta acidesa es deu a la fàcil pèrdua del protó que es troba en la posició metilènica de l'anell, originant-se així un anió fortament estabilitzat (**Fig.3.3**), però n'hi ha d'haver alguna altre.

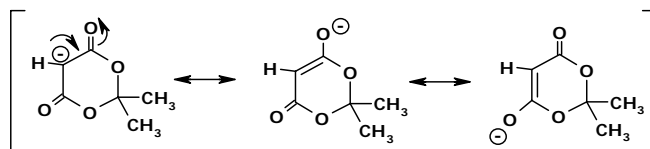


**Fig.3.3.** Estabilització de l'anió de l'àcid de Meldrum

Sorprenentment, les propietats tautomèriques de la 5,5-dimetil-1,3-diona i de l'àcid de Meldrum són bastant diferents. En la primera la càrrega negativa recau principalment en l'oxigen i en l'àcid de Meldrum en el

<sup>96</sup> A. N. Meldrum, J. Chem. Soc., **93**, 598-600 (1908).

<sup>97</sup> D. Davidson, S. A. Bernhard, J. Amer. Chem. Soc., **70**, 3426-3428 (1948).

<sup>98</sup> K. Pihlaja, M. Seilo, Acta. Chem. Scand., **22**, 3053-3062 (1968).

<sup>99</sup> E. M. Arnett, J. A. Jr. Harrelson, J. Am. Chem. Soc., **109**, 809-812 (1987).



carboni.<sup>100</sup> Tot i així, no sembla ser una explicació suficient per justificar la seva acidesa anòmala, ja que generalment els esters són menys enolitables que les cetones.<sup>101</sup> Diferents estudis conformacionals,<sup>99,102,103,104</sup> de moments dipolars<sup>105</sup> i de raigs X,<sup>106</sup> entre d'altres, no han arribat a una completa explicació de l'acidesa d'aquest compost.

Aquest capítol es centrarà en l'estudi de la copolimerització catiónica de la reina epoxi de diglicidil èter de bisfenol A (DGEBA) amb l'àcid de Meldrum (MA) i tres dels seus derivats en diferents proporcions molars. La reacció entre la reina epoxi i la lactona passa per la formació d'un espiroortoester com a intermedi el qual, posteriorment, polimeritza (**Esquema 3.1**). Les copolimeritzacions catióniques de l'àcid de Meldrum s'han portat a terme amb dos triflats de lantànid, el Yb(OTf)<sub>3</sub> i el La(OTf)<sub>3</sub>. S'han emprat diferents proporcions d'iniciador per tal d'estudiar la influència del catió metàl·lic en el curat de la mescla de la reina epoxi de DGEBA amb MA i en les propietats finals dels materials.

Les proporcions d'iniciador estudiades són 0.003, 0.0015 i 0.00075 mols d'iniciador per equivalent reactiu de monòmer. Tenint en compte que el DGEBA té dos equivalents per mol i que l'àcid de Meldrum o derivats en té un, en mescles de DGEBA/lactona amb una relació molar entre comonòmers 3:1, el nombre d'equivalents és set i en mescles amb una relació molar entre comonòmers 2:1, el nombre d'equivalents és cinc. Per tant, el tercer número que apareix en les formulacions resulta de multiplicar la corresponent proporció d'iniciador pel nombre d'equivalents de la mescla.

Cal assenyalar que es va decidir treballar amb mols d'iniciador per equivalent de reina amb el propòsit de mantenir la formulació reina/comonòmer/iniciador en relacions molars i no amb phr (parts d'iniciador per cent parts de mescla de monòmers), magnitud utilitzada habitualment en el món de la indústria. D'aquesta manera es contempla que els iniciadors i els comonòmers emprats tenen diferents pesos moleculars i per tant queda reflectit en la formulació final de les diferents composicions.

Les copolimeritzacions catióniques dels derivats de l'àcid de Meldrum també s'han portat a terme amb Yb(OTf)<sub>3</sub> i La(OTf)<sub>3</sub>. No obstant, per a comparar, en algun dels sistemes també s'ha estudiat el curat de la de la mescla amb Sc(OTf)<sub>3</sub> i BF<sub>3</sub>·MEA. La proporció d'iniciador estudiada és de 0.003 mols d'iniciador per equivalent reactiu de monòmer en el cas dels

<sup>100</sup> M. Eigen, G. Ilgenfritz and W. Kruse, Chem. Ber., **98**, 1623-1638 (1965).

<sup>101</sup> A. Gero, J. Org. Chem., **19**, 1960-1970 (1954).

<sup>102</sup> P. Åyräs, P. Partanen, Finn. Chem. Letters, 110 (1976).

<sup>103</sup> X. Wang, K. N. Houk, J. Am. Chem. Soc., **110**, 1870-1872 (1988).

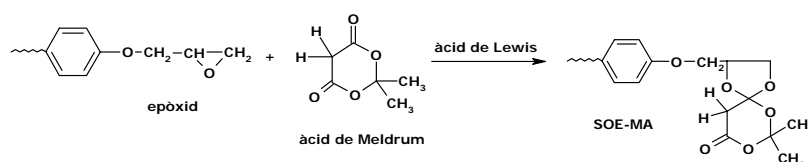
<sup>104</sup> K. Byun, Y. Mo, J. Gao, J. Am. Chem. Soc., **123**, 3974-3979 (2001).

<sup>105</sup> (a) D. Körberl, P. Schuster, Monatsh., **103**, 1483 (1972); D. Körberl, O. E. Polansky, Monatsh., **104**, 1421 (1973); (c) E. N. Klimovitskii, L. K. Yudasheva, B. A. Arbutov, Izvest. Akad. Nauk. S.S.S.R., Ser. Khim., 1527 (1973).

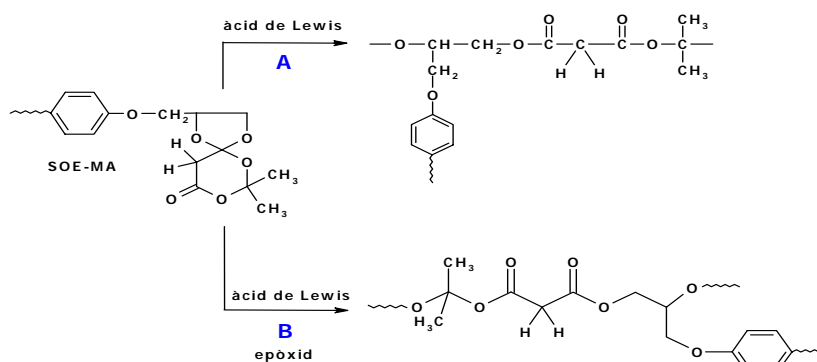
<sup>106</sup> P. G. Jones, O. Kennard, Cryst. Struct. Comm., **6**, 97 (1977).

triflats de terres rares ( $\text{Yb}(\text{OTf})_3$ ,  $\text{La}(\text{OTf})_3$  i  $\text{Sc}(\text{OTf})_3$ ) i 0.048 mols d'iniciador per equivalent reactiu de monòmer en el cas del  $\text{BF}_3 \cdot \text{MEA}$ .

- *Formació de l'epiroortoester*



- *Homopolimerització del SOE-MA (A) i copolimerització de DGEBA amb el SOE-MA (B)*



Esquema 3.1. Reaccions en el procés de curat

Dels resultats obtinguts en la copolimerització del DGEBA amb l'àcid de Meldrum s'ha pogut deduir que els protons àcids de la posició metilènica de l'anell podien desenvolupar un paper rellevant en la reactivitat del procés de curat i, com a conseqüència, en les propietats finals dels polímers. Per tant, es va decidir incorporar diferents substituents en aquesta posició per evitar així que el mecanisme de polimerització es veiés influït per la presència d'aquests protons i per veure com aquests substituents afecten a les propietats finals dels materials termoestables.

Els derivats de l'àcid de Meldrum utilitzats són: el 2,2,5,5-tetrametil-4,6-dioxo-1,3-dioxà (**MDM**), la 6,6-dimetil-5,7-dioxaspiro[2.5]octan-4,8-diona (**MCP**) i la 7,7-dimetil-6,8-dioxaspiro[3.5]nonan-5,9-diona (**MCB**) (**Fig.3.4.**). D'aquests tres compostos, l'únic que és comercial és el MCP. Els altres dos han estat prèviament sintetitzats en el laboratori.

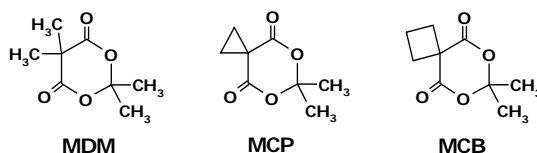


**Fig.3.4.** Derivats de l'àcid de Meldrum (MA)

Els resultats d'aquest treball es reflecteixen en diferents articles:

**3.2.** "New Thermosets Obtained from DGEBA and Meldrum Acid with Lanthanum and Ytterbium Triflates as Cationic Initiators".

L. González, X. Ramis, J. M. Salla, A. Mantecón, A. Serra.  
Eur. Polym. J. En premsa

**3.3.** "Reduction of the Shrinkage of Thermosets by Cationic Curing of Mixtures of Diglycidyl Ether of Bisphenol A and 6,6-Dimethyl-(5,7-dioxaspiro [2.5]octane-4,8-dione)".

L. González, X. Ramis, J. M. Salla, A. Mantecón, A. Serra.  
J. Polym. Sci. Part A: Polym. Chem. 44, 6869-6879 (2006)

**3.4.** "The Degradation of New Thermally Degradable Thermosets Obtained by cationic curing of mixtures of DGEBA and 6,6-Dimethyl-(5,7-dioxaspiro [2.5]octane-4,8-dione)".

L. González, X. Ramis, J.M. Salla, A. Mantecón, A. Serra  
Polym. Degrad. Stab. 92, 596-604 (2007)

**3.5.** "Kinetic Analysis by DSC of the Cationic Curing of Mixtures of DGEBA and 6,6-Dimethyl-(5,7-dioxaspiro[2.5]octane-4,8-dione)".

L. González, X. Ramis, J.M. Salla, A. Mantecón, A. Serra  
Thermochim. Acta. 464, 35-41 (2007)

**3.6.** "Study of the Cationic Curing of DGEBA and 2,2,5,5-Tetramethyl-4,6-dioxo-1,3-dioxane and the Degradation of the Thermosets Obtained".

L. González, X. Ramis, J. M. Salla, A. Mantecón, A. Serra  
J. Appl. Polym. Sci. 108, 1229-1237 (2008)

**3.7.** "New Poly(ether-ester) Thermosets Obtained by Cationic Curing of DGEBA and 7,7-Dimethyl-6,8-dioxaspiro[3.5]nonane-5,9-dione with Several Lewis Acids as Initiators".

L. González, X. Ramis, J.M. Salla, A. Mantecón, A. Serra  
J. Polym. Sci. Part A. Polym. Chem. 46, 1229-1239 (2008)



## 3.2.

*NEW THERMOSETS OBTAINED FROM DGEBA AND MELDRUM  
ACID WITH LANTHANUM AND YTTERBIUM TRIFLATES  
AS CATIONIC INITIATORS*



**NEW THERMOSETS OBTAINED FROM DGEBA AND MELDRUM ACID  
WITH LANTHANUM AND YTTERBIUM TRIFLATES  
AS CATIONIC INITIATORS**

Lidia González,<sup>1</sup> Xavier Ramis,<sup>2</sup> Josep Maria Salla,<sup>2</sup>  
Angels Serra<sup>1</sup>, Ana Mantecón<sup>1\*</sup>

<sup>1</sup>Departament de Química Analítica i Química Orgànica. Universitat Rovira i Virgili. Marcel·lí Domingo s/n, 43007 Tarragona, Spain

<sup>2</sup>Laboratori de Termodinàmica, ETSEIB. Universitat Politècnica de Catalunya, Av. Diagonal 647, 08028 Barcelona, Spain

---

**Abstract**

Ytterbium and lanthanum triflates were used as cationic initiators to cure mixtures of diglycidylether of bisphenol A (DGEBA) and Meldrum acid (MA) in several proportions of comonomers and initiators. The evolution of the epoxy and lactone groups during curing and the linear ester formed in the final materials were evaluated by Fourier Transform Infrared in the attenuated-total-reflection mode (ATR/FTIR). The global evolution of the curing process was investigated by calorimetric analysis and the activation energy was calculated by isoconversional procedures. Shrinkage on curing and thermal degradability of the final materials on varying the initiator and the proportion of Meldrum acid in the mixtures were evaluated. The expandable character of MA was confirmed. The materials obtained were more degradable than conventional epoxy resins due to the tertiary ester groups incorporated into the network by copolymerization, especially those obtained with ytterbium triflate. On increasing the proportion of initiator the degradability was also increased.

**Keywords:** Epoxy resins, Meldrum acid, cationic polymerization, cross-linking, thermosets

## 1. INTRODUCTION

Epoxy thermosets are widely applied, among others, in the microelectronic industry as coatings and encapsulants. However, the curing of epoxy resins is generally accompanied by shrinkages of 4-5 % because covalent bonds, which form between chains, increase the density of the materials. Shrinkage can be reduced to 3 % when the cure is made by ring-opening mechanism. Shrinkage during curing is a big problem because it could lead to the formation of microvoids and microcracks, which reduce the durability of the material and worsen the properties, especially in the presence of geometrical constraints. A possible solution to overcome this problem is the use of expanding monomers, such as spirobicyclic compounds, which were proposed by Bailey several years ago.<sup>1</sup> The most useful monomers are spiroorthoesters (SOEs), which lead by cationic homopolymerization to poly(ether-ester) chains with zero shrinkage or even expansion.<sup>2</sup> Because SOEs can be formed by reaction of epoxides and lactones in presence of a Lewis acid<sup>3</sup>, the copolymerization of epoxy resins with lactones could reduce the shrinkage during curing and therefore the subsequent internal stress<sup>4</sup>, eliminating the need of the previous synthesis of SOEs. This is the consequence of three main factors: a) ring opening leads to less contraction than other mechanisms of polymerization, b) spiroorthoesters (SOEs) can be formed "in situ", and c) SOEs homopolymerize in the last steps of the cationic

curing and therefore expand in volume and reduce the internal stress when it is usually originated, after gelation. Furthermore, when a monomer with a functionality of two, as a lactone, is added to another with a functionality of four, as DGEBA when it participates in a ring-opening polymerization, the network's crosslink density diminishes and the degree of conversion at the gelation point increases.<sup>5,6</sup> This leads to a lower shrinkage after gelation, when the material lacks of mobility and it is the cause of the internal stresses in the material, which worsen its properties. Moreover, it is reported<sup>2</sup> that the degree of shrinkage is related to the size of the ring being opened; in general, the larger the ring, the smaller the shrinkage.

Meldrum acid (2,2-dimethyl-4,6-dioxo-1,3-dioxane, MA) is a structurally and chemically interesting cyclic diester, which was first synthesized by A.N. Meldrum in 1908<sup>7</sup> from malonic acid and acetone in cold acetic anhydride and sulphuric acid as catalyst. Meldrum acid has a great reactivity, analogous to malonic esters, and a great acidity ( $pK_a = 4.83$  in water)<sup>8</sup> and therefore is widely applied in organic synthesis.

In a previous study<sup>9</sup> Meldrum acid was used in the preparation of new epoxy powder coatings with a lanthanide triflate as curing agent. The results obtained showed that the on adding MA to the epoxy powder an acceleration of the curing process was observed and the coatings had a better impact resistance and a higher adhesion to the metallic substrates, which was attributed to the reduction in the shrinkage on

curing. However, the reduction of the shrinkage could not be experimentally quantified and a detailed study of the reaction progress was not made.

In the present work, we studied the cationic crosslinking of a liquid DGEBA epoxy resin with different proportions of MA, using ytterbium and lanthanum triflates in different quantities to investigate the curing evolution and the shrinkage and the thermal degradability of the materials obtained.

In previous works<sup>10,11</sup> we demonstrated an enhanced degradability of epoxy thermosets when we added Meldrum acid derivatives because of the introduction of tertiary ester groups into the polymeric network, which suffers a  $\beta$ -elimination process at relatively low temperature. This enhanced thermal degradability is an advantage to recycle, repair and reuse the electronic components coated with this type of materials.<sup>12,13</sup>

Lanthanide triflates were selected as initiators because they have been proved to be excellent Lewis acids, commercially available, stable in water and environmentally friendly catalysts<sup>14</sup> capable of copolymerizing epoxy resins with lactones by a ring-opening mechanism through the formation of spirocyclic compounds.<sup>6,10,11</sup>

## 2. EXPERIMENTAL

### 2.1. Materials

Diglycidylether of bisphenol A (DGEBA) EPIKOTE RESIN 827 from Shell Chemicals (Epoxy

Equiv. = 182.08 g/eq), Meldrum acid (2,2-dimethyl-4,6-dioxo-1,3-dioxane, MA) (Aldrich) were used as received.

Lanthanum (III) and ytterbium (III) trifluoromethanesulfonates (Aldrich) were used without purification.

### 2.2. Preparation of the curing mixtures

The samples were prepared by mixing and manual stirring in a mortar the selected initiator with the corresponding amount of MA and DGEBA. The prepared mixtures were kept at  $-18^{\circ}\text{C}$  before use. Lanthanide triflates were added in a molar ratio of 0.006, 0.003 and 0.0015 mols per mol of DGEBA and adding 0.003, 0.0015 and 0.00075 mols per mol of MA respectively. The compositions of all formulations are detailed in the corresponding tables.

### 2.3. Characterization and measurements

Calorimetric studies were carried out on a Mettler DSC-821e thermal analyzer in covered Al pans under  $\text{N}_2$  at  $10^{\circ}\text{C}/\text{min}$ . The calorimeter was calibrated using an indium standard (heat flow calibration) and an indium-lead-zinc standard (temperature calibration). The samples weighed approximately 7-9 mg. In the dynamic curing process the degree of conversion by DSC ( $\alpha_{DSC}$ ) was calculated as follows:

$$\alpha_{DSC} = \frac{\Delta H_T}{\Delta H_{dyn}} \quad (1)$$

where  $\Delta H_T$  is the heat released up to a temperature  $T$ , obtained by integration of the calorimetric signal up to this temperature, and  $\Delta H_{dyn}$  is the total reaction heat associated with the complete conversion of all reactive groups.

The glass transition temperature for each material ( $T_g$ ) was calculated after complete curing, by means of a second scan, as the temperature of the half-way point of the jump in the heat capacity when the material changed from the glassy to the rubbery state.

The isothermal curing process at 150°C was monitored with a FTIR spectrophotometer FTIR-680PLUS from JASCO with a resolution of 4  $\text{cm}^{-1}$  in the absorbance mode. An attenuated-total-reflection accessory with thermal control and a diamond crystal (Golden Gate heated single-reflection diamond ATR, Specac-Teknokroma) was used to determine FTIR spectra. The conversions of the reactive groups were determined from the normalized changes in the absorbance by the Lambert-Beer law, as we explained previously.<sup>15-17</sup> After isothermal curing in the FTIR-ATR device, a dynamic scan by DSC was always carried out to prove that the curing was complete.

Thermogravimetric analyses (TGAs) were carried out with a Mettler TGA/SDTA 851e thermobalance. Cured samples with an approximate mass of 7 mg were degraded between 30 and 600°C at a heating rate of 10°C/min in  $\text{N}_2$

(200  $\text{cm}^3/\text{min}$ ) measured in normal conditions.

Shrinkage was determined from the densities of the samples before and after curing. The densities were determined using a Gas Pycnometer Micromeritics AccuPyc 1330 thermostated at 30°C. This is based in the gas displacement technique. A weighed quantity of sample is introduced in the cell. Then, the selected temperature should be reached and maintained. The pycnometer measures automatically the difference of volume of gas on comparing with the volume of the empty cell. From this volume and the weight of sample introduced, the density of the sample is automatically calculated.

#### 2.4. Kinetic analysis

Integral non-isothermal kinetic analysis was used to determine the kinetic triplet (A pre-exponential factor, E activation energy and  $g(\alpha)$  integral function of degree of conversion).

Non-isothermal kinetic analysis may start with the kinetic equation:

$$\beta \frac{d\alpha}{dT} = A \exp\left(\frac{-E}{RT}\right) f(\alpha) \quad (2)$$

where  $\beta$  is the heating rate,  $\alpha$  is the conversion,  $R$  is the universal gas constant,  $T$  is the temperature and  $f(\alpha)$  is the differential conversion function.

By using the Coats-Redfern<sup>18</sup> approximation to resolve the so-called temperature integral and considering that  $2RT/E$  is much lower than 1, the Kissinger-



Akahira-Sunose (KAS) equation may be written as:<sup>19</sup>

$$\ln \frac{\beta}{T^2} = \ln \left[ \frac{AR}{g(\alpha)E} \right] - \frac{E}{RT} \quad (3)$$

For each conversion degree, the linear representation of  $\ln[\beta/T^2]$  versus  $T^{-1}$  enables  $E$  and  $\ln[AR/g(\alpha)E]$  to be determined from the slope and the ordinate in the origin.

### 3. RESULTS AND DISCUSSION

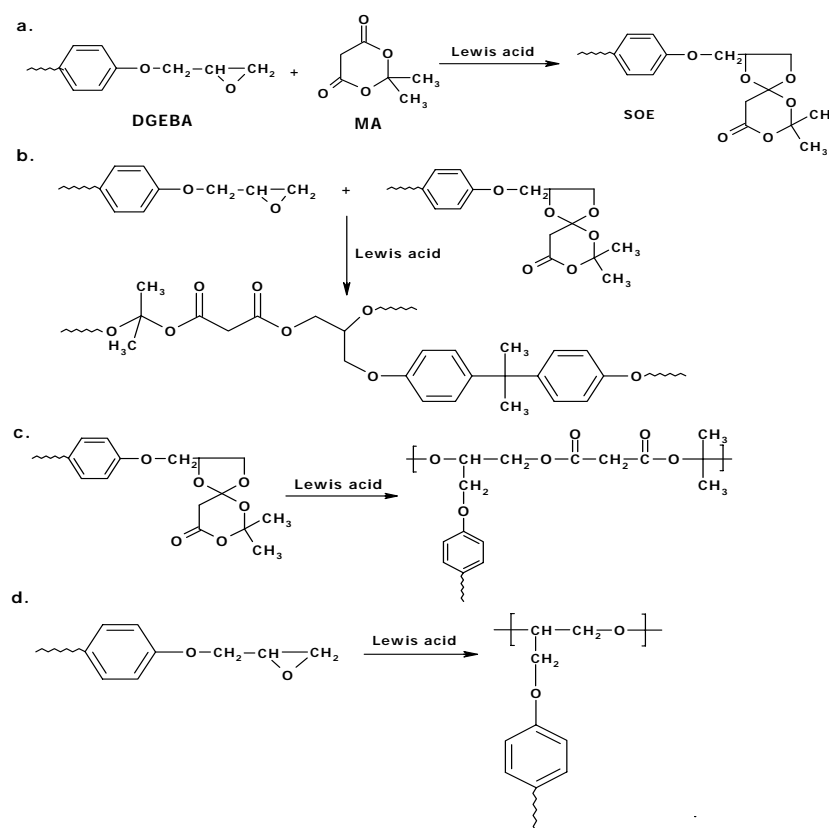
As we saw in previous studies for similar structures<sup>10,20</sup> cationic copolymerization of DGEBA and MA is a complex process where four different reactions can occur in a different extension, which depends on the proportion of co-monomers in the mixture and on the initiator used and its proportion. These reactions that are represented in **Scheme 1** are: a) formation of the spiroorthoesters (SOEs); b) copolymerization of SOEs and epoxy groups; c) homopolymerization of SOEs and d) homopolymerization of epoxy groups, which are in excess. It was experimentally proved that substituted MA derivatives did not homopolymerize in these conditions<sup>10,20</sup> but MA, due to the presence of an activated methylene, is described to be more reactive.<sup>21,22</sup> For example, it is reported that MA on heating produces ketene, acetone and carbon dioxide as is shown in **Scheme 2.a**.<sup>21</sup>

#### 3.1. FTIR-ATR studies

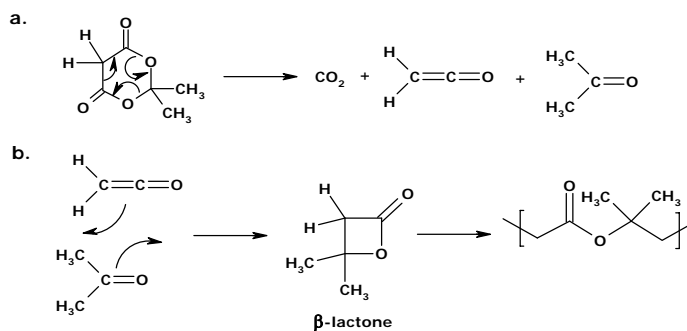
To see if the decomposition of MA occurs at moderate temperature in the presence of a lanthanide triflate we followed the evolution of a mixture of MA with 0.003 mol of ytterbium or lanthanum triflate per mol of MA at 150°C in the ATR/FTIR. **Figure 1** shows the FTIR spectra registered before and after reaction. The most significant bands in the initial spectrum are the carbonyl absorption at 1749  $\text{cm}^{-1}$  with a shoulder at 1783  $\text{cm}^{-1}$ , attributable to symmetric and asymmetric stretching of the two carbonylic groups and the band at 968  $\text{cm}^{-1}$ , which was assigned to the Meldrum acid ring the deformation<sup>10</sup>. Moreover, a band at 1825  $\text{cm}^{-1}$  appears which is not present in pure MA without initiator. In the final spectrum all these bands have been disappeared and a new absorption at 1710  $\text{cm}^{-1}$  can be observed, which was attributed to a linear ester. Thus, at first sight, it seems that Meldrum acid polymerizes in these conditions and no ketene is formed. However, if we observe the evolution of the carbonyl bands (see **Figure 2**), we can see how the band at 1749  $\text{cm}^{-1}$  steadily transforms into another at 1710  $\text{cm}^{-1}$  and how the little absorption at 1825  $\text{cm}^{-1}$  increases until a maximum and then decreases until total disappearance. This band can be attributed to the carbonyl of a strained lactone ( $\beta$ -lactone).<sup>23</sup>

The appearance of the band at  $1825\text{ cm}^{-1}$  from the very beginning of the reaction, before the first

spectrum could be recorded, is a consequence of the high temperature of the ATR ( $150^\circ\text{C}$ ), which suddenly started the reaction.



Scheme 1



Scheme 2

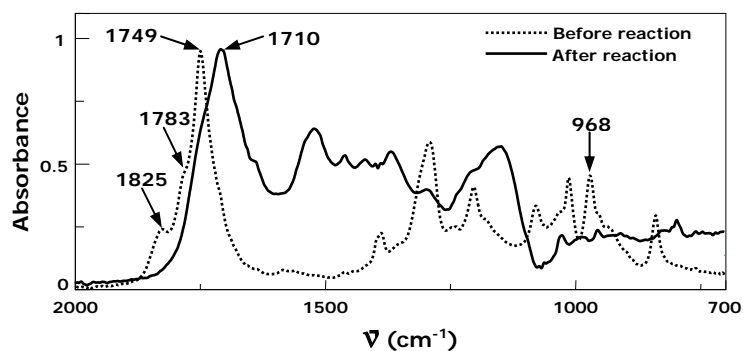


Figure 1. ATR-FTIR spectra of a mixture of MA with 0.003 mol of  $\text{Yb}(\text{OTf})_3$  before and after reaction at  $150^\circ\text{C}$

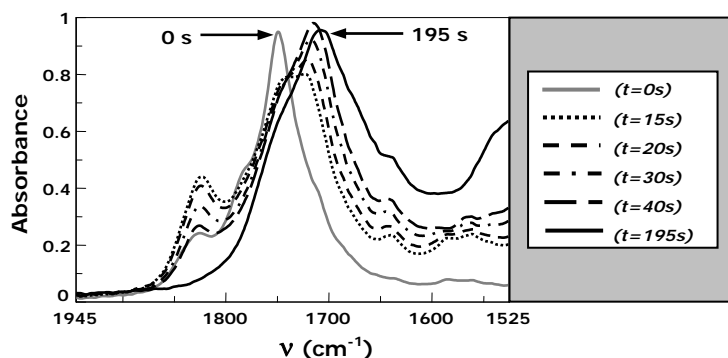


Figure 2. ATR-FTIR spectra of a mixture MA with 0.003 mol of  $\text{Yb}(\text{OTf})_3$  during reaction at  $150^\circ\text{C}$

The evolution of this band can be explained if we take into account a first decomposition of Meldrum acid into ketene and acetone (**Scheme 2.a**) and the subsequent 2+2 cycloaddition reaction between them to form  $\beta$ -isovalerolactone. Its formation is described to be promoted by Lewis acids<sup>24,25</sup> (**Scheme 2.b**). The evolution of some bubbles of  $\text{CO}_2$  on the ATR support this process. The  $\beta$ -isovalerolactone formed polymerizes under cationic conditions to give the corresponding polyester.<sup>25</sup>

To investigate if this reaction takes place in our reactive system we followed the curing of a mixture DGEBA/MA 2:1 mol/mol with 0.015 mol of  $\text{Yb}(\text{OTf})_3$ . In any intermediate spectrum the band at  $1825\text{ cm}^{-1}$  appeared and the final spectrum showed a carbonylic absorption at  $1737\text{ cm}^{-1}$ , analogous to the spectra of the materials obtained from Meldrum acid derivatives/DGEBA mixtures.<sup>10,20</sup>

Therefore, the formation of SOEs from MA in the presence of epoxide is more favored than the formation of ketene and acetone. In the final spectrum we could see the total disappearance of the epoxy absorption at  $912\text{ cm}^{-1}$ , which indicates that the complete curing was reached.

spectra with those obtained from Meldrum acid derivatives MCP (with a cyclopropenyl group in 5 position) and MDM (with two methylene groups in 5 position)<sup>10,20</sup> we observe a higher incorporation of linear ester into the network for MA. This could be due to the steric hindrance caused by the substi-

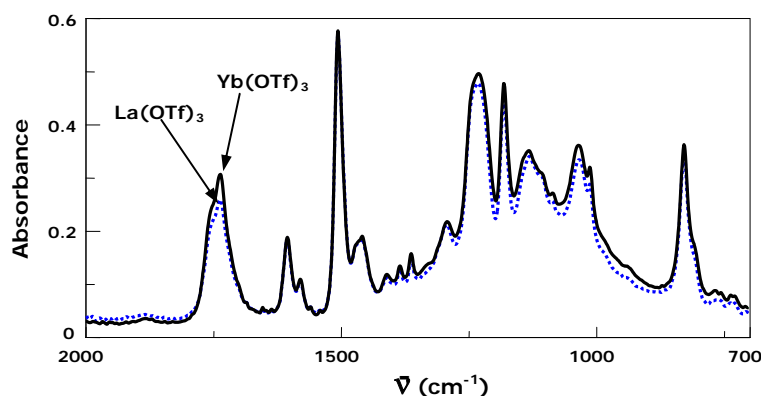


**Figure 3.** ATR-FTIR spectra of different materials obtained from DGEBA/MA mixtures 2:1 (mol/mol) with 0.015 mol of ytterbium and lanthanum triflates after curing at  $150^{\circ}\text{C}$

In **Figure 3** we can see the final spectra of the materials obtained from the same mixture initiated by ytterbium and lanthanum triflates, in which we observe that are similar but ytterbium triflate leads to a higher linear ester absorption. The band at  $968\text{ cm}^{-1}$  completely disappears with both initiators and therefore we can conclude that all MA was transformed into SOE, which on opening forms the linear ester. Although from the FTIR measurements we cannot assure the total transformation of SOE into linear ester with the ytterbium salt, it can be stated that lanthanum triflate leaves some unreacted SOE in the final material. On comparing these

tients in 5 position of the MA ring that makes difficult the SOE polymerization. It can be established that an increase of the volume of the substituents in 5 position decreases the ability of SOE groups to be polymerized.

From the area of the band at  $1737\text{ cm}^{-1}$  and taking the absorption at  $1605\text{ cm}^{-1}$  of the aromatic ring, which does not change during curing, as a reference, we can calculate the normalized areas of the linear ester band in the final network. These values were then referred to the maximum incorporation achieved. The relative proportion of ester groups are included in **Tables 1 and 2** for  $\text{Yb}(\text{OTf})_3$  and  $\text{La}(\text{OTf})_3$  respectively

for all the mixtures studied. As is expected, the higher proportion of MA in the initial mixture the higher the linear ester proportion.

We also studied the effect of the amount of initiator on the linear ester proportion. In a previous work<sup>26</sup> we could prove that a lower proportion of initiator led to a higher proportion of linear ester in the curing of DGEBA/ $\gamma$ -butyrolactone mixtures whereas a higher proportion favors the homopolymerization of epoxide. Since it was confirmed that the copolymerization of SOEs with epoxides was favored in front of SOEs homopolymerization<sup>15</sup>, the slower homopolymerization of epoxides, when we used a little proportion of initiator, should increase the linear ester formation.

Relative values of linear ester incorporation collected in **Tables 1 and 2** indicate a contrary trend in the case of DGEBA/MA mixtures. Thus, entries 4 and 7 in both tables show that the highest proportion of initiator is the most suitable to get the highest linear ester incorporation in final materials. One possible explanation to this different behaviour could be found in the different structure of the lactone and the corresponding SOE.

The evolution of MA and epoxy on changing the proportion of both initiators for DGEBA/MA 2:1 mol/mol mixtures was followed by FTIR and they are represented in **Figure 4**. We can see a different evolution of conversions of MA and epoxide on changing the initiator and its proportion.

**Table 1.** Calorimetric data and activation energies of the system studied initiated by different proportions of  $Yb(OTf)_3$

Entry	Formulation <sup>a</sup>	Linear Ester <sup>b</sup>	Tg <sup>c</sup> (°C)	$\Delta H$ <sup>d</sup> (J/g)	$\Delta H$ <sup>e</sup> (kJ/ee)	T <sub>max</sub> <sup>f</sup> (°C)	Ea <sup>g</sup> (kJ/mo)
1	DGEBA/Yb(OTf) <sub>3</sub> 1:0.006	0	135	519.7	95.6	184	90.7
2	DGEBA/Yb(OTf) <sub>3</sub> 1:0.003	0	120	534.5	97.8	206	85.2
3	DGEBA/Yb(OTf) <sub>3</sub> 1:0.0015	0	115	536.8	98.1	217	83.3
4	DGEBA/MA/Yb(OTf) <sub>3</sub> 3:1:0.021	0.33	120	445.1	92.7	166	86.0
5	DGEBA/MA/Yb(OTf) <sub>3</sub> 3:1:0.0105	0.31	109	465.5	96.5	200	84.5
6	DGEBA/MA/Yb(OTf) <sub>3</sub> 3:1:0.00525	0.30	108	471.4	97.6	203	74.9
7	DGEBA/MA/Yb(OTf) <sub>3</sub> 2:1:0.015	0.65	118	415.0	91.3	160	73.2
8	DGEBA/MA/Yb(OTf) <sub>3</sub> 2:1:0.0075	0.56	107	448.8	98.6	187	73.4
9	DGEBA/MA/Yb(OTf) <sub>3</sub> 2:1:0.00375	0.42	105	455.6	99.7	206	75.4
10	DGEBA/MA/Yb(OTf) <sub>3</sub> 1:1:0.009	1	110	353.0	90.7	168	75.6

- a. The composition of the formulations is given in molar ratios  
 b. Proportion of linear ester in the network calculated from FTIR-ATR experiments  
 c. Glass transition temperatures obtained by DSC in the second scan after dynamic curing  
 d. Enthalpy per gram of mixture  
 e. Enthalpy per equivalent of epoxy groups  
 f. Temperature of the maximum of the curing  
 g. Values of activation energies were evaluated by the isoconversional integral method (Eq. (3)) applied at conversion of 0.5

**Table 2.** Calorimetric data and activation energies of the system studied initiated by different proportions of  $La(OTf)_3$

Entry	Formulation <sup>a</sup>	Linear Ester <sup>b</sup>	T <sub>g</sub> <sup>c</sup> (°C)	ΔH <sup>d</sup> (J/g)	ΔH <sup>e</sup> (kJ/ee)	T <sub>max</sub> <sup>f</sup> (°C)	E <sub>a</sub> <sup>g</sup> (kJ/mo)
1	DGEBA/La(OTf) <sub>3</sub> 1:0.006	0	127	513.5	94.4	192	79.8
2	DGEBA/La(OTf) <sub>3</sub> 1:0.003	0	117	520.3	95.3	206	77.9
3	DGEBA/La(OTf) <sub>3</sub> 1:0.0015	0	106	525.1	95.8	231	82.6
4	DGEBA/MA/La(OTf) <sub>3</sub> 3:1:0.021	0.31	110	440.2	91.6	170	77.4
5	DGEBA/MA/La(OTf) <sub>3</sub> 3:1:0.0105	0.29	106	466.2	96.7	190	80.2
6	DGEBA/MA/La(OTf) <sub>3</sub> 3:1:0.00525	0.28	105	473.5	97.8	201	75.4
7	DGEBA/MA/La(OTf) <sub>3</sub> 2:1:0.015	0.56	109	410.0	90.3	173	68.5
8	DGEBA/MA/La(OTf) <sub>3</sub> 2:1:0.0075	0.44	108	453.7	99.5	186	74.9
9	DGEBA/MA/La(OTf) <sub>3</sub> 2:1:0.00375	0.38	104	456.5	99.9	200	75.4
10	DGEBA/MA/La(OTf) <sub>3</sub> 1:1:0.009	0.81	96	345.1	89.6	167	95.8

- a. The composition of the formulations is given in molar ratios  
 b. Proportion of linear ester in the network calculated from FTIR-ATR experiments  
 c. Glass transition temperatures obtained by DSC in the second scan after dynamic curing  
 d. Enthalpy per gram of mixture  
 e. Enthalpy per equivalent of epoxy groups  
 f. Temperature of the maximum of the curing  
 g. Values of activation energies were evaluated by the isoconversional integral method (Eq.(3) applied at conversion of 0.5

To understand these evolutions, we should take into account the composition of the reactive mixtures and the functionality of each monomer. For example, for DGEBA/MA 2:1 proportion there are four epoxy groups per one MA. As can be seen in the figure, the disappearance of epoxide and MA is quicker with ytterbium triflate and with the highest proportion of initiator. The successive increase in the proportion of the initiator on the epoxy evolution has a greater effect with ytterbium than with lanthanum salt.

On comparing the times needed to reach a complete disappearance of epoxide in MA, MCP and MDM mixtures, we can conclude that MA systems cure at

much short time. Thus, for example, in DGEBA/MA 2:1 systems with 0.015 mol of Yb(OTf)<sub>3</sub> only 480s are enough for the complete disappearance, whereas DGEBA/MCP 2:1 needs 6280s and DGEBA/MDM 2:1 2400s. For the analogous La(OTf)<sub>3</sub> systems the time for MA mixtures is 885s, for MCP is 7370s and for MDM about 3000s. The great difference in the reactivity could not only be due to the steric hindrances before mentioned but to the catalytic effect of methylene protons of the Meldrum acid ring. The great reactivity of the MA mixtures was previously observed in the curing of epoxy powder coatings.<sup>9</sup>

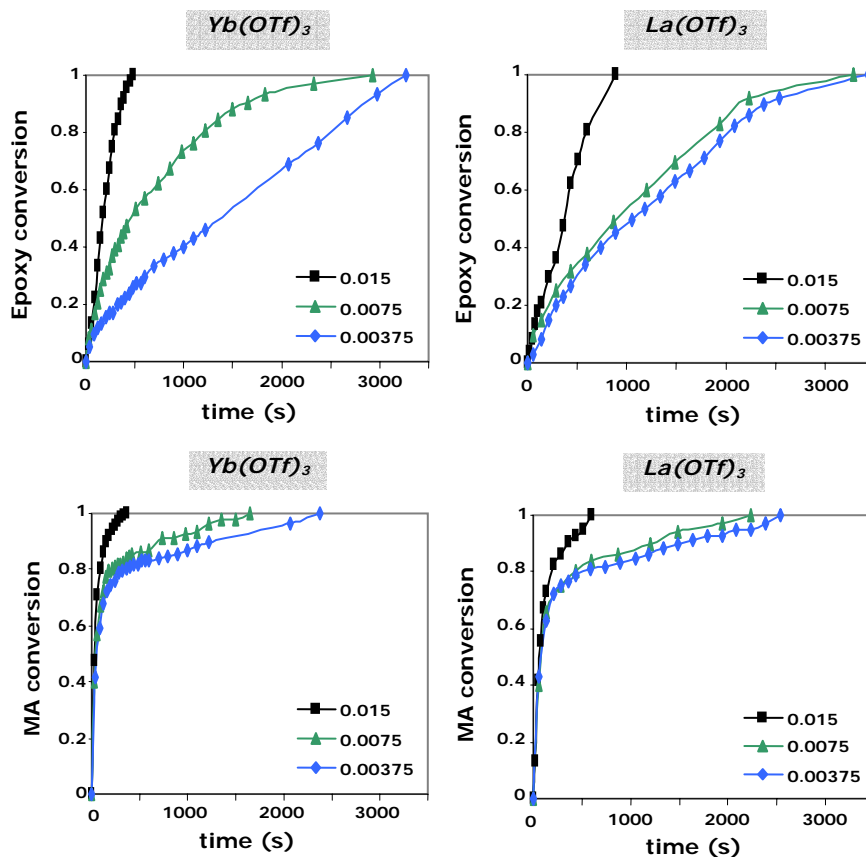


**Figure 4.** Epoxy ( $912\text{ cm}^{-1}$ ) and MA ( $968\text{ cm}^{-1}$ ) conversion degrees versus time for the DGEBA/MA 2:1 (mol/mol) formulation with different proportions of ytterbium and lanthanum triflates during curing at  $150^\circ\text{C}$  in the ATR-FTIR

### 3.2. Calorimetric studies

In previous works we studied the curing of mixtures of DGEBA epoxy resin with spiranic Meldrum acid derivatives using lanthanide triflates as initiators.<sup>20,27</sup> We saw that the addition of these compounds to DGEBA accelerated the curing process and some kinetic differences were observed on changing the initiator.

By means of calorimetry the overall curing process for DGEBA/MA mixtures was studied. **Figure 5** shows the dynamic calorimetric curves for both initiators for 3:1 and 2:1 DGEBA/MA mixtures with three proportions of initiator. In general, MA formulations led to curves with a complex shape with a big exotherm accompanied by one or more little exo-

therms at lower temperature. With the highest proportion of  $\text{Yb}(\text{OTf})_3$ , the exotherm is split off but the maxima are too close to be deconvoluted. The apparition of these two

cess depicted in **Scheme 2** because, in the presence of epoxide, this lactone can react instantaneously to form the corresponding SOE.

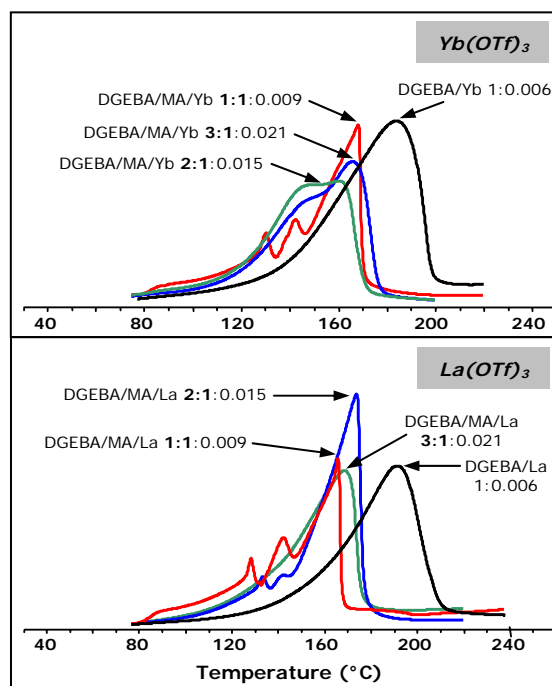


**Figure 5.** DSC curves of the curing of DGEBA and DGEBA/MA (mol/mol) mixtures in different molar ratios initiated by ytterbium and lanthanum triflates at a heating rate of 10°C/min

overlapped exotherms can be attributed to the competition between two propagation mechanisms related to the epoxide homopolymerization: AM (monomer activated) and ACE (activated chain end), which were previously observed in DGEBA/ $\gamma$ -butyrolactone mixtures at high proportions of initiator.<sup>26</sup> However, although we did not see the band at 1825  $\text{cm}^{-1}$ , we cannot discard a possible formation of the  $\beta$ -isovalerolactone through the pro-

We can see in the figure that the addition of MA advances the curing initiated by lanthanum and ytterbium triflates at lower temperatures. In general, we can also see that the curing with ytterbium triflate takes place at lower temperature than using lanthanum triflate. In previous studies with DGEBA/ $\gamma$ -lactone mixtures initiated by lanthanide triflates<sup>28</sup> we concluded that, in general, when Lewis acidity is increased, the initia-



tor becomes more active and the curing process accelerates.

**Tables 1 and 2** show calorimetric data and activation energies for the curing of pure DGEBA and its mixtures with MA and both initiators in different proportions. Total enthalpies per epoxy equivalent are similar and, with an only exception, all  $T_g$  values are higher than  $100^\circ\text{C}$ .  $T_g$ s slightly diminish when the proportion of MA increases or the proportion of initiator decreases. Ytterbium initiator leads to materials with a higher  $T_g$  indicating a higher degree of cross-linking.

The dependence of the apparent activation energy on the degree of conversion, calculated using the isoconversional method (Eq. 3)<sup>29</sup> is represented in **Figure 6** for DGEBA/MA 3:1 and 2:1 mixtures with 0.021 and 0.015 mol of each initiator respectively. The plots are practically horizontal for the curing in the range 20-80% of conversion, but with higher energy values for the ytterbium salt. The relative high values in the initial stage can be attributed to the formation of the initiating active species.

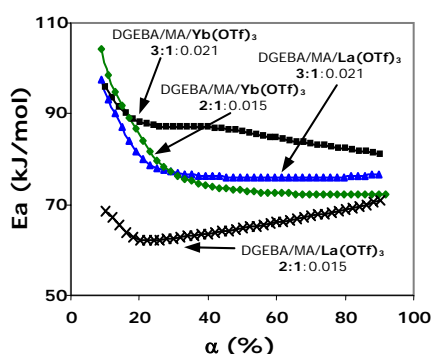


**Figure 6.** Dependence of  $E_a$  on the degree of conversion obtained by DSC of different mixtures DGEBA/MA (mol/mol) initiated by ytterbium and lanthanum triflates

As can be seen, in **Tables 1 and 2** the activation energies in mixtures initiated by ytterbium triflate are slightly higher. The activation energy values are not significant and do not clearly show the acceleration effect of the initiators due to the compensation effect between the activation energy and the pre-exponential factor.<sup>30</sup> However, the experimental conversion-temperature curves clearly show the order of reactivity observed (see **Figure 7**). This figure shows the accelerative effect of the addition of MA to the reactive mixture for ytterbium and lanthanum triflates. Although, in general, a higher Lewis acidity of the initiator accelerates the curing process, this behavior is not strictly accomplished for mixtures with MA and the reason could be found in the existence of acidic protons in the methylene carbon, which can act as co-initiator.

### 3.3. Shrinkage

**Table 3** shows the densities of the mixtures before and after curing and the calculated global shrinkage. We have added in this table the values of densities for pure DGEBA formulation to compare the effect of the addition of MA to the reactive mixture. On adding MA steadily increases the density, which could be attributed to the high dipolar moments in the cyclic MA structure, which originate great attractive forces between molecules. These dipolar moments decrease on the opening of the MA ring similarly to that described for cyclic carbonate polymerizations.<sup>31</sup> Thus, the addition of MA leads to a

reduction of shrinkage on curing, more important for ytterbium salt, attributable to the opening of a higher proportion of SOEs.

This reduction of the global shrinkage experimented in the DGEBA/MA curing further confirms the expandable character of the Meldrum acid structure.<sup>10,20</sup>

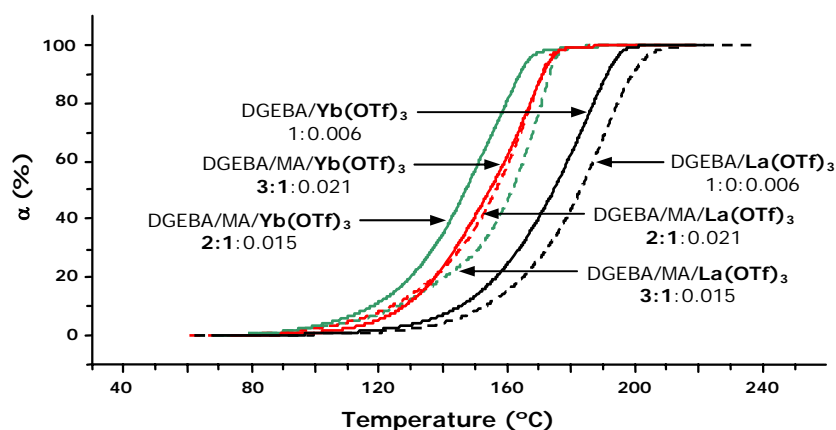


**Figure 7.** Conversion degree against temperature of the curing of DGEBA and DGEBA/MA (mol/mol) mixtures in different molar ratios initiated by Yb(OTf)<sub>3</sub> and La(OTf)<sub>3</sub> obtained through dynamic DSC experiments

**Table 3.** Densities and shrinkage of the systems studied initiated by different Lewis Acids

Entry	Formulation <sup>a</sup>	$\delta_{\text{initial mixture}}^b$ (g/cm <sup>3</sup> )	$\delta_{\text{final material}}^b$ (g/cm <sup>3</sup> )	Shrinkage (%)
1	DGEBA/Yb(OTf) <sub>3</sub> 1:0.006	1.158	1.192	2.9
2	DGEBA/MA/Yb(OTf) <sub>3</sub> 3:1:0.021	1.182	1.201	1.6
3	DGEBA/MA/Yb(OTf) <sub>3</sub> 2:1:0.015	1.183	1.198	1.3
4	DGEBA/La(OTf) <sub>3</sub> 1:0.006	1.158	1.193	3.0
5	DGEBA/MA/La(OTf) <sub>3</sub> 3:1:0.021	1.181	1.203	1.9
6	DGEBA/MA/La(OTf) <sub>3</sub> 2:1:0.015	1.184	1.202	1.5

<sup>a</sup> The compositions of the formulation is given in molar ratios

<sup>b</sup> Densities before and after curing process

It should be commented that the formation of SOEs, which takes place at the beginning of curing, occurs with shrinkage whereas its opening occurs with expansion at the end of the process and thus shrinkage in the gel state is much lower.

Previously<sup>9</sup> we demonstrated the improved adhesion to metal substrates on adding MA to DGEBA powder coatings, which was attributed to the lower shrinkage on curing, but no measurements of densities could be made because the microbubbles

in the cured material, as are usually formed in this type of coatings. The lower shrinkage on adding MA reported in the present paper confirms the hypothesis made to explain the improvement of the adhesion.

### 3.4. Thermogravimetric studies

In previous works,<sup>10,20</sup> we demonstrated the enhanced degradability of the thermosets obtained by copolymerization of DGEBA with Meldrum acid derivatives due to the formation of linear tertiary ester groups in the network. We could also observe that the temperatures at which the ruptures took place depended on the initiator and on the chemical structure of the thermoset. **Figure 8** shows the TGA and DTG curves for the degradation of the materials obtained from the formulation DGEBA/MA 2:1 (mol/mol) initiated with both Lewis acids in the three proportions studied.

DTG curves are unimodal but a little splitting is observed in case of materials obtained with the highest proportion of initiator. As we can see, on increasing the proportion of initiator the degradability increases confirming the influence of the initiator in the degradative process.<sup>11</sup> The thermogravimetric data are collected in **Tables 4 and 5**, where we can see that the materials obtained with  $\text{Yb}(\text{OTf})_3$  are more thermally degradable. This could be attributed to two different effects: a higher proportion of linear ester in the network and a greater catalytic activity of the ytterbium triflate on the degradation. The addition of MA to DGEBA samples and the proportion of initiator used mainly affect the initial steps of the degradative process, which is worth in order to increase the reworkability of electronic devices. The temperatures of the highest rate of degradation ( $T_{\text{max}}$ ), which is mainly

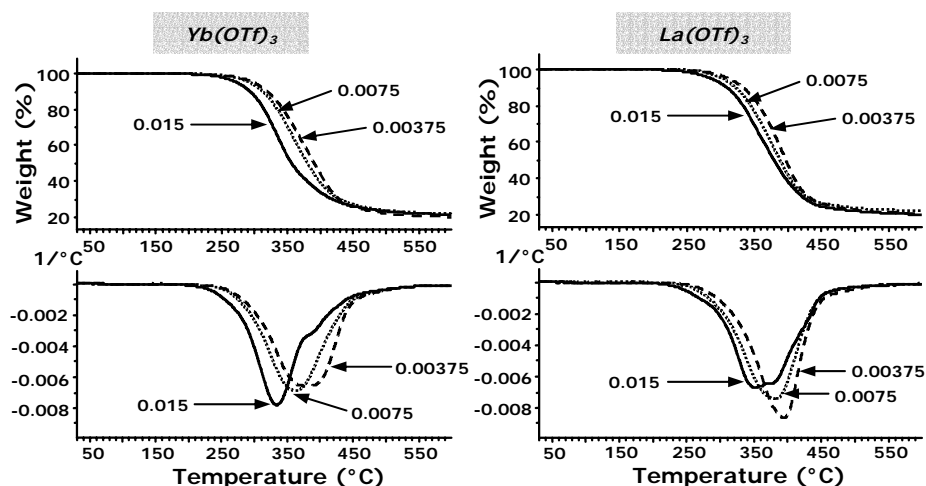


**Figure 8.** TG and DTG curves at 10°C/min in  $\text{N}_2$  atmosphere of several thermosetting materials obtained from DGEBA/MA 2:1 (mol/mol) formulation initiated by different proportions of ytterbium and lanthanum triflates

related to the rupture of ether linkages, are practically unaltered on changing the proportion of MA, but they increase on decreasing the amount of initiator. The lower shrinkage and the higher thermal

degradability which show these materials made it useful for coating applications when a re-workability of the coated material is desirable. Although mechanical properties has not been until yet

**Table 4.** Thermogravimetric data for the materials obtained with *Ytterbium Triflate*

Entry	Formulation <sup>a</sup>	T <sub>2%</sub> <sup>b</sup> (°C)	T <sub>max</sub> (°C)	% Char (T <sup>a</sup> =600°C)
1	DGEBA/Yb(OTf) <sub>3</sub> 1:0.006	287	345	20
2	DGEBA/Yb(OTf) <sub>3</sub> 1:0.003	294	391	20
3	DGEBA/Yb(OTf) <sub>3</sub> 1:0.0015	302	406	18
4	DGEBA/MA/Yb(OTf) <sub>3</sub> 3:1:0.021	246	343	21
5	DGEBA/MA/Yb(OTf) <sub>3</sub> 3:1:0.0105	268	364	21
6	DGEBA/MA/Yb(OTf) <sub>3</sub> 3:1:0.00525	277	377	20
7	DGEBA/MA/Yb(OTf) <sub>3</sub> 2:1:0.015	244	337	21
8	DGEBA/MA/Yb(OTf) <sub>3</sub> 2:1:0.0075	265	363	21
9	DGEBA/MA/Yb(OTf) <sub>3</sub> 2:1:0.00375	270	376	20
10	DGEBA/MA/Yb(OTf) <sub>3</sub> 1:1:0.009	243	335	22

<sup>a</sup> The composition of the formulations is given in molar ratios

<sup>b</sup> Temperature of a 2% of weight loss calculated by thermogravimetry

**Table 5.** Thermogravimetric data for the materials obtained with *Lanthanum Triflate*

Entry	Formulation <sup>a</sup>	T <sub>2%</sub> <sup>b</sup> (°C)	T <sub>max</sub> (°C)	% Char (T <sup>a</sup> =600°C)
1	DGEBA/La(OTf) <sub>3</sub> 1:0.006	303	354	19
2	DGEBA/La(OTf) <sub>3</sub> 1:0.003	308	385	19
3	DGEBA/La(OTf) <sub>3</sub> 1:0.0015	320	405	19
4	DGEBA/MA/La(OTf) <sub>3</sub> 3:1:0.021	272	353	20
5	DGEBA/MA/La(OTf) <sub>3</sub> 3:1:0.0105	279	383	20
6	DGEBA/MA/La(OTf) <sub>3</sub> 3:1:0.00525	287	396	20
7	DGEBA/MA/La(OTf) <sub>3</sub> 2:1:0.015	256	352	21
8	DGEBA/MA/La(OTf) <sub>3</sub> 2:1:0.0075	278	383	22
9	DGEBA/MA/La(OTf) <sub>3</sub> 2:1:0.00375	285	395	20
10	DGEBA/MA/La(OTf) <sub>3</sub> 1:1:0.009	253	350	21

<sup>a</sup> The composition of the formulations is given in molar ratios

<sup>b</sup> Temperature of a 2% of weight loss calculated by thermogravimetry

studied, powder coatings obtained following a similar procedure showed higher impact resistance and adherence to metallic substrates, than commercially available epoxy powder coatings.<sup>9</sup>

#### 4. CONCLUSIONS

The modification of DGEBA by copolymerization with MA using lanthanide triflates as initiators leads to poly(ether-ester) network structures. Ytterbium triflate leads to a higher proportion of linear ester groups. This proportion increases with the proportion of initiator.

The addition of MA to the DGEBA resins accelerates the curing process being the curing rate higher with the ytterbium salt.

On adding MA to the DGEBA the T<sub>g</sub> of the materials is reduced but on increasing the proportion of initiator this value increases. The use of ytterbium triflate as initiator leads to materials with higher T<sub>g</sub>s than the lanthanum salt.

The expandable character of MA has been demonstrated by the reduction of the global shrinkage on curing DGEBA/MA mixtures.

The thermal degradability of these materials increases in reference to pure DGEBA and the materials obtained with ytterbium triflate are more degradable. On increasing the amount of initiator the degradability also increases.

#### Acknowledgements

*The authors from the Universitat Politècnica de Catalunya would like to thank CICYT and FEDER (MAT2004-04165-C02-02) for their financial support. The authors from the Rovira i Virgili University would like to thank the CICYT (Comisión Interministerial de Ciencia y Tecnología) and FEDER (Fondo Europeo de Desarrollo Regional) (MAT2005-01806)*

#### 5. REFERENCES

1. Bailey WJ. *J Elastoplast* 1973; 5: 142-152.
2. Sadhir RK, Luck MR, Ed. *Expanding Monomers. Synthesis, Characterization and Applications*. Boca Raton: CRC Press, 1992.
3. Bodenbenner K. *Justus Liebigs Ann* 1959, 623, 183-191.
4. Fedtke M, Haufe J, Kahlert E, Müller G. *Angew Makromol Chem* 1998; 255: 53-59.
5. Flory PJ. *Principles of Polymer Chemistry*. Ithaca, NY: Cornell University Press, 1953. p. 347-398.
6. González S, Fernández-Francos X, Salla JM, Serra A, Mantecón A, Ramis X. *J Polym Sci Part A: Polym Chem* 2007; 45: 1968-1979.
7. Meldrum NA. *J Chem Soc* 1908; 93: 598-601.
8. Pihlaja K, Sello M. *Acta Chem Scand* 1968; 22: 3053-3062.
9. Garcia SJ, Serra A, Suay J. *J Polym Sci Part A: Polym Chem* 2007; 45: 2316-2327.
10. González L, Ramis X, Salla JM, Mantecón A, Serra A. *J Polym Sci Part A: Polym Chem* 2006; 44: 6969-6979.

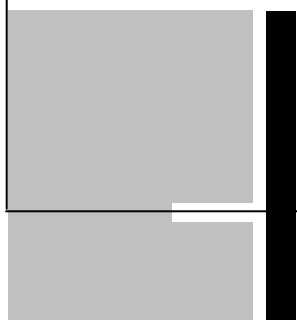
- 11.** González L, Ramis X, Salla JM, Mantecón A, Serra A. *Polym Degrad Stab* 2007; 92: 596-604.
- 12.** Chen JS, Ober CK, Poliks MD, Zhang Y, Wiesner U, Cohen C. *Polymer* 2004; 45: 1939-1950.
- 13.** Wang L, Li H, Wong CP. *J Polym Sci Part A: Polym Chem* 2000; 38: 3771-3782.
- 14.** Kobayashi S, Ed. *Lanthanides: Chemistry and Use in Organic Synthesis. Topics in Organometallic Chemistry*, Berlin: Springer Verlag, 1999.
- 15.** Mas C, Ramis X, Salla JM, Mantecón A, Serra A. *J Polym Sci Part A: Polym Chem* 2003; 41: 2794-2808.
- 16.** Arasa M, Ramis X, Salla JM, Mantecón A, Serra A. *J Polym Sci Part A: Polym Chem* 2007; 45: 2129-2141.
- 17.** Giménez R, Fernández-Francos X, Salla JM, Serra A, Mantecón A, Ramis X. *J Polym Sci Part A: Polym Chem* 2005; 46: 10637-10647.
- 18.** Coats AW, Redfern JP. *Nature* 1964; 201: 68-69.
- 19.** Kissinger HE. *Anal Chem* 1957; 29: 1702-1706.
- 20.** González L, Ramis X, Salla JM, Mantecón A, Serra A. *J Polym Sci Part A: Polym Chem* 2008; 46: 1229-1239.
- 21.** McNab H. *Chem Soc Rev* 1978; 7: 345-358.
- 23.** Pretsch E, Clerc T, Seibl J, Simon W. *Tablas para la Determinación Estructural por Métodos Espectroscópicos*, Springer Verlag Ibérica, Barcelona, 1998.
- 24.** Pons JM, Oblin M, Pommier A, Rajzmann M, Liotard D. *J Am Chem Soc* 1997; 119: 3333-3338.
- 25.** Gresham TL, Jansen JE, Shaver FW, Beears WL. *J Am Chem Soc* 1953; 76: 486-488.
- 26.** Salla JM, Fernández-Francos X, Ramis X, Mas C, Mantecón A, Serra A. *J Therm Anal Cal*, in press.
- 27.** González L, Ramis X, Salla JM, Mantecón A, Serra A. *Therm Chim Acta*, 2007, 464, 35-41.
- 28.** Mas C, Mantecón A, Serra A, Ramis X, Salla JM. *J Polym Sci Part A: Polym Chem* 2004; 42: 3782-3791.
- 29.** Vyazovkin S, Lenikovich A. *Thermochim Acta* 1992; 203: 177-185.
- 30.** Vyazovkin S, Linert W. *J Solid State Chem* 1995; 114: 392-398.
- 31.** Kricheldorf HR, Dunsing R, Serra A. *Makromol Chem* 1987; 188: 2453-2466.



### 3.3.



*REDUCTION OF THE SHRINKAGE OF THERMOSETS BY CATIONIC CURING OF MIXTURES OF DIGLYCIDYL ETHER OF BISPHENOL A AND 6,6-DIMETHYL-(5,7-DIOXASPIRO[2.5]OCTANE-4,8-DIONE)*



**REDUCTION OF THE SHRINKAGE OF THERMOSETS BY CATIONIC  
CURING OF MIXTURES OF DIGLYCIDYL ETHER OF BISPHENOL A AND  
6,6-DIMETHYL-(5,7-DIOXASPIRO[2.5]OCTANE-4,8-DIONE)**

Lidia González,<sup>1</sup> Xavier Ramis,<sup>2</sup> Josep Maria Salla,<sup>2</sup>  
Ana Mantecón,<sup>1</sup> Angels Serra<sup>1\*</sup>

<sup>1</sup>Departament de Química Analítica i Química Orgànica. Universitat Rovira i Virgili. Marcel·lí Domingo s/n, 43007 Tarragona, Spain

<sup>2</sup>Laboratori de Termodinàmica, Escola Tècnica Superior d'Enginyeria Industrial de Barcelona, Universitat Politècnica de Catalunya, Av. Diagonal 647, 08028 Barcelona, Spain

*Received 6 July 2006; accepted 5 September 2006*

*DOI: 10.1002/pola.21776*

---

**Abstract**

Ytterbium and lanthanum triflates were used as initiators to cure mixtures of diglycidyl ether of bisphenol A and 6,6-dimethyl-(5,7-dioxaspiro[2.5]octane-4,8-dione) in several proportions. The evolution of the epoxy and 6,6-dimethyl-(5,7-dioxaspiro[2.5]octane-4,8-dione) bands during curing and the linear ester groups in the final materials were evaluated with Fourier transform infrared in the attenuated-total-reflection mode. The use of a conventional cationic initiator, boron trifluoride monoethylamine, was also studied to test the advantages of lanthanide triflates. The shrinkage after curing and the thermal degradability of the materials with variations in the comonomer ratio and the initiator were evaluated and related to the chemical structure of the final network.



**Keywords:** cationic polymerization; copolymerization; crosslinking; epoxy resins; FT-IR; initiators; lactones; networks; thermosets

---

## 1. INTRODUCTION

Epoxy resins are among the most important thermosetting materials in the electronics industry because of their good characteristics. However, they have some disadvantages, such as the shrinkage produced during curing, their permanency in the environment when their service life is over, and their fragility, which should be reduced to improve their quality.

The shrinkage during curing can cause serious problems when they are used in coatings because it leads to the appearance of microvoids, microcracks, and internal stress, which reduce the adhesion of epoxy resins to the substrate and worsen the durability and mechanical properties of the coatings.<sup>1</sup> Thus, in the preparation of thermosets, the copolymerization of epoxy resins with monomers such as spiroorthoesters (SOEs), spiroorthocarbonates (SOCs),<sup>2,3</sup> and carbonates,<sup>4</sup> which expand on polymerizing, could be a good strategy to solve this problem. However, SOEs and SOC are not easy to synthesize; therefore, from an economic point of view, their use is not advisable.

Cyclic carbonates are expandable monomers<sup>4</sup> because in the polymerization process there is a change in the dipolar moments, which are higher for the cyclic carbonate and lower for the polymer. This change leads to a

decrease in the density of the material during polymerization and therefore to an expansion in the process. However, the copolymerization of epoxy resins and cyclic carbonates is usually accompanied by a loss of CO<sub>2</sub>, which results in a deterioration of some properties of the materials and an increase in the contraction on curing.<sup>5</sup>

Because SOEs can be prepared in situ from epoxy and lactones in the presence of a Lewis acid, in previous works we have studied the copolymerization of diglycidyl ether of bisphenol A (DGEBA) with several lactones.<sup>6-8</sup> From these studies, we can observe that the global shrinkage during curing is, in general, not lower, but the shrinkage after gelation is notably reduced; this is important because internal stresses appear in the material when there is no mobility in the network.

Among the polymerization methods, ring opening is the one that leads to the lowest shrinkage during curing because when a cyclic monomer opens, a covalent bond is converted into a Van der Waals distance, and this reduces the shrinkage produced in the formation of covalent bonds between monomer molecules.<sup>1</sup> This method has other advantages, such as the possibility of copolymerizing cyclic monomers with different functional groups and functionalities and the selection of the initiator and its proportion, which influences the ki-

netics and mechanism of the polymerization process.

In reference to the permanency in the environment of thermosets when their service life is over, one strategy is the introduction of more labile linkages into the structure. Carbonate and ester groups are thermally cleavable and therefore facilitate the reworking of the thermosets in which they are chemically incorporated.<sup>9-12</sup> Some authors<sup>11</sup> have incorporated tertiary ester groups into the network by polymerizing cycloaliphatic epoxy resins including these moieties in their structure. This method has the drawback that the epoxy monomers have to be synthesized previously and that cycloaliphatic epoxides are more difficult to crosslink than glycidyl ones. Thus, the copolymerization of DGEBA with monomers that introduce breakable groups into the structure could be advantageous for increasing the degradability of modified epoxy thermosets.

Because catalytic systems generally lead to a higher density of crosslinking and more fragile materials, another advantage of the copolymerization route is the improvement in the mechanical properties of epoxy resins. Thus, introducing flexible chains into the structure by copolymerization with a monocyclic lactone or carbonate is an adequate way of reducing the fragility of epoxy thermosets.

This study deals with the copolymerization of a commercially available monomer with two ester groups in its structure, 6,6-dimethyl-(5,7-dioxaspiro [2.5] octane-4,8-dione) (MCP; see Scheme 1),<sup>13</sup> and a DGEBA resin promoted by ytterbium or lanthanum triflates as

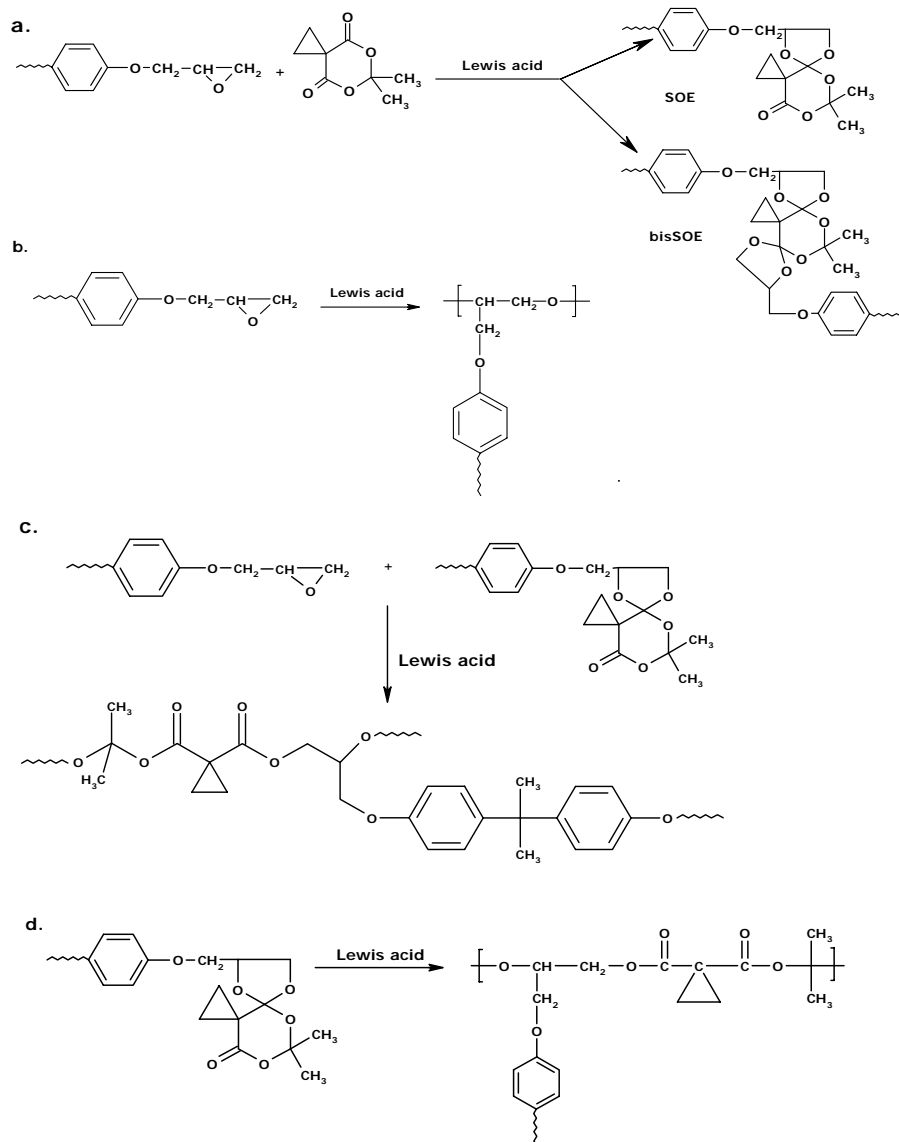
cationic initiators. The functionalities of MCP and DGEBA in this process are two and four, respectively and therefore this copolymerization leads to three-dimensional networks. MCP was selected because it has two tertiary ester groups in its structure, which facilitate the  $\beta$ -degradation process, and a relatively high dipolar moment, which can involve an expandable behavior. Lanthanide triflates were selected as initiators because they have been proved to be excellent Lewis acids, are commercially available, are stable in water, and are environmentally friendly catalysts<sup>14</sup> capable of copolymerizing epoxy resins with lactones<sup>6-8</sup> by a ring-opening mechanism through the formation of spirocyclic compounds. To prove the good capability of lanthanide triflates as initiators, we have conducted a parallel study using a conventional cationic initiator, boron trifluoride monoethylamine ( $\text{BF}_3 \cdot \text{MEA}$ ).

## 2. EXPERIMENTAL

### 2.1. Materials

DGEBA (Epikote Resin 827 from Shell Chemicals; epoxy equivalent = 182.08 g/equiv) was used as received. MCP (Aldrich) was used as received. Lanthanum (III) and ytterbium (III) trifluoromethane sulfonates and  $\text{BF}_3 \cdot \text{MEA}$  (Aldrich) were used without purification.

### 2.2. Preparation of the Curing Mixtures



Scheme 1

The samples were prepared by the mixing of the selected initiator in the corresponding proportion of DGEBA with manual stirring. The prepared mixtures were kept at  $-18^{\circ}\text{C}$  before use. Lanthanide triflates were added in a molar ratio of 0.006 mols per mol of DGEBA and 0.003 mols per mol of MCP.  $\text{BF}_3\cdot\text{MEA}$  was added in a molar ratio of 0.096 mols per mol of DGEBA and 0.048 mols per mol of MCP.

### 2.3. Characterization and Measurements

Calorimetric studies were carried out on a Mettler DSC821e thermal analyzer in covered Al pans under  $\text{N}_2$  at  $10^{\circ}\text{C}/\text{min}$ . The calorimeter was calibrated with an indium standard (heat flow calibration) and an indium–lead–zinc standard (temperature calibration). The samples weighed approximately 5 mg.

The glass transition temperatures ( $T_g$ 's) were calculated after complete curing, by means of a second scan, as the temperature of the half-way point of the jump in the heat capacity when the material changed from the glassy state to the rubbery state.

The isothermal curing process at  $150^{\circ}\text{C}$  was monitored with a Fourier transform infrared (FTIR) spectrophotometer (FTIR-680 Plus from Jasco) with a resolution of  $4\text{ cm}^{-1}$  in the absorbance mode. An attenuated total reflection (ATR) accessory with thermal control and a diamond crystal (a Golden Gate heated, single-reflection, diamond ATR accessory from Specac Teknokroma) was used to determine the

FTIR spectra. The conversions of the reactive groups were determined from the normalized changes in the absorbance by the Lambert-Beer law, as we explained previously.<sup>6</sup> After isothermal curing by means of FTIR, a dynamic scan by differential scanning calorimetry (DSC) was always carried out to prove that the curing was complete.

Thermogravimetric analyses (TGAs) were carried out with a Mettler TGA/SDTA 851e thermobalance. Cured samples with an approximate mass of 5 mg were degraded between 30 and  $600^{\circ}\text{C}$  at a heating rate of  $10^{\circ}\text{C}/\text{min}$  in  $\text{N}_2$  ( $200\text{ cm}^3/\text{min}$ ) under normal conditions.

The densities of the materials before and after curing were determined with a Microteritics AccuPyc 1330 gas pycnometer thermostated at  $30^{\circ}\text{C}$ .

## 3. RESULTS AND DISCUSSION

In previous works, we studied the curing of mixtures of a DGEBA epoxy resin with  $\gamma$ -butyrolactone ( $\gamma$ -BL) with lanthanide triflates as initiators in an attempt to obtain thermosets with breakable ester groups in the polymeric chain and low shrinkage during curing.<sup>6,15</sup> By FTIR spectroscopy, we could prove that the reaction of the epoxide and lactone took place through an intermediate SOE compound, which could homo or copolymerize with epoxides to form poly(ether-ester) structures. Similar systems with  $\text{BF}_3\cdot\text{MEA}$  and a lower proportion of lactone were previously reported by Matějka et

al.<sup>16</sup> The formation of SOE occurred with great shrinkage, but its polymerization led to expansion. This fact produced an increase in the global shrinkage on curing but a notable reduction of the contraction after gelation, which was related to the polymerization of SOEs in the last steps of the curing.<sup>6</sup> Moreover, the addition of a bifunctional monomer, such as  $\gamma$ -BL or MCP, to a tetrafunctional one (DGEBA) increases the conversion in the gelation on curing; therefore, the shrinkage after gelation is notably reduced.<sup>17</sup> This reduction is very convenient to minimize the appearance of stresses in the material because of the low mobility of the polymeric structure after this point.

For thermodynamic reasons,  $\gamma$ -BL could not homopolymerize, but there is no information about the polymerizability of MCP. To test if the homopolymerization of MCP would take place, we registered calorimetric curves of this compound with a small proportion of ytterbium or lanthanum triflates, and in any case, exothermic processes were detected, though only the melting endotherm of the pure compound. Moreover, we maintained at 150°C a mixture of this compound with the corresponding amount of an initiator for 2h, and we registered the FTIR spectrum before and after this time. According to a comparison of the spectra, no change was evident, and this indicated that this compound was not able to homopolymerize under these conditions.

**Scheme 1** shows the individual reactions expected in the global curing process of these mixtures. The first reaction **(a)** is the

formation of an intermediate SOE from epoxide and MCP. The presence of two ester groups in MCP could lead to the formation of the corresponding MCP transformed into bis(espiroorthoester) by reaction of both ester groups with epoxides (bisSOE) [this is represented in **Scheme 1**], but this process should be negligible because of the great steric hindrance. The second process **(b)** is the homopolymerization of DGEBA, which leads to poly(ether) chains; the third **(c)** is the copolymerization of DGEBA with the SOE intermediate, which produces poly(ether-ester) chains, and the fourth **(d)** is the homopolymerization of the SOE. Processes a and b lead to shrinkage, whereas c and d, in which SOE opens, should reduce the contraction or even expand.

ATR-FTIR experiments allowed us to observe the evolution of the reactive process when the composition of the mixture was varied. **Figure 1** shows the FTIR spectra of the 2:1 DGEBA /MCP formulation with ytterbium triflate as the initiator before and after curing at 150°C. In the spectrum of the uncured sample, there is a strong absorption at 1747 cm<sup>-1</sup> and a weak absorption at 1770 cm<sup>-1</sup> attributable to the stretching of the carbonyl groups of MCP, a medium band at 965 cm<sup>-1</sup> due to the deformation of the six-membered Meldrum ring, and a medium band at 912 cm<sup>-1</sup> due to the deformation of the oxirane ring.

The band at 965 cm<sup>-1</sup> was assigned on the basis of the calculations made with the program Gaussian 98.<sup>18</sup> In the spectrum of the cured sample, the 912 and 965 cm<sup>-1</sup> absorption completely

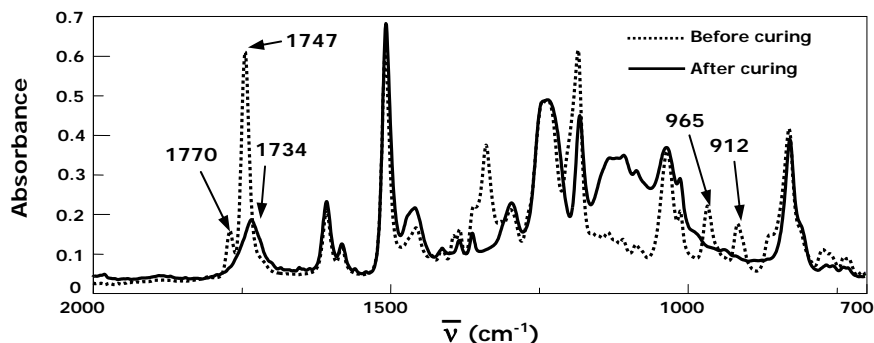


**Figure 1.** ATR-FTIR spectra of a mixture of DGEBA/MCP 2:1 (mol/mol) with 0.015 mol of  $\text{Yb}(\text{OTf})_3$  before and after curing at 150°C

disappear, and this indicates that epoxide and MCP are incorporated into the network.

The disappearance of the band at  $965\text{ cm}^{-1}$  should indicate that MCP has reacted with epoxide to form the corresponding SOE, which on opening leads to an absorption at  $1734\text{ cm}^{-1}$  due to the linear carbonyl ester group. Because of the partial overlapping of cyclic and linear carbonyl ester absorptions, a quantification of the evolution of linear ester formation during curing, such as those we made in other studies, was not possible.<sup>6,8</sup>

**Figures 2 and 3** show the evolution of the normalized intensity of the 912 and  $965\text{ cm}^{-1}$  infrared bands versus time, respectively, and allow us to compare the incorporation of epoxide and MCP into the material when we used the ytterbium and lanthanum triflates and the boron trifluoride complex as initiators.

As we can see in **Figure 2**, ytterbium triflate leads to the fastest epoxide reaction in a short time (ca. 2000s) until the conversion reaches a value of 0.95, but

the boron complex leads to running out at a shorter time than the others. Thus, to reach the complete consumption of epoxide, the ytterbium salt needs 6280s, the lanthanum salt needs 7370s, and the boron complex needs 4900s at 150°C. However, not as big differences can be observed in **Figure 3** in the evolution of the MCP infrared band at shorter times for the three different initiators, although the total consumption of MCP is reached first with the boron complex. The times needed to run out MCP are 5500, 10780, and 11870 s for  $\text{BF}_3\cdot\text{MEA}$ ,  $\text{Yb}(\text{OTf})_3$  and  $\text{La}(\text{OTf})_3$ , respectively. As we can see, with  $\text{BF}_3\cdot\text{MEA}$  as the initiator, MCP and epoxide react completely at the same time, but lanthanide triflates lead to the consumption of epoxide before the disappearance of MCP. Thus, some reaction of MCP occurs during the final stages of the curing, probably with the SOEs formed, which are present until the last steps of the curing.

**Table 1** shows the comparative incorporation of linear ester groups in the network.

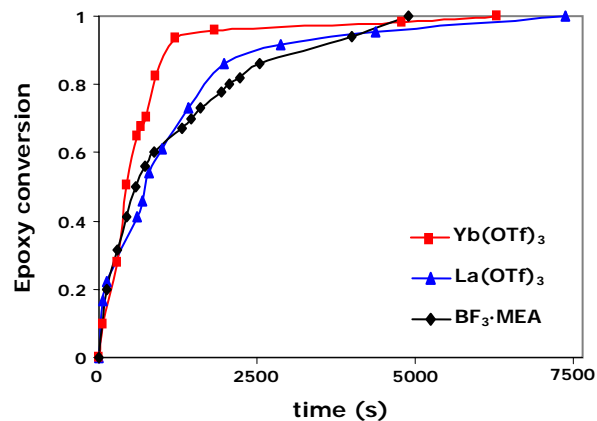


**Figure 2.** Epoxy conversion degree (912 cm<sup>-1</sup>) versus time for the DGEBA/MCP 2:1 (mol/mol) formulation with different initiators during curing at 150°C by ATR-FTIR

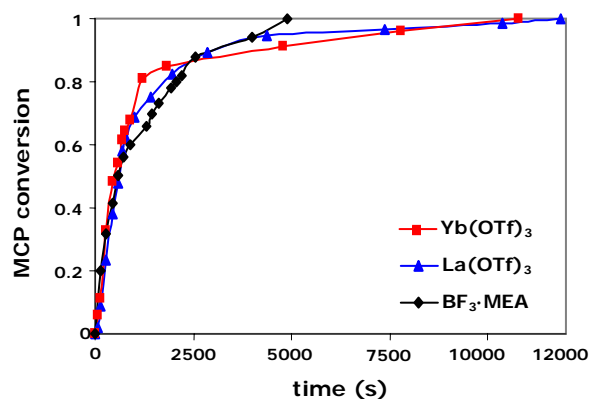


**Figure 3.** MCP conversion degree (965 cm<sup>-1</sup>) versus time for the DGEBA/MCP 2:1 (mol/mol) formulation with different initiators during curing at 150°C by ATR-FTIR

To do this comparison, the absorptions at 1734 cm<sup>-1</sup> were normalized to the reference band at 1605 cm<sup>-1</sup>, and then a value of 1 was given to the material with a greater band at 1734 cm<sup>-1</sup> independently of the composition of the initial mixture. The other linear ester absorptions (after normalization to the band at 1605 cm<sup>-1</sup>)

were normalized to this. Thus, the value of 1 was given to entry 4, in which a mixture with a 1:1 molar ratio of DGEBA/MCP with ytterbium triflate was crosslinked.

As can be seen, the maximum incorporation was achieved when ytterbium triflate was used as the initiator for all the proportions studied, and the lowest was achieved

**Table 1.** Calorimetric and thermogravimetric data, densities and shrinkage of all the systems studied

Entry	Formulation <sup>a</sup>	Linear Ester <sup>b</sup>	T <sub>g</sub> <sup>c</sup> (°C)	ΔH <sup>d</sup> (J/g)	ΔH <sup>e</sup> (kJ/ee)	δ <sub>im</sub> (g/cm <sup>3</sup> )	δ <sub>fm</sub> (g/cm <sup>3</sup> )	Shrinkage (%)	T <sup>f</sup> (°C)	T <sub>max</sub> <sup>g</sup> (°C)
1	DGEBA/Yb(OTf) <sub>3</sub> 1:0.006	0	135	519.7	95.6	1.158	1.192	2.9	287	345
2	DGEBA/MCP/Yb 3:1:0.021	0.46	117	430.3	91.5	1.174	1.194	1.7	241	335
3	DGEBA/MCP/Yb 2:1:0.015	0.83	110	388.0	88.2	1.176	1.193	1.5	230	332
4	DGEBA/MCP/Yb 1:1:0.009	1	105	314.4	84.4	-	-	-	214	319
5	DGEBA/La(OTf) <sub>3</sub> 1:0.006	0	127	513.5	94.4	1.158	1.193	3.0	303	354
6	DGEBA/MCP/La 3:1:0.021	0.44	105	418.6	89.1	1.173	1.202	2.5	250	350
7	DGEBA/MCP/La 2:1:0.015	0.62	100	386.8	87.7	1.175	1.200	2.1	233	348
8	DGEBA/MCP/La 1:1:0.009	0.72	95	307.4	83.4	-	-	-	216	344
9	DGEBA/BF <sub>3</sub> ·MEA 1:0.096	0	160	460.0	86.6	1.155	1.191	3.1	332	360-433
10	DGEBA/MCP/BF <sub>3</sub> 3:1:0.336	0.30	156	391.0	84.5	1.165	1.199	2.9	296	333-429
11	DGEBA/MCP/BF <sub>3</sub> 2:1:0.240	0.40	147	337.1	78.0	1.166	1.198	2.7	288	330-425

<sup>a</sup> The composition of the formulations is given in molar ratios

<sup>b</sup> Proportion of linear ester in the network calculated from FTIR experiments

<sup>c</sup> Obtained by DSC in the second scan after dynamic curing

<sup>d</sup> Enthalpy per gram of mixture

<sup>e</sup> Enthalpy per equivalent of epoxy groups

<sup>f</sup> Temperature of a 2 % of weight loss calculated by thermogravimetry

<sup>g</sup> Temperature of the maximum degradation rate calculated by thermogravimetry

δ = Density

for the materials crosslinked with BF<sub>3</sub>·MEA. This comparison is put into evidence in **Figure 4**, which shows the FTIR spectra of the cured materials obtained from a DGEBA/MCP (2:1 mol/mol) formulation with all the initiators studied. FTIR showed that the initial MCP disappeared completely in all the cured samples. Thus, the lower the band was at 1734 cm<sup>-1</sup>, the higher the amount was of unreacted SOE that did not polymerize, particu-

larly when the boron complex was used as the initiator. In the figure, we can see that the absorption at 1034 cm<sup>-1</sup> is higher, whereas the broad band at about 1110 cm<sup>-1</sup> is lower, for this material.

Bodenbenner<sup>19</sup> assigned the band at nearly 1034 cm<sup>-1</sup> to the SOE group, and the broad band at 1110 cm<sup>-1</sup> is due to the polyether structure. From the relative intensity of these bands, we can confirm that the material ob-



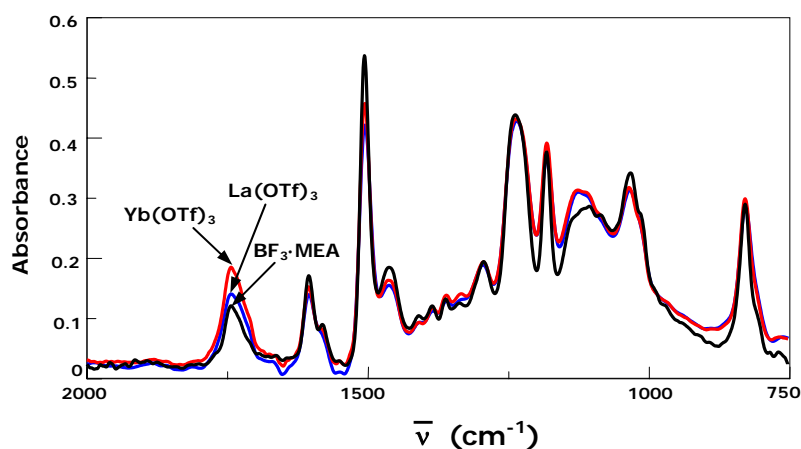


**Figure 4.** ATR-FTIR spectra of different materials obtained after curing at 150°C from DGEBA/MCP 2:1 (mol/mol) mixtures with 0.015 mol of lanthanide triflates and 0.240 mol of  $\text{BF}_3\cdot\text{MEA}$

tained with  $\text{BF}_3\cdot\text{MEA}$  as the initiator has a higher proportion of unreacted SOE. From our previous experience, we know that  $\text{BF}_3\cdot\text{MEA}$  favors the homopolymerization of epoxides over their copolymerization with lactones. Moreover, from previous results, we have put into evidence that SOEs more easily copolymerize with epoxides than homopolymerize.<sup>6</sup> Therefore, if the homopolymerization of epoxides is favored, SOE cannot copolymerize, and because its homopolymerization is hindered, it remains unreacted in the final material.

In the same table, the  $T_g$  values of the cured materials are also collected because of their meaning in industrial applications. The addition of an increasing proportion of MCP leads to a slight diminution of this parameter because of the higher flexibility of the network and the greater distances between crosslinks. Previously reported systems<sup>5,6,8</sup> obtained by the copolymerization of DGEBA and cyclic aliphatic structures led to a

higher diminution of  $T_g$ , but the presence of a cyclopropenylic group and the tertiary ester groups in MCP mixtures reduce the mobility of the moiety introduced, leading to a less flexible network. The materials with higher  $T_g$ 's were those obtained with the boron complex, possibly because of the greater proportion of rigid SOE that remained unreacted. The differences between the materials obtained with ytterbium and lanthanum triflates are less significant, but the ytterbium salt leads to higher values. The lower values of the  $T_g$ 's of the materials obtained with the lanthanide salts in comparison with those obtained with the boron complex could be due to the formation of macrocyclic structures in the former by backbiting processes favored by the template effect of the lanthanides.<sup>20</sup> The macrocycles cannot be detected by spectroscopic procedures but could change the calorimetric characteristics, acting as plasticizers. A similar trend of  $T_g$

values was obtained in the copolymerization of DGEBA with propylene carbonate with these initiators.<sup>21</sup>

If we look at the enthalpies that evolve during the curing process, we can observe that with the addition of MCP to the mixture, the reaction enthalpy diminishes. However, if the enthalpy is related to the epoxy equivalents in the reaction mixture, we can observe only a slight diminution. This means that the curing degree should be comparable. Although the evolved enthalpies are similar for the different initiators studied, there are differences in the  $T_g$ 's of the materials obtained with the boron trifluoride complex, which are much higher than the  $T_g$ 's of those obtained with the lanthanide triflates. By FTIR, we have seen that the proportion of linear ester group is lower for  $BF_3 \cdot MEA$  initiated thermosets. The presence of rigid and bulky, unreacted SOE groups, besides the absence of macrocycles, could justify the higher  $T_g$ 's observed.

In the same table, the densities of the mixtures before and after curing and the calculated global shrinkage are shown. As we can see, the addition of MCP leads to a reduction of the shrinkage, probably because of a change in the dipolar moment when MCP opens to linear ester chains; this is similar to an observation for the polymerization of cyclic carbonates.<sup>1</sup> Again, ytterbium triflate reduces to the greatest extent the contraction upon the addition of MCP to DGEBA, and this can be attributed to the expansion produced in the opening of the intermediate SOEs. This is more im-

portant for this initiator, as reflected in the higher absorption of linear ester groups. This expansion partially compensates the contraction produced on curing. Moreover, the opening of SOE groups occurs in the final stages of the curing process; therefore, the higher the polymerization is of SOE groups, the lower the contraction should be after gelation. From the shrinkage results, it seems that MCP could be considered a new expandable monomer.

To evaluate the degradability of the materials synthesized, we performed TGA measurements. **Figure 5** shows as an example the differential thermogravimetry (DTG) curves for the materials cured with lanthanum triflate as the initiator.

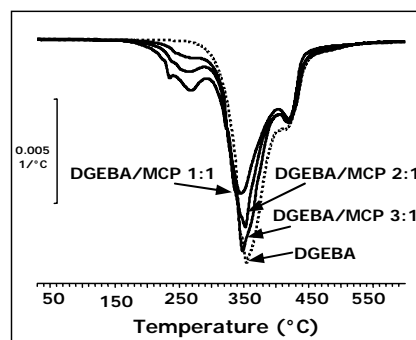


**Figure 5.** DTG curves at 10°C/min in a  $N_2$  atmosphere of several thermosetting materials obtained from DGEBA and DGEBA/MCP (mol/mol) mixtures initiated by  $La(OTf)_3$

The addition of MCP leads to the appearance of a new degradation step at a lower temperature, which increases as the proportion of MCP increases. Thus, it should be related to the ester

group rupture produced by a thermal  $\beta$ -elimination process.<sup>22</sup>

Therefore, the progressive addition of MCP to DGEBA increases the thermal degradability of the epoxy thermosets. The influence of the initiator on the degradability can be observed in **Figure 6**, which shows that the materials obtained with lanthanide salts are significantly more degradable. Thus, materials obtained with both lanthanum and ytterbium salts begin their degradation at lower temperatures and this can be attributed to the presence of a higher proportion of ester linkages in the network. However, from the temperatures of 2% weight loss and of the maximum degradation rate of pure DGEBA with the different initiators (see **Table 1**, entries 1, 5, and 9), it can be observed that lanthanide triflates lead to greater degradability, which can be attributed to participation of the lanthanide triflates in the degradation process acting as catalysts.  $\text{BF}_3 \cdot \text{MEA}$  leads to more stable materials, with two maxima of the degradation rate at about 330 and 430°C, the latter being the more important.

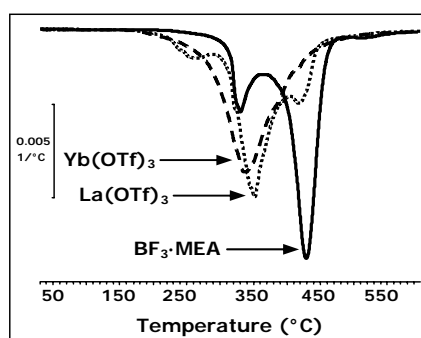


**Figure 6.** DTG curves at 10°C/min in an atmosphere of  $\text{N}_2$  of several thermosetting materials obtained from DGEBA/MCP formulation 2:1 (mol/mol) initiated by different Lewis acids

Journal of Polymer Science: Part A: Polymer Chemistry, Vol. 44, 6869-6879 (2006)

In **Table 1**, the 2% weight loss and the temperature of the maximum decomposition rate are collected for all the materials. As we can see, the incorporation of MCP into the curing mixtures led to a reduction in these parameters with all the initiators tested, and this confirms that the materials are more thermally degradable. Mechanical and thermomechanical characteristics will be reported in a forthcoming publication.

#### 4. CONCLUSIONS

The modification of DGEBA by its copolymerization with MCP initiated by lanthanide triflates and  $\text{BF}_3 \cdot \text{MEA}$  incorporated tertiary linear ester moieties into the chemical structure of the network, although some proportion of SOE remained unreacted in the material. The proportion of linear ester depended on the initiator used and was higher for lanthanide triflates. The addition of MCP slightly reduced the  $T_g$  values of the materials, which were higher when we used  $\text{BF}_3 \cdot \text{MEA}$  as the initiator.

The addition of MCP to the DGEBA resins reduced the global shrinkage on curing; therefore, MCP could be used as expandable monomer in this type of copolymerization.

The incorporation of MCP into DGEBA epoxy resins increased the thermal degradability of the final materials, especially in those obtained with lanthanide triflates as initiators.

### Acknowledgements

The authors thank Dr. Josep Manel Ricart for the calculations made with the program Gaussian 98. The authors from Rovira i Virgili University thank the Comisión Interministerial de Ciencia y Tecnología and Fondo Europeo de Desarrollo Regional (MAT2005-01806). The authors from Universitat Politècnica de Catalunya also thank the Comisión Interministerial de Ciencia y Tecnología and Fondo Europeo de Desarrollo Regional (MAT2004-04165-C02-02) for their financial support.

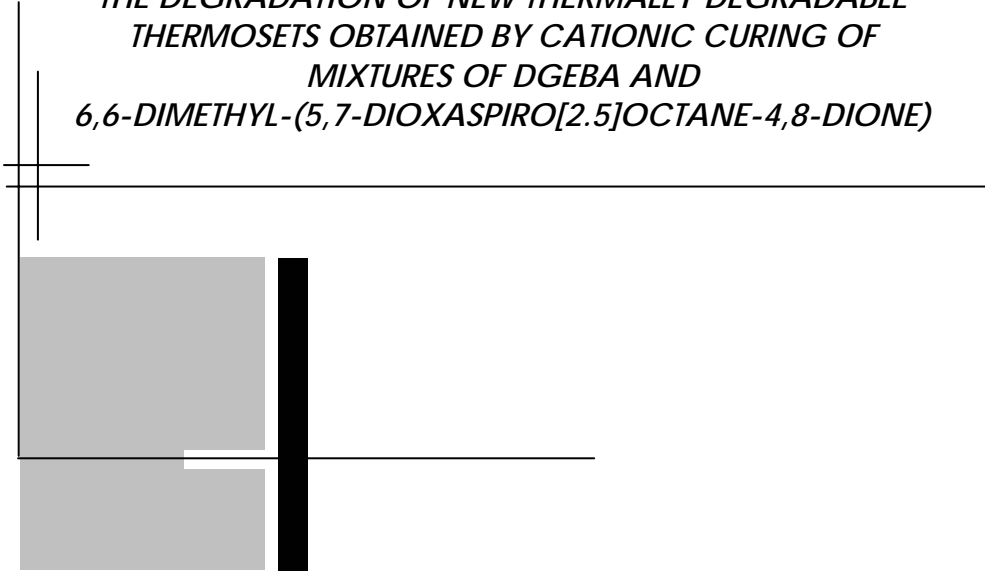
### 5. REFERENCES

1. Expanding Monomers: Synthesis, Characterization and Applications; Sathir, R. K.; Luck, M. R., Eds.; CRC: Boca Raton, FL, 1992.
2. Bailey, W. J.; Sun, R. L. Polym Prepr (Am Chem Soc Div Polym Chem) 1972, 13, 281.
3. Takata, T.; Endo, T. Prog Polym Sci 1993, 18, 839–870.
4. Rokicki, G. Prog Polym Sci 2000, 25, 259–342.
5. Cervellera, R.; Ramis, X.; Salla, J. M.; Mantecón, A.; Serra, A. J Polym Sci Part A: Polym Chem 2005, 43, 5799–5813.
6. Mas, C.; Ramis, X.; Salla, J. M.; Mantecón, A.; Serra, A. J Polym Sci Part A: Polym Chem 2003, 41, 2794–2808.
7. Giménez, R.; Fernández-Francos, X.; Salla, J. M.; Serra, A.; Mantecón, A.; Ramis, X. J Polym Sci Part A: Polym Chem 2005, 46, 10637–10647.
8. Mas, C.; Ramis, X.; Salla, J. M.; Mantecón, A.; Serra, A. J Polym Sci Part A: Polym Chem 2006, 44, 1711–1721.
9. Wang, L.; Li, H.; Wong, C. P. J Polym Sci Part A: Polym Chem 2000, 38, 3771–3782.
10. Li, H.; Wong, C. P. IEEE Trans Adv Packaging 2004, 27, 165–172.
11. Chen, J.-S.; Ober, C. K.; Poliks, M. D.; Zhang, Y.; Wiesner, U.; Cohen, C. Polymer 2004, 45, 1939–1950.
12. Ogino, K.; Chen, J.-S.; Ober, C. K. Chem Mater 1998, 10, 1475–1482.
13. Singh, R. K.; Danishefsky, S. J Org Chem 1975, 40, 2969–2970.
14. Lanthanides: Chemistry and Use in Organic Synthesis; Kobayashi, S., Ed.; Topics in Organometallic Chemistry; SpringerVerlag: Berlin, 1999.
15. Mas, C.; Mantecón, A.; Serra, A.; Ramis, X.; Salla, J. M. J Polym Sci Part A: Polym Chem 2004, 42, 3782–3791.
16. Matějka, L.; Chabanne, P.; Tighzert, L.; Pascault, J. P. J Polym Sci Part A: Polym Chem 1994, 32, 1447–1458.
17. Flory, P. J. Principles of Polymer Chemistry; Cornell University Press: Ithaca, NY, 1953.
18. Lee, I.; Han, I. S.; Kim, C. K.; Lee, H. W. Bull Korean Chem Soc 2003, 24, 1141–1149.
19. Bodenbenner, K. Justus Liebigs Ann 1959, 625, 183–191.
20. Aspinall, H. C.; Dwyer, J. L. M.; Greeves, N.; McIver, E. G.; Wooley, J. C. Organometallics 1998, 17, 1884–1888.
21. Cervellera, R.; Ramis, X.; Salla, J. M.; Mantecón, A.; Serra, A. J Appl Polym Sci 2006, 102, 2086–2093.
22. Chen, J.-S.; Ober, C.; Poliks, M. D. Polymer 2002, 43, 131–139.



## 3.4.

*THE DEGRADATION OF NEW THERMALLY DEGRADABLE  
THERMOSETS OBTAINED BY CATIONIC CURING OF  
MIXTURES OF DGEBA AND  
6,6-DIMETHYL-(5,7-DIOXASPIRO[2.5]OCTANE-4,8-DIONE)*



THE DEGRADATION OF NEW THERMALLY DEGRADABLE THERMOSETS  
OBTAINED BY CATIONIC CURING OF MIXTURES OF DGEBA AND  
6,6-DIMETHYL-(5,7-DIOXASPIRO[2.5]OCTANE-4,8-DIONE)

Lidia González,<sup>1</sup> Xavier Ramis,<sup>2</sup> Josep Maria Salla,<sup>2</sup>  
Ana Mantecón,<sup>1\*</sup> Angels Serra<sup>1</sup>

<sup>1</sup>Departament de Química Analítica i Química Orgànica. Universitat Rovira i Virgili. Marcel·lí Domingo s/n, 43007 Tarragona, Spain

<sup>2</sup>Laboratori de Termodinàmica, ETSEIB. Universitat Politècnica de Catalunya, Av. Diagonal 647, 08028 Barcelona, Spain

*Received 7 September 2006; received in revised form 14 December 2006; accepted 1 January 2007*

*DOI: 10.1016/j.polymdegradstab.2007.01.07*

---

**Abstract**

The thermal degradation of thermosetting materials prepared by cationic copolymerization of mixtures of different proportions of diglicidylether of bisphenol A (DGEBA) with 6,6-dimethyl(5,7-dioxaspiro[2.5]octane-4,8-dione) (MCP) initiated by ytterbium or lanthanum triflate or using a conventional initiator, BF<sub>3</sub>·MEA was investigated. To study the thermal degradation, several techniques were used such as thermogravimetry (TGA), infrared spectroscopy (FTIR) and calorimetry (DSC) and the volatiles evolved during degradation were identified by mass spectrometry. The materials prepared possess the characteristics of thermally degradable thermosets, due to the presence of ester groups in the polymer chain, which are broken at the beginning of degradation. The degradability increased when lanthanide triflates were used in the curing, especially the ytterbium salt and when the proportion of MCP in the material increased.

**Keywords:** Epoxy resins; Degradation; Thermosets; Cationic polymerizations; Reworkability

---

## 1. INTRODUCTION

The widespread use of epoxy materials in technological applications is due to their excellent adhesive and thermomechanical properties, as well as their easy processing. Once cured these resins form highly crosslinked networks with a high thermal stability, which can be a disadvantage from an ecological point of view. For example, microelectronic applications need degradable thermosets, because if a component of an electronic device is defective the entire circuit board must be thrown away. Because the electronic device can be reused, some authors<sup>1</sup> applied the term "reworkable" to the epoxy thermoset. However, this term does not mean that the polymeric material can be reused or recycled. The concept of reworkable thermoset can be defined as the ability to breakdown under controlled conditions in order to remove it from the substrate. The application of these degradation conditions to these materials diminishes the crosslinking density and therefore their mechanical properties under controlled circumstances. Rework enables the straight forward repair, replacement or recycling of electronic devices assembled with such materials. These thermosets have applications as underfills, which fill the gap between an integrated circuit chip and the substrate and encap-

sulate the solder interconnects. These products are adhesives, which reduce the strain in the solder joints by transferring some of the strain energy into the underfill layer. The underfill provides enhancement of solder fatigue life and also corrosion protection to the integrated circuit chip, resulting in 10- to 100-fold improvement in fatigue life as compared to an unencapsulated package.<sup>2</sup>

Several authors designed new molecular structures, which on curing introduce breakable groups into the three-dimensional network. Thus, Sastri and Tesoro<sup>3</sup> introduced cleavable disulfide linkages; Buchwalter and Kosbar<sup>4</sup> put hydrolysable ketal groups; Malik et al.<sup>5</sup> incorporated sterically hindered urea linkages; Shirai and co-workers<sup>6</sup> sulfonate ester moieties and recently Liu and Hsieh<sup>7</sup> formed thermally reversible bicyclic structures from a Diels-Alder reaction between maleimide and furan functionalized polymers. However, the most extended and easiest approach to prepare reworkable epoxy thermosets introduces thermally labile secondary and tertiary ester groups. Among the research groups that follow this route should be considered the work reported by Ober<sup>8,1</sup> Shirai<sup>9,10</sup> and Wong.<sup>11,12</sup>

Most of the work done in the field of thermally reworkable epoxy thermosets is based on cycloaliphatic structures which con-

tain ester groups. Cycloaliphatic epoxides should be cross-linked with anhydrides or catalytic systems because they do not react with nucleophilic agents such as amines. Moreover, they usually lead to high crosslinking densities, which reduce their mechanical characteristics. Thus, these reworkable systems lack of versatility and the mechanical properties should be improved for several applications.

In previous papers we reported a new route of introducing ester or carbonate groups in thermosetting materials by copolymerizing commercial epoxy resins with lactones<sup>13-15</sup> and cyclic carbonates<sup>16,17</sup> by a ring-opening mechanism. This strategy presents some advantages, such as the possible modulation of the properties of the final materials by changing the characteristics of the epoxy resin and the comonomer and their feed ratio. Moreover, the type of initiator used can also change the characteristics of the final materials. Following this route we could introduce thermally breakable groups into the network, to reduce the shrinkage on curing and therefore the internal stress generated by the shrinkage. We could also delay the gelation point until greater conversions, which reduces the shrinkage after gelation. In this way the mechanical properties could be increased.

In the present work we report a thermal degradation study of a series of new materials obtained by cationic copolymerization of DGEBA epoxy resin with 6,6-dimethyl (5,7-dioxaspiro[2.5]octane-4,8-dione) (MCP) initiated by ytterbium or lanthanum triflates or

using a conventional catalyst,  $\text{BF}_3 \cdot \text{MEA}$ . In previous work<sup>18</sup> we studied this curing and could prove that the global shrinkage on curing decreases on adding MCP to the epoxy resin and that the proportion of ester groups in the material depends on the feed ratio of comonomers and the initiator used. The aim of this work is to understand the thermal degradation chemistry, the kinetics, and their influence on the reworkability of the proposed materials.

## 2. EXPERIMENTAL

### 2.1. Materials

Diglycidylether of bisphenol A (DGEBA) EPIKOTE RESIN 827 from Shell Chemicals (epoxy equiv. = 182.08 g/eq) was used as received.

6,6-Dimethyl-(5,7-dioxaspiro[2.5]octane-4,8-dione) (MCP) (Aldrich) was used as received.

Lanthanum (III) and ytterbium (III) trifluoromethanesulfonates and borontrifluoride monoethylamine ( $\text{BF}_3 \cdot \text{MEA}$ ) (Aldrich) were used without purification.

### 2.2. Preparation of the materials

The samples were prepared by mixing the selected initiator in the corresponding amount of MCP and adding the required proportion of DGEBA with manual stirring. The prepared mixtures were kept at  $-18^\circ\text{C}$  before use. The mixture was crosslinked by pouring it into a silanized glass mould and then cured in an oven at  $140^\circ\text{C}$  for 3 h, followed by post-curing at



160°C for 2h (at 170°C for BF<sub>3</sub>·MEA). The samples were then allowed to cool at room temperature. It was confirmed by DSC that they were completely cured.

### 2.3. Characterization and measurements

Calorimetric studies were carried out on a Mettler DSC-821e thermal analyzer in covered Al pans under N<sub>2</sub> at 10 °C/min. The calorimeter was calibrated using an indium standard (heat flow calibration) and an indium-lead-zinc standard (temperature calibration). The samples weighed approximately 7 mg.

The glass transition temperatures (T<sub>gs</sub>) of the cured and semi-degraded materials were calculated as the temperature of the half-way point of the jump in heat capacity when the material changed from the glassy to rubbery state.

The FTIR spectra were recorded with a Jasco FTIR-680PLUS spectrophotometer with a resolution of 4 cm<sup>-1</sup> in the absorbance mode, equipped with an attenuated-total-reflection accessory with thermal control and a diamond crystal (golden gate heated single-reflection diamond ATR, Specace Teknokroma). The conversions of the reactive groups were determined from the normalized changes in absorbance by the Lambert-Beer law, as we explained previously.<sup>13</sup>

Thermogravimetric analyses (TGAs) were carried out with a Mettler TGA/SDTA 851e thermobalance. Cured samples with an approximate mass of 7 mg were

degraded between 30 and 600°C at a heating rate of 10°C/min in N<sub>2</sub> (100 ml/min) measured under normal conditions. Non-isothermal thermogravimetric tests were carried out at rates of 2, 5, 10 and 20°C/min to evaluate the kinetic parameters. Isothermal studies at selected temperatures were also carried out.

The degradation of the materials was performed in nitrogen atmosphere in a Carbolite tubular oven at 200 and then at 250°C and at selected times several fractions of volatile matter evolved were trapped in a flask refrigerated by liquid nitrogen. The fractions collected were diluted in acetonitrile and then studied by gas chromatography (Hewlett-Packard 5890 equipped with a capillary column Ultra 2) coupled to a Hewlett-Packard 5989<sup>a</sup> quadrupole detector equipped with a double source ionization by electronic impact and chemical ionization to identify the structures formed. The residues produced maintaining the materials in an oven at 200 and 225°C temperatures at different times were investigated by FTIR-ATR spectra and T<sub>gs</sub> were determined in order to follow the degradation of the materials by these procedures.

### 2.4. Kinetic analysis

Integral non-isothermal kinetic analysis was used to determine the kinetic triplet (A pre-exponential factor, E activation energy and g(α) integral function of degree of conversion).

The degree of conversion as the mass loss is defined as:

$$\alpha = \frac{m_0 - m}{m_0 - m_\infty} \quad (1)$$

where  $m$  is the mass corresponding to temperature  $T$ ,  $m_0$  is the initial mass and  $m_\infty$  is the mass of the substance at the end of the experiment.

If we accept that the dependence of the rate constant on the temperature follows the Arrhenius equation, non-isothermal kinetic analysis may start with the kinetic equation:

$$\frac{d\alpha}{dt} = \beta \frac{d\alpha}{dT} = \left(-\frac{E}{RT}\right) f(\alpha) \quad (2)$$

where  $\beta$  is the heating rate,  $d\alpha/dt$  is the rate of conversion,  $R$  is the universal gas constant,  $T$  is the temperature and  $f(\alpha)$  is the differential conversion function. By using the Coats-Redfern<sup>19</sup> approximation to resolve the so-called temperature integral and considering that  $2RT/E \ll 1$  the Kissinger-Akahira-Sunose equation (KAS) may be written as:

$$\ln \frac{\beta}{T^2} = \ln \left[ \frac{AR}{g(\alpha)E} \right] - \frac{E}{RT} \quad (3)$$

For each conversion degree, the linear representation of  $\ln [\beta/T^2]$  versus  $T^{-1}$  enables  $E$  and  $\ln [AR/g(\alpha)E]$  to be determined from the slope and the ordinate in the origin. If the reaction model,  $g(\alpha)$ , is known, for each conversion the corresponding pre-exponential factor can be calculated for every activation energy. Integration of rate equation in isothermal condi-

tions gives the isoconversional expression:

$$\ln t = \ln \left[ \frac{g(\alpha)}{A} \right] + \frac{E}{RT} \quad (4)$$

where  $t$  is cure time.

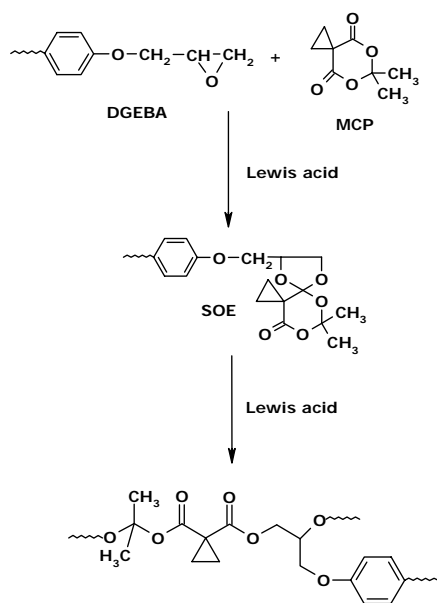
It can be observed how the isothermal constant  $\ln[g(\alpha)/A]$  (Eq. (4)) is directly related by  $R/E$  for every value of  $\alpha$  to the constant  $\ln [AR/g(\alpha)E]$  of the non-isothermal adjustment (Eq. (3)). Thus, taking the non-isothermal data  $\ln[AR/g(\alpha)E]$  and  $E$  from Eq. (3), we can determine the isothermal parameters of Eq. (3) and simulate isothermal curing without knowing  $g(\alpha)$ .

In this study, we used the reduced master curves procedure of Criado<sup>20</sup> and the Coats-Redfern method to assign a reaction model to the systems studied.<sup>21</sup> Different kinetic models have been studied: diffusion ( $D_1$ ,  $D_2$ ,  $D_3$  and  $D_4$ ), Avrami-Erofeev ( $A_2$ ,  $A_3$  and  $A_4$ ), power law, phase-boundary-controlled reaction ( $R_2$  and  $R_3$ ), autocatalytic ( $n + m = 2$  and  $3$ ) and order  $n$  ( $n = 1, 1.5, 2$  and  $3$ ). The rate constant,  $k$ , was calculated with  $E$  and  $A$  determined at conversion of 0.5, using the Arrhenius equation.

### 3. RESULTS AND DISCUSION

The reaction of DGEBA and MCP in cationic conditions leads to the formation of poly(ether-ester) structures through the formation of intermediate spiroorthoesters (SOEs). **Scheme 1** shows the chemical structure of the three-

dimensional polymer formed. In previous work<sup>18</sup> we have studied this curing by FTIR experiments using ytterbium and lanthanum triflates and  $\text{BF}_3\cdot\text{MEA}$  as initiators and confirmed the formation of an intermediate spiroorthoester. We also proved that MCP does not homopolymerise in the conditions used. From these experiments we

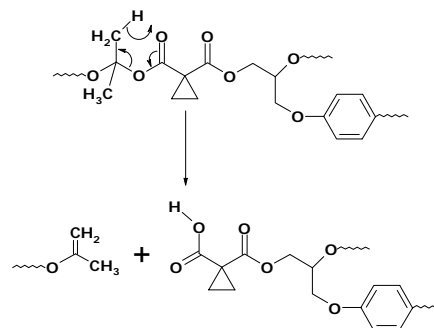


Scheme 1.

could determine that ytterbium triflate leads to the highest proportion of ester linkages in the network and the boron complex to the lowest. We also detected that some proportion of SOE remained unreacted in the materials and therefore the proportion of ester groups is in some cases lower than expected. As we can see in the scheme, the use of MCP as comonomer leads to the formation of tertiary ester groups in the polymeric chain, but the excess of

epoxy groups in the formulations contributes to a higher amount of poly(ether) units. Thus, the higher the proportion of MCP in the mixture the higher is the proportion of ester group in the material for a selected initiator.

Ester groups are thermally cleavable by a  $\beta$ -elimination mechanism<sup>22</sup>, which leads to the formation of acid and vinyl ether groups as chain ends; such is represented in **Scheme 2**. Tertiary



Scheme 2.

esters are more easily thermally degraded than primary or secondary ones. Each time an ester group is cleaved, the local cross-link density decreases and therefore, the higher the proportion of tertiary esters the more degradable character of the modified epoxy resin should be.

**Fig. 1** shows the TGA and DTG curves of the materials obtained from DGEBA/MCP 2:1 (mol/mol) mixtures using the corresponding amount of the three initiators tested. **Table 1** collects the thermal data obtained for all the materials studied. As we can see, the thermal stability of  $\text{BF}_3\cdot\text{MEA}$  initiated materials is much higher than when we used lanthanide triflates.

**Table 1.** Calorimetric and thermogravimetric data of all systems studied

Entry	Formulation <sup>a</sup>	T <sub>g</sub> <sup>b</sup> (°C)	T <sup>c</sup> (°C)	T <sub>max</sub> <sup>d</sup> (°C)	Char Yield <sup>e</sup> (%)
1	DGEBA/Yb(OTf) <sub>3</sub> 1:0.006	150	287	345	20
2	DGEBA/MCP/Yb(OTf) <sub>3</sub> 3:1:0.021	132	241	335	19
3	DGEBA/MCP/Yb(OTf) <sub>3</sub> 2:1:0.015	124	230	332	19
4	DGEBA/MCP/Yb(OTf) <sub>3</sub> 1:1:0.009	107	214	319	18
5	DGEBA/La(OTf) <sub>3</sub> 1:0.006	145	303	354	19
6	DGEBA/MCP/La(OTf) <sub>3</sub> 3:1:0.021	127	250	350	18
7	DGEBA/MCP/La(OTf) <sub>3</sub> 2:1:0.015	121	233	348	17
8	DGEBA/MCP/La(OTf) <sub>3</sub> 1:1:0.009	100	216	344	17
9	DGEBA/BF <sub>3</sub> ·MEA 1:0.096	165	332	433	19
10	DGEBA/MCP/BF <sub>3</sub> ·MEA 3:1:0.336	160	296	429	19
11	DGEBA/MCP/BF <sub>3</sub> ·MEA 2:1:0.240	154	288	425	18

- a. The composition of the formulations is given in molar ratios  
 b. Glass transition temperatures of the materials cured at 140°C for 3h and at 160°C for 2h (at 170 °C for BF<sub>3</sub>·MEA)  
 c. Temperature of a 2 % of weight loss calculated by thermogravimetry  
 d. Temperature of the maximum degradation rate calculated by thermogravimetry  
 e. Char Yield at 600°C

This could be attributed to a lower proportion of ester groups or to a higher cross-linking density.

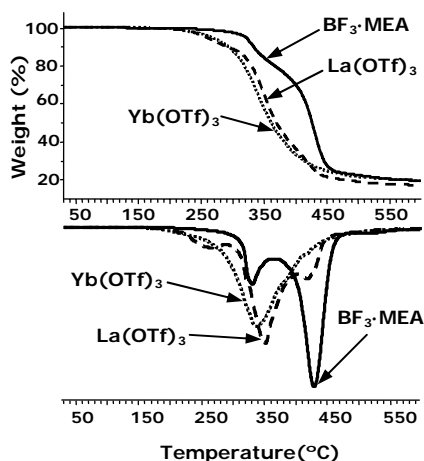


**Fig. 1.** Thermogravimetric and DTG curves at 10°/min in N<sub>2</sub> atmosphere of several thermosetting materials obtained from DGEBA/MCP 2:1 (mol/mol) formulation initiated by lanthanide triflates and BF<sub>3</sub>·MEA

However, from the TGA and the DTG curves for DGEBA homopolymer samples (**Fig. 2**) and the values collected in **Table 1** (entries 1, 5 and 9), we can conclude that the presence of lanthanide triflates in the materials initiated the degradation at lower temperatures. Thus, it seems that lanthanide triflates play a catalytic role in degradation. Moreover, the higher the Lewis acidity (ytterbium is more acidic than lanthanum) the greater is this effect. If we look at the plot of the derivatives in **Figs. 1** and **2**, we can see different shapes for all the samples tested. Thus, the material obtained with the ytterbium catalyst has a broad peak for both the co- and homopolymer, which indicates that all the degradation processes overlap. The material obtained with lanthanum triflate leads to degradation in two stages for DGEBA alone and to

a three peak curve for the copolymer. Thus, it seems that the weak broad maximum at 250°C should correspond to the decomposition of chains in which the presence of ester groups is higher.

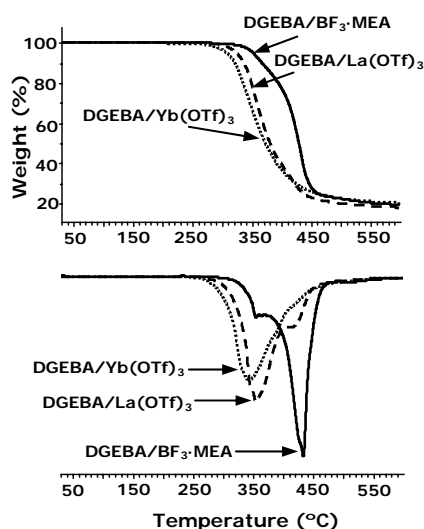


**Fig. 2.** Thermogravimetric and DTG curves at 10°C/min in N<sub>2</sub> atmosphere of several thermosetting materials obtained from DGEBA cured with lanthanide triflates and BF<sub>3</sub>·MEA

Therefore, lanthanum and ytterbium triflates act differently in the thermal degradation, because of their different capabilities to catalyze the individual degradative processes. Thus, by several  $\beta$ -elimination mechanisms little fragments could be originated giving place to a weight loss at these temperatures. BF<sub>3</sub>·MEA leads to the appearance of two peaks, more definite for the copolymeric material and at slightly lower temperature. However, there are not big differences in the initial degradation temperatures for the ytterbium

and lanthanum triflates initiated materials (see entries 3 and 7 in **Table 1**) but much more differences with the boron initiated material (entry 11). It must be said that in order to get reworkable materials the most significant parameter is the initial degradation temperature. Thus, the use of lanthanide triflates as initiators increases the reworkability of the thermosets.

As expected, there is also an increase in the degradability of the materials on increasing the proportion of MCP in the reactive mixture. **Fig. 3** shows the thermogravimetric and their derivatives for materials initiated with lanthanum triflate. On increasing the proportion of ester groups the first peak in the DTG curves increases steadily. Thus, it can be confirmed that this peak is due to a weight loss in which ester groups are broken. The second peak, with the highest rate of decomposition decreases slightly in magnitude and temperature on increasing the proportion of ester groups in the material and therefore it should be related to the breakage of ether group in the network.

The values collected in **Table 1** for all the initiators show that the maximum variations on the degradation parameters on increasing the proportion of MCP in the sample occurs in the initial degradation temperature and only slight differences can be noted in  $T_{max}$  because this temperature is related to the cleavage of ether groups. Moreover, the introduction of ester groups significantly increases the degradability with referent to the pure DGEBA.

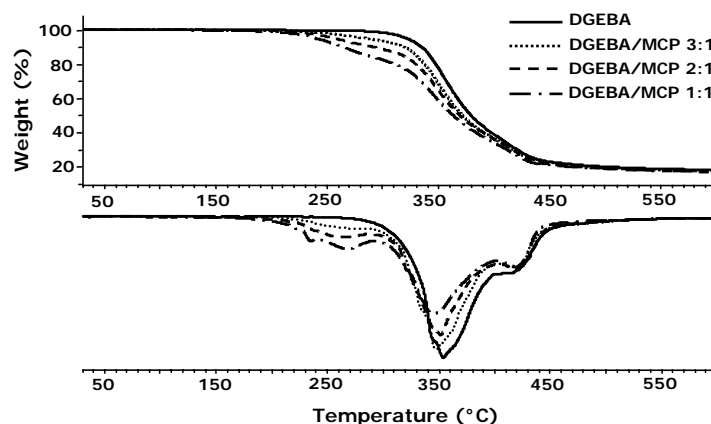


**Fig. 3.** Thermogravimetric and DTG curves at 10°C/min in N<sub>2</sub> atmosphere of several thermosetting materials obtained from different formulations of DGEBA/MCP cured with La(OTf)<sub>3</sub>

Thus, in the proportion DGEBA/MCP 3:1 the initial degradation temperature is reduced about 40-50°C with reference to the pure DGEBA, whereas an additional increase of MCP produces a lower decrease. It must be noted that big differences in the thermal degradability of the materials are obtained with lanthanide triflates and MCP in comparison to conventional DGEBA/BF<sub>3</sub>·MEA system (entry 9) which reduces both the initial and the maximum rate degradation temperatures. Lower initial degradation temperatures are not desirable because degradation could occur on curing or during use. With reference to the residues after heating until 600 °C there are not big differences among the materials, and only a slight decrease was observed on increasing the proportion of MCP.

The degradability was also tested by isothermal thermogravimetry. **Fig. 4** shows the plot of weight loss versus time at 275°C.

We can see that ytterbium triflate at longer times raises the weight loss with reference to the lanthanum salt, although in the initial steps of degradation there are only little differences, although lanthanum salt increases the initial degradability. Moreover, the effect of increasing the proportion of MCP in the sample is higher for materials initiated by lanthanum than by ytterbium salts.

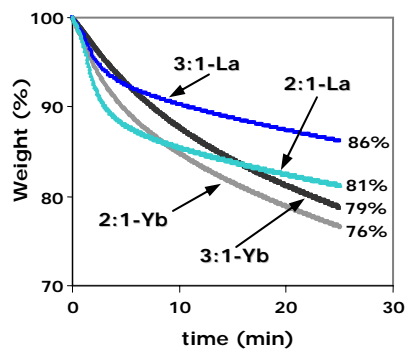


**Fig. 4.** Isothermal thermogravimetric curves at 275°C for 25 min in N<sub>2</sub> atmosphere of several thermosetting materials obtained from formulations DGEBA/MCP 3:1 and 2:1 (mol/mol) cured with Yb(OTf)<sub>3</sub> and La(OTf)<sub>3</sub>

Thermogravimetric analysis has been widely used to estimate the kinetic parameters of degradation processes, such as activation energy ( $E_a$ ), kinetic model, Arrhenius pre-exponential factor ( $A$ ) and rate constant ( $k$ ).<sup>23,24</sup> The effect of the initiators and the formulations used to prepare the samples were dynamically studied by TGA. For each material the tests carried out at different rates provided the weight loss and the rate of weight loss depending on the temperature. These data were standardised by means of Eq. (1) to find the degree of conversion with the temperature at a rate of 10 °C/min.

To find the kinetic parameters associated with the set of thermogravimetric curves obtained for different materials, we applied the isoconversional KAS equation, Eq. (3), at a conversion of 0.5. We used the reduced master curves procedure of Criado<sup>20</sup> and the Coats-Redfern method<sup>19</sup> to assign a reaction model to the degradative processes studied.

By this procedure we calculated the apparent activation energies associated with the simultaneous degradation processes and the pre-exponential factor for the  $n=3$  kinetic model. The fact that the shape of the curves have more than one peak for lanthanum triflate and  $\text{BF}_3 \cdot \text{MEA}$  cured materials (**Fig. 1**) make the comparison of the kinetics of degradation difficult. Thus, the kinetic study was only done for the ytterbium triflate cured materials, which shows a unimodal degradation curve. The results are summarized in **Table 2**. The activation energy at  $\alpha$  conversion of 0.5 and the pre-exponential factor do not show a clear tendency when the proportion of MCP was varied. Because of the compensation effect between the activation energy and the frequency factor it would be more accurate to analyze the degradation rate using the rate constant calculated by the Arrhenius equation. Thus, the values of  $k$  confirm a quicker degradation of the material when a higher proportion of MCP was added in the modification of DGEBA.

**Table 2.** Kinetic parameters calculated from the thermogravimetry of the materials obtained using ytterbium triflate as initiator

Entry	Formulation <sup>a</sup>	$E_a$ <sup>b</sup> (kJ/mol)	$\ln A$ <sup>c</sup> (s <sup>-1</sup> )	$k_{300^\circ\text{C}}^d \cdot 10^3$ (s <sup>-1</sup> )
1	DGEBA/Yb(OTf) <sub>3</sub> 1:0.006	155.4	23.43	0.1016
2	DGEBA/MCP/Yb(OTf) <sub>3</sub> 3:1:0.021	164.5	25.78	0.1574
3	DGEBA/MCP/Yb(OTf) <sub>3</sub> 2:1:0.015	163.3	25.66	0.1778
4	DGEBA/MCP/Yb(OTf) <sub>3</sub> 1:1:0.009	168.5	27.49	0.3750

a. The composition of the formulations is given in molar ratios

b. Values of activation energies were evaluated by the isoconversional integral method (Eq.(3)) applied at conversion of 0.5

c. The values of pre-exponential factor for kinetic model with  $n=3$  kinetic model

$g(\alpha)=2^{-1}[-1+(1-\alpha)^{-2}]$

d. The values of the rate constants at 300°C were calculated using the Arrhenius equation

$$\ln k = \ln A - \frac{E}{RT}$$

By applying the isoconversional procedure, Eqs. (3) and (4), we can predict the time necessary to reach a determined degree of weight loss at a selected temperature. **Fig. 5** shows the plot of weight loss against time at 275°C for the different formulations cured with lanthanide triflates.

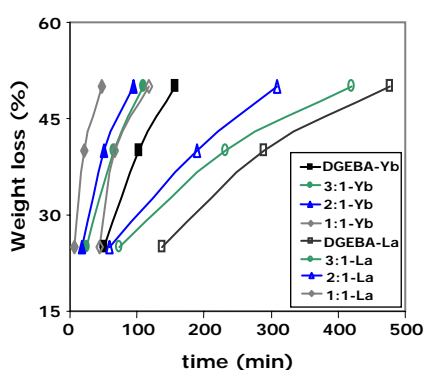


**Fig. 5.** Predicted evolution of weight loss (%) against time at 275°C of several thermosetting materials obtained from DGEBA/MCP (mol/mol) formulations cured with ytterbium and lanthanum triflate

As a general trend, the materials cured by ytterbium salts show a much better reworkability. Shorter times are needed for the degradation of the materials obtained from DGEBA/MCP 1:1 formulation for both initiators. Whereas at weight losses of 25% the differences in time to reach this conversion in all the samples are not much (in a range of 130 min) when the weight loss is about 50% these differences increase notably (about 450 min). This behaviour can be related to the initial degradation of ester groups, which should lead to more volatile fragments.

**Fig. 6** shows the dependence of the activation energy on the degree of conversion; calculated using the isoconversional method, Eq. (3)<sup>25</sup>, for the materials prepared using ytterbium triflate as initiator.

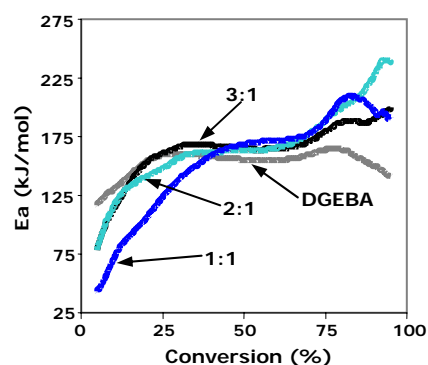


**Fig. 6.** Dependence of activation energy on the degree of conversion obtained by applying isoconversional analysis to thermogravimetric curves of several thermosetting materials prepared from DGEBA, and DGEBA/MCP (mol/mol) formulations cured with ytterbium triflate

As we can see, at lower degrees of conversion the lowest energy is the one of the material with a higher proportion of MCP. This can be attributed to the fact that degradation may begin by the cleavage of ester groups. However, at conversions about 0.5 there is no clear tendency because mainly the ether groups in the network are broken. **Fig. 7** shows the dependence of activation energy on the degree of conversion for the materials obtained from DGEBA/MCP 3:1 formulation cured with the three initiators. The materials prepared with lanthanide triflates show a similar evolution, but during the whole process the material with the ytterbium salt



degrades with lower activation energy. The material obtained with the boron complex has a completely different behaviour, because the initial value is much higher, then decreases until a 30% of conversion and finally increases steadily until the end of the degradation. This behaviour can be related to the two maximum observed in the DTG curves.

Several authors<sup>1</sup> studied the change in the glass transition temperature ( $T_g$ ) of the reworkable thermosets as a function of the thermal treatment, because there is a relationship between this parameter and the crosslink density, as  $T_g$  varies inversely with  $M_c$  and affects the mechanical properties of the material. In contrast to using TGA, where only the loss of volatiles is measured, the determination of the  $T_g$  by DSC during degradation reveals a more direct information on the behaviour of the network. Initial  $T_g$  determined from the materials cured in isothermal conditions are collected in **Table 1**.

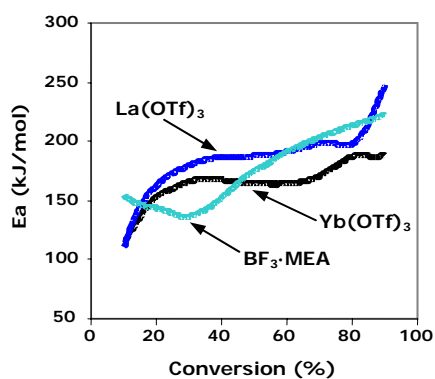


**Fig. 7.** Dependence of activation energy on the degree of conversion obtained applying isoconversional analysis to thermogravimetric curves of several thermosetting materials obtained from DGEBA/MCP 3:1 (mol/mol) formulation cured with lanthanide triflates and  $\text{BF}_3 \cdot \text{MEA}$

**Fig. 8** shows the variation of  $T_g$  of the materials initiated by ytterbium triflate at a temperature of 200 and 225°C. As we can see, an increase in the proportion of MCP in the sample leads to a notable reduction of the  $T_g$  of the material by applying the same thermal treatment.

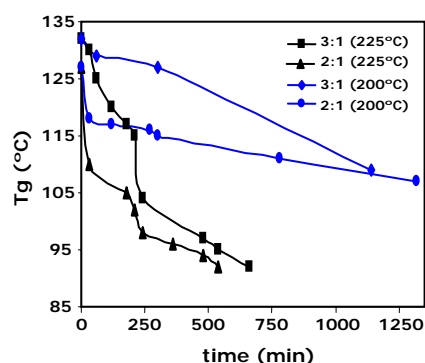


**Fig. 8.** Evolution of  $T_g$  against time for the materials obtained from DGEBA/MCP 3:1 and 2:1 (mol/mol) formulations cured with ytterbium triflate after degradation at 200 and 225°C in an oven

The diminution of the  $T_g$  is more evident at the beginning and increases noteworthy with the proportion of ester in the network, which is in accordance with the cleavage of ester groups that reduce the crosslinking density but does not produce a significant weight loss. On increasing the temperature from 200 to 225°C the effect is much more evident.

In order to follow the chemical processes involved in the degradation we recorded the FTIR spectra of the materials maintained at 200 and 225°C for 20h and integrated the ester absorption at  $1734 \text{ cm}^{-1}$  and the reference band at  $1605 \text{ cm}^{-1}$  of the

DGEBA aromatic ring. **Fig. 9** shows the variation of the normalized absorption of the ester group against time at 200 and 225°C for two different formulations initiated by ytterbium triflate. In this way, we can monitor the disappearance of ester groups and therefore the cleavage of the main chain. As we can see, on increasing the temperature from 200 to 225°C there is a rapid variation in the evolution of ester groups. Thus, 30min at 225°C leads to a loss of 39% of ester groups of the sample 2:1 and 25% of the sample 3:1, whereas at 200°C only a 19% and a 2%, respectively, disappear. This indicates that a temperature of 225°C is much better than 200°C to degrade the sample and to rework the materials. In fact, it is necessary to heat for 480 min at 200°C to cleave half of the ester groups in the formulation 2:1 and 540 min for the formulation 3:1.

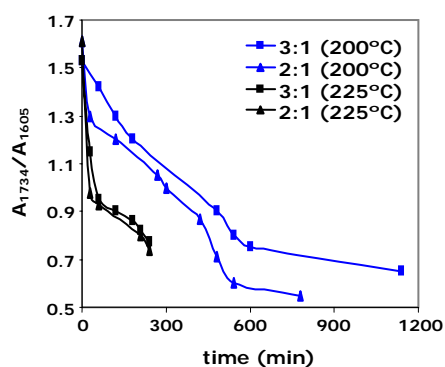
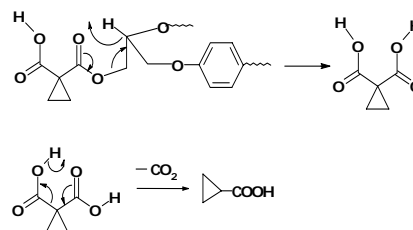


**Fig. 9.** Evolution by FTIR spectroscopy of the  $A_{1734}/A_{1605}$  ratio against time for the degradation in an oven in  $N_2$  atmosphere at 200 and 225°C of the materials obtained from 3:1 and 2:1 (mol/mol) formulations cured with  $Yb(OTf)_3$

In order to know the identity of volatile fragments produced in the degradation of the thermosets, we put the material obtained from a DGEBA/MCP (2:1) mixture cured with ytterbium triflate into an oven at 200°C for 7h and then at 250°C for 3 and 9h. The volatiles evolved were collected in three fractions trapping them in liquid nitrogen and then studied by gas chromatography coupled with mass spectrometry. Several products could be identified, which gave some information about the degradative processes. In the first fraction, obtained after 7h at 200°C, we could identify phenol and isopropyl phenol, which are formed by the breakage of ether linkages of the units introduced by DGEBA and cyclopropane carboxylic acid which can be formed by a double  $\beta$ -elimination of the diester group introduced by MCP and decarboxylation such as the one represented in **Scheme 3**. Thus, at temperatures of 200°C not only ester groups are broken but also ether groups and C-C linkages. In the fractions collected at 250°C, the second and the third after 3 and 9h, respectively, only the former contained cyclopropane carboxylic acid, which means that ester groups are broken much easier than ether or carbon-carbon linkages.

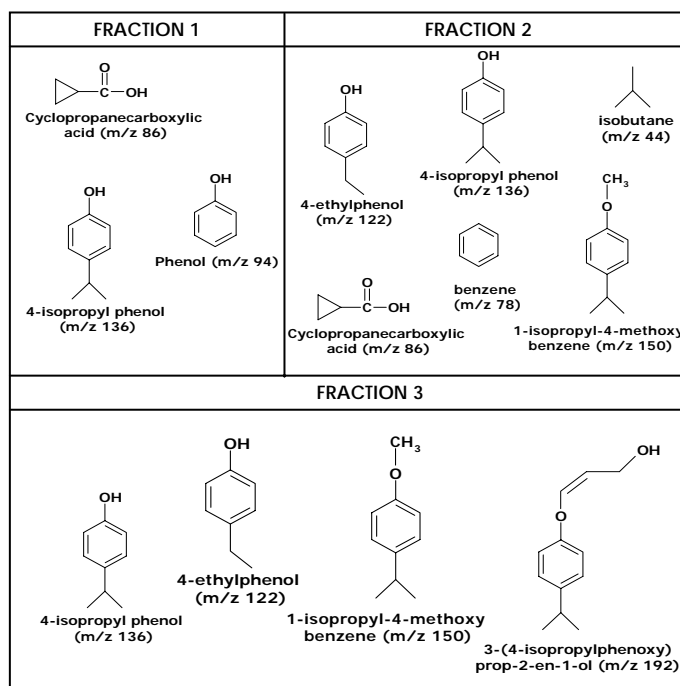


**Scheme 3.**

Moreover, in this fraction and in the third we could identify other products represented in **Scheme 4**.

In a previous article about the preparation of this type of thermosetting materials we proved that the increase of MCP in the materials reduced the global shrinkage, especially when we used ytterbium triflate as initiator.<sup>18</sup> In the present study we confirm that a higher proportion of MCP in the material and the use of ytterbium triflate are also advantageous in order to reach the highest reworkability of these thermosets.

Thus, lanthanide triflates are better than the conventional cationic  $\text{BF}_3\cdot\text{MEA}$  initiator in order to reduce the shrinkage and to increase the degradability of this type of thermosets. Moreover, the addition of MCP to the samples does not worsen the  $T_g$  values of the materials due to the structure of the comonomer with a tertiary ester and a cyclopropenyl group which restrict the internal mobility of the polymeric chain. Thus, it seems that the strategy of modification of DGEBA by copolymerization with MCP allows the enhancement of some properties of the thermosetting materials at the same time.



Scheme 4.

#### 4. CONCLUSIONS

The copolymerization of DGEBA and MCP increases the thermal degradability of epoxy resins through the cleavage of ester groups introduced into the polymer chain. The higher the proportion of MCP in the reactive mixture the more degradable the materials are.

Lanthanide triflates lead to more degradable materials than the conventional  $\text{BF}_3\cdot\text{MEA}$  cationic initiator.

From the volatiles evolved during degradation and the evolution followed by FTIR spectroscopy of the residues an initial  $\beta$ -elimination of the tertiary ester groups can be confirmed.

#### Acknowledgements

*The authors from the Universitat Politècnica de Catalunya would like to thank CICYT and FEDER (MAT-2004-04165-C02-02) for their financial support. The authors from the Rovira i Virgili University would like to thank the CICYT (Comisión Interministerial de Ciencia y Tecnología) and FEDER (Fondo Europeo de Desarrollo Regional) (MAT-2005-01806).*

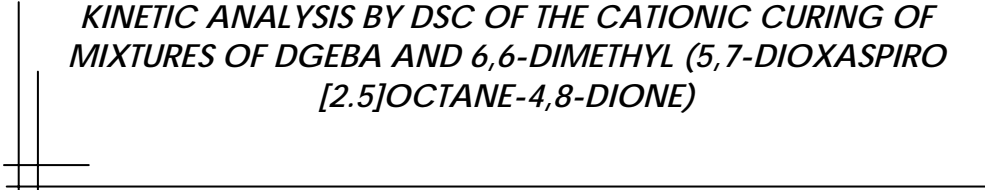
#### 5. REFERENCES

1. Chen JS, Ober CK, Poliks MD. *Polymer* 2002; 43: 131-139.
2. Wang L, Li H, Wong CP. *IEEE Trans Electron Packag Manuf* 2001; 24: 115-122.
3. Sastri VR, Tesoro GC. *J Appl Polym Sci* 1990; 39: 1425-1437; Sastri VR, Tesoro GC. *J Appl Polym Sci* 1990; 39: 1439-1457.
4. Buchwalter SL, Kosbar LL. *J Polym Sci Part A Polym Chem* 1996; 34: 249-260.
5. Malik J, Goldslager K, Clarson SJ. *J Appl Polym Sci* 2002; 85: 856-864.
6. Shin Y, Kawaue A, Okamura H, Shirai M. *React Funct Polym* 2004; 61: 293-302.
7. Liu YL, Hsieh CY. *J Polym Sci Part A Polym Chem* 2006; 44: 905-913.
8. Yang S, Chen JS, Corner H, Breiner T, Ober CK, Poliks MD. *Chem Mater* 1998; 10: 1475-1482.
9. Shirai M, Morishita S, Okamura H, Tsunnoka M. *Chem Mater* 2002; 14: 334-340.
10. Shirai M, Kawaue A, Okamura H, Tsunnoka M. *Chem Mater* 2003; 15: 4075-4081.
11. Wang L, Li H, Wong CP. *J Polym Sci Part A Polym Chem* 2000; 38: 3771-3782.
12. Wong CP, Wang L, Shi S-H. *Mat Res Innovat* 1999; 2: 232-247.
13. Mas C, Ramis X, Salla JM, Mantecón A, Serra A. *J Polym Sci Part A Polym Chem* 2003; 41: 2794-2808.
14. Giménez R, Fernández-Francos X, Salla JM, Serra A, Mantecón A, Ramis X. *J Polym Sci Part A Polym Chem* 2005; 46: 10637-10647.
15. Mas C, Ramis X, Salla JM, Mantecón A, Serra A. *J Polym Sci Part A Polym Chem* 2006; 44: 1711-1721.
16. Cervellera R, Ramis X, Salla JM, Mantecón A, Serra A. *J Polym Sci Part A Polym Chem* 2005; 43: 5799-5813.
17. Cervellera R, Ramis X, Salla JM, Serra A, Mantecón A. *J Polym Sci Part A Polym Chem* 2006; 44: 4546-4558.
18. González L, Ramis X, Salla JM, Mantecón A, Serra A. *J Polym Sci Part A Polym Chem* 2006; 44: 6869-6879.

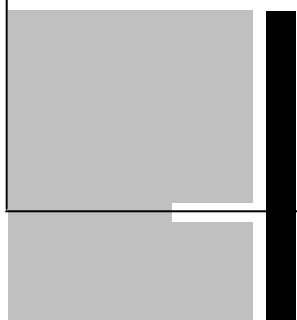
- 19.** Coats AW, Redfern JP. *Nature* 1964; 201: 68-69.
- 20.** Criado JM. *Thermochim Acta* 1978; 24: 186-9.
- 21.** Ramis X, Salla JM, Cadenato A, Morancho JM. *J Therm Anal Cal* 2003; 72: 707-718.
- 22.** Sivasamy P, Palaniandavar M, Vijayakumar CT, Ledered K. *Polym Degrad Stab* 1992; 38: 15-21.
- 23.** Morancho JM, Salla JM, Ramis X, Cadenato A. *Thermochim Acta* 2004; 419: 181-187.
- 24.** Liu YL, Wei WL, Chen YJ, Wu CS, Tsai MH. *Polym Degrad Stab* 2004; 86: 135-145.
- 25.** Ramis X, Cadenato A, Morancho JM, Salla JM. *Polymer* 2003; 44: 2067-2079.



## 3.5.



*KINETIC ANALYSIS BY DSC OF THE CATIONIC CURING OF  
MIXTURES OF DGEBA AND 6,6-DIMETHYL (5,7-DIOXASPIRO  
[2.5]OCTANE-4,8-DIONE)*



KINETIC ANALYSIS BY DSC OF THE CATIONIC CURING OF MIXTURES  
OF DGEBA AND 6,6-DIMETHYL(5,7-DIOXASPIRO  
[2.5]OCTANE-4,8-DIONE)

Lidia González,<sup>1</sup> Xavier Ramis,<sup>2</sup> Josep Maria Salla,<sup>2\*</sup>  
Ana Mantecón,<sup>1</sup> Angels Serra<sup>1</sup>

<sup>1</sup>Departament de Química Analítica i Química Orgànica. Universitat Rovira i Virgili. Marcel·lí Domingo s/n, 43007 Tarragona, Spain

<sup>2</sup>Laboratori de Termodinàmica, Escola Tècnica Superior d'Enginyeria Industrial de Barcelona, Universitat Politècnica de Catalunya, Av. Diagonal 647, 08028 Barcelona, Spain

*Received 20 March 2007; received in revised form 21 June 2007; accepted 3 July 2007*  
*DOI: 10.1016/j.tca.2007.07.09*

---

### Abstract

The kinetics of the thermal cationic cure reaction of mixtures in different proportions of diglycidylether of bisphenol A (DGEBA) with 6,6-dimethyl(5,7-dioxaspiro[2.5]octane-4,8-dione) (MCP) initiated by ytterbium or lanthanum triflates or using a conventional initiator,  $\text{BF}_3 \cdot \text{MEA}$  was investigated. The non-isothermal differential scanning calorimetry (DSC) experiments at a controlled heating rate was used for obtaining the kinetic parameters of the reactive systems.  $\text{BF}_3 \cdot \text{MEA}$  and lanthanide triflates initiated curing systems follow a complete different kinetic model. Among lanthanide triflates the ytterbium is the most active initiator.

**Keywords:** Epoxy resins, kinetics, thermosets, cationic polymerization, calorimetry.

---

## 1. INTRODUCTION

The extraction of the maximum relevant information from non-isothermal data obtained by differential scanning calorimetry (DSC) techniques and the modelling of the kinetic process are common tasks in calorimetric data treatments. DSC is an experimental technique that can be used to evaluate the kinetics of a reactive system. The results of the kinetic study can be used for various purposes, i.e. to analyze how an initiator or different proportions of a coreactant can affect a reactive system or how the temperature can affect the evolution of the reaction.<sup>1</sup>

The cure reaction of thermosetting polymers have been studied extensively,<sup>2,3</sup> among them epoxy resins studies are relevant because of their industrial applications.<sup>4,5,6</sup> However, most of the studies have been performed on epoxy-amine traditional systems and few studies are based on cationic systems.<sup>7,8</sup>

The present study deals with the kinetics of the copolymerization reaction of diglycidylether of bisphenol A (DGEBA) with 6,6-dimethyl (5,7-dioxaspiro[2.5]octane-4,8-dione) (MCP) mixtures in several proportions using ytterbium and lanthanum triflates or  $\text{BF}_3 \cdot \text{MEA}$  as initiators. The materials obtained with lanthanide triflates have been demonstrated to be more degradable than conventionally crosslinked DGEBA materials<sup>9</sup> and that their curing takes place with a lower shrinkage.<sup>10</sup> The cationic copolymerization reaction between DGEBA and lactones are scarcely studied from the point of

view of the kinetics.<sup>11,12,13,14</sup> As has been previously demonstrated<sup>9</sup> the copolymerization mechanism is rather complex, because lactones and epoxides react to form spiro orthoesters (SOEs) intermediates, which can polymerize or copolymerize with epoxies to form poly(ether-ester) structures. Moreover, epoxides can homopolymerize leading to polyether structures. In addition to these four elemental processes, cationic ring-opening polymerizations of cyclic monomers can occur by the activated chain end (ACE) or by the activated monomer (AM) mechanisms and also back-biting processes can take place.<sup>15</sup> All these processes overlap during curing and therefore only the global kinetic parameters of curing can be calculated. Moreover, physical processes also take place during curing (gelation and vitrification) that can affect not only the curing process but also the physical properties of the material.

## 2. EXPERIMENTAL

### 2.1. Materials

Diglycidylether of bisphenol A (DGEBA) EPIKOTE RESIN 827 from Shell Chemicals (Epoxy Equiv. = 182.08 g/eq) was used as received.

6,6-Dimethyl-(5,7-dioxaspiro[2.5]octane-4,8-dione) (MCP) (Aldrich) was used as received.

Lanthanum (III) and ytterbium (III) trifluoromethanesulfonates and borontrifluoride monoethyl-



amine ( $\text{BF}_3 \cdot \text{MEA}$ ) (ALDRICH) were used without purification.

## 2.2. Preparation of the Curing Mixtures

The samples were prepared by mixing the selected initiator in the corresponding amount of MCP and adding the required proportion of DGEBA with manual stirring. The prepared mixtures were kept at  $-18^\circ\text{C}$  before use. Lanthanide triflates were added in a proportion of 0.006 mol/mol of DGEBA and 0.003 mol/mol of MCP. Previous experiments showed that with  $\text{BF}_3 \cdot \text{MEA}$  it was necessary to add 0.096 mol/mol of DGEBA and 0.048 mol/mol of MCP to reach complete curing.

## 2.3. Characterization and Measurements

Calorimetric studies were carried out on a Mettler DSC-821e thermal analyzer in covered Al pans under  $\text{N}_2$  at 2, 5, 10 and  $15^\circ\text{C}/\text{min}$ . The calorimeter was calibrated using an indium standard (heat flow calibration) and an indium-lead-zinc standard (temperature calibration). The samples weighed approximately 5 mg.

## 3. RESULTS AND DISCUSSION

In a previous work<sup>9</sup> we studied the curing of mixtures of DGEBA/MCP initiated by ytterbium and lanthanum triflates and  $\text{BF}_3 \cdot \text{MEA}$  as Lewis acids. The proportions of DGEBA/MCP were 3:1,

2:1 and 1:1. We observed a moderate decrease of the  $T_g$  values on increasing the proportion of MCP in the material in addition to a decrease in the global shrinkage during curing, which put into evidence the nature of MCP as expandable monomer. By FTIR spectroscopy we could prove the formation of linear ester linkages in the network and the complete curing of the mixtures. We observed the total disappearance of the epoxy absorption band, although several proportion of the intermediate SOE remained unreacted in the material.

In previous works<sup>16,17</sup> we observed that the higher the Lewis acidity of the lanthanide triflates (from lanthanum to ytterbium) the higher the curing rate. However, the  $\text{BF}_3$  complex usually follows a different trend to the lanthanide triflates because of the formation of the active specie of initiator  $\text{HBF}_4$  and that lanthanide triflates lead to the consumption of epoxide before the disappearance of MCP, while MCP and epoxide react completely at the same time with  $\text{BF}_3 \cdot \text{MEA}$ . Thus, a higher proportion of the boron initiator is always needed to reach the total curing and the materials showed a higher  $T_g$ , which seems to indicate that the curing proceeds by a different way. The differences in the structure of the cured materials could be proved by the degradation behaviour by thermogravimetric analysis (TGA).<sup>9,10</sup>

In the present work we studied the kinetic of the curing process of these materials. Many exothermic polymerizations have difficulties for the determination of the heat of reaction trough iso-

thermal experiments and the subsequent deduction of the kinetic from these values. When reactions are performed at high temperatures, some of the heat may be lost during the stabilization of the apparatus, whereas at low temperatures, the heat is released slowly and can fall below the sensitivity of the calorimeter. Another problem arises when a physical phenomenon (e.g. vitrification) takes place. One alternative in both cases is to simulate isothermal curing with non-isothermal data.<sup>18</sup> Thus, in this work we used the non-isothermal differential scanning calorimetry experiments at a controlled heating rate as the most suitable procedure for obtaining the kinetic parameters of the reactive systems.

Thermal data obtained from non-isothermal DSC for all the samples studied are collected in **Table 1**. As can be seen the total enthalpy per gram of the curing strongly decreases as the proportion of MCP increases. However, if we consider the enthalpy per epoxy equivalent this diminution is lower. We should take into account that the heat release is mainly due to the opening of the strained epoxy ring. If we consider the heat evolved during curing for the DGEBA/MCP samples cured with the different initiators, we observed that the ytterbium salt leads to the maximum heat and boron trifluoride to the lowest, which can be related to the proportion of the unreacted SOE remaining in the final material as observed by FTIR.<sup>9</sup> Moreover, when a higher proportion of MCP is present in the mixture the higher the proportion of unreacted SOE is.

**Figures 1 and 2** show the variation of the conversion degree and the rate of conversion against the temperature of these formulations studied at a heating rate of 10°C/min. **Figure 1** shows that all curing processes are activated above 80°C and they are completed at 220°C for lanthanide salts and even higher for the BF<sub>3</sub>·MEA initiated systems. The most reactive systems at low temperatures are those initiated by BF<sub>3</sub>·MEA and the ytterbium triflate systems are more active than the ones initiated by the lanthanum salt in all the range of temperatures. Similar trends are observed in **Figure 2**. Moreover, the plots show that BF<sub>3</sub>·MEA initiated systems have a very different kinetic behaviour. Thus, these systems reach the maximum curing rate at low conversions, whereas lanthanide triflates lead to the highest curing rate at high conversions. Moreover a broad exotherm appears at low temperatures (100-130°C), which is due to the formation of the initiating active species.<sup>19,20</sup> By increasing the amount of BF<sub>3</sub>·MEA an important increase in this exotherm is observed. Moreover, by FTIR of the BF<sub>3</sub>·MEA at 120°C has been observed the conversion of BF<sub>3</sub> to HBF<sub>4</sub> which are the true initiator species. This conversion has been shown by the appearance of an absorption band at 1034 cm<sup>-1</sup> caused by BF<sub>4</sub><sup>-</sup> (asymmetric B-F stretch) and for the decrease of the bands caused by B-F asymmetric and symmetric stretching in BF<sub>3</sub>. **Figure 2** also shows that the samples with lanthanum triflate present a bimodal curve of curing with

**Table 1.** Calorimetric and thermogravimetric data of all systems studied

Entry	Formulation <sup>a</sup>	T <sub>g</sub> (°C)	ΔH <sup>b</sup> (J/g)	ΔH <sup>c</sup> (KJ/ee)	T <sup>d</sup> (°C)	T <sub>max</sub> <sup>e</sup> (°C)
1	DGEBA/Yb(OTf) <sub>3</sub> 1:0.006	135	519.7	95.6	287	345
2	DGEBA/MCP/Yb(OTf) <sub>3</sub> 3:1:0.021	117	430.3	91.5	241	335
3	DGEBA/MCP/Y(OTf) <sub>3</sub> b 2:1:0.015	110	388.0	88.2	230	332
4	DGEBA/MCP/Yb(OTf) <sub>3</sub> 1:1:0.009	105	314.4	84.4	214	319
5	DGEBA/La(OTf) <sub>3</sub> 1:0.006	127	513.5	94.4	303	354
6	DGEBA/MCP/La(OTf) <sub>3</sub> 3:1:0.021	105	418.6	89.1	250	350
7	DGEBA/MCP/La(OTf) <sub>3</sub> 2:1:0.015	100	386.8	87.7	233	348
8	DGEBA/MCP/La(OTf) <sub>3</sub> 1:1:0.009	95	307.4	83.4	216	344
9	DGEBA/BF <sub>3</sub> ·MEA 1:0.096	160	460.0	86.6	332	360-433
10	DGEBA/MCP/BF <sub>3</sub> ·MEA 3:1:0.336	156	391.0	84.5	296	333-429
11	DGEBA/MCP/BF <sub>3</sub> ·MEA 2:1:0.240	147	337.1	78.0	288	330-425

- a. The composition of the formulations is given in molar ratios  
 b. Enthalpies of curing per gram of mixture  
 c. Enthalpies of curing expressed by the equivalent of epoxy groups  
 d. Temperature of a 2 % of weight loss calculated by thermogravimetry  
 e. Temperature of the maximum degradation rate calculated by thermogravimetry

the higher peak at higher temperatures. This fact could be attributed to the SOE homopolymerization that takes place at higher temperatures.<sup>21</sup> This explanation has also been demonstrated in these DSC experiments by recording FTIR spectra of partially cured samples. The lowest reactivity of the lanthanum triflate in comparison to the ytterbium salt could explain the

appearance of a second exotherm which appears overlapped in the ytterbium initiated curing. The isoconversional dynamic procedure was used to obtain the kinetic parameters, given by the following equation:

$$\frac{d\alpha}{dt} = \beta \frac{d\alpha}{dT} = kf(\alpha) = Af(\alpha) \exp\left(-\frac{E}{RT}\right) \quad (1)$$

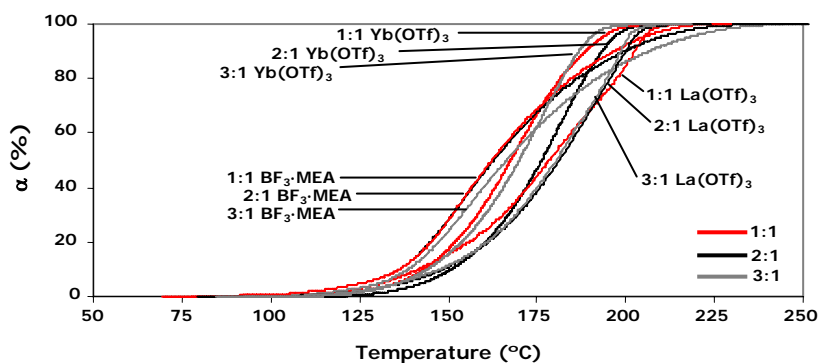


**Figure 1.** Conversion degree against temperature for the curing of several DGEBA/MCP (mol/mol) formulations initiated by different Lewis Acids obtained through dynamic DSC experiments

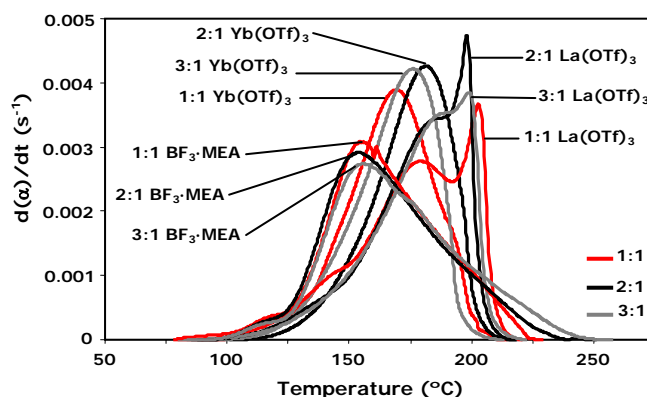


**Figure 2.** Variation of the rate of conversion with the temperature of several DGEBA/MCP (mol/mol) formulations initiated by different Lewis Acids obtained through dynamic DSC experiments

where  $\alpha$  is the degree of conversion, determined from the fractional areas of the DSC exotherm,  $T$  is the absolute temperature,  $t$  is the time,  $\beta$  is the linear heating rate,  $k$  is the constant rate,  $A$  is the pre-exponential factor,  $E$  is the activation energy,  $R$  is the gas constant, and  $f(\alpha)$  the differential conversion function (reaction model).

The isoconversional method presupposes that the reaction rate at a constant conversion is only a function of temperature. For each conversion, the activation energy  $E_\alpha$  is related to the rate of conversion and temperature by:<sup>22,23</sup>

$$\left[ \frac{d \left( \ln \left( \beta \frac{d\alpha}{dT} \right) \right)}{d(1/T)} \right]_\alpha = -\frac{E_\alpha}{R} \quad (2)$$

From the calorimetric curves at different heating rates and applying the Eq. (2), we obtained the

activation energy, for each degree of conversion in all the formulations studied. **Figure 3** shows the apparent activation energy and conversion rates against of degree of conversion (10°C/min) for the DGEBA/MCP 3:1 (mol/mol) formulation with the three initiators tested. We can observe that lanthanide initiated systems have a similar activation energy with the exception of the last part of the curve (over 70% of conversion) in which lanthanum triflate leads to an increase, which could be related to the homopolymerization of SOE groups in the second maximum observed in **Figure 2**. This result is supported by the activation energy (94.9kJ/mol) calculated for the homopolymerization of SOE groups in a previous study.<sup>21</sup>

In **Figure 3** we can also observe that the activation energy for the curing with  $\text{BF}_3 \cdot \text{MEA}$  is higher than with lanthanides in the main range of the conversion and slightly increases in all the range. The relative low values in the initial stage can be attributed to the

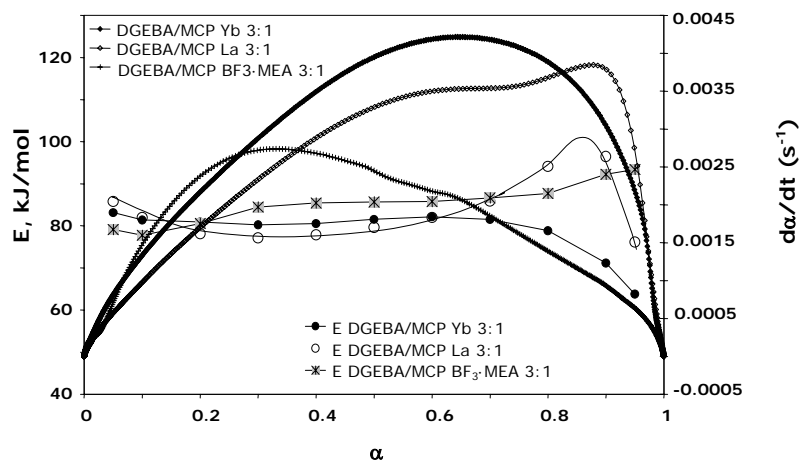


Figure 3. Apparent activation energies and conversion rates against degree of conversion (10°C/min)

formation of initiating active species. This fact produces that at low temperatures the samples initiated by  $\text{BF}_3 \cdot \text{MEA}$  react faster than samples initiated by triflates.

In spite of the multi-stage cure mechanisms, the isoconversional analysis of all the samples reflects, for an important part of the reaction process, that the apparent activation energy varies slightly with the conversion degree, as can be seen in **Figure 3**. We have used this fact to obtain and average single kinetic triplet ( $E$ ,  $A$ ,  $f(\alpha)$ ) for each mixture in order to compare and to better understand the differences between the analyzed samples. The most representative numerical values of this analysis are collected in **Table 2**. To obtain them, the following steps were necessary.

To calculate the frequency factor from the activation energies obtained from the isoconversional procedure, firstly we determined the kinetic model which better fits

with the experimental results. We used the differential reduced master curves procedure<sup>24,25</sup> that consist in comparing the experimental curves with the theoretical calculated for the different models like  $n$ -th reaction-order, autocatalytic, diffusion, Avrami-Erofeev and contraction. These models have not been described here because they are widely documented in the literature.<sup>13,24</sup>

Using as a reference point  $\alpha = 0.5$ , the following differential master equation is easily derived from Eq. (1):

$$\frac{f(\alpha)}{f(\alpha_{0.5})} = \frac{(d\alpha/dt)}{(d\alpha_{0.5}/dt)} \cdot \exp\left(\frac{E_{\alpha_{0.5}}}{R} \left(\frac{T_{\alpha_{0.5}} - T}{T_{\alpha_{0.5}} \cdot T}\right)\right) \quad (3)$$

where  $d(\alpha_{0.5})/dt$ ,  $T_{\alpha_{0.5}}$  and  $f(\alpha_{0.5})$  are respectively the reaction rate, the temperature reaction and the differential conversion function at  $\alpha=0.5$ .  $E_{\alpha_{0.5}}$  is the activation energy calculated by the isoconversional method for a degree of

**Table 2.** Apparent activation energies, pre-exponential factors and kinetic models for the systems studied

Entry	Formulation <sup>a</sup>	E <sup>b</sup> (kJ/mol)	A <sup>c</sup> (s <sup>-1</sup> )	K <sub>423K</sub> <sup>d</sup> (s <sup>-1</sup> )	Kinetic model, f(α) function <sup>e</sup>
1	DGEBA/MCP/Yb 3:1:0.021	75.8	5.42·10 <sup>6</sup>	2.37·10 <sup>-3</sup>	N <sub>1</sub> , f(α)=(1-α)
2	DGEBA/MCP/Yb 2:1:0.015	79.4	1.02·10 <sup>7</sup>	1.62·10 <sup>-3</sup>	N <sub>1</sub> , f(α)=(1-α)
3	DGEBA/MCP/Yb 1:1:0.009	68.8	7.04·10 <sup>5</sup>	2.28·10 <sup>-3</sup>	N <sub>1</sub> , f(α)=(1-α)
4	DGEBA/MCP/La 3:1:0.021	89.0	1.22·10 <sup>8</sup>	1.25·10 <sup>-3</sup>	N <sub>1</sub> , f(α)=(1-α)
5	DGEBA/MCP/La 2:1:0.015	87.6	8.77·10 <sup>7</sup>	1.36·10 <sup>-3</sup>	N <sub>1</sub> , f(α)=(1-α)
6	DGEBA/MCP/La 1:1:0.009	77.1	4.46·10 <sup>6</sup>	1.34·10 <sup>-3</sup>	N <sub>1</sub> , f(α)=(1-α)
7	DGEBA/MCP/BF <sub>3</sub> 3:1:0.336	77.7	1.72·10 <sup>7</sup>	4.38·10 <sup>-3</sup>	Autocatha., f(α)=α <sup>0.15</sup> (1-α) <sup>1.85</sup>
8	DGEBA/MCP/BF <sub>3</sub> 2:1:0.240	84.8	7.37·10 <sup>7</sup>	2.53·10 <sup>-3</sup>	Autocatha., f(α)=α <sup>0.15</sup> (1-α) <sup>1.85</sup>
9	DGEBA/MCP/BF <sub>3</sub> 1:1:0.240	89.9	6.69·10 <sup>8</sup>	5.43·10 <sup>-3</sup>	Autocatha., f(α)=α <sup>0.15</sup> (1-α) <sup>1.85</sup>

<sup>a</sup> The compositions of the formulations is given in molar ratios

<sup>b</sup> The values of activation energies have been taken for an interval 0.1 < α < 0.9

<sup>c</sup> The values of pre-exponential factor have been calculated considering the kinetic model

<sup>d</sup> Values of rate constant at 423 K calculated using the Arrhenius equation

<sup>e</sup> The selected model was the one that best correlate the experimental results

conversion  $\alpha = 0.5$ . It was assumed  $E_{\alpha 0.5}$  and the pre-exponential factor constant. The left side of Eq. (3), is a reduced theoretical curve which is characteristic of each kinetic function. The right side of the equation is associated with the reduced rate and can be obtained from experimental data if the activation energy is known. The comparison of both sides of Eq. (3) tells us which kinetic model describes an experimental reaction process.

**Figure 4** represents the  $f(\alpha)/f(\alpha_{0.5})$  function for the usual kinetic models in addition to the experimental data obtained at 10°C/min for the different formulations studied. We can observe that any formulation perfectly fits any kinetic model in all the conversion range. The formulations initiated by lanthanide triflates follow simi-

lar kinetic models, but different from those followed by the BF<sub>3</sub>·MEA initiated systems. In basis of these results, we selected an autocatalytic model  $f(\alpha) = \alpha^{0.15}(1-\alpha)^{1.85}$  for the curing of the samples initiated with BF<sub>3</sub>·MEA and a n=1 model for the samples containing lanthanide triflates. Although these models do not fit perfectly with our experimental values, we selected them because they are the most applied in the curing of epoxy resins.<sup>19,20</sup> Thus, the frequency factors and constant rates will be comparable for all the systems initiated by lanthanide triflates but not with those initiated by BF<sub>3</sub>·MEA.

Known the activation energy and the kinetic model and using the eq. 1 we can obtain the frequency factor  $A_{\alpha}$  for each conver-

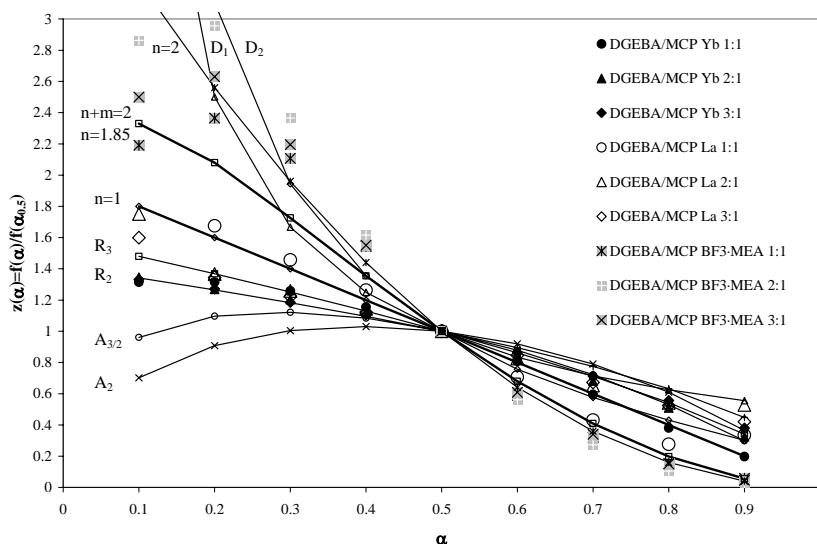


**Figure 4.** Comparison of the theoretical differential master plots of  $f(\alpha)/f(0.5)$  versus  $\alpha$  with the experimental master curve. The symbols correspond to the experimental values determined for the curing of the reactive mixtures studied

sion through the following equation:

$$A_{\alpha} = \left( \frac{d\alpha/dt}{f(\alpha)} \right) \cdot \exp \left( \frac{E_{\alpha}}{RT_{\alpha}} \right) \quad (4)$$

where  $d\alpha/dt$  and  $T_{\alpha}$  are obtained experimentally and  $E_{\alpha}$  is the activation energy calculated by the isoconversional procedure. The obtained values of  $A_{\alpha}$  are not reproduced because they reflect the same behaviour than  $E_{\alpha}$  which has already represented in **Figure 3**.

The different kinetic model obtained for  $\text{BF}_3 \cdot \text{MEA}$  and lanthanide triflates initiated systems can be related with the formation of different active species in both cases. When we used lanthanide triflates the kinetic model is of  $n$  order being the maximum curing

rate at zero conversion. When the reaction progress there are less active species in the reaction medium and the topological hindrance increases. When we use  $\text{BF}_3 \cdot \text{MEA}$ , at the beginning of the curing process, the difficulty of the  $\text{BF}_3 \cdot \text{MEA}$  of initiating the reactive process until active species ( $\text{HBF}_4$ ) are formed,<sup>19,20</sup> might explain the different behaviour with regard the triflate initiation and, in accordance with figure 3, is better fitted with an autocatalytic model than one of order  $n$ . After the highest curing rate is reached (about  $\alpha = 0.2$ ) the curing declines as it occurs in the case of lanthanide triflates.

To obtain a single pair ( $E$ ,  $A$ ) for each reactive system, we used the so called reduced constant rate defined by the following equation:

$$k_r = \left( \frac{\beta(d\alpha/dT)}{f(\alpha)} \right) \quad (5)$$

By comparing equations 1 and 5, extracting logarithms and rearranging terms the following equation can be obtained:

$$\ln k_r = \ln A - \frac{E}{RT} \quad (6)$$

In equation 6 do not appear the subscripts  $\alpha$  to mean that if the activation energy and A are independent of the conversion degree and the reduced constant rate turns into the actual constant rate that only depends on the temperature.

If the plot of the  $\ln k_r$  values (obtained from experimental data and using the selected kinetic model) against  $1/T$  fits a straight line, the kinetic process is well defined by the kinetic triplet ( $f(\alpha)$ , E and A) being E and A the values obtained from the slope and the intercept respectively of the regression line.

**Figure 5** shows, as an example, the comparative analysis made with the constant rates of the  $\text{BF}_3 \cdot \text{MEA}$  catalytic systems, using all the heating rate values (2, 5, 10 and 15 °C/min) and all conversions between 0.1 and 0.9. The correlations obtained are good enough to consider the activation energies and pre-exponential factors, collected in **Table 2**, as representative average values for these systems. From the **Figure 5** it could be put into evidence the different accelerative effect that an increase in the proportion of MCP

causes in the different stages of the curing. The amount of MCP in the samples makes to increase the rate constant. But this influence is not the same at the beginning of reaction (at low temperature is practically unappreciable) than later.

An analogous analysis was made for the formulations initiated by lanthanide triflates. In **Figure 6** are represented the results for the formulation DGEBA/MCP 3:1 (mol/mol) for both initiators. We can observe the greater catalytic effect of the ytterbium triflate. Similar behaviour was observed for the DGEBA/MCP 2:1 and 1:1 (mol/mol) formulations.

From the average values collected in **Table 2** we can see that the activation energies are lower for the systems initiated by the ytterbium salt. As commented earlier, these differences probably reflects de different ability of the initiators to produce copolymerization of SOE and epoxy with the consequence that the remaining SOE homopolymerizes at higher temperatures. For both lanthanide triflate initiators, the increase of MCP in the reactive mixture reduces the activation energies and pre-exponential factors. These results show that the differences cannot be explained exclusively by the changes produced by the combined effect of temperature and medium viscosity when the amount of MCP is increased. The contrary trend is observed when the amount of MCP increases in the samples with the boron initiator. It is difficult to explain this behaviour only on the basis of the kinetic processes.



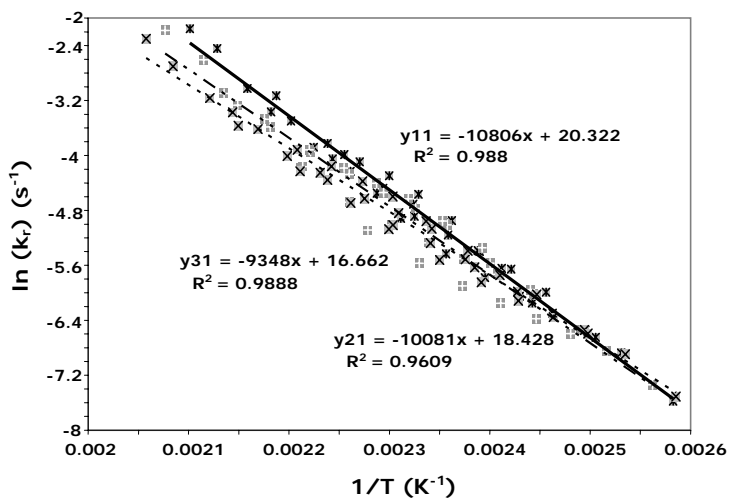


Figure 5. Analysis by the reduced rate constant of the DGEBA/MCP (mol/mol) formulations initiated by  $\text{BF}_3 \cdot \text{MEA}$

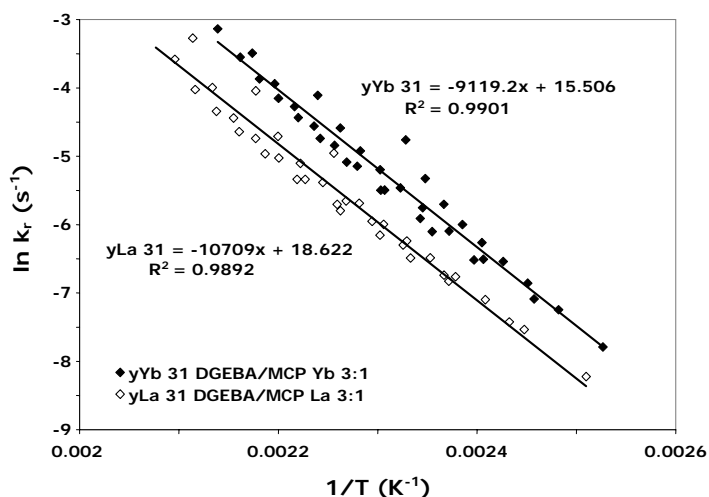


Figure 6. Analysis by the reduced rate constant of the DGEBA/MCP (3:1 mol/mol) formulations initiated by lanthanum and ytterbium triflates

For these samples, the pre-exponential factor increases with MCP addition but not enough to compensate the increment of the activation energy so there is not appreciable effect on the constant rate. The differences of pre-expo-

nenial factors and constant rate values for lanthanide triflates and  $\text{BF}_3 \cdot \text{MEA}$  initiated samples in table 2 are not comparable because they were obtained from different kinetic models. All these facts put into evidence the complexity of the ca-

tionic curing of these systems. Although the kinetic analysis performed allowed to find out differences between the samples with different initiators and proportions of MCP, we must accept that the results obtained are not enough to explain in detail the curing behaviour and the properties of the cured materials. The competitive reaction processes, whose extension depends on the initiator and on the composition of the mixtures, are only a partial cause of the cure kinetics and the final structure of the material. In addition, the formation of intermediate SOEs, the possibility of separated phases, the amount of poly(ether-ester) and polyether structures depending on homopolymerization- copolymerization extensions, produce a physical change of the substrate that plays a relevant role as a complementary cause in the explanation of the complex kinetics and the final properties of the cured samples.<sup>9,10</sup>

#### 4. CONCLUSIONS

This work shows that the kinetics of the thermal cationic cure reaction of mixtures of DGEBA with MCP must be analyzed as a multi-stage cure mechanisms highly dependent on the initiator system (conventional  $\text{BF}_3\cdot\text{MEA}$  or lanthanide triflates). Based on the results of DSC isoconversional kinetic analysis, the apparent activation energy of the  $\text{BF}_3\cdot\text{MEA}$  systems is higher than lanthanide triflates systems in the most part of conversion.

The lower reactivity of the mixtures initiated with  $\text{BF}_3\cdot\text{MEA}$  correlates well with the higher activation energy obtained in comparison to the lanthanide triflates ones. The relative low  $E$  values of the  $\text{BF}_3\cdot\text{MEA}$  in the initial cure stage can be explained by the nature of the initiating active species.

The analysis of reduced constant rate allows to obtain a single kinetic triplet ( $E$ ,  $A$ ,  $f(\alpha)$ ) for each mixture in order to a better understanding of the effect of the initiator proportion and the amount of MCP in the DGEBA/MCP mixtures. In all the samples analyzed, the reactivity increases with the proportion of MCP. The increase in the amount of MCP produces an acceleration effect that is notorious in advanced steps of the reaction but not in the initial stage. Although the kinetic of mixtures initiated by ytterbium and lanthanum triflates are very similar, the ytterbium triflate is more active than lanthanum triflate due to the higher Lewis acidity of the ytterbium cation.

#### Acknowledgements


*The authors from the Rovira i Virgili University would like to thank the CICYT (Comisión Interministerial de Ciencia y Tecnología), FEDER (Fondo Europeo de Desarrollo Regional) (MAT2005-01806). The authors from the Universitat Politècnica de Catalunya would like to thank CICYT and FEDER (MAT2004-04165-C02-02) for their financial support.*

## 5. REFERENCES

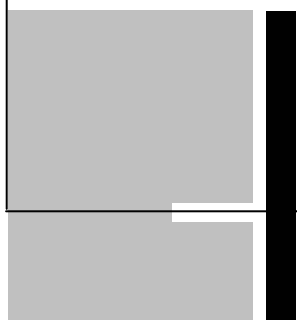

1. Salla, J.M.; Ramis, X.; Morancho, J.M.; Cadenato, A. *Thermochim Acta* 2002, 388, 355-370.
2. Leroy, E., Dupuy, J.; Maazouz, A. *Macromol Chem Phys* 2001, 202, 465-474.
3. Han, J.L.; Hsieh, K.H.; Chiu, W.Y. *J Appl Polym Sci* 1993, 50, 1099-1106.
4. Sbirrazzuoli, N.; Vyazovkin, S.; Mititelu, A.; Sladic, C.; Vincent, L. *Macromol Chem Phys* 2003, 204, 1815-1821.
5. Zvetkov, V.L. *Polymer* 2002, 43, 1069-1080.
6. Blanco, M.; Corcuera, M.A.; Riccardi, C.C.; Mondragón, I. *Polymer* 2005, 46, 7989-8000.
7. Grazulevicius, J.V.; Kublickas, R.; Kavaliunas, R. *J Macromol Sci Part A Pure Appl Chem* 1994, A31, 1303-1313.
8. García, S.J.; Ramis, X.; Serra, A.; Suay, J. *J Termal Anal Cal* 2006, 83, 429-438.
9. González, L.; Ramis, X.; Salla, J.M.; Mantecón, A.; Serra, A. *J Polym Sci Part A Polym Chem* 2006, 44, 6869-6879.
10. González, L.; Ramis, X.; Salla, J.M.; Mantecón, A.; Serra, A. *Polym Degrad Stab* 2007, 92, 596-604.
11. Chabanne, P.; Tighzert, L.; Pascault, J.P. *J Appl Polym Sci* 1994, 53, 787-806.
12. Matejka, L.; Dusek, K.; Chabanne, P.; Pascault, J.P. *J Polym Sci Part A Polym Chem* 1997, 35, 665-672.
13. Ramis, X.; Salla, J.M.; Mas, C.; Mantecón, A.; Serra, A. *J Appl Polym Sci* 2004, 92, 381-393.
14. Salla, J.M.; Fernández-Francos, X.; Ramis, X.; Mas, C.; Mantecón, A.; Serra, A. *J Therm Anal Calorim*, in press
15. Penczek, S. *J Polym Sci Part A Polym Chem* 2000, 38, 1919-1933
16. Mas, C.; Mantecón, A.; Serra, A.; Ramis, X.; Salla, J.M. *J Polym Sci Part A Polym Chem* 2004, 42, 3782-3791.
17. Cervellera, R.; Ramis, X.; Salla, J.M.; Mantecón, A.; Serra, A. *J Polym Sci Part A Polym Chem* 2005, 43, 5799-5813.
18. Ramis, X.; Salla, J.M.; Puiggali, J. *J Polym Sci Part A Polym Chem* 2005, 43, 1166-1176
19. Ghaemy, M. *Eur Polym J* 1998, 34, 1151-1156.
20. Li, Y.; Li, M.; Chang, F. *J Polym Sci Part A Polym Chem* 1999, 37, 3614-3624
21. Mas, C.; Ramis, X.; Salla, J.M.; Mantecón, A.; Serra, A. *J Polym Sci Part A Polym Chem* 2003, 41, 2794-2808.
22. Vyazovkin, S.; Sbirrazzuoli, N. *Macromol Rapid Commun* 2006, 27, 1515-1532.
23. Friedman, H. *J Polym Sci Part C* 1964-5, 6, 183.
24. Gotor, F.J.; Criado, J.M.; Málek, J.; Koga, N. *J Phys Chem A* 2000, 104, 10777-10782.
25. Criado, J.M.; Pérez-Maqueda, L.A.; Gotor, F.J.; Málek, J.; Koga, N. *J Therm Anal Cal* 2003, 72, 901-906.



3.6.



*STUDY OF THE CATIONIC CURING OF DGEBA AND 2,2,5,5-  
TETRAMETHYL-4,6-DIOXO-1,3-DIOXANE AND THE  
DEGRADATION OF THE THERMOSETS OBTAINED*



## STUDY OF THE CATIONIC CURING OF DGEBA AND 2,2,5,5-TETRAMETHYL-4,6-DIOXO-1,3-DIOXANE AND THE DEGRADATION OF THE THERMOSETS OBTAINED

Lidia González,<sup>1</sup> Xavier Ramis,<sup>2</sup> Josep Maria Salla,<sup>2</sup>  
Ana Mantecón,<sup>1</sup> Angels Serra<sup>1\*</sup>

<sup>1</sup>Departament de Química Analítica i Química Orgànica. Universitat Rovira i Virgili. Marcel·lí Domingo s/n, 43007 Tarragona, Spain

<sup>2</sup>Laboratori de Termodinàmica, ETSEIB. Universitat Politècnica de Catalunya, Av. Diagonal 647, 08028 Barcelona, Spain

*Received 21 May 2007; accepted 9 November 2007*

*DOI: 10.1002/app.27758*

---

### Abstract

Ytterbium and lanthanum triflates were used as cationic initiators to cure mixtures of diglycidylether of bisphenol A and 2,2,5,5-tetramethyl-4,6-dioxo-1,3-dioxane in several proportions. The evolution of the epoxy and lactone during curing and the linear ester groups in the final materials were evaluated by Fourier Transform Infrared in the attenuated-total-reflection mode. The shrinkage after curing and the thermal degradability of the materials on varying the comonomer ratios and the initiator used were evaluated and related to the chemical structure of the final network. The expandable character of 2,2,5,5-tetramethyl-4,6-dioxo-1,3-dioxane was confirmed. The obtained materials were more degradable than conventional epoxy resins because of the tertiary ester groups incorporated into the network by copolymerization. The kinetic parameters of the curing and degradation processes were calculated with differential scanning calorimetry and thermogravimetric analysis, respectively, with isoconversional procedures applied in both cases.

**Keywords:** Epoxy resins; lactones, cationic polymerization, crosslinking, thermosets

---

## 1. INTRODUCTION

Epoxy resins are thermosetting materials which are very used in electronic applications as encapsulants or coatings because their good characteristics as insulators. However, they present some disadvantages such as the shrinkage produced during curing, their permanency in the environment when their service life is over and their fragility. All these drawbacks should be reduced to improve their applicability.

Ring-opening is the polymerization mechanism that leads to the lowest shrinkage during curing, because when a cyclic monomer opens a covalent bond is converted into a van der Waals distance, which reduces the shrinkage produced in the formation of covalent bonds between monomer molecules.<sup>1</sup> This method has other advantages such as the possibility of copolymerizing heterocyclic monomers with different groups and functionalities. Moreover, the selection of the initiator and its proportion influences the kinetics and mechanism of the polymerization process. A disadvantage of the catalytically cured epoxy resins is that they generally are fragile because of their high density of crosslinking. Copolymerization enables the improvement of their mechanical properties be-

cause it allows the introduction of flexible chains into the structure with adequate heterocyclic comonomers and also diminishes the crosslinking density.

Previous publications of our research group have dealt with the copolymerization of commercially available lactone monomers with commercial epoxy resins.<sup>2,3,4</sup> In these studies, we demonstrated that the shrinkage after gelation is notably reduced by this way, and even in some cases, the global shrinkage of the material during curing is even lowered.

One strategy for reducing the permanency of thermosets in the environment, when their service life is over is the introduction of labile linkages, such as ester groups, into the structure. Ester groups are thermally cleavable over 200°C and therefore facilitate the reworking of the thermosets in which they are chemically incorporated.<sup>5,6,7</sup> Among ester groups, the tertiary ones are the most easily breakable, and so we considered in a previous study their introduction by the copolymerization of diglycidyl ether of bisphenol A (DGEBA) resins with a Meldrum acid derivative, 6,6-dimethyl-(4,8-dioxaspiro[2.5]octane-5,7-dione) (MCP), with an spiranic skeleton.<sup>8,9</sup> MCP was selected because it allows the introduction of tertiary ester groups

into the network, which facilitates the degradation process of the thermoset. The expandable behaviour of MCP on curing was also demonstrated. Moreover, other studies<sup>10</sup> have demonstrated that the copolymerization of MA and DGEBA solid epoxy resins improves the adhesion and the mechanical properties.

In our studies, lanthanide triflates have been selected as initiators because they have been proved to be excellent Lewis acids, are commercially available, are stable in water, and can be considered environmentally friendly catalysts.<sup>11</sup> These initiators have been proved to be capable of copolymerizing epoxy resins with lactones by a ring-opening mechanism through the formation of intermediate spirocyclic compounds, spiroorthoesters (SOEs).<sup>2</sup> The presence of lanthanide triflates in the cured material also facilitates the thermal degradation of the thermoset.<sup>9</sup>

## 2. EXPERIMENTAL

### 2.1. Materials

Diglycidylether of bisphenol A (DGEBA) EPIKOTE RESIN 827 from Shell Chemicals (Epoxy Equiv.= 182.08g/eq), methyl iodide (Fluka); silver oxide (Fluka) and 2,2-dimethyl-4,6-dioxo-1,3-dioxane (Meldrum acid; Aldrich) were used as received.

Lanthanum (III) and ytterbium (III) trifluoromethanesulfonates (ALDRICH) were used without purification.

Organic solvents were purified by standard methods.

### 2.2. Synthesis of 2,2,5,5-tetramethyl-4,6-dioxo-1,3-dioxane (MDM)

Into a suspension of 10g (0.043mol) of Ag<sub>2</sub>O in a mixture of 50ml of acetonitrile and 8ml (0.129mol) of methyl iodide was dropped a solution of 5.56g (0.039mol) of MA in 20ml of acetonitrile during stirring at 10°C for 1h. After stirring overnight, the silver oxide/silver iodide was filtered, and then the solvent eliminated by distillation below 60°C in the vacuum of water pump. The residual oil was treated with water, and after 10min, the product solidified. The suspension was transferred to a mortar, and the solid was broken up to facilitate washing. After filtration by suction and washing with water, the product was dried *in vacuo* and sublimated. Yield 3.1g (46%) of white crystals. m.p: 60-62°C (lit 62°C).<sup>12</sup> H<sup>1</sup>-NMR (CDCl<sub>3</sub>, δ, ppm): 1.64 (s, 6H, -CH<sub>3</sub>-C-O-); 1.74 (s, 6H, CH<sub>3</sub>-C=O). C<sup>13</sup>-NMR (CDCl<sub>3</sub>, δ, ppm): 25.77; 29.01; 44.74; 104.93; 171.22. IR (cm<sup>-1</sup>): 1778, 1733, 1455, 1387, 1288, 1193, 1166, 1058, 1008, 966.

### 2.3. Preparation of the curing mixtures

The samples were prepared through the mixing of the selected initiator in the corresponding amount of MDM and the addition of the required proportion of DGEBA with manual stirring. The prepared mixtures were kept at -

18°C before use. Lanthanide triflates were added in a molar ratio of 0.006 mol/mol of DGEBA and 0.003 mol/mol of MDM.

#### 2.4. Characterization and measurements

Calorimetric studies were carried out on a Mettler DSC-821e thermal analyzer in covered Al pans under N<sub>2</sub> at 10°C/min. The calorimeter was calibrated using an indium standard (heat flow calibration) and an indium-lead-zinc standard (temperature calibration). The samples weighed approximately 7-9 mg. In the dynamic curing process the degree of conversion by DSC ( $\alpha_{DSC}$ ) was calculated as follows:

$$\alpha_{DSC} = \frac{\Delta H_T}{\Delta H_{dyn}} \quad (1)$$

where  $\Delta H_T$  is the heat released up to a temperature  $T$ , obtained by integration of the calorimetric signal up to this temperature, and  $\Delta H_{dyn}$  is the total reaction heat associated with the complete conversion of all reactive groups. The glass transition temperatures (Tg's) were calculated after complete curing, by means of a second scan, as the temperature of the half-way point of the jump in the heat capacity when the material changed from the glassy to the rubbery state.

The isothermal curing process at 150°C was monitored with an FTIR-680PLUS Fourier transform infrared (FTIR) spectrophotometer from Jasco (Tokyo, Japan) with a resolution of 4 cm<sup>-1</sup> in the absorbance mode. An attenuated-

total-reflection (ATR) accessory with thermal control and a diamond crystal (Golden Gate heated, single-reflection diamond ATR, Specac-Teknokroma) was used to determine FTIR spectra. The conversions of the reactive groups were determined from the normalized changes in absorbance by the Lambert-Beer law, as we explained previously.<sup>2</sup> After isothermal curing by means of FTIR, a dynamic scan by DSC was always carried out to prove that the curing was complete.

Thermogravimetric analyses (TGAs) were carried out with a Mettler TGA/SDTA 851e thermobalance. Cured samples with an approximate mass of 7 mg were degraded between 30 and 600°C at a heating rate of 10°C/min in N<sub>2</sub> (200 cm<sup>3</sup>/min) measured in normal conditions.

Shrinkage was determined from the densities of the samples before and after curing. These densities were determined with a Micromeritics (USA) AccuPyc 1330 gas pycnometer thermostated at 30°C.

#### 2.5. Kinetic analysis

Integral nonisothermal kinetic analysis was used to determine the kinetic triplet (pre-exponential factor (A), activation energy (E), and integral function of the degree of conversion  $g(\alpha)$ ).

Nonisothermal kinetic analysis can start with the kinetic equation:

$$\beta \frac{d\alpha}{dT} = A \exp\left(\frac{-E}{RT}\right) f(\alpha) \quad (2)$$



where  $\beta$  is the heating rate,  $\alpha$  is the conversion,  $R$  is the universal gas constant,  $T$  is the temperature and  $f(\alpha)$  is the differential conversion function.

By using the Coats-Redfern<sup>13</sup> approximation to resolve the so-called temperature integral and considering that  $2RT/E$  is much lower than 1, the Kissinger-Akahira-Sunose equation as follows:<sup>14,15,16</sup>

$$\ln \frac{\beta}{T^2} = \ln \left[ \frac{AR}{g(\alpha)E} \right] - \frac{E}{RT} \quad (3)$$

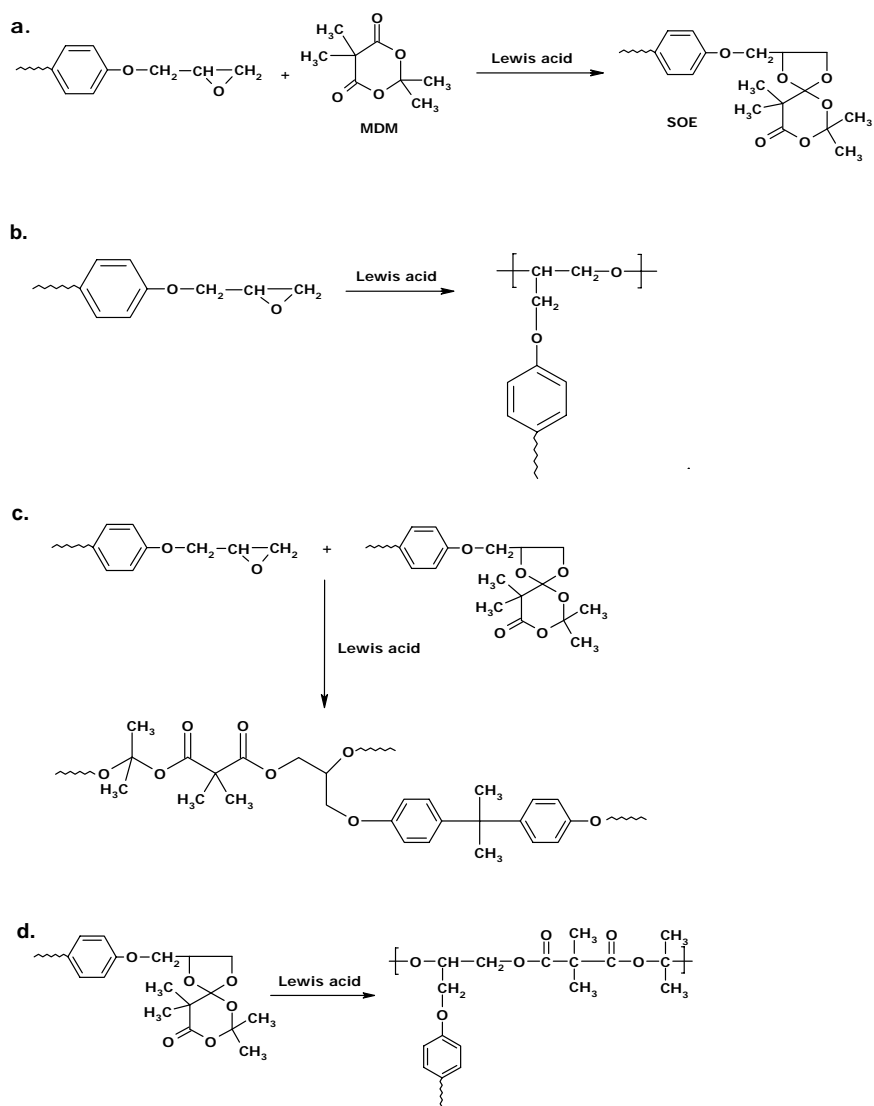
For each conversion degree, the linear representation of  $\ln[\beta/T^2]$  versus  $T^{-1}$  enables  $E$  and  $\ln[AR/g(\alpha)E]$  to be determined from the slope and the ordinate in the origin. If the reaction model,  $g(\alpha)$ , is known, for each conversion the corresponding value of  $A$  can be calculated for every value of  $E$ . In this article, to assign a reaction model to the systems studied, we used Criado's reduced master curve procedure,<sup>17</sup> which is described elsewhere.<sup>18</sup> Different kinetic models have been studied: diffusion ( $D_1$ ,  $D_2$ ,  $D_3$  and  $D_4$ ), Avrami-Erofeev ( $A_2$ ,  $A_3$  and  $A_4$ ), power law, phase-boundary-controlled reaction ( $R_2$  and  $R_3$ ), autocatalytic ( $n+m = 2$  and  $3$ ) and  $n$ -order ( $n=1, 2$  and  $3$ ).<sup>17</sup> We found that the curing of the studied systems follows a kinetic model of the surface-controlled reaction type  $R_3$  with  $g(\alpha)=[1-(1-\alpha)^{1/3}]$  and the degradation processes follow an  $n$ -order model with  $n=3$  and  $g(\alpha)=2^{-1}[-1+(1-\alpha)^{-2}]$ . The rate constant ( $k$ ) values were calculated with  $E$

and  $A$  determined at  $\alpha = 0.5$  with the Arrhenius equation.

### 3. RESULTS AND DISCUSSION

In a previous work,<sup>8</sup> we studied the curing of mixtures of DGEBA epoxy resin with a cyclopropenylic spiranic MA derivative (MCP), using lanthanide triflates as initiators. We observed that the higher the proportion of MCP in the curing mixture, the lower the global shrinkage was. Because of the characteristics of this spiranic compound with a highly strained cyclopropenylic ring, a double ring opening of the skeleton could be suspected, which could justify the expandable behaviour observed. Some spiranic compounds can be considered as expandable monomers according to the definition proposed by Bailey and others.<sup>19,20</sup> In this work, we synthesized another MA derivative with a similar structure but with no spiranic skeleton, MDM, to determine whether the lower shrinkage observed in the copolymerization could be attributed to a double ring opening of MCP upon copolymerization or to the expandable character of the six-membered ring.

The copolymerization of DGEBA and MDM is a complex process in which four different reactions can occur to different extents that depend on the proportions of comonomers in the mixture and on the lanthanide triflate used. These reactions are represented in **Scheme 1**. It has been experimentally proved that MDM does not homopolymerize in under these conditions.



**Scheme 1.** Reactive process during curing

### 3.1. Study by FTIR-ATR

By FTIR we followed the evolution of the different species that are implied in the global curing. **Figure 1** shows the initial and final spectra of the 2:1 (mol/mol) DGEBA/MDM mixture with 0.015 mol of  $\text{Yb}(\text{OTf})_3$  at 150°C. In the initial spectrum, we can see two carbonylic bands at 1782 and 1745  $\text{cm}^{-1}$  attributable to the unsymmetrical and symmetrical stretching of ester groups and two bands at 962 and 912  $\text{cm}^{-1}$  due to the deformation of the six-membered lactone ring and the deformation of the oxirane group, respectively. All these absorptions disappear in the final spectrum, and a new band at 1734  $\text{cm}^{-1}$  appears because of the linear ester group that forms. The disappearance of the absorptions indicates the complete consumption of the initial species. Because MDM does not homopolymerize, the disappearance of the bands at 1782, 1745 and 962  $\text{cm}^{-1}$  must be attributed to the formation of the corresponding SOE, from which the poly(ether-ester) units are formed upon polymerization.

The partial overlapping of cyclic and linear carbonyl ester absorptions hindered a quantification of the evolution of the linear ester group on curing. However, the disappearance of MDM could be quantified from the 962  $\text{cm}^{-1}$  absorption. The incorporation of the epoxy group into the network was followed by the diminution of the 912  $\text{cm}^{-1}$  band. The evolution of MDM and epoxy with both initiators is represented in **Figures 2 and 3**, respectively. We can see a different evolution of the conversions of MDM with both initiators, whereas there are not big differences in the evolution of epoxy groups. To understand the reactive process, we should take into account that in the reactive mixture there are four epoxy groups per MDM group. Thus, lanthanum salt, in the initial steps, leads to a quicker evolution of MDM in comparison with epoxide, and this indicates that in addition to the formation of SOE, a superficial elimination, facilitated by the easy sublimation, also occurs. This fact is related to the low proportion of linear ester groups in the final material (**Figure 4**).

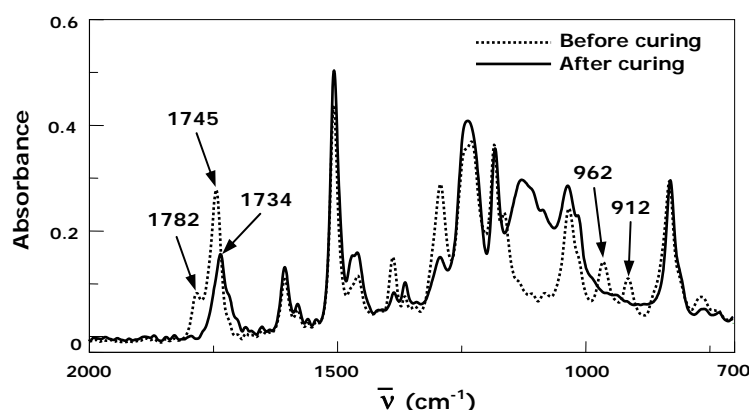


**Figure 1.** ATR-FTIR spectra of a mixture of DGEBA and MDM 2:1 (mol/mol) with 0.015 mol of  $\text{Yb}(\text{OTf})_3$  before and after curing at 150°C

In contrast, with the ytterbium salt, the SOE formation and the homopolymerization of epoxide occur simultaneously from the beginning of curing, and a much lower elimination by sublimation of MDM occurs (**Figure 2**). This is confirmed by the FTIR spectrum of the final material, in which the use of  $\text{Yb}(\text{OTf})_3$  produces a high proportion of linear ester.

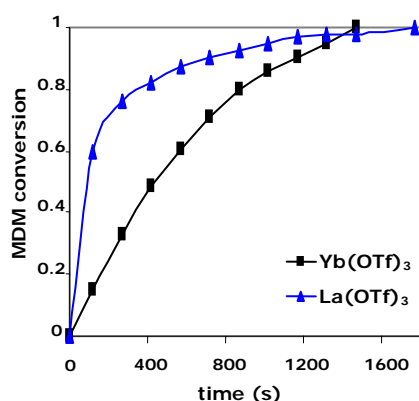


**Figure 2.** MDM conversion degree ( $965\text{ cm}^{-1}$ ) versus time for the DGEBA/MDM 2:1 (mol/mol) formulation with both initiators during curing at  $150^\circ\text{C}$  by ATR-FTIR

This different behaviour can be related to the higher Lewis acid character of the ytterbium cation, which leads to a quicker curing, and so a lower elimination of MDM by sublimation occurs. From the normalized areas of the carbonyl linear ester absorption in both spectra (**Figure 4**), we can estimate that the relation of linear ester groups in both materials is about 3.5.

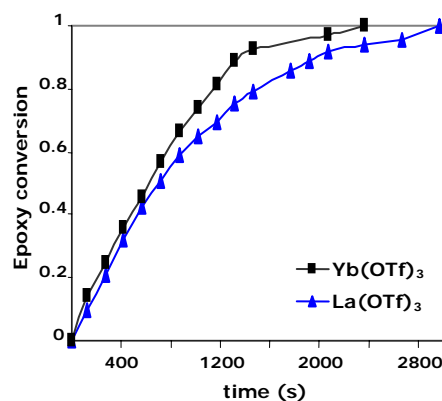


**Figure 3.** Epoxy conversion degree ( $912\text{ cm}^{-1}$ ) versus time for the DGEBA/MDM 2:1 (mol/mol) formulation with both initiators during curing at  $150^\circ\text{C}$  by ATR-FTIR

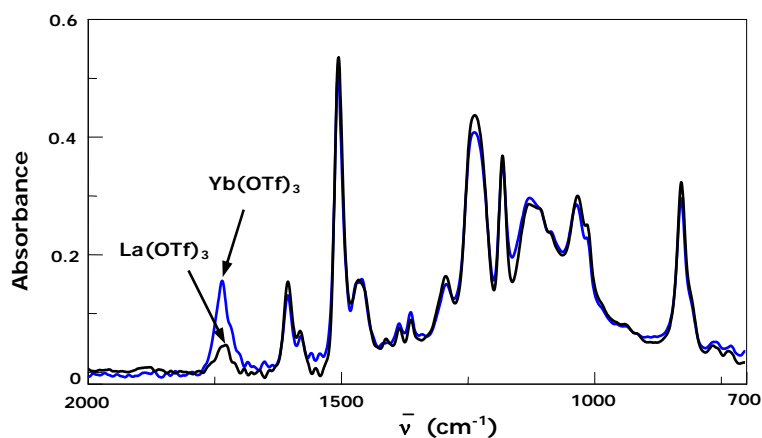


**Figure 4.** ATR-FTIR spectra of the materials obtained after curing at  $150^\circ\text{C}$  from DGEBA/MDM mixtures (2:1 mol/mol) with 0.015 mol of ytterbium or lanthanum triflates

### 3.2. Calorimetric studies

The curing of the mixtures was studied, and  $T_g$  of the materials was determined by means of calorimetry. **Table 1** shows the results obtained.  $T_g$ 's are similar for both initiators, but with the amount of MDM in the mixture increasing,  $T_g$  slightly decreases because of the flexibility introduced by the linear ester moiety. The experimental reaction enthalpy decreases when the proportion of MDM increases. This is due to the low opening enthalpy that has evolved from the nonstrained MDM ring. The heat released per epoxy equivalent is not as different but is slightly lower when lanthanum

triflate is the initiator, and this can be justified by the endothermic sublimation process of MDM. The values from the curing of pure DGEBA with both initiators were added to the table for comparison with the mixtures. The maximum of the curing exotherm shifts to lower temperatures as the proportion of MDM increases, but it is higher for the lanthanum initiator, indicating lower reactivity.

**Table 1** shows the kinetic parameters associated with the dynamic curing by DSC for a conversion of 0.5. The values of the activation energies are similar for all the mixtures, but they are higher for the systems initiated by ytterbium triflate.

**Table 1.** Calorimetric data and kinetic parameters of the curing of several formulations initiated by Lanthanide Triflates

Entry	Formulation <sup>a</sup>	$T_g^b$ (°C)	$\Delta H^c$ (J/g)	$\Delta H^d$ (kJ/ee)	$T_{max}^e$ (°C)	$E_a^f$ (kJ/mol)	$\ln A^g$ (s <sup>-1</sup> )	$k_{150^\circ C} \cdot 10^3^h$ (s <sup>-1</sup> )
1	DGEBA/Yb 1:0.006	135	519.7	95.6	184	90.7	18.09	0.45
2	DGEBA/MDM/Yb 3:1:0.021	111	427.6	91.1	175	86.5	17.35	0.70
3	DGEBA/MDM/Yb 2:1:0.015	107	396.5	90.1	174	87.9	17.74	0.71
4	DGEBA/MDM/Yb 1:1:0.009	96	325.4	88.2	174	90.1	18.46	0.78
5	DGEBA/La 1:0.006	127	513.5	94.4	192	79.8	14.59	0.30
6	DGEBA/MDM/La 3:1:0.021	110	422.1	89.8	190	81.6	15.40	0.41
7	DGEBA/MDM/La 2:1:0.015	105	394.1	89.6	188	80.4	15.15	0.44
8	DGEBA/MDM/La 1:1:0.009	91	308.6	84.8	176	76.6	14.05	0.45

- a. The composition of the formulations is given in molar ratios  
 b. Glass-transition temperature obtained by DSC in the second scan after dynamic curing  
 c. Enthalpy per gram of mixture  
 d. Enthalpy per equivalent of epoxy groups  
 e. Temperature of the maximum degradation rate calculated by thermogravimetry  
 f. Activation energy evaluated by the isoconversional integral method (Eq.(3)) applied at conversion of 0.5  
 g. Pre-exponential factor for kinetic model  $R_3$  in which  $g(\alpha)=[1-(1-\alpha)^{1/3}]$   
 h. Rate constant at 150°C calculated with the Arrhenius equation:

$$\ln k = \ln A - \frac{E}{RT}$$

This trend is not very significant and does not clearly show the acceleration effect of the MDM due to the compensation effect between the activation energy and the pre-exponential factor.<sup>16,21</sup>

To show more clearly the effect of MDM on the curing kinetics, the rate constant at 150°C was calculated. It can be seen that the addition of MDM increases the rate constant, causing the curing reaction to accelerate. Ytterbium triflate leads to higher rate constants, which can be attributed to the higher Lewis acidity of the cation. **Figure 5** shows plots of the conversion degree against the temperature for the mixtures with different proportions of MDM initiated by ytterbium and lanthanum triflates. In both cases, the addition of MDM accelerates the curing process in the entire range in comparison with pure DGEBA. However, there are some slight differences between the effects of both initiators. With ytterbium triflate, the increase in the proportion of MDM in the curing

mixture leads to a slight progressive acceleration in the entire range. On the other hand, lanthanum triflate leads to a different behaviour before and after 50% conversion, especially with the mixture containing the highest proportion of MDM. This behaviour could be explained on the basis of the sublimation process of MDM previously mentioned and by the different extent to which each reaction occurs during curing.

**Figure 6** shows the dependence of the activation energy on the degree of conversion calculated with the isoconversional method (Eq. (3))<sup>22</sup> for all the samples studied. As we can see, with ytterbium triflate, the higher the proportion is of MDM, the higher the initial activation energy is, but over 40% conversion, the differences among them are slight, and all are lower than that of pure DGEBA, which has been introduced as a reference. However, a different trend is observed for lanthanum triflate initiated curing.

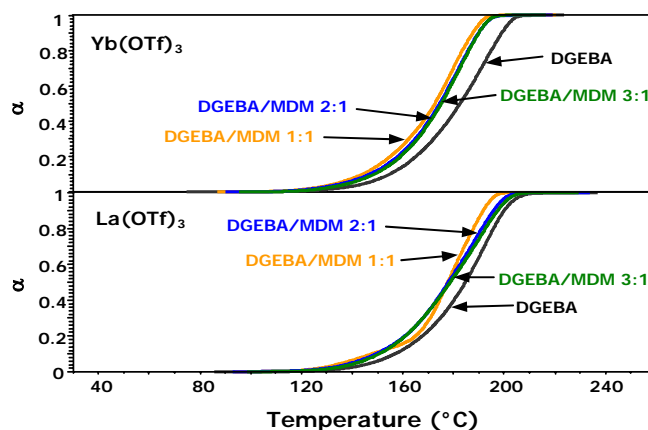


**Figure 5.** Conversion degree ( $\alpha$ ) versus the temperature of curing for DGEBA and DGEBA/MDM mixtures with different molar ratios initiated by  $\text{Yb}(\text{OTf})_3$  or  $\text{La}(\text{OTf})_3$  from dynamic DSC experiments

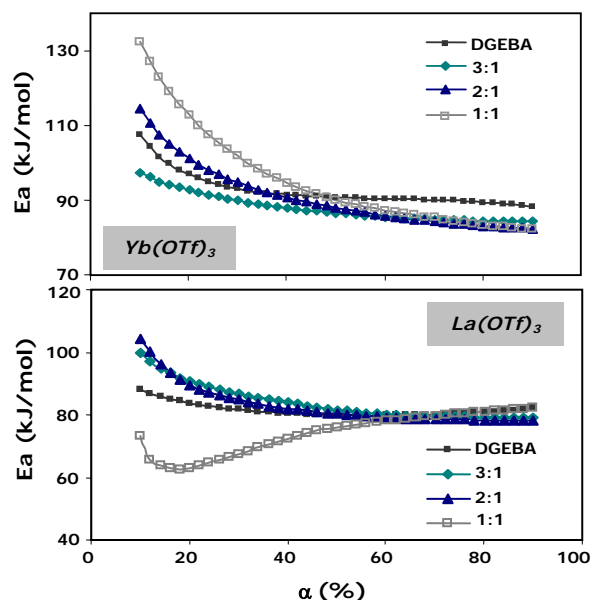


**Figure 6.** Dependence of activation energy ( $E_a$ ) on the degree of conversion ( $\alpha$ ) for DGEBA and DGEBA/MDM (mol/mol) formulations initiated  $Yb(OTf)_3$  or  $La(OTf)_3$

In this case, lower activation energy in the first part of the process is observed for the DGEBA/MDM 1:1 (mol/mol) mixture, whereas similar values are observed for the other samples, possibly because of the sublimation process, which overlaps with curing. With over 60% conversion, all the samples have similar activation energies. The general decrease observed between degrees of conversion of 10-60% can be related to the autocatalytic effect.

### 3.3. Thermogravimetric studies

In a previous study<sup>9</sup> we demonstrated the enhanced degradability of thermosets obtained by copolymerization of DGEBA with MCP due to the formation of ter-

tiary ester groups in the network. From the analysis of the volatiles that evolved on heating, we could detect the rupture of these ester groups but also the breakage of the ether linkages. These ruptures occurred at lower temperatures when ytterbium triflate was used as the initiator.

**Figure 7** shows the TGA and differential thermogravimetry (DTG) curves for the degradation of the materials obtained from the DGEBA/MDM 2:1 (mol/mol) formulation initiated with ytterbium and lanthanum salts. The thermal stability of the material obtained with lanthanum triflate is higher, and the bimodal shape of its DTG curve is most characteristic. In the previous study with MCP,<sup>9</sup> we ob-

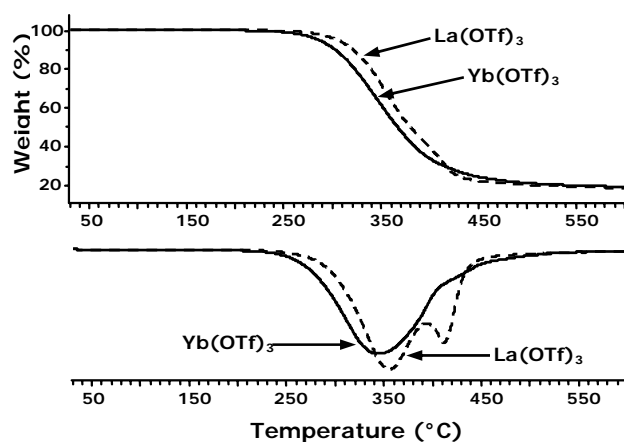


**Figure 7.** TGA and DTG curves at 10°C/min in a N<sub>2</sub> atmosphere of two thermosetting materials obtained from DGEBA/MDM 2:1 (mol/mol) formulation initiated by 0.015 mol of ytterbium or lanthanum triflates

served a three modal DTG curve for the analogous material, with a broad peak at a lower temperature, which is not found in the MDM curves. Therefore, we think that the spiranic structure of MCP facilitated the degradative process.

**Table 2** collects the thermogravimetric data obtained for all the formulations studied. Again, in this work, we can confirm that when the proportion of the lactone is increased, the degradability of the material also increases, and the materials obtained with ytterbium triflate begin their degradation at lower temperatures than those obtained with lanthanum triflate. This fact may be related to the higher content of linear ester group in the network and also to the catalytic effect of ytterbium in the degradation. The catalytic effect should contribute because the same trend can be observed in samples 1 and 5, in which there are no ester groups. The addition of lactone to DGEBA sam-

ples mainly affects the initial steps of the process, and this is worth it to increase the reworkability of the electronic devices. If we compare the temperatures of the initial degradation with those previously published, we can conclude that the spiranic MCP lactone favors degradation.<sup>9</sup>

The kinetic parameters for the degradation ( $E_a$ ,  $A$  and  $k$ ) were calculated only for the ytterbium triflate cured materials, which show a unimodal degradation curve, because the appearance of more than one peak for lanthanum triflate cured materials makes the kinetic comparison difficult. Using a procedure similar to that previously described for the curing of DGEBA/MDM mixtures, we obtained the values collected in **Table 3**. The values of  $k$  confirm a quicker degradation of the materials when a higher proportion of MDM is added for the modification of DGEBA. Moreover, the values of  $k$  are slightly lower than those



**Table 2.** Thermogravimetric data, densities and shrinkage of the materials obtained from the different formulations studied

Entry	Formulation <sup>a</sup>	T <sup>b</sup> (°C)	T <sub>max</sub> <sup>c</sup> (°C)	Char Yield <sup>d</sup> (%)	δ <sub>im</sub> (g/cm <sup>3</sup> )	δ <sub>fm</sub> (g/cm <sup>3</sup> )	Shrinkage (%)
1	DGEBA/Yb 1:0.006	287	345	20	1.158	1.192	2.9
2	DGEBA/MDM/Yb 3:1:0.021	265	337	19	1.165	1.191	2.2
3	DGEBA/MDM/Yb 2:1:0.015	262	340	18	1.167	1.190	2.0
4	DGEBA/MDM/Yb 1:1:0.009	253	355	17	-	-	-
5	DGEBA/La 1:0.006	303	354	19	1.158	1.193	3.0
6	DGEBA/MDM/La 3:1:0.021	286	361	18	1.161	1.192	2.7
7	DGEBA/MDM/La 2:1:0.015	282	355	18	1.164	1.193	2.5
8	DGEBA/MDM/La 1:1:0.009	272	373	17	-	-	-

- a. The composition of the formulations is given as molar ratios  
 b. Temperature of 2 % weight loss calculated by thermogravimetry  
 c. Temperature of the maximum degradation rate calculated by thermogravimetry  
 d. At 600°C

**Table 3.** Kinetic parameters of the thermal decomposition of Ytterbium Triflate initiated materials

Entry	Formulation <sup>a</sup>	Ea <sup>b</sup> (kJ/mol)	ln A <sup>c</sup> (s <sup>-1</sup> )	k <sub>300°C</sub> · 10 <sup>3</sup> (s <sup>-1</sup> ) <sup>d</sup>
1	DGEBA/Yb 1:0.006	155.4	23.43	0.1016
2	DGEBA/MDM/Yb 3:1:0.021	160.8	24.83	0.1340
3	DGEBA/MDM/Yb 2:1:0.015	144.0	21.55	0.1715
4	DGEBA/MDM/Yb 1:1:0.009	105.2	14.00	0.3016

- a. The composition of the formulations is given as molar ratios  
 b. Activation energy evaluated by the isoconversional integral method applied at a conversion of 0.5  
 c. Pre-exponential factor for the kinetic model with n=3, in which g(α)=2<sup>-1</sup>[-1+(1-α)<sup>2</sup>]  
 d. Rate constant at 300 °C calculated with the Arrhenius equation:

$$\ln k = \ln A - \frac{E}{RT}$$

obtained from the modification of DGEBA with MCP.

### 3.4. Shrinkage

In a previous work<sup>8</sup> we put into evidence the expandable character of MCP in its cationic copolymerization with DGEBA, in which we observed that the higher the proportion was of MCP in the sample, the lower the overall shrinkage was. However, the most important fact is the shrinkage after gelation because it occurs in the gel state

when the material lacks mobility and is the cause of the internal stresses in the material, which make its properties as a coating worse.<sup>20</sup> Furthermore, when a monomer with a functionality of two (MCP or MDM) is added to another with a functionality of four (DGEBA), the network's crosslink density decreases, and the degree of conversion at the gelation point increases.<sup>23,24</sup> This fact was experimentally proved in similar systems by thermomechanical analyses.<sup>4</sup>

The expandable character of MCP was proved and attributed to the change in the dipolar moment by opening of the lactone ring.<sup>8</sup> Moreover, the amount of shrinkage is related to the size of the ring being opened; in general, the larger the ring is, the smaller the shrinkage is.<sup>20</sup> Therefore, six-membered lactones should produce a larger expansion on polymerizing than the five-membered lactones. However, as we said before, we cannot discard a possible influence of the spiranic structure. Therefore, the evaluation of the shrinkage during curing of DGEBA/MDM mixtures could shed light on the origin of the expandable character.

**Table 2** shows the densities of the mixtures before and after curing and the calculated global shrinkage. As we can see, the addition of MDM leads to a higher density of the uncured mixture and to a reduction of the shrinkage, which is more important for the ytterbium salt initiated curing because of the incorporation of a higher proportion of MDM. The lower shrinkage is a result of the higher extension extent of the polymerization reactions in which SOEs open. It should be mentioned that the formation of SOE, which takes place at the beginning of the curing, occurs with shrinkage whereas its opening occurs with expansion at the end of the process. In this way, the shrinkage in the gel state is much lower. Because of the reduction of the global shrinkage found experimentally in the DGEBA/MDM curing, we could confirm the expandable character of the substituted MA ring, which on opening

should reduce the interactions between the polymeric chains, because of the change in the dipolar moment. In previous studies with other five-membered lactones,<sup>2,4</sup> we did not observe a reduction of the global shrinkage, but the shrinkage after gelation was reduced when the proportion of lactone was increased in the reactive mixture.

The results obtained in this study allow us confirm that the copolymerization of DGEBA epoxy resins with functional cyclic monomers is a convenient route to simultaneously improve some properties of epoxy therosets.

#### 4. CONCLUSIONS

The modification of DGEBA by copolymerization with MDM using ytterbium and lanthanum triflates as initiators incorporated tertiary linear ester moieties into the network (in higher proportions with ytterbium triflate).

The addition of MDM to the DGEBA resins accelerates the curing process, the curing rate being higher in the ytterbium-initiated samples because of the higher Lewis acidity of the cation. The addition of MDM to DGEBA slightly reduces Tg of the materials.

The expandable character of MDM has been demonstrated by the reduction of the global shrinkage upon curing of mixtures of DGEBA and MDM.

The degradability of the materials increases with the proportion of MDM, and ytterbium triflate leads to a higher degradability.

### Acknowledgements

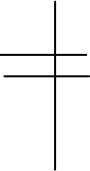
The authors from the Universitat Politècnica de Catalunya would like to thank CICYT and FEDER (MAT2004-04165-C02-02) for their financial support. The authors from the Rovira i Virgili University would like to thank the CICYT (Comisión Interministerial de Ciencia y Tecnología) and FEDER (Fondo Europeo de Desarrollo Regional) (MAT2005-01806).

### 5. REFERENCES

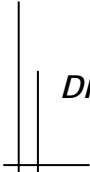
1. Ivin, J.K.; Saegusa, T. "Ring Opening Polymerization" Vol. 1; 1. Ivin J.K.; Saegusa, T., Eds.; Elsevier Science: New York, 1984.
2. Mas, C.; Ramis, X.; Salla, J.M.; Mantecón, A.; Serra, A. J Polym Sci Part A: Polym Chem 2003, 41, 2794-2808.
3. Giménez, R.; Fernández-Francos, X.; Salla, J.M.; Serra, A.; Mantecón, A.; Ramis, X. J Polym Sci Part A: Polym Chem 2005, 43, 10637-10647.
4. Mas, C.; Ramis, X.; Salla, J.M.; Mantecón, A.; Serra, A. J Polym Sci Part A: Polym Chem 2006, 44, 1711-1721.
5. Wang, L.; Li, H.; Wong, C.P. J Polym Sci Part A: Polym Chem 2000, 38, 3771-3782.
6. Li, H.; Wong, C.P. IEEE Trans Adv Packaging 2004, 27, 165-172.
7. Chen, J-S.; Ober, C.K.; Poliks, M.D.; Zhang, Y.; Wiesner, U.; Cohen, C.; Polymer 2004, 45, 1939-1950.
8. González, L.; Ramis, X.; Salla, J.M.; Mantecón, A.; Serra, A. J Polym Sci Part A: Polym Chem 2006, 44, 6869-6879.
9. González, L.; Ramis, X.; Salla, J.M.; Mantecón, A.; Serra, A. Polym Degrad Stab 2007, 92, 596-604.
10. Garcia, S.J.; Serra, A.; Suay, J.; J Polym Sci Part A: Polym Chem in press
11. Kobayashi, S., Ed. "Lanthanides: Chemistry and Use in Organic Synthesis" Topics in Organometallic Chemistry, Springer Verlag, Berlin, 1999.
12. Davidson, D.; Bernhard, A. S. J Am Chem Soc 1948; 70: 3426-3428.
13. Coats, A.W.; Redfern, J.P. Nature 1964; 201: 68-69.
14. Kissinger, H.E. Anal Chem 1957; 29: 1702-1706.
15. Boey, F.Y.C.; Qiang, W. Polymer 2000; 41: 2081-2094.
16. Xiong, Y.; Boey, F.Y.C.; Rath, S.K. J Appl Polym Sci 2003, 90, 2229-2240.
17. Criado, J.M. Thermochim Acta 1978; 24: 186-189.
18. Ramis, X.; Salla J.M.; Cadenato, A.; Morancho, J.M. J Therm Anal Cal 2003; 72: 707-718.
19. Bailey, W.J.; Sun, R.L. Polym Prepr ACS div, Polym Chem 1972; 13: 281.
20. Sadhir, R.K.; Luck, M.R. Ed. "Expanding Monomers. Synthesis, Characterization and Applications" CRC Press, Boca Raton, 1992.
21. Vyazovkin, S.; Linert, W., J Solid State Chem 1995; 114: 392-398.
22. Vyazovkin, S.; Lesnikovich, A. Thermochim Acta 1992; 203: 177-185.
23. Flory, P.J. "Principles of Polymer Chemistry" Cornell University Press, Thac, New York, 1953.
24. González, S.; Fernández-Francos, X.; Salla, J.M.; Serra, A.; Mantecón, A.; Ramis, X. J Polym Sci Part A: Polym Chem 2007, 45, 1968-1979.




**3.7.**



*NEW POLY (ETHER-ESTER) THERMOSETS OBTAINED BY  
CATIONIC CURING OF DGEBA AND 7,7-DIMETHYL-6,8-  
DIOXASPIRO[3.5]NONANE-5,9-DIONE WITH SEVERAL LEWIS  
ACIDS AS INITIATORS*



---



**NEW POLY(ETHER-ESTER) THERMOSETS OBTAINED BY CATIONIC  
CURING OF DGEBA AND 7,7-DIMETHYL-6,8-DIOXASPIRO[3.5]  
NONANE-5,9-DIONE WITH SEVERAL LEWIS ACIDS AS INITIATORS**

Lidia González,<sup>1</sup> Xavier Ramis,<sup>2</sup> Josep Maria Salla,<sup>2</sup>  
Ana Mantecón,<sup>1</sup> Angels Serra<sup>1\*</sup>

<sup>1</sup>Departament de Química Analítica i Química Orgànica. Universitat Rovira i Virgili. Marcel·lí Domingo s/n, 43007 Tarragona, Spain

<sup>2</sup>Laboratori de Termodinàmica, ETSEIB. Universitat Politècnica de Catalunya, Av. Diagonal 647, 08028 Barcelona, Spain

*Received 2 July 2007; accepted 10 October 2007*

*DOI: 10.1002/pola. 22464*

---

**Abstract**

Scandium, ytterbium and lanthanum triflates and boron trifluoride monoethylamine were used as cationic initiators to cure a mixture 2:1 (mol/mol) of diglycidylether of bisphenol A (DGEBA) and 7,7-dimethyl-6,8-dioxaspiro[3.5]nonane-5,9-dione (MCB). The evolution of the epoxy and lactone during curing and the linear ester groups in the final materials were evaluated by Fourier Transform Infrared in the attenuated-total-reflection mode. The kinetic parameters of the curing process were calculated from DSC analysis applying isoconversional procedures. The shrinkage on curing and the thermal degradability of the materials on varying the initiator used were evaluated. The expandable character of MCB was confirmed. The materials obtained were more degradable than conventional epoxy resins due to the tertiary ester groups incorporated in the network by copolymerization.

**Keywords:** Epoxy resins, lactones, cationic polymerization, cross-linking, thermoset

---

## 1. INTRODUCTION

Epoxy thermosets are applied in many industrial applications such as castings, coatings, mould replication and microelectronics. However, the shrinkage during curing, which leads to poor adhesion to the substrate, delamination and microvoids and microcracks formation, reduces the durability of the materials and produces internal stress. Bailey<sup>1</sup> introduced the term *expanding monomers*, which refers to monomers that lead to low shrinkage or even expansion on polymerizing. Among them, spiroorthoesters (SOEs), which can be synthesized from epoxy groups and lactones in the presence of a Lewis acid, leads to polymerization in cationic conditions with low or zero volume change. Moreover, ring-opening polymerization leads to a lower shrinkage during curing than other mechanisms, because when a cyclic monomer opens, a covalent bond is converted into a Van der Waals distance, which reduces the shrinkage produced in the formation of covalent bonds between monomer molecules.<sup>2</sup> It is reported that the degree of shrinkage is related to the size of the ring being opened; in general, the larger the ring, the smaller the shrinkage.<sup>2</sup> Therefore, six membered lactones should produce a lower shrinkage on polymerizing than the five membered lactones,

which were used in previous studies.<sup>3,4,5</sup> However, the most important feature is the shrinkage after gelation, because it occurs in the gel state, when the material lacks mobility and shrinkage is the cause of the internal stresses in the material, which make worse the properties of the materials as coating. Furthermore, when a monomer with a functionality of two, as a lactone, is added to another with a functionality of four, as DGEBA, the network's crosslink density diminishes and the degree of conversion at the gelation point increases.<sup>6,7</sup>

This article focuses on the preparation of new materials by copolymerization of a conventional epoxy resin (DGEBA) with 7,7-dimethyl-6,8-dioxaspiro [3.5] nonane-5,9-dione (MCB), which through the formation of an intermediate SOE leads to poly(ether-ester) three-dimensional structures and a reduction of the shrinkage during curing, specially after gelation.

Rare earth triflates are commercially available Lewis acids that maintain their catalytic activities even in water and are regarded as environmentally friendly catalyst.<sup>8,9</sup> Generally, scandium triflate shows a higher catalytic activity than lanthanide triflates due to its higher Lewis acidity attributed to its small ionic radius. Lanthanide triflates can act as cationic initiators in the curing of epoxy resins.<sup>10</sup> Thus, in this work we test

the effectiveness of scandium, ytterbium and lanthanum triflates and we compare them with the conventionally used  $\text{BF}_3 \cdot \text{MEA}$  complex.

In addition to the reduction of the shrinkage, another advantage of the copolymerization of epoxy resins with lactones is the introduction of polyester moieties in the network making it more thermally degradable, because they have more labile links than polyethers, and therefore, some authors insert ester groups into the networks for preparing reworkable thermosets.<sup>11,12</sup> The polymeric material cannot be recycled but it can be breakdown under controlled conditions to remove it from the substrate, enabling the repairing or recycling of electronic devices assembled with such materials.

In addition, catalytic epoxy curing usually leads to brittle materials because of the high density of crosslinking achieved. The copolymerization with lactones reduces the crosslinking density and increases the flexibility. Thus, the mechanical properties can be improved by this strategy such as it was demonstrated by curing mixtures of DGEBA and Meldrum acid initiated with erbium triflate.<sup>13</sup>

## 2. EXPERIMENTAL

### 2.1. Materials

DGEBA EPIKOTE RESIN 827 from Shell Chemicals (Epoxy Equiv.=182.08 g/eq), cyclobutane-1,1-dicarboxylic acid (Aldrich) and

isopropenylacetate (Aldrich) were used as received.

Lanthanum (III), ytterbium (III) and scandium (III) trifluoromethanesulfonates and borontrifluoride monoethylamine (Aldrich) were used without purification.

Organic solvents were purified by standard methods.

### 2.2. Synthesis of MCB

The synthesis was performed following the detailed procedure described for a similar compound.<sup>14</sup> To a stirred suspension of cyclobutane-1,1-dicarboxylic acid (2.88g, 0.002mol) and isopropenyl acetate (2.20g, 0.022mol) was added dropwise over 30min 0.36g of concentrated sulphuric acid. The resulting clear solution was stirred for an additional 30min and maintained at 0°C overnight. Upon dilution with 20ml of cool water, a solid was obtained by filtration. The solid was twice washed with 5ml portions of cool water and dried to afford the pure MCB (yield 85 %). M.p. 77-78 °C, (lit.<sup>15</sup> 81°C)

$^1\text{H}$  NMR ( $\text{CDCl}_3$ ,  $\delta$  (ppm)): 1.69 (singlet, 6H,  $\text{CH}_3^-$ ); 2.30 (quintuplet, 2H,  $\text{CH}_2$ ), 2.76 (triplet, 4H,  $\text{CH}_2$ ).

$^{13}\text{C}$  NMR ( $\text{CDCl}_3$ ,  $\delta$  (ppm)): 16.36, 28.67, 30.71, 46.46, 104.78, 169.89

IR ( $\text{cm}^{-1}$ ): 1769, 1731, 1396, 1383, 1360, 1306, 1202, 1168, 1099, 1073, 1054, 997, 976, 938, 842.

Elemental Analysis ( $\text{C}_9\text{H}_{12}\text{O}_4$ ) (%) Calc: C 58.69, H 66.62; Found C, 57.41, H 67.12

### 2.3. Preparation of the curing mixtures

The samples were prepared by mixing the selected initiator in the corresponding amount of MCB and adding the required proportion of DGEBA with manual stirring. The prepared mixtures were kept at  $-18^{\circ}\text{C}$  before use. Rare earth triflates were added in a molar ratio of 0.006 mols per mol of DGEBA and 0.003 mols per mol of MCB.  $\text{BF}_3\cdot\text{MEA}$  was added in a molar ratio of 0.096 mols per mol of DGEBA and 0.048 mols per mol of MCB. Previous experiments showed that these amounts are necessary to reach the complete curing rare earth triflates and for  $\text{BF}_3\cdot\text{MEA}$  respectively.

### 2.4. Characterization and measurements

Calorimetric studies were carried out on a Mettler DSC-821e thermal analyzer in covered Al pans under  $\text{N}_2$  at  $10^{\circ}\text{C}/\text{min}$ . The calorimeter was calibrated using an indium standard (heat flow calibration) and an indium-lead-zinc standard (temperature calibration). The samples weighed approximately 7-9mg. In the dynamic curing process the degree of conversion by DSC ( $\alpha_{\text{DSC}}$ ) was calculated as follows:

$$\alpha_{\text{DSC}} = \frac{\Delta H_T}{\Delta H_{\text{dyn}}} \quad (1)$$

where  $\Delta H_T$  is the heat released up to a temperature  $T_i$  obtained by integration of the calorimetric signal up to this temperature, and

$\Delta H_{\text{dyn}}$  is the total reaction heat associated with the complete conversion of all reactive groups. The glass transition temperature for each material ( $T_g$ ) was calculated after complete curing, by means of a second scan, as the temperature of the half-way point of the jump in the heat capacity when the material changed from the glassy to the rubbery state.

The isothermal curing process at  $150^{\circ}\text{C}$  was monitored with a Fourier Transform Infrared (FTIR) spectrophotometer FTIR-680PLUS from JASCO with a resolution of  $4\text{cm}^{-1}$  in the absorbance mode. An attenuated-total-reflection (ATR) accessory with thermal control and a diamond crystal (Golden Gate heated single-reflection diamond ATR, Specac-Teknokroma) was used to determine FTIR spectra. The conversions of the reactive groups were determined from the normalized changes in absorbance by the Lambert-Beer law, as we explained previously.<sup>3</sup> After isothermal curing in the FTIR-ATR device, a dynamic scan by DSC was always carried out to prove that the curing was complete.

Thermogravimetric analyses (TGAs) were carried out with a Mettler TGA/SDTA 851e thermobalance. Cured samples with an approximate mass of 7mg were degraded between 30 and  $600^{\circ}\text{C}$  at a heating rate of  $10^{\circ}\text{C}/\text{min}$  in  $\text{N}_2$  ( $200\text{ cm}^3/\text{min}$ ) measured in normal conditions.

The densities of the materials before and after curing were determined using a Gas Pycnometer Micromeritics AccuPyc 1330 thermostated at  $30^{\circ}\text{C}$ .



## 2.5. Kinetic analysis

Integral nonisothermal kinetic analysis was used to determine the kinetic triplet ( $A$  pre-exponential factor,  $E$  activation energy and  $g(\alpha)$  integral function of degree of conversion).

Nonisothermal kinetic analysis may start with the kinetic equation:

$$\beta \frac{d\alpha}{dT} = A \exp\left(\frac{-E}{RT}\right) f(\alpha) \quad (2)$$

where  $\beta$  is the heating rate,  $\alpha$  is the conversion,  $R$  is the universal gas constant,  $T$  is the temperature and  $f(\alpha)$  is the differential conversion function.

By using the Coats-Redfern<sup>16</sup> approximation to resolve the so-called temperature integral and considering that  $2RT/E$  is much lower than 1, the Kissinger-Akahira-Sunose (KAS) equation may be written as:<sup>17</sup>

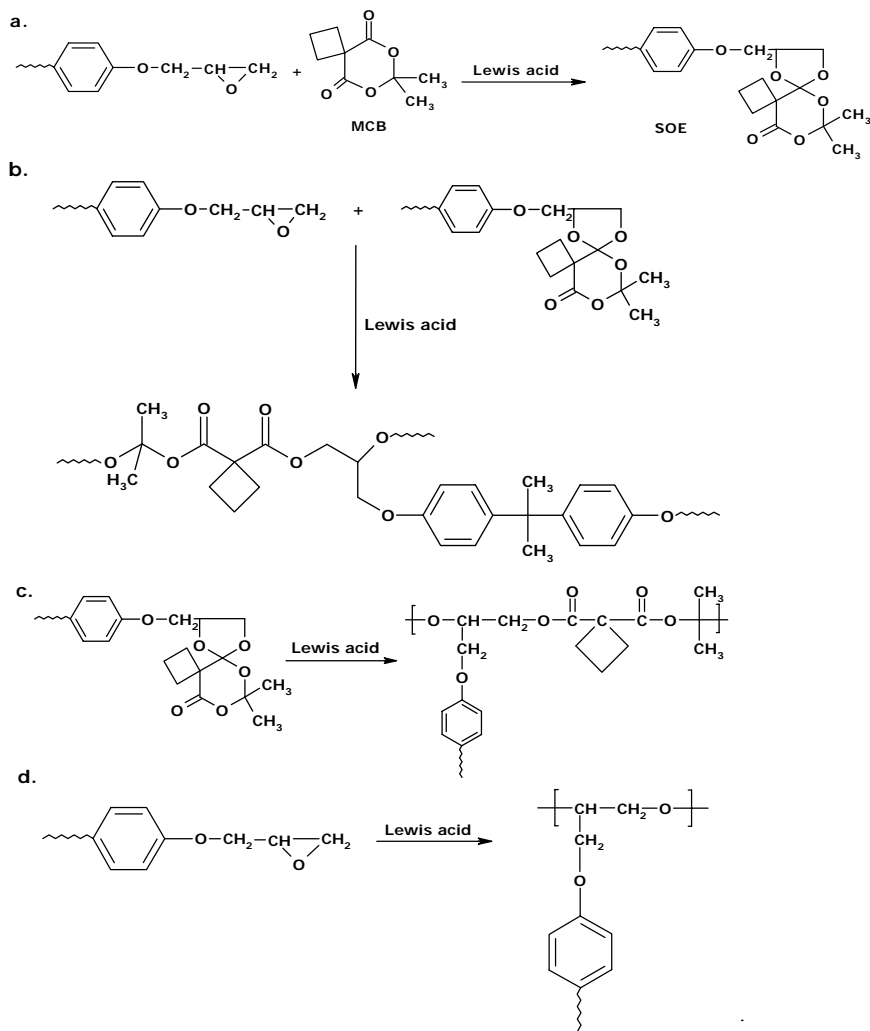
$$\ln \frac{\beta}{T^2} = \ln \left[ \frac{AR}{g(\alpha)E} \right] - \frac{E}{RT} \quad (3)$$

For each conversion degree, the linear representation of  $\ln[\beta/T^2]$  versus  $T^{-1}$  enables  $E$  and  $\ln[AR/g(\alpha)E]$  to be determined from the slope and the ordinate in the origin. If the reaction model,  $g(\alpha)$ , is known, for each conversion the corresponding pre-exponential factor can be calculated for every activation energy. In this article, to assign a reaction model to the systems studied, we used the Criado's reduced master curves procedure,<sup>18</sup> which is described elsewhere.<sup>19</sup> Different kinetic models have been studied: diffusion ( $D_1$ ,

$D_2$ ,  $D_3$  and  $D_4$ ), Avrami-Erofeev ( $A_2$ ,  $A_3$  and  $A_4$ ), power law, phase-boundary-controlled reaction ( $R_2$  and  $R_3$ ), autocatalytic ( $n+m = 2$  and  $3$ ) and  $n$  order ( $n = 1, 2$  and  $3$ ).<sup>18</sup> We found that the curing of the systems studied follows a kinetic model of the surface-controlled reaction type  $R_3$ , with  $g(\alpha)=[1-(1-\alpha)^{1/3}]$ . The rate constants,  $k$ , were calculated with  $E$  and  $A$  determined at  $\alpha = 0.5$ , using the Arrhenius equation.

## 3. RESULTS AND DISCUSSION

In previous works we studied the curing of mixtures of DGEBA epoxy resin with a cyclopropenylic spiranic Meldrum acid derivative (MCP) using lanthanide triflates and  $\text{BF}_3 \cdot \text{MEA}$  as initiators.<sup>20,21,22</sup> The thermosets obtained showed a good thermal degradability and a lower shrinkage on curing than pure DGEBA materials. Moreover, the addition of MCP to DGEBA accelerated the curing process, which is more important in advanced steps of curing. Some kinetic differences were observed on changing the initiator. MCP has the advantage of being commercially available but the high stress of the cyclopropanic ring can lead to unexpected reactions, which could be the reason for the expandable character of MCP and its influence on the curing evolution. Therefore, we synthesized a less strained Meldrum acid derivative, MCB, which is not a commercial product.



Scheme 1

MCB presents a cyclobutenyl instead of the cyclopropenyl group of MCP in Meldrum acid (**Scheme 1**). One of the aims of our studies is the introduction of a high proportion of ester groups into the network. However, in the basis of our experience with other

lactones, we selected the proportion DGEBA/MCB 2:1 (mol/mol), which led to better features of the final materials than equimolecular mixtures.<sup>3,20</sup>

To prepare MCB, firstly we tested the direct alkylation of Meldrum acid<sup>23</sup> with 1,3-dibromo-

propane, sodium carbonate and DMF under inert atmosphere obtaining an unsatisfactory yield. Therefore, we followed a procedure described for analogous spiranic derivatives of Meldrum acid. This procedure, which involves the reaction of cyclobutane-1,1-dicarboxylic acid with isopropenyl acetate, gave the expected product with a high yield. The preparation of MCB was described by the *in situ* formation of isopropenyl acetate from acetone, acetic anhydride and sulphuric acid and reaction with cyclobutane-1,1-dicarboxylic acid.<sup>15</sup>

### 3.1. Study of the curing process by DSC

The copolymerization of DGEBA and MCB is a complex process where four different reactions can occur in a different extension, which depends on the proportion of comonomers in the mixture and on the type of initiator used. These reactions are represented in **Scheme 1**. These reactions are: (a) formation of the SOE; (b) copolymerization of SOE and epoxy groups; (c) homopolymerization of SOE; and (d) homopolymerization of epoxy groups, which are in excess. It was experimentally proved that MCB does not homopolymerize in these conditions and therefore it was not included in the scheme.

By means of calorimetry the overall curing process was studied. **Figure 1** shows the calorimetric curves and the conversion degrees against temperature for all the initiators for pure DGEBA and DGEBA/MCB mixtures.  $\text{BF}_3\cdot\text{MEA}$  initiated curings exhibit exotherms

and evolutions of conversion degrees with a different shape than rare earth triflates. This fact seems to indicate a different kinetic behaviour. Thus, the systems with  $\text{BF}_3\cdot\text{MEA}$  reach the maximum curing rates at low conversions, whereas rare earth triflates lead to the highest curing rate at high conversions. This different behaviour was previously observed in the curing of DGEBA/MCP formulations.<sup>22</sup> MCP formulations led to a bimodal DSC curve when we used  $\text{La}(\text{OTf})_3$  as initiator, with a sharp maximum at higher temperatures, which was attributed to the homopolymerization of SOE, which occurs at the end of the curing.<sup>22</sup> However, in the present study, the lanthanum triflate initiated curing leads to a broad but unimodal curve indicating that all the reactions are more or less simultaneous. In previous studies with DGEBA/ $\gamma$ -lactones mixtures initiated by lanthanide triflates<sup>24</sup> we concluded that, in general, when Lewis acidity is increased, the initiator becomes more active and the curing process accelerates. It is reported that oxophilicity (acidity) of Sc, Yb and La is 2.37, 2.09 and 1.36 respectively.<sup>25</sup> In the present study, in spite of the highest acidity of scandium cation, this initiator leads to the slower curing, and then the acidity should not be the only factor that influences the reaction rate. We can see in the figure that the addition of MCB accelerates the curing initiated by lanthanum and ytterbium triflates, but the addition of MCB to DGEBA in the sample with scandium triflate or  $\text{BF}_3\cdot\text{MEA}$  practically does not produce any acceleration. This result could be related to the

different extension of the four reactions implied in the global curing. Scandium cation is less bulky than lanthanides and the real initiator for  $\text{BF}_3 \cdot \text{MEA}$  is a proton.<sup>26,27</sup> Sc, due to its small size, and the proton are more able to coordinate to the MCB, which has bulky substituents, whereas this coordination is more difficult for lanthanides.

metric data and the kinetic parameters of the curing of pure DGEBA and its mixtures with MCB with the four initiators tested. As can be seen, the total enthalpy per epoxy equivalent for rare earth triflates is similar, whereas  $\text{BF}_3 \cdot \text{MEA}$  leads to lower enthalpies but to a higher  $T_g$  value indicating a more rigid structure of the network than the others.

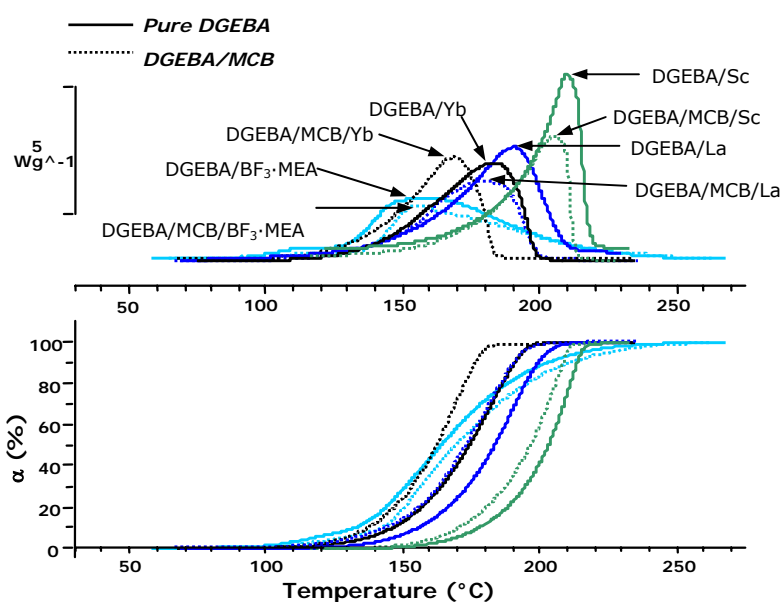


**Figure 1.** DSC scanning curves and conversion degree against temperature of the curing of DGEBA and DGEBA/MCB 2:1 (mol/mol) mixtures initiated by different Lewis Acids at a heating rate of 10°C/min and obtained through dynamic DSC experiments, (Green (Sc), Black (Yb), Blue (La) and Sky-blue (BF<sub>3</sub>))

In this way, a lower amount of epoxide is activated by the Sc and the proton and the homopolymerization of epoxide and its copolymerization with MCB are retarded. Thus, MCB has no accelerative effect on the curing of mixtures with  $\text{BF}_3 \cdot \text{MEA}$  and  $\text{Sc}(\text{OTf})_3$ .

**Table 1** shows the calori-

We previously observed the higher  $T_g$  values in  $\text{BF}_3 \cdot \text{MEA}$  initiated materials,<sup>20</sup> due to the fact that rare earths triflates induce reorganization reactions, specially in case of scandium,<sup>4</sup> that reduce the cross-linking density of the network,<sup>28</sup> thus producing more flexible materials.

**Table 1.** Calorimetric data, kinetic parameters and relative linear ester content in the curing of DGEBA and DGEBA/MCB 2:1 mol/mol mixtures initiated by different Lewis Acids

Entry	Formulation <sup>a</sup>	T <sub>g</sub> <sup>b</sup> (°C)	ΔH <sup>c</sup> (J/g)	ΔH <sup>d</sup> (kJ/ee)	T <sub>max</sub> <sup>e</sup> (°C)	E <sub>a</sub> <sup>f</sup> (kJ/mol)	ln A <sup>g</sup> (s <sup>-1</sup> )	k <sub>170°C</sub> · 10 <sup>3</sup> h (s <sup>-1</sup> )	Abs <sub>ester</sub> / Abs <sub>1605</sub>	linear ester
1	DGEBA/Yb(OTf) <sub>3</sub> 1:0.006	135	519.7	95.6	184	90.7	18.09	1.45	-	-
2	DGEBA/MCB/Yb 2:1:0.015	104	433.4	99.8	170	81.8	16.31	2.74	1.95	1
3	DGEBA/La(OTf) <sub>3</sub> 1:0.006	127	513.5	94.4	192	79.8	14.59	0.83	-	-
4	DGEBA/MCB/La 2:1:0.015	90	430.1	98.7	181	82.9	16.03	1.54	1.05	0.54
5	DGEBA/Sc(OTf) <sub>3</sub> 1:0.006	107	535.5	96.7	210	76.4	12.92	0.40	-	-
6	DGEBA/MCB/Sc 2:1:0.015	102	440.5	101.2	205	98.7	12.92	0.42	1.27	0.65
7	DGEBA/BF <sub>3</sub> ·MEA 1:0.096	160	460.0	86.6	158	87.5	-	-	-	-
8	DGEBA/MCB/BF <sub>3</sub> 1:0.240	139	308.6	83.4	157	99.4	-	-	-	0.31

- a. The compositions of the formulation is given in molar ratios  
 b. Glass transition temperatures obtained by DSC in the second scan after dynamic curing  
 c. Enthalpy per gram of mixture  
 d. Enthalpy per equivalent of epoxy group  
 e. Temperature of the maximum of the curing exotherm  
 f. Values of activation energies were evaluated by the isoconversional integral method (Eq.(3)) applied at conversion of 0.5  
 g. The values of pre-exponential factor for kinetic model with R<sub>3</sub> kinetic model ( $g(\alpha)=1-(1-\alpha)^{1/3}$ )  
 h. The values of rate constants at 170°C were calculated using the Arrhenius equation  $\ln k = \ln A - \frac{E}{RT}$

The dependence of the apparent activation energy on the degree of conversion calculated using the isoconversional method (Equation (3))<sup>29,30</sup> is represented in **Figure 2** for the curing of mixtures DGEBA/MCB. The plots are practically horizontal for the curing with rare earth triflates in the range 10-80% of conversion, but with much higher energy values for the scandium salt. BF<sub>3</sub>·MEA shows a steadily increase in the activation energy along the conversion range. The relative low values in the initial stage can be attributed to the formation of initiating active species.<sup>26,27</sup>

To calculate the frequency factors from the isoconversional kinetic parameters calculated previously (Eq 3), we determined the kinetic model which better fits with the experimental results. We used the differential reduced master curves procedure<sup>18</sup> that consists in comparing the experimental curves with the theoretical calculated for the different models mentioned in the experimental part. We selected the R<sub>3</sub> model for the curing initiated by rare earth triflates, however the curing with BF<sub>3</sub>·MEA follows a different and more complex kinetic model, as it shows in the strongly increase in the activation energy

(Figure 2), and therefore the kinetic parameters have not been calculated for this sample.

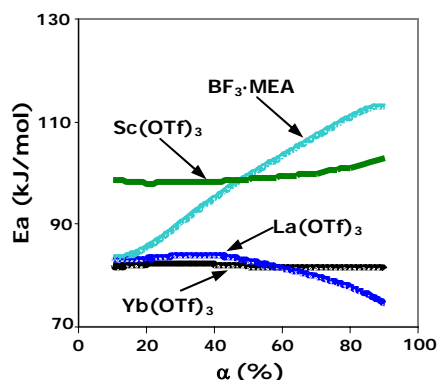
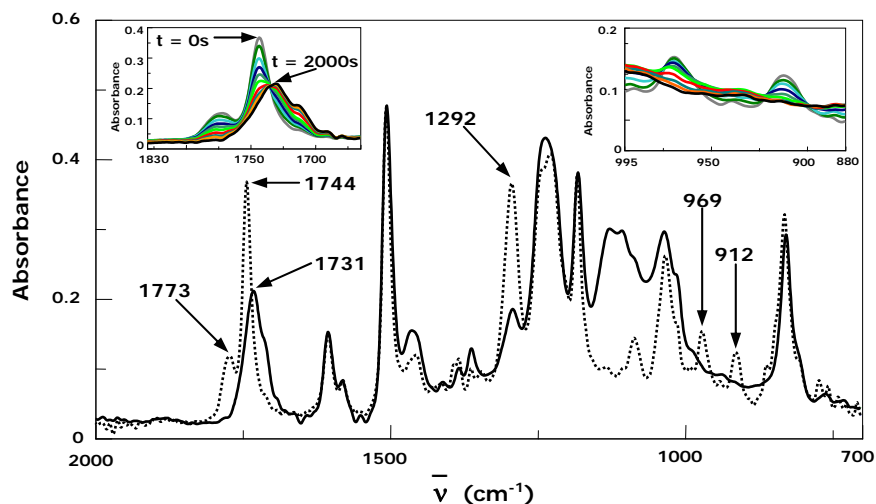


Figure 2. Dependence of  $E_a$  on the degree of conversion obtained by DSC of different mixtures from DGEBA/MCB 2:1 (mol/mol) formulation initiated by different Lewis acids

Table 1 shows the kinetic parameters associated with the dynamic curing by DSC for 0.5 of conversion. The values of the activation energies are similar for mixtures initiated by ytterbium and lanthanum triflates, but are higher for the other initiators. However, this trend is not observed for pure DGEBA, in which the scandium salt leads to the lowest activation energy. The activation energy values are not significant and do not clearly show the acceleration effect of the initiators due to the compensation effect between the activation energy and the pre-exponential factor.<sup>18,31</sup> However, the calculated constant rates clearly show the order of reactivity observed by DSC. The constant rates show the accelerative effect of the addition of MCB to the reactive mixture for ytterbium and lanthanum triflates, but this effect is negligible for the scandium salt.

### 3.2. Study of the curing process by FTIR

To study the individual reactions, that take place during the curing process and to establish the evolution of the different reactive groups, the curing of DGEBA/MCB 2:1 (mol/mol) formulation with each initiator at 150°C was followed by ATR/FTIR. Figure 3 shows the initial and final spectra of the DGEBA/MCB 2:1 (mol/mol) mixture with 0.015 mol of  $Yb(OTf)_3$  at 150°C. The inset of the regions 1850-1650 and 1000-800 $cm^{-1}$  are included. In the initial spectrum we can see two carbonylic bands at 1773 and 1744 $cm^{-1}$  attributable to the unsymmetric and symmetric stretching of ester groups of MCB and two bands at 969 and 912 $cm^{-1}$  due to the deformation of the six membered MCB ring and the oxirane group respectively. All these absorptions disappear in the final spectrum and a new band at 1731  $cm^{-1}$  appears due to the linear ester group formed. The disappearance of the absorptions indicates the complete consumption of the initial species and also that the chemical reactions takes place simultaneously. Because MCB does not homopolymerize, the disappearance of the bands at 1773, 1744 and 969  $cm^{-1}$  must be attributed to the formation of the corresponding SOE, from which the poly(ether-ester) unities are formed on polymerizing. The partial overlapping of cyclic and linear carbonyl ester absorptions hindered a quantification of the evolution of linear ester group on curing. However, the disappearance of MCB could be quantified from the 969 $cm^{-1}$  absorption.



**Figure 3.** ATR-FTIR spectra of a mixture DGEBA/MCB 2:1 (mol/mol) with 0.015 mol of  $\text{Yb}(\text{OTf})_3$  before (discontinues line) and after (continues line) curing at  $150^\circ\text{C}$ . Insets, evolution of carbonyl, ring deformation of MCB, and epoxy bands during curing

The chemical incorporation of the epoxy group into the network was followed by the diminution of the  $912\text{cm}^{-1}$  band. The evolution of MCB and epoxy with both initiators are represented in **Figures 4 and 5**, respectively. We can see a different evolution of the conversions of MCB and epoxide on changing the initiator. To understand the reactive process, we should take into account that in the reactive mixture there are four epoxy groups per one MCB group. The disappearance of epoxide and MCB using  $\text{BF}_3\cdot\text{MEA}$  are the slowest at high conversions, specially the former, whose complete disappearance needs 12000s of curing. With scandium triflate both MCB and epoxide are run out at around 5400s and the homopoly-

merization of epoxide occurs from the beginning, since MCB conversion takes values between two and four times the values of the epoxide conversion.

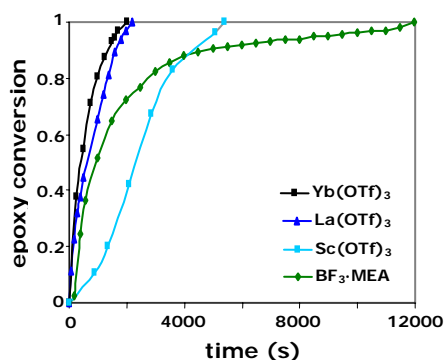


**Figure 4.** Epoxy conversion degree ( $912\text{cm}^{-1}$ ) versus time for the DGEBA/MCB 2:1 (mol/mol) formulation with different initiators during curing at  $150^\circ\text{C}$  by ATR-FTIR

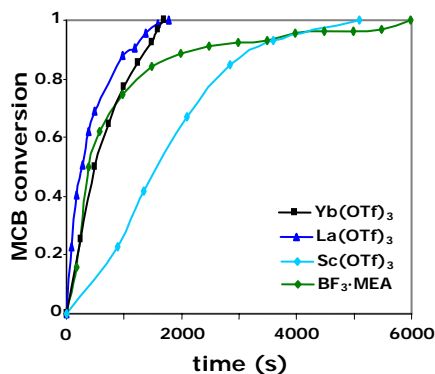


**Figure 5.** MCB conversion degree ( $969\text{ cm}^{-1}$ ) versus time for the DGEBA/MCB 2:1 (mol/mol) formulation with different initiators during curing at  $150^\circ\text{C}$  by ATR-FTIR

On comparing the evolution of samples initiated by ytterbium and lanthanum salts, ytterbium favors the epoxide consumption and lanthanum favors the MCB consumption by formation of SOE. With these initiators MCB and epoxide are run out before 2000s, which agree with their higher constant rate values determined by DSC. **Figure 6** shows the final FTIR spectrum of all cured DGEBA/MCB mixtures. From these spectra we can see that the highest proportion of linear ester is achieved when we used ytterbium triflate as initiator. From the areas of the band at  $1731\text{cm}^{-1}$  and taking the absorption at  $1605\text{cm}^{-1}$  of the aromatic ring, that not change during curing, as reference we can calculate the relative areas of linear ester in the final network. These values are collected in **Table 1**, together with the relative proportions of ester groups referred to the maximum achieved for ytterbium. We can see that all the rare earth triflates lead to a higher modification than  $\text{BF}_3\cdot\text{MEA}$ . Because in the

final spectra we cannot see any remaining MCB, some proportion of SOE must remain unreacted in the final material. In a previous work<sup>4</sup> on the curing of DGEBA/ $\gamma$ -valerolactone formulations with the same initiators we saw that the higher proportion of linear ester in the thermosets was achieved with the ytterbium initiator, but the explanation in that case was a depolymerization process observed at long curing times when we used the scandium salt. In the present study no depolymerization process was observed and therefore the results obtained should be related to the coordination ability of the cation to the oxygen atoms of SOE and its polymerizability.

### 3.3. Determination of the shrinkage

**Table 2** shows the densities of the mixtures before and after curing and the calculated global shrinkage. We have added in the table the values of densities for pure DGEBA formulation, in order to compare the effect of the addition of MCB. As we can see, the addition of MCB leads to a reduction of the shrinkage, which is more important for the ytterbium salt initiated curing, which could be attributed to the incorporation of a higher proportion of the lactone. The lower shrinkage is a consequence of the higher extension of the polymerization reactions in which SOEs open. It should be commented that the formation of SOE, which takes place at the beginning of the curing, occurs with shrinkage whereas its opening



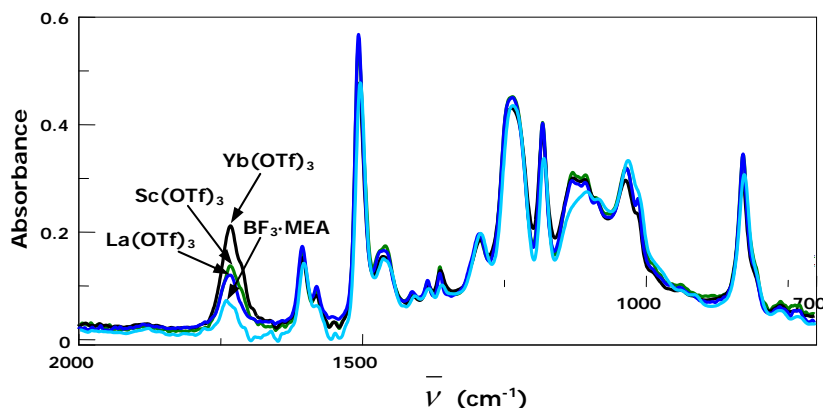


**Figure 6.** ATR-FTIR spectra of different materials obtained after curing at 150°C from DGEBA/MCB mixtures (2:1 mol/mol) with 0.015 mol of rare earth triflates or 0.240 mol of BF<sub>3</sub>·MEA

**Table 2.** Densities and shrinkage of the systems studied initiated by different Lewis Acids

Entry	Formulation <sup>a</sup>	$\rho_{\text{initial mixture}}^b$ (g/cm <sup>3</sup> )	$\rho_{\text{final material}}^b$ (g/cm <sup>3</sup> )	Shrinkage (%)
1	DGEBA/Yb(OTf) <sub>3</sub> 1:0.006	1.158	1.192	2.9
2	DGEBA/MCB/Yb(OTf) <sub>3</sub> 2:1:0.015	1.171	1.191	1.7
3	DGEBA/La(OTf) <sub>3</sub> 1:0.006	1.158	1.193	3.0
4	DGEBA/MCB/La(OTf) <sub>3</sub> 2:1:0.015	1.168	1.195	2.3
5	DGEBA/Sc(OTf) <sub>3</sub> 1:0.006	1.158	1.194	3.1
6	DGEBA/MCB/Sc(OTf) <sub>3</sub> 2:1:0.015	1.171	1.202	2.6
7	DGEBA/BF <sub>3</sub> ·MEA 1:0.096	1.155	1.191	3.1
8	DGEBA/MCB/ BF <sub>3</sub> ·MEA 2:1:0.240	1.166	1.198	2.7

<sup>a</sup> The compositions of the formulation is given in molar ratios

<sup>b</sup> Densities before and after curing process

occurs with expansion at the end of the process and thus the shrinkage in the gel state is much lower. However, the dependence of a higher SOE polymerization with a lower shrinkage should not be the only reason, because scandium leads to a greater proportion of linear ester and also to a greater shrinkage than lanthanum initiator.

Because of the reduction of

the global shrinkage experimented in the DGEBA/MCB curing, it could be confirmed the expandable character of the substituted Meldrum acid ring, which on opening should reduce the interactions between the polymeric chains.<sup>20</sup> Moreover, as we told in the introduction in ring opening polymerization, the shrinkage is related to the size of the ring being opened,<sup>2</sup> and there-

fore, six membered lactones should produce a larger expansion on polymerizing than the five membered ones. Moreover, on comparing these results with those obtained from MCP formulations we cannot discard a possible influence of the spiranic structure, because MCP leads to an even lower shrinkage during curing than MCB.

### 3.4. Study of the thermal degradability

In a previous study<sup>22</sup> we demonstrated the enhanced degradability of the thermosets obtained by copolymerization of DGEBA with MCP due to the formation of tertiary ester groups in the network. From the analysis of the volatiles evolved on heating we could detect the rupture of these ester groups but also the breakage of the ether linkages. We could observe that the temperatures at which the ruptures took place depended on the initiator.

**Figure 7** shows the TGA and DTG curves for the degradation of the materials obtained from the formulation DGEBA/MCB 2:1 (mol/mol) initiated with the four Lewis acids. As we can see, the thermal stability of the material obtained with  $\text{BF}_3 \cdot \text{MEA}$  is the highest and the material obtained with  $\text{Yb}(\text{OTf})_3$  is the most degradable. It could be expected that the higher the proportion of linear ester the higher the degradability will be. This trend is observed in the TGA curves, but this should not be the only factor, because the temperature of the 2% of weight loss does not exactly reflect the ester content (*see Table 3*). If you look at

the DGEBA degradation temperatures in **Table 3** the type of initiator starkly influences the initial degradation temperatures. We can see that the higher the Lewis acidity of the rare earth triflate the lower the initial degradation temperature is. The degree of crosslinking ( $T_g$ ) also can influence in the thermal stability. If other factors do not act, the lower  $T_g$  the higher thermal degradability will be. The broadness and shape of the DTG curves indicates the complexity of the degradative processes for the materials obtained with rare earth triflates, whereas the material obtained with  $\text{BF}_3 \cdot \text{MEA}$  shows a unimodal and sharp curve at high temperature. In the previous study with MCP<sup>21</sup> we observed that the weight loss took place at lower temperatures than MCB thermosets. Moreover, the DTG curves had two or three peaks, with a broad peak at lower temperature for lanthanum initiated thermoset. Therefore, it seems that the more strained spiranic structure of the MCP also contributes to the degradative process.

**Table 3** collects the thermogravimetric data obtained for all the formulations studied. To compare, we have also introduced the values for DGEBA and DGEBA/MCP formulations. The addition of a lactone to DGEBA samples mainly affects the initial steps of the process, which is worth in order to increase the reworkability of the electronic devices. The higher thermal stability of the materials obtained with  $\text{BF}_3 \cdot \text{MEA}$  could be related to their higher crosslinking density, which is reflected in their higher  $T_g$  values.

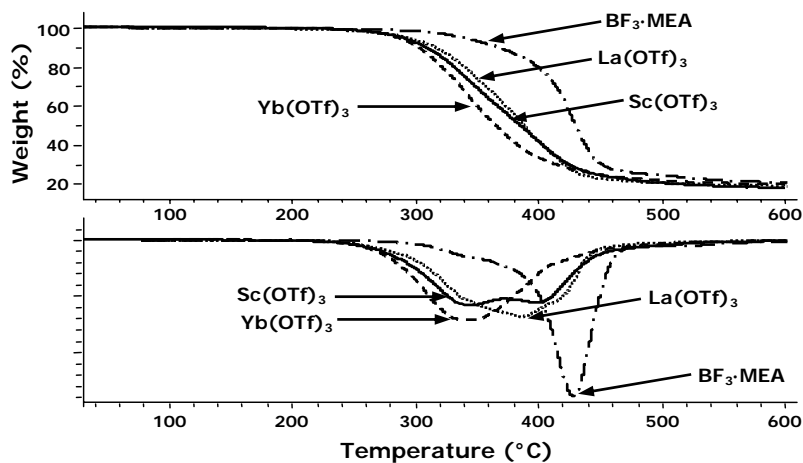


**Figure 7.** TGA and DTG curves at 10°C/min in a N<sub>2</sub> atmosphere of several thermosetting materials obtained from DGEBA/MCB (2:1 mol/mol) formulations initiated by different Lewis Acids

**Table 3.** Thermogravimetric data of DGEBA and DGEBA/lactone 2:1 (mol/mol) mixtures initiated by different Lewis Acids

Entry	Formulation	Mol Initiator <sup>a</sup>	T <sup>b</sup> (°C)	T <sub>max</sub> (°C)	% Char (T=600°C)
1	DGEBA/Yb(OTf) <sub>3</sub>	0.006	287	345	20
2	DGEBA/MCB/Yb(OTf) <sub>3</sub>	0.015	258	342	20
3	DGEBA/MCP/Yb(OTf) <sub>3</sub>	0.015	230	332	19
4	DGEBA/La(OTf) <sub>3</sub>	0.006	303	354	19
5	DGEBA/MCB/La(OTf) <sub>3</sub>	0.015	262	386	19
6	DGEBA/MCP/La(OTf) <sub>3</sub>	0.015	233	348	17
7	DGEBA/Sc(OTf) <sub>3</sub>	0.006	266	354	20
8	DGEBA/MCB/Sc(OTf) <sub>3</sub>	0.015	262	334	18
9	DGEBA BF <sub>3</sub> ·MEA	0.096	332	433	19
10	DGEBA/MCB/BF <sub>3</sub> ·MEA	0.240	302	428	21
11	DGEBA/MCP/BF <sub>3</sub> ·MEA	0.240	288	425	18

<sup>a</sup> The proportion of initiator is given in mol per 2 mol of DGEBA and 1 mol of monomer (MCP and MCB)

<sup>b</sup> Temperature of a 2% of weight loss calculated by thermogravimetry

#### 4. CONCLUSIONS

The modification of DGEBA by copolymerization with MCB using rare earth triflates as initiators incorporated a higher proportion of tertiary linear ester moieties than  $\text{BF}_3 \cdot \text{MEA}$  in the network.

The addition of MCB to the DGEBA resins accelerates the curing process when we used lanthanide triflates as initiators.

The addition of MCB to the DGEBA slightly reduces the  $T_g$  of the materials.  $\text{BF}_3 \cdot \text{MEA}$  leads to higher  $T_g$  values of the materials than rare earth triflates.

The expandable character of MCB has been demonstrated by the reduction of the global shrinkage on curing mixtures of DGEBA/ MCB.

The thermal degradability of these materials increases in reference to pure DGEBA and the initiation with ytterbium triflate leads to the highest degradable materials.

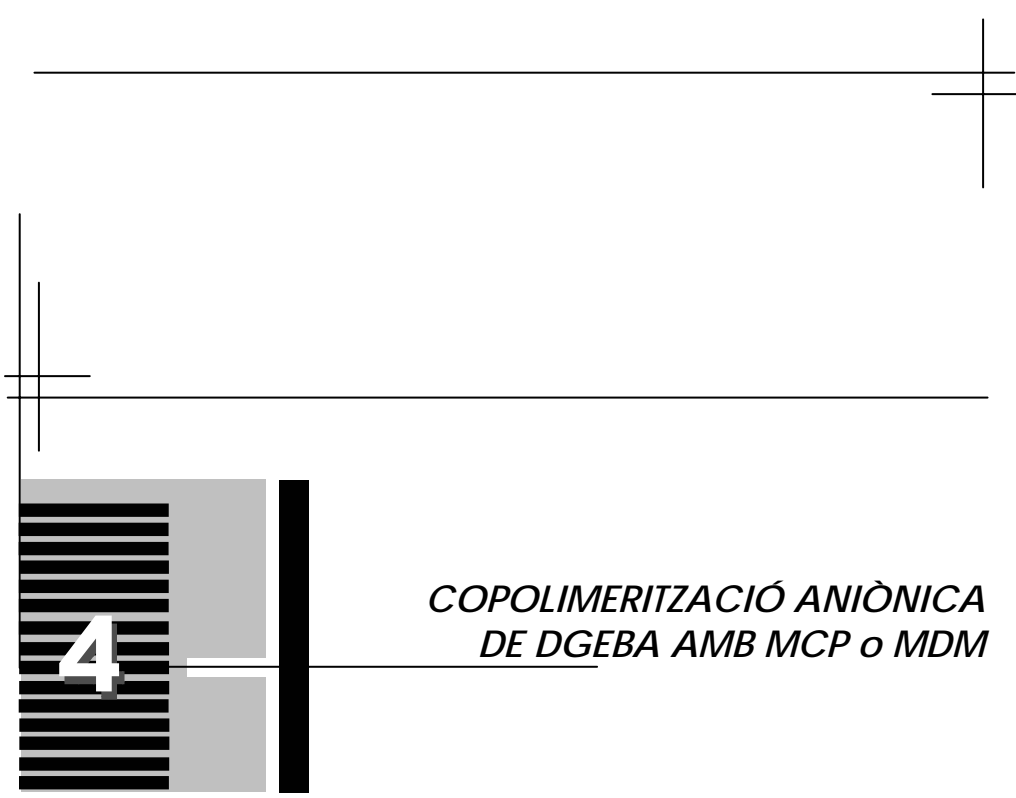
#### Acknowledgements

The authors from the Universitat Politècnica de Catalunya would like to thank CICYT and FEDER (MAT2004-04165-C02-02) for their financial support. The authors from the Rovira i Virgili University would like to thank the CICYT (Comisión Interministerial de Ciencia y Tecnología) and FEDER (Fondo Europeo de Desarrollo Regional) (MAT2005-01806)

#### 5. REFERENCES

1. Bailey, W.J. *J Elastoplast* 1973, 5, 142-152.
2. Sadhir, R.K.; Luck, M.R. Ed. *Expanding Monomers. Synthesis, Characterization and Applications* CRC Press, Boca Raton, 1992.
3. Mas, C.; Ramis, X.; Salla, J.M.; Mantecón, A.; Serra, A. *J Polym Sci Part A: Polym Chem* 2003, 41, 2794-2808.
4. Arasa, M.; Ramis, X.; Salla J.M., Mantecón, A.; Serra, A. *J Polym Sci Part A: Polym Chem* 2007, 45, 2129-2141.
5. Giménez, R.; Fernández-Francos, X.; Salla, J.M.; Serra, A.; Mantecón, A.; Ramis, X. *J Polym Sci Part A: Polym Chem* 2005, 46, 10637-10647.
6. Flory, P.J. *Principles of Polymer Chemistry* Cornell University Press: Ithaca, NY, 1953, 347-398.
7. González, S.; Fernández-Francos, X.; Salla, J.M.; Serra, A.; Mantecón, A.; Ramis, X. *J Polym Sci Part A: Polym Chem* 2007, 45, 1968-1979.
8. Kobayashi, S., Ed. *Lanthanides: Chemistry and Use in Organic Synthesis* Topics in Organometallic Chemistry, Springer Verlag, Berlin, 1999.
9. Kobayashi, S.; Sugiura, M.; Kitagawa, H.; Lam, W.W.L. *Chem Rev* 2002, 102, 2227-2302.
10. Castell P.; Galià, M.; Serra, A; Salla, J.M.; Ramis, X. *Polymer* 2000, 41, 8465-8474.

11. Chen, J-S.; Ober, C.K.; Poliks, M.D.; Zhang, Y.; Wiesner, U.; Cohen, C.; *Polymer* 2004, 45, 1939-1950.
12. Wang, L.; Li, H.; Wong, C.P. *J Polym Sci Part A: Polym Chem* 2000, 38, 3771-3782.
13. García, S.J.; Serra, A.; Suay, J.; *J Polym Sci Part A: Polym Chem* 2007, 45, 2316-2327.
14. Singh, R.K.; Danishefsky, S. *J Org Chem* 1975, 40, 2969-70, *ibid* *Collective Organic Syntheses* 1990, VII, 411-414.
15. Baxter, G.J.; Brown, R.F.C.; Eastwood, F.W.; Harrington, K.J. *Tetrahedron Lett* 1975, 48, 4283-4284.
16. Coats, A.W.; Redfern, J.P. *Nature* 1964, 201, 68-69.
17. Kissinger, H.E. *Anal Chem* 1957, 29, 1702-1706.
18. Criado, J.M. *Thermochim Acta* 1978, 24, 186-189.
19. Ramis, X.; Salla J.M.; Cadenato, A.; Morancho, J.M. *J Therm Anal Cal* 2003, 72, 707-718.
20. González, L.; Ramis, X.; Salla, J.M.; Mantecón, A.; Serra, A. *J Polym Sci Part A: Polym Chem* 2006, 44, 6969-6979.
21. González, L.; Ramis, X.; Salla, J.M.; Mantecón, A.; Serra, A. *Polym Degrad Stab* 2007, 92, 596-604.
22. González, L.; Ramis, X.; Salla, J.M.; Mantecón, A.; Serra, A. *Thermochim Acta* 2007, 464, 35-41.
23. Desai, D.G.; Mane, R.B. *Chem Ind* 1982, 20, 809.
24. Mas, C.; Mantecón, A.; Serra, A.; Ramis, X.; Salla, J.M. *J Polym Sci Part A: Polym Chem* 2004, 42, 3782-3791.
25. Luo, S.; Zhu, L.; Talukdar, A.; Zhang, G.; Mi, X.; Cheng, J.P.; Wang, P.G. *Mini-Rev Org. Chem.* 2005, 2, 546-564.
26. Ghaemy, M. *Eur Polym J* 1998, 34, 1151-1156.
27. Li, Y.; Li, M.; Chang, F. *J Polym Sci Part A: Polym Chem* 1999, 37, 3614-3624
28. Fernández-Francos, X.; Salla J.M.; Cadenato, A.; Morancho, J.M.; Mantecón, A.; Serra, A.; Ramis, X. *J Polym Sci Part A: Polym Chem*, in press
29. Vyazovkin, S.; Sbirrazzuoli, N. *Macromol Rapid Commun* 2006, 27, 1515-1532
30. Cadenato, A.; Morancho, J.M.; Fernández-Francos, X.; Salla J.M.; Ramis, X. *J Therm Anal Cal* 2007, 89, 233-244
31. Vyazovkin, S.; Linert, W. *J Solid State Chem* 1995, 114, 392-398



*COPOLIMERITZACIÓ ANIÒNICA  
DE DGEBA AMB MCP o MDM*



4.1.



*INTRODUCCIÓ*

## 4. COPOLIMERITZACIÓ ANIÒNICA DEL DGEBA AMB MCP o MDM

### 4.1. Introducció

Un cop realitzats els diferents estudis sobre la copolimerització catiònica de la reïna epoxi de diglicidilèter de bisfenol A (DGEBA) amb els diversos diesters cíclics de sis baules proposats, es decidí abordar la copolimerització aniònica d'alguns derivats de l'àcid de Meldrum, el MCP i el MDM.

Dell'Erba i Williams<sup>16</sup> van realitzar un estudi sobre l'homopolimerització de monòmers epoxídics (DGEBA i PGE) iniciada amb 4-(N,N-dimetilamino)piridina (DMAP). En aquest estudi van observar que quan s'utilitzava DMAP la reacció de polimerització tenia lloc a una velocitat major que amb les típiques amines terciàries i que el valor de la Tg del material obtingut era superior. Aquesta amina ja havia estat utilitzada pel nostre grup de recerca en l'entrecruament de reïnes epoxi amb bons resultats.<sup>107,108</sup>

L'homopolimerització aniònica de grups epoxi iniciada per amines terciàries i imidazoles N-substituïdes és una reacció complexa i presenta dos inconvenients: (a) velocitats de reacció baixes, i (b) formació de cadenes principals curtes degut a l'elevada velocitat de les reaccions de transferència de cadena.<sup>10,109</sup>

A la **fig. 4.1** es representa l'activitat relativa i els valors de les càrregues netes dels nitrògens d'algunes amines emprades com a iniciadors.<sup>110</sup>

<sup>107</sup> M. Galià, A. Serra, A. Mantecón, V. Cádiz, J. Appl. Polym. Sci. **56**, 193-200 (1995).

<sup>108</sup> D. Ribera, A. Mantecón, A. Serra, J. Polym. Sci. Part A: Polym. Chem. **40**, 3916-3926 (2002).

<sup>109</sup> Pascault, J. P.; Sautereau, H.; Verdu, J.; Williams, R. J. J.; *Thermosetting Polymers*, Marcel Dekker, New York 2002.

<sup>110</sup> Murayama, M.; Sanda, F.; Endo, T.; *Macromolecules* **31**, 919-923, (1998).



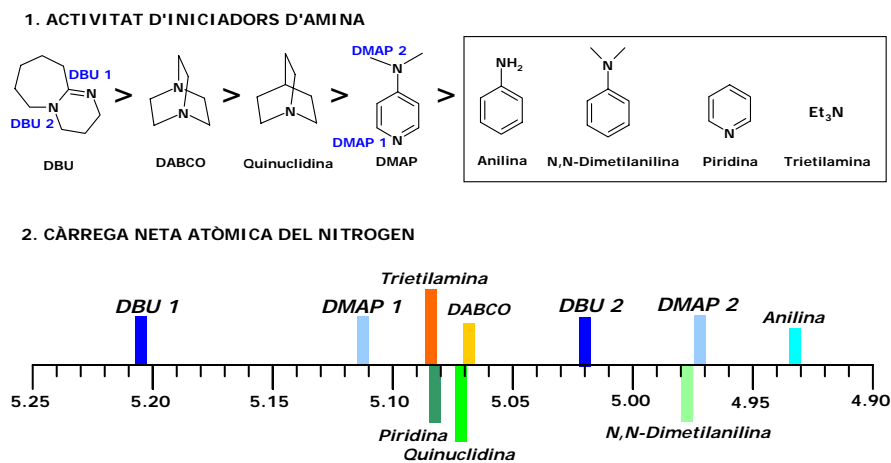


Fig.4.1. Activitat d'iniciadors d'amina i càrregues netes dels nitrogens

Malgrat l'aparent major activitat del DBU com a iniciador, en el nostre grup de recerca s'ha demostrat que una base anàloga, el DBN que presenta dos carbonis menys en l'anell que tan sols conté un nitrogen, no permet el curat complet del DGEBA.<sup>111</sup>

La necessitat d'una concentració crítica de DMAP per aconseguir una total conversió de grups epoxi està relacionada amb la presència d'un procés de terminació on es consumeixen les espècies actives. El procés de terminació podria ser la formació d'èters cíclics (**Fig.4.2**). Aquesta possibilitat es troba postulada a la literatura per reaccions amb piridina i poli(vinilpiridina) amb compostos epoxi.<sup>16,112,113</sup>

<sup>111</sup> X. Fernández-Francos, J.M. Salla, A. Mantecón, A. Serra, X. Ramis, J. Appl. Polym. Sci., *in press*

<sup>112</sup> G. Xue, H. Ishida and J. L. Koenig, Makromol. Chem. Rapid Commun., **7**, 37-41 (1986).

<sup>113</sup> G. Xue, H. Ishida and J. L. Koenig, Angew. Makromol. Chem., **142**, 17-27 (1986).

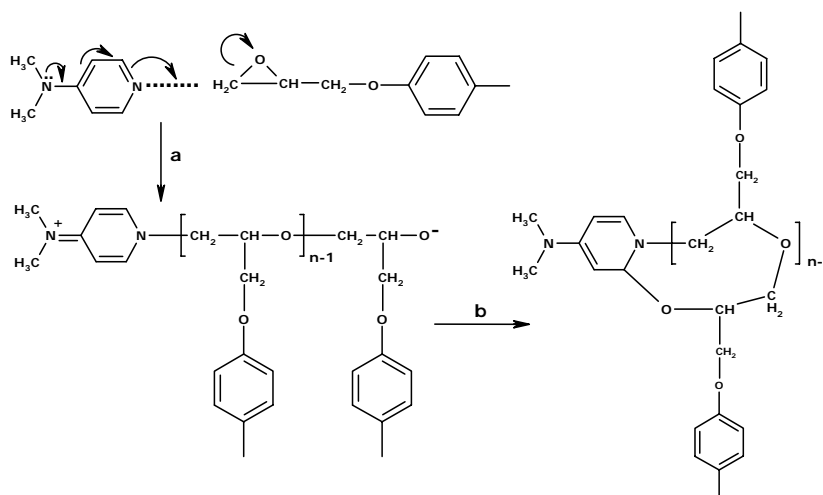


**Fig.4.2.** Mecanismes d'iniciació (a) i terminació (b) proposats en l'homopolimerització de PGE iniciat per DMAP

Brady i col. van dur a terme diversos estudis sobre la copolimerització aniónica de monòmers bicíclics (**Fig.4.3**) amb reines epoxi amb la finalitat de controlar l'encongiment durant el procés de polimerització.<sup>114</sup> Mitjançant copolimerització aniónica de reines epoxi amb petites quantitats de  $\gamma$ -lactones espirocícliques van aconseguir reduir l'encongiment.<sup>115</sup> No obstant, van observar que la reducció de la contracció només es produïa a l'estadi inicial de la copolimerització, probablement perquè la quantitat de comonòmers bicíclics i espirocíclics era massa petita per tal de suprimir totalment la contracció.

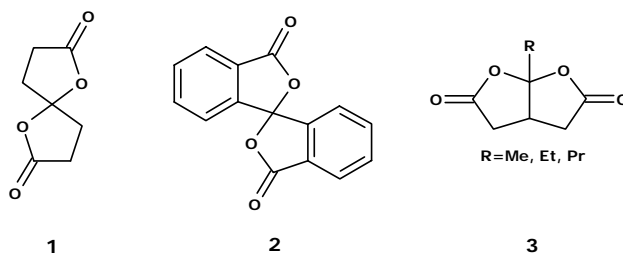


**Fig.4.3.** Espirobislactones (1 i 2) i bis( $\gamma$ -lactona) bicíclica (3)

<sup>114</sup> Brady, R. F., Jr.; Simon, F. E. J. *Polym. Sci. Part A: Polym. Chem.*, **25**, 231 (1987).

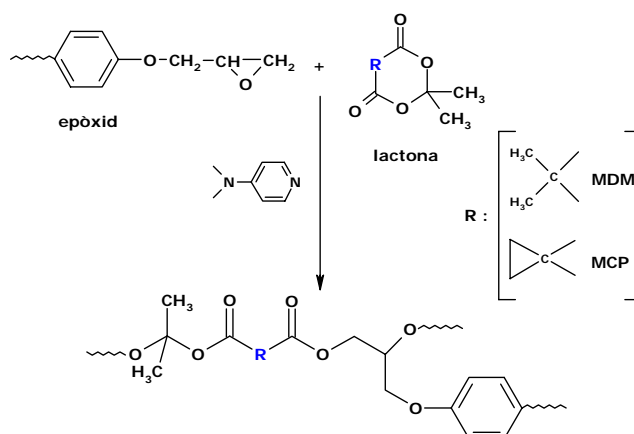
<sup>115</sup> Sikes, A. M.; Brady, R. F.; *J. Polym. Sci. Part A: Polym. Chem.*, **28**, 2533-2546 (1990).

Endo i col. han trobat que les bis( $\gamma$ -lactones) bicícliques i espirobicícliques no donen homopolimerització però presenten una bona copolimeritzabilitat amb epòxids per donar copolímers alternats via doble obertura d'anell, concloent així que la parcial reducció de l'encongiment en l'estadi inicial de les copolimeritzacions descrites per Brady i col·laboradors s'expliquen per la copolimerització aniónica alternada.<sup>116,117</sup> En estudis realitzats en el nostre grup sobre el curat de reines epoxi amb bislactones espiràniques s'ha observat també una copolimerització alternada.<sup>111</sup>

En el present treball s'han portat a terme les copolimeritzacions anióniques del DGEBA amb MCP o MDM emprant 4-(N,N-dimetilamino)piridina (**DMAP**) ja que es troba descrit a la literatura que és un iniciador eficaç en polimeritzacions anióniques d'obertura d'anell.<sup>16,110,111</sup>

A **l'esquema 4.1** es representen les reaccions que poden tenir lloc en la copolimerització aniónica d'un epòxid i una lactona, en aquest cas derivada de l'àcid de Meldrum:

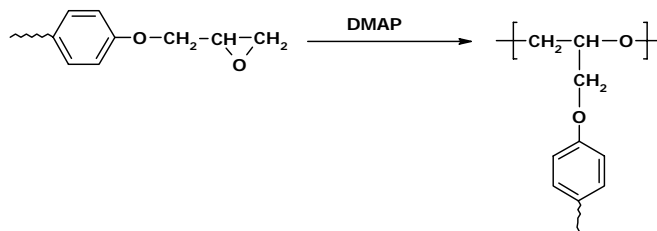
- *Copolimerització de l'epòxid amb MCP o MDM*



<sup>116</sup> Takata, T.; Tadokoro, A.; Endo, T.; *Macromolecules* **25**, 2782-2783 (1992).

<sup>117</sup> Tadokoro, A.; Takata, T.; Endo, T.; *Macromolecules* **26**, 4400 (1993).

- *Homopolimerització del DGEBA*



- *Homopolimerització del MCP o MDM*



Els resultats d'aquest estudi es presenten a l'article:

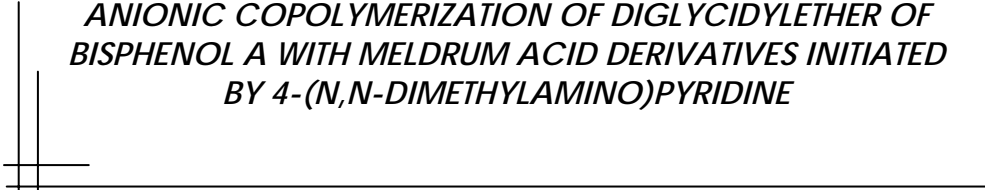
**4.2.** "Anionic Copolymerization of Diglycidyl Ether of Bisphenol A with Two Meldrum Acid Derivatives Initiated by 4-(N,N-Dimethylamino)Pyridine".

L. González, X. Ramis, J. M. Salla, A. Mantecón, A. Serra.

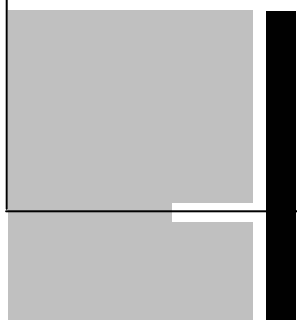
J. Polym. Sci. Part A: Polym. Chem. *En revisió menor*



## 4.2.



*ANIONIC COPOLYMERIZATION OF DIGLYCIDYLETHER OF  
BISPHENOL A WITH MELDRUM ACID DERIVATIVES INITIATED  
BY 4-(N,N-DIMETHYLAMINO)PYRIDINE*



**ANIONIC COPOLYMERIZATION OF DIGLYCIDYLETHER OF BISPHENOL  
A WITH MELDRUM ACID DERIVATIVES INITIATED  
BY 4-(N,N-DIMETHYLAMINO)PYRIDINE**

Lidia González,<sup>1</sup> Xavier Ramis,<sup>2</sup> Josep Maria Salla,<sup>2</sup>  
Ana Mantecón<sup>1</sup>, Angels Serra<sup>1\*</sup>

<sup>1</sup>Departament de Química Analítica i Química Orgànica. Universitat Rovira i Virgili. Marcel·lí Domingo s/n, 43007 Tarragona, Spain

<sup>2</sup>Laboratori de Termodinàmica, ETSEIB. Universitat Politècnica de Catalunya, Av. Diagonal 647, 08028 Barcelona, Spain

---

**Abstract**

The anionic copolymerization of diglycidylether of bisphenol A (DGEBA) with 2,2,5,5-tetramethyl-4,6-dioxo-1,3-dioxane (MDM) or 6,6-dimethyl-(5,7-dioxaspiro[2.5]octane-4,8-dione) (MCP) using 4-(N,N-dimethylamino)pyridine (DMAP) as initiator to form thermosets was studied by differential scanning calorimetry (DSC) and the kinetics evaluated by isconversional procedures. The evolution during curing of the bands due to the epoxide, lactone and linear ester groups was evaluated by Fourier Transform Infrared in the attenuated-total-reflection mode (ATR/FTIR) to clarify the reactive process that takes place.

The shrinkage during curing, thermomechanical characteristics and the thermal degradability of the materials obtained on varying the structure of the Meldrum acid derivative were evaluated and related to the chemical structure of the final network. The materials obtained were compared with those prepared by cationic mechanisms.

**Keywords:** Epoxy resins, lactones, anionic polymerization, crosslinking, thermosets.

---

## 1. INTRODUCTION

The shrinkage during curing can origin serious problems when epoxy resins are used in coatings because it leads to the apparition of microvoids, microcracks, and internal stress, which reduce the adhesion of epoxy resins to the substrate and makes worse the durability, the mechanical properties and the capacity of protection of the coatings.<sup>1</sup>

The cationic copolymerization of epoxy resins with lactones using several Lewis acids as initiators has been widely studied.<sup>2,3</sup> Several studies developed in our research of group<sup>4,5,6</sup> demonstrated that on copolymerizing  $\gamma$ -lactones and DGEBA by a cationic mechanism the global shrinkage during curing is, in general, not lower but the shrinkage after gelation is notably reduced, which is important because of internal stresses appear in the material when there is no mobility in the network. This copolymerization that leads to poly(ether-ester) networks takes place through the *in situ* formation of spiroorthoesters (SOEs) and the subsequent ring-opening polymerization during the curing process. Spiroorthoesters (SOEs) are considered expandable monomers, which can expand on polymerizing, being their use a good strategy to solve the shrinkage but it is necessary the

previous synthesis of these monomers, which in some cases is very tedious.<sup>7</sup> Moreover, Meldrum acid and its derivatives have demonstrated their expandable character on copolymerizing with epoxy resins using lanthanide triflates as cationic initiators, which leads to thermosets with a lower global shrinkage than pure epoxy resins.<sup>8,9,10</sup>

Brady et al.<sup>11</sup> reported that bicyclic monomers undergo copolymerization with epoxy resins via an anionic mechanism to control the polymerization shrinkage of such resins. Furthermore, they have succeeded in the reduction of volume shrinkage which is achieved by addition of small amounts of spirocyclic  $\gamma$ -lactones to the anionic copolymerization systems with epoxy resins.<sup>12</sup> However, in these copolymerizations, suppression of volume shrinkage is achieved only in the initial stage of the copolymerization and the final volume change leads to shrinkage. Endo et al.<sup>13,14</sup> suggested that this copolymerization follows an alternant pathway, with certain degree of homopolymerization depending on the feed ratio of the reactants. Nevertheless, they proposed that the homopolymerization of bislactone was not feasible. These authors<sup>13,14</sup> used potassium *t*-butoxide or methyl lithium as anionic initiators. However, tertiary amines, such as benzyldimethylamine, pyridine, triethylamine, imidazoles, 2,4,6-tris-(dimethyl-

aminomethyl) phenol<sup>15,16</sup> or 4-(N,N-dimethylamino) pyridine<sup>17,18</sup> are compounds which are more suitable as initiators for the technological curing of epoxy materials because of they can be used in air atmosphere.

Spiro( $\gamma$ -bislactones) and DGEBA was copolymerized using 4-(N,N-dimethylamino) pyridine (DMAP), 1,5-diazabicyclo[4.3.0]non-5-ene (DBN) and 1-methylimidazole (1MI) as anionic initiators and the alternating character of the copolymerization was demonstrated.<sup>19</sup> Among these initiators, the most efficient one was DMAP. The different activities of these initiators might be attributed to the intrinsic activity of the tertiary nitrogens, but also to the chances of undergoing termination reactions which allow refreshing the initiator and keeping a sufficient amount of active species in the reaction medium. The alternating copolymers obtained in this way should be advantageous as "reworkable thermosets" due to the presence of ester groups in the network. These labile groups lend higher thermal and hydrolytical degradability, which reduces the permanency of these thermosets in the environment when their service life is over.<sup>20</sup>

Some authors<sup>20,21,22,23</sup> incorporate tertiary ester groups into the network by polymerizing cycloaliphatic epoxy resins including these moieties into their structure. This way has the drawback that the epoxy monomers had to be synthesized previously and that cycloaliphatic epoxides are more difficult to crosslink than glycidyl ones and they do not polymerize with anionic initiators. Thus, the

copolymerization of DGEBA with monomers which introduce breakable groups into the structure could be advantageous to increase the degradability of modified epoxy thermosets, to enhance the versatility of the materials and to reduce the economic costs, because DGEBA is the most conventional and cheap epoxy resin.

In the present paper we report the anionic copolymerization of DGEBA with two different Meldrum acid derivatives: 2,2,5,5-tetramethyl-4,6-dioxo-1,3-dioxane (MDM) and 6,6-dimethyl-(5,7-dioxaspiro[2.5]octane-4,8-dione) (MCP) using 4-(N,N-dimethylamino)pyridine (DMAP) as initiator, the most efficient in our previous study.<sup>19</sup>

In previous papers we reported the cationic copolymerization of DGEBA epoxy resin with MCP<sup>8,24,25</sup> or MDM<sup>9</sup> using several Lewis acids as cationic initiators and the reduction in the shrinkage was confirmed. In the present study we want to compare the overall curing processes and to test if the global shrinkage is also reduced in anionic conditions. In the curing process, the functionalities of MCP and MDM are two and the functionality of DGEBA is four. Therefore, this copolymerization leads to three-dimensional networks with a poly(ether-ester) structure, in which the addition to DGEBA of MCP or MDM increases the distance between crosslinks, which should reduce the fragility, and retard the gelation point up to higher conversions.<sup>26</sup> In this way the contraction after gelation is reduced and the internal stresses originated are much lower. MCP and MDM were selected because they have two



tertiary ester groups in their structure, which facilitates the thermal  $\beta$ -degradation process and a relatively high dipolar moment and a six membered cyclic structure which can imply an expandable behaviour.

## 2. EXPERIMENTAL PART

### 2.1. Materials

Diglycidylether of bisphenol A (DGEBA) EPIKOTE RESIN 827 from Shell Chemicals (Epoxy Equiv =182.08 g/eq) was used as received.

6,6-Dimethyl-(5,7-dioxaspiro[2.5]octane-4,8-dione) (MCP) (Aldrich) was used as received and 2,2,5,5-tetramethyl-4,6-dioxo-1,3-dioxane (MDM) was prepared according to the reported method.<sup>9</sup>

4-(N,N-dimethylamino) pyridine (DMAP) and phenylglycidylether (PGE) (Aldrich) were used without further purification.

### 2.2. Preparation of the curing mixtures

The samples were prepared by mixing DMAP in the corresponding amount of MDM or MCP and adding the required proportion of DGEBA with manual stirring in a mortar. The prepared mixtures were kept at -18°C before use. DMAP was added in a molar ratio of 0.088 mols per mol of DGEBA and 0.044 mols per mol of MDM or MCP. Thus, mixtures of 3 mol of DGEBA with a 1 mol of lactone contain 0.308 mols of initiator.

### 2.3. Characterization and measurements

Calorimetric studies were carried out on a Mettler DSC-821e thermal analyzer in covered Al pans under N<sub>2</sub> at 10 °C/min. The calorimeter was calibrated using an indium standard (heat flow calibration) and an indium-lead-zinc standard (temperature calibration). The samples weighed approximately 7-9 mg. In the dynamic curing process the degree of conversion by DSC ( $\alpha_{DSC}$ ) was calculated as follows:

$$\alpha_{DSC} = \frac{\Delta H_T}{\Delta H_{dyn}} \quad (1)$$

where  $\Delta H_T$  is the heat released up to a temperature  $T$ , obtained by integration of the calorimetric signal up to this temperature, and  $\Delta H_{dyn}$  is the total reaction heat associated with the complete conversion of all reactive groups. The glass transition temperature for each material ( $T_g$ ) was calculated after complete curing, by means of a second scan, as the temperature of the half-way point of the jump in the heat capacity when the material changed from the glassy to the rubbery state.

The isothermal curing process at 150°C was monitored with a FTIR spectrophotometer FTIR-680PLUS from JASCO with a resolution of 4 cm<sup>-1</sup> in the absorbance mode. An attenuated-total-reflection accessory with thermal control and a diamond crystal (Golden Gate heated single-reflection diamond ATR, Specac-Teknokroma) was used to determine FTIR spectra.

The conversions of the reactive groups were determined from the normalized changes in absorbance by the Lambert-Beer law, as we explained previously.<sup>4</sup> After isothermal curing, in the FTIR/ATR, a dynamic scan by DSC was always carried out to prove that the curing was complete. In any case, residual enthalpy was observed.

Thermogravimetric analyses (TGAs) were carried out with a Mettler TGA/SDTA 851e thermobalance. Cured samples with an approximate mass of 7 mg were heated between 30 and 600°C at a heating rate of 10°C/min in N<sub>2</sub> (200 cm<sup>3</sup>/min) measured in normal conditions.

The shrinkage was calculated from the densities of the materials before and after curing, which were determined using a Gas Pycnometer Micromeritics AccuPyc 1330 thermostated at 30°C.

The dynamic mechanical thermal analyses (DMTA) were carried out with a TA Instruments DMTA 2980 analyzer. The samples were cured isothermally in a mold at 140°C for 3h and subjected to a post-curing for 2h at 160°C. Three point bending of 10mm was performed on cylindrical samples (10 x 4.05 mm<sup>2</sup>, approximately). The instrument operated dynamically, at 3°C/min, from 35 to 200°C at a frequency of 1 Hz.

## 2.4. Kinetic Analysis

Integral non-isothermal kinetic analysis was used to determine the kinetic triplet (A pre-exponential factor, E activation energy and g(α) integral function of degree of conversion).

Non- isothermal kinetic analysis may start with the kinetic equation:

$$\beta \frac{d\alpha}{dT} = A \exp\left(\frac{-E}{RT}\right) f(\alpha) \quad (2)$$

where β is the heating rate, α is the conversion, R is the universal gas constant, T is the temperature and f(α) is the differential conversion function.

By using the Coats-Redfern<sup>27</sup> approximation to resolve the so-called temperature integral and considering that 2RT/E is much lower than 1, the Kissinger-Akahira-Sunose (KAS) equation may be written as:<sup>28</sup>

$$\ln \frac{\beta}{T^2} = \ln \left[ \frac{AR}{g(\alpha)E} \right] - \frac{E}{RT} \quad (3)$$

For each conversion degree, the linear representation of ln[β/T<sup>2</sup>] versus T<sup>-1</sup> enables E and ln[AR/g(α)E] to be determined from the slope and the ordinate in the origin. If the reaction model, g(α), is known, for each conversion the corresponding pre-exponential factor can be calculated for every activation energy. In this paper, to assign a reaction model to the systems studied, we used the Criado's reduced master curves procedure, which is described elsewhere.<sup>30</sup>

Different kinetic models have been studied: diffusion (D<sub>1</sub>, D<sub>2</sub>, D<sub>3</sub> and D<sub>4</sub>), Avrami-Erofeev (A<sub>2</sub>, A<sub>3</sub> and A<sub>4</sub>), power law, phase-boundary-controlled reaction (R<sub>2</sub> and R<sub>3</sub>), autocatalytic (n+m = 2 and 3) and n order (n = 1, 1.5, 2 and 3).<sup>30</sup> We found that the curing of the systems studied follows a kinetic model of order n (n=1.5), with g(α)=

$2[-1+(1-\alpha)^{1/2}]$ . The rate constant,  $k$ , were calculated with  $E$  and  $A$  determined at  $\alpha = 0.5$ , using the Arrhenius equation.

### 3. Results and Discussion

In previous works we reported the cationic copolymerization of DGEBA with Meldrum acid derivatives (MCP and MDM). Due to the characteristics of MCP, with a high strained cyclopropenylic ring, a double ring opening of the skeleton could be suspected, which could justify the expandable behaviour observed.<sup>8</sup> However, MDM also showed an expandable character.<sup>9</sup> Therefore, the opening of the Meldrum acid ring should be the responsible of these results.

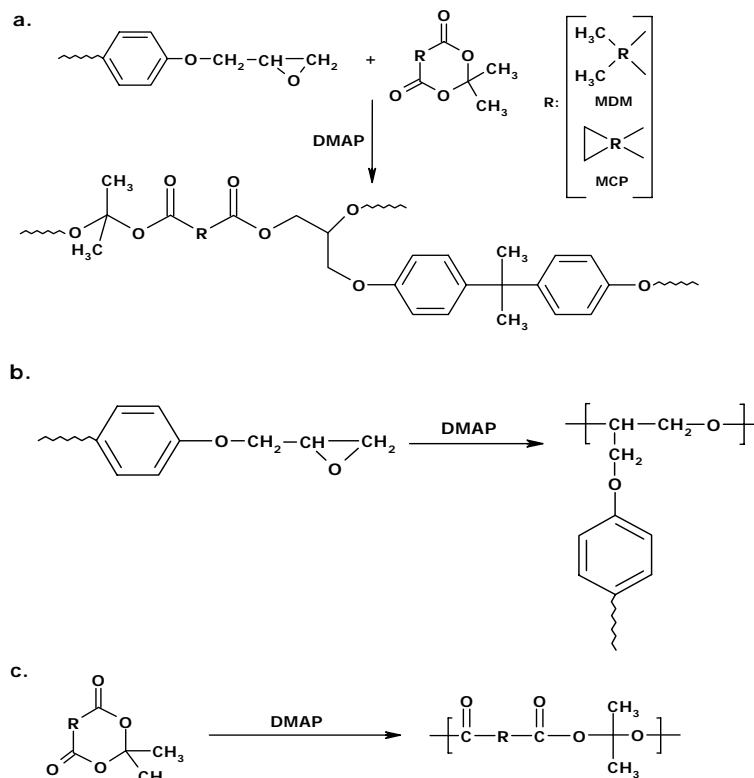
In the present work we studied the copolymerization of DGEBA and these two lactones using DMAP as anionic initiator because DMAP has proved to be stable in air atmosphere and to have a great nucleophilicity.<sup>17,18</sup> In **Scheme 1** is depicted the structure of the initial products and the reactive processes that could be expected. In anionic systems the reactions between epoxide and  $\gamma$ -lactones are reported to have an alternating character<sup>13,14</sup> but there are not reported studies in the anionic copolymerization with Meldrum acid derivatives (**Scheme 1.a**). In addition, if epoxide is in excess in the reactive mixture its homopolymerization should also occur (**Scheme 1.b**).<sup>31</sup> The polymerization of lactones was studied several years ago<sup>32</sup> and it was reported that the polymerizability of six-membered carbonyl-containing cyclic monomers depends marked-

ly on the class of compound involved. Alkyl and aryl substituents on a ring always decrease the polymerizability and therefore the homopolymerization of MCP or MDM is uncertain (**Scheme 1.c**). The DGEBA/lactone proportion of the formulations studied, 3:1 mol/mol, reduces the probability of this homopolymerization process.

#### 3.1. Study of the curing by calorimetry

**Figure 1** shows the calorimetric curves and the conversion degrees against temperature for pure DGEBA, DGEBA/MDM and DGEBA/MCP mixtures initiated by DMAP. The curing of DGEBA exhibits a unimodal exotherm and higher conversion degrees at lower temperatures than the curing of DGEBA/lactone mixtures. On adding lactone the calorimetric curve exhibit a more complex shape, due to the concurrence of the different reactive processes. Among Meldrum acid derivatives, MCP produced a higher deceleration than MDM. The addition of both Meldrum derivatives to DGEBA delay the curing process. This fact could be attributed to the presence of carboxylate and alkoxide chain ends, being the former less reactive than the latter.

In **Table 1** the calorimetric results and the kinetic parameters of the curing process of pure DGEBA and its mixtures with MDM or MCP are collected. As can be seen, the addition of lactone, leads to a decrease in the Tg values of the materials because of the increased length between cross-



**Scheme 1**

links and the flexibility introduced by the lactone structure. The total enthalpy per epoxy equivalent for the formulations DGEBA/MDM and DGEBA/MCP are quite similar between them and higher than the pure DGEBA epoxy resin, which can be due to the heat evolved by the ring-opening of the lactone.

The dependence of the apparent activation energy on the degree of conversion calculated using the isoconversional method (Eq. 3) is represented in **Figure 2** for the samples studied.

There is not a big variation of activation energy values in the curing of DGEBA or its mixture with MCP, but the  $E_a$  of the curing of the sample that contains MDM shows a pronounced decrease from 85 to 45 kJ/mol in the range 10-80% of conversion.

To calculate the frequency factors from the activation energies we determined the kinetic model which better fits with the experimental results.

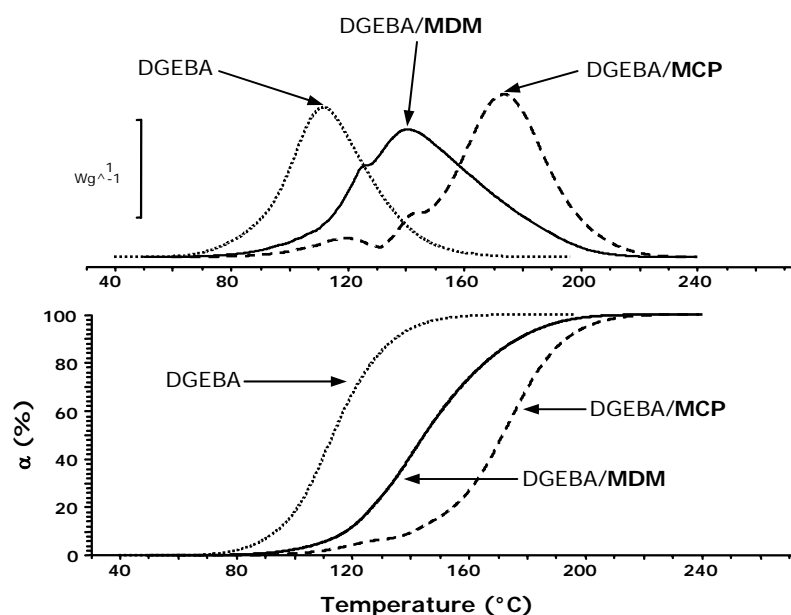


**Figure 1.** DSC scanning curves and conversion degrees against temperature of the curing of DGEBA and DGEBA/lactone 3:1 (mol/mol) mixtures initiated by DMAP at a heating rate of 10°C/min

**Table 1.** Calorimetric data and kinetic parameters of the different systems studied

Entry	Formulation <sup>a</sup>	T <sub>g</sub> <sup>c</sup> (°C)	ΔH <sup>d</sup> (J/g)	ΔH <sup>e</sup> (kJ/ee)	T <sub>max</sub> <sup>f</sup> (°C)	E <sub>a</sub> <sup>g</sup> (kJ/mol)	ln A <sup>h</sup> (s <sup>-1</sup> )	k <sub>150°C</sub> · 10 <sup>3</sup> (s <sup>-1</sup> )
1	DGEBA/DMAP 1:0.088	140	466.4	84.9	112	65.2	15.40	42.94
2	DGEBA/MCP/DMAP 3:1:0.308	116	427.3	92.5	175	67.3	13.12	2.44
3	DGEBA/MCP/DMAP 3:1:0.308	97	423.1	91.8	141	59.6	12.12	8.03

a. The composition of the formulations is given in molar ratios

b. In entries 2 and 3 the glass transition temperatures were obtained by DSC in a second scan after dynamic curing. For entry 1 it was evaluated from the sample cured isothermally at 140°C for 3 hours and a post-curing for 2 hours at 160°C

c. Enthalpy per gram of mixture

d. Enthalpy per equivalent of epoxy group

e. Temperature of the maximum of the curing exotherm

f. Values of activation energies were evaluated by the isoconversional integral method (Eq. (3)) applied at conversion of 0.5

g. The values of pre-exponential factor for kinetic model with  $n=1.5$  ( $g(\alpha) = 2[-1+(1-\alpha)^{1/2}]$ ) per  $\alpha=50\%$

h. The values of the rate constants at 150°C were calculated using the Arrhenius equation  $\ln k = \ln A - \frac{E}{RT}$

We used the reduced master curves procedure of Criado<sup>29</sup> that consists in comparing the experimental curves with the theoretical ones calculated for the different models mentioned in the experimental part.

The activation energies for each theoretical model by the Coats-Redfern method<sup>27</sup> were also calculated and compared with the experimental values. The results, using both Criado and Coats-Redfern methods showed that the

$n=1.5$  kinetic model presented the best correlation between experimental and predicted kinetic data.

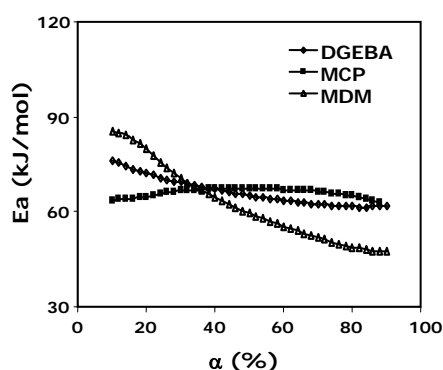


**Figure 2.** Dependence of activation energy on the degree of conversion obtained by DSC in the curing of DGEBA and DGEBA/lactone formulations

Known the activation energy and the kinetic model and using the equation 3, we can obtain the frequency factors  $A\alpha$  for a conversion of 0.5.<sup>33</sup> To obtain the kinetic constants we used the Arrhenius equation.

**Table 1** also collects the kinetic parameters of the curing for the samples studied at a conversion of 0.5. The calculated constant rates clearly show the order of reactivity observed by DSC (see **Figure 1**). In a previous work<sup>34</sup> we studied the anionic polymerization of DGEBA with some six membered cyclic carbonates initiated by DMAP. We could observe a reduction in the  $T_g$  of the materials obtained on adding the comonomer, due to the aliphatic structure introduced, and also a decrease in the curing rate.

### 3.2. Study of the reactions on curing

Because of the homopolymerizability of MCP or MDM is uncertain, first of all we studied if these processes can occur in the presence of DMAP as initiator. By DSC (**Figure 3**) the thermal behaviour of mixtures of each lactone and DMAP was investigated. As can be seen, the MCP curve shows after melting an exothermic process, which could be attributed to the homopolymerization. The enthalpy per mol calculated from the DSC was 24.3kJ/mol. On the other hand, MDM only shows a broad endotherm, which can be related to their melting and sublimation ability.

By ATR/FTIR it could be confirmed that MDM completely disappeared on heating at 150°C in the presence of DMAP by sublimation. In contrast, MCP reacted because of the initial carbonyl lactone bands at 1768 and 1742 $\text{cm}^{-1}$  disappeared and a new band at 1732 $\text{cm}^{-1}$  attributable to the linear ester was formed. Moreover, the band at 962 $\text{cm}^{-1}$  due to the deformation of the six-membered ring completely disappeared. This band was assigned in the basis of the calculations made with the program Gaussian 98.<sup>35</sup> However, the most striking observation was the complete disappearance of the absorption at 3115 $\text{cm}^{-1}$ , which is typical from the C-H stretching of cyclopropenylic structures. This leads to the conclusion that DMAP can attack the cyclopropenylic ring, similarly to the results described by some authors with other nucleophiles.<sup>36,37</sup>

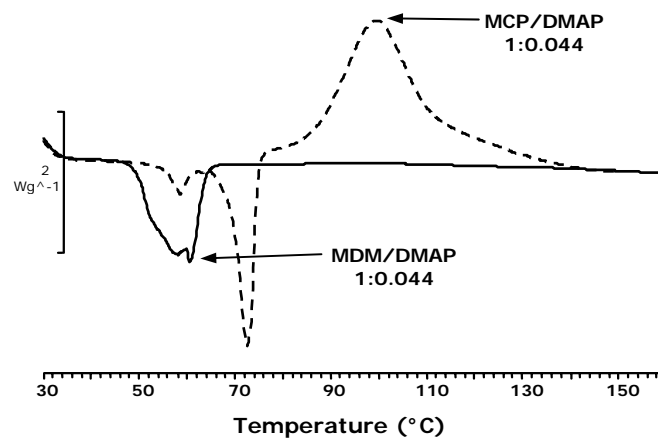


**Figure 3.** DSC scanning curves against temperature of both Meldrum acid derivatives and 0.044 mol of DMAP per mol of lactone at a heating rate of 10°C/min

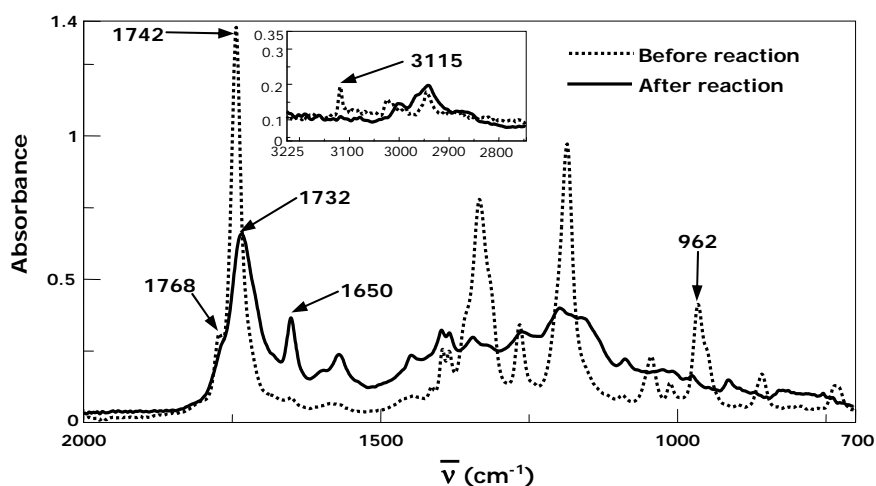


**Figure 4.** ATR-FTIR spectra of a mixture of MCP/DMAP initiated by DMAP before and after reaction at 150°C

**Figure 4** shows the ATR/FTIR spectra obtained from a MCP/DMAP mixture before and after reaction. To establish the structure of the product obtained we heated at 150°C for 2 hours a convenient amount of the reactive mixture in a reaction tube and

then we tried to record NMR spectra, but the product was partially insoluble in common deuterated solvents. This indicates that some crosslinking occurred and that MCP behaved as it had functionality higher than two. These facts allowed confirming

that pure MCP can homopolymerize when heated with DMAP with opening of the cyclopropenylic ring, but this result does not imply that the homopolymerization must occur in the copolymerization with DGEBA.

**Figures 5 and 6** show the ATR/FTIR spectra of the DGEBA/MCP and DGEBA/MDM 3:1 (mol/mol) formulations using 0.308 mol of DMAP as initiator before and after curing at 150°C. The evolution of the carbonyl region during curing is shown in the insets. In the spectra of the uncured samples, there are two carbonylic absorptions at 1771 and 1747 cm<sup>-1</sup> (MCP) and 1782 and 1743 cm<sup>-1</sup> (MDM), attributable to the stretching of the carbonyl groups

the six-membered ring and a band at 912cm<sup>-1</sup> due to the deformation of the oxirane ring. In the spectra of the both cured samples, the epoxide and the lactone ring deformation absorptions are absent, indicating that the epoxide and the lactone are fully incorporated into the network. The times needed to achieve the complete reaction were 4335s and 1830s for MCP and MDM mixtures, respectively.

The disappearance of the band at 965 or 962 cm<sup>-1</sup> should indicate that MCP or MDM have reacted leading to an absorption at 1733 or 1734 cm<sup>-1</sup> due to the linear carbonyl ester group. This band is more intense in the MDM sample, which indicates that the proportion of linear carbonyl ester

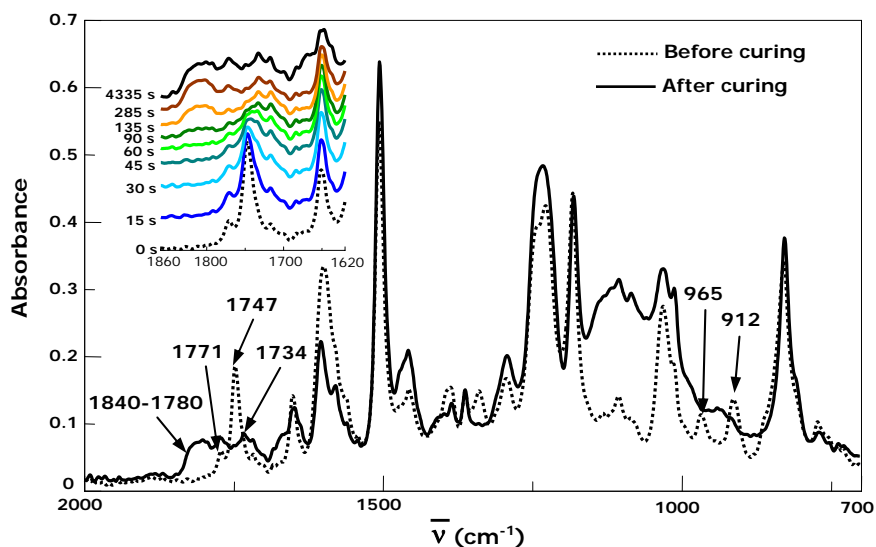


**Figure 5.** ATR-FTIR spectra of a mixture of DGEBA/MCP 3:1 (mol/mol) formulation initiated by DMAP before and after curing at 150°C. The inset show the evolution of the region between 1600-1880 cm<sup>-1</sup> during curing

of the initial lactones, a band at 965cm<sup>-1</sup> (MCP) and 962cm<sup>-1</sup> (MDM) due to the deformation of

groups in the network is higher in this case. The disappearance of the band at 965 cm<sup>-1</sup> indicates that the



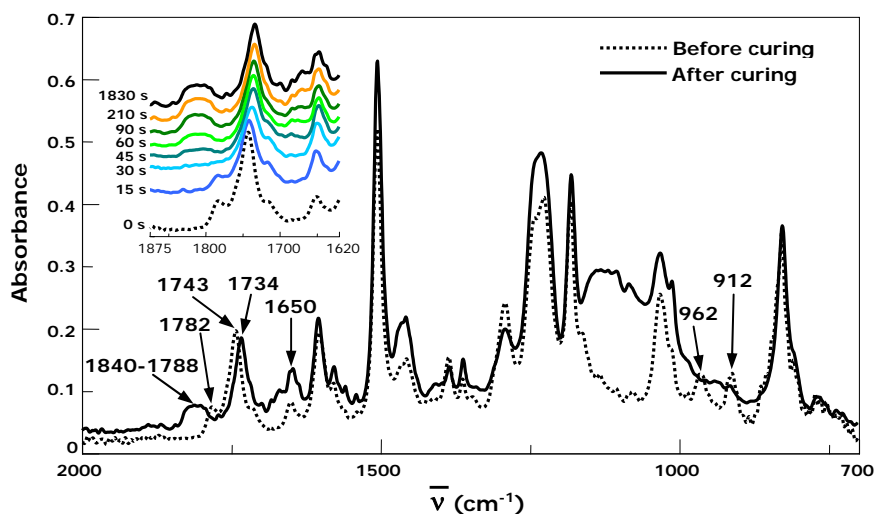


**Figure 6.** ATR-FTIR spectra of a mixture of DGEBA/MDM 3:1 (mol/mol) formulation initiated by DMAP before and after curing at 150°C. The inset show the evolution of the region between 1600-1880  $\text{cm}^{-1}$  during curing

lactone ring is opened. Therefore, the low linear ester absorption in MCP mixture is an unexpected result. In fact, when pure MCP with DMAP polymerized (**Figure 4**), the linear ester band at 1732  $\text{cm}^{-1}$  clearly appeared. One possible explanation to this difference could be found in the reactivity of the spiroacetal structure of MCP, which is susceptible to be attacked by a variety of nucleophiles to give ring-opened products bearing a stabilized carbanion. When the MCP is copolymerized with DGEBA, DMAP firstly opens the oxirane ring forming an alkoxide, which can attack the cyclopropenylic structure finally leading to a different structure than the formed by the direct attack of DMAP. However, we could not observe any difference in the zone of 3100  $\text{cm}^{-1}$  corresponding to the cyclopropanic C-H st. because of the proportion

of MCP in the DGEBA/MCP reactive mixture. Thus, in the curing of the mixtures we could not experimentally prove the opening of the cyclopropenylic ring.

MDM was not able to homopolymerize with DMAP in the previous experiments, but the copolymerization with DGEBA resulted in the formation of linear ester. This seems to indicate that DMAP is not capable to attack directly to the lactone ester group, but the alkoxide formed in the opening of oxirane ring is reactive enough to open the lactone structure.

**Figure 7** shows the evolution of the lactone during curing by monitoring the diminution of the band at 962 (MDM) or 965  $\text{cm}^{-1}$  (MCP) corresponding to the deformation of the lactone ring. As can be seen, MDM reacts faster and at 360s completely disappears, whereas MCP needs 1185s to com-

plete the reaction. Both lactones react at a high rate in the first stages of the curing, but the reaction of MCP slows down at a conversion of 0.55, at lower conversion than MDM.

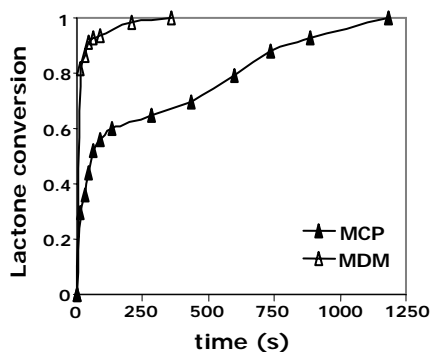


Figure 7. Conversion of lactone against time in the curing of mixtures DGEBA/lactone initiated by DMAP obtained from FTIR spectra

Figure 8 shows the evolution of epoxide groups during curing in both mixtures by monitoring the disappearance of the band at  $912\text{ cm}^{-1}$ . The disappearance of epoxy group in the MDM mixture takes place very fast until a conversion of 0.8 is reached. A different behaviour shows the epoxy conversion curve in the mixture with MCP. The disappearance of epoxide is slower from the very beginning and slows down after a conversion of 0.5. Taking into account the molar relation between epoxide and lactone, the results indicate that homopolymerization of epoxide occurs from the first stages in the mixture with MDM. In the MCP mixture the monomer consumption occurs more simultaneously in the first stages of the curing. For example, in Figure 7 it can be seen that at

250s the lactone conversion is 0.6, which should correspond to an epoxy conversion of 0.1 if an alternate copolymerization occurs. Figure 8 shows that at 250 s the conversion of epoxide are 0.1, which implies a consumption of 0.6 mol of epoxy because of the molar ratio of the mixture.

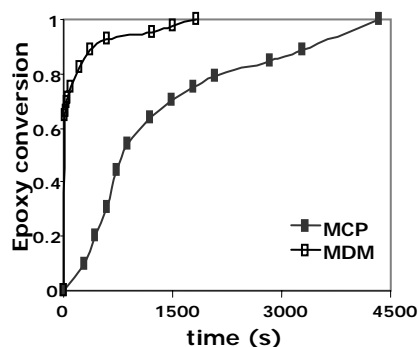


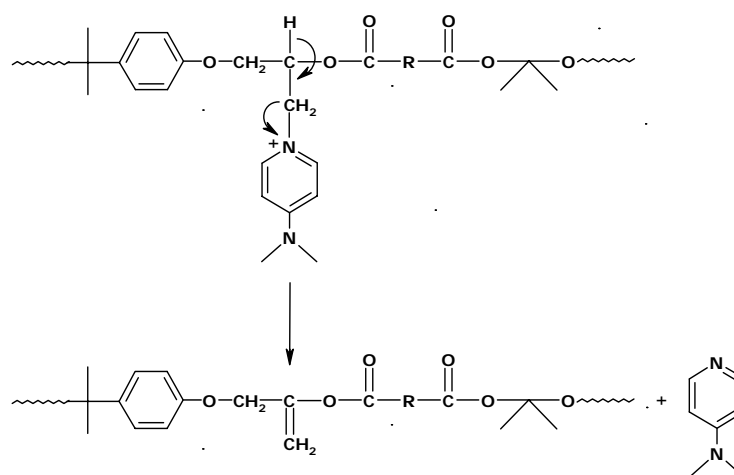
Figure 8. Conversion of epoxide against time in the curing of mixtures DGEBA/lactone initiated by DMAP obtained from FTIR spectra

However, from the FTIR spectrum in Figure 5, we cannot observe the expected intensity in the linear ester absorption and therefore the alternate copolymerization cannot be confirmed, because of some lactone reacts in another way.

Figures 5 and 6, in addition to the expected absorptions, show a broad band above  $1780\text{ cm}^{-1}$  in the spectra recorded after curing. Among the carbonyl groups which absorbs at this high wave number the most probably in our reactive medium could be anhydrides or vinylic esters. The formation of vinylic ethers was described in the homopolymerization of epoxide with DMAP,<sup>31</sup> the reaction mechanism to form vinylic esters seems to be probable and it implies the attack of the alkoxide to

the lactone ring and the posterior elimination reaction to refresh DMAP. This mechanism is depicted in **Scheme 2**. Dell'Erba et al.<sup>31</sup> assigned the vinylic ether peaks to the band at  $1642\text{ cm}^{-1}$ .

From the FTIR data and TGA experiments, the formation of both, vinyl esters and anhydride moieties, can be suspected in our curing systems and their presence can justify the broadness of the

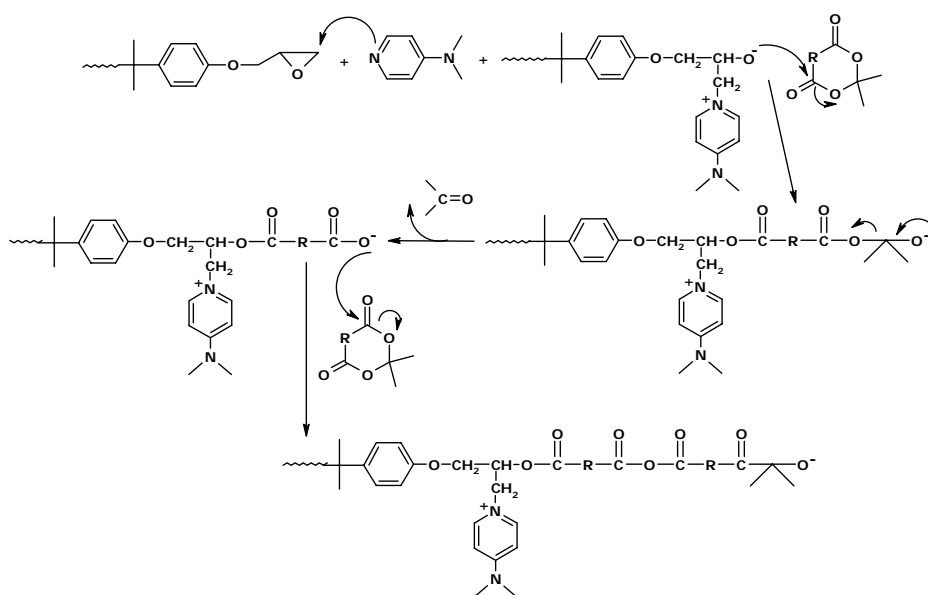


**Scheme 2**

Vinyl esters should produce an absorption in the region  $1690\text{--}1650\text{ cm}^{-1}$  due to the  $\text{C}=\text{C}$  stretch in addition to the carbonylic absorption.<sup>39</sup> In the insets of **Figures 5** and **6** we can clearly see a band in this zone that broadens when the curing progresses, which seems to confirm the presence of these groups. Moreover, a possible mechanism that leads to the formation of anhydride moieties, which implies the loss of acetone, is shown in **Scheme 3**. The loss of acetone, occurring in this mechanism, could be related with a clear weight loss at about  $70^\circ\text{C}$  observed on curing mixtures of DGEBA/MCP or DGEBA/MDM in the presence of DMAP in the thermobalance.

absorptions in the carbonylic region.

In a previous study<sup>34</sup> on the copolymerization of DGEBA and six membered cyclic carbonates initiated by DMAP an unexpected broad centered at  $1820\text{ cm}^{-1}$  could be observed by FTIR spectroscopy and was attributed to the formation of a five membered cyclic carbonate formed by a back-biting process. Furthermore, the linear carbonate absorption was much lower than expected. These observations can support the formation of the unexpected moieties that we postulated in the present study, produced by the high reactivity of the anionic groups at the end of the growing chains.



Scheme 3

In order to go deeply in the reactions that take place during the curing process some experiments using phenylglycidylether (PGE) as a model compound, were made maintaining at 150°C for 3 h in the presence of DMAP. **Figure 9** shows the initial and final FTIR spectra and the evolution of the 1875-1615  $\text{cm}^{-1}$  range in the ATR during reaction of a mixture PGE/MCP 6:1 mol/mol. In contrast to that observed in the spectrum of DGEBA/MCP mixture (**Figure 5**), the model compound shows a big linear ester absorption after polymerization. However, looking at the inset of the figure at 600 seconds a broad absorption about 1800  $\text{cm}^{-1}$  is clearly seen, but it diminishes with the progress of the reaction. The appearance of this band can be attributed to the formation of an anhydride, which

can be transformed into ester group by reaction with an alkoxide. This last reaction is possible in this model study but it is hindered by topological reasons in the curing of DGEBA/MCP, because of the lack of mobility in the growing network. Thus, anhydride can remain unreacted and a low linear ester proportion is formed in the thermoset. There is no evidence of the formation of vinylic ester in this model study, because the band at 1650  $\text{cm}^{-1}$  does not broaden as observed in the curing mixture.

### 3.3. Study of the shrinkage

One of the goals of our research is to reduce the shrinkage during curing that reduces the stresses in the final materials; therefore the densities of the mixtures

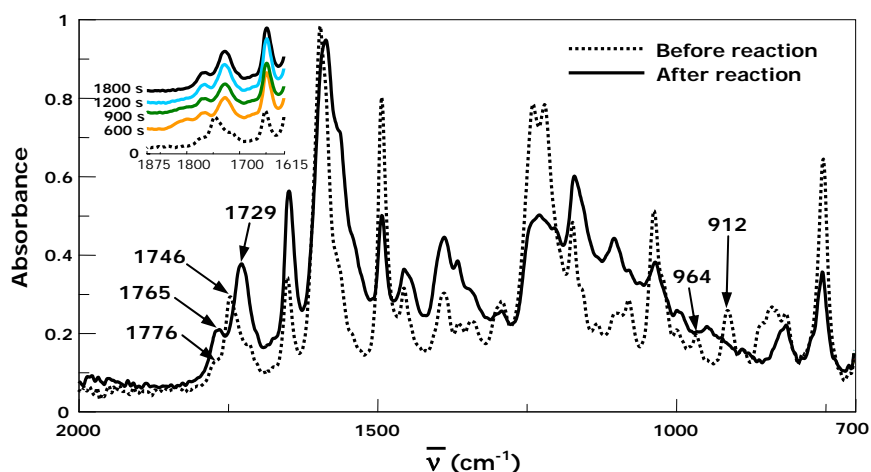


**Figure 9.** ATR-FTIR spectra of a mixture of PGE/MCP 6:1 (mol/mol) formulation initiated by DMAP before and after reaction at 150°C. The inset show the evolution of the region between 1600-1880  $\text{cm}^{-1}$  during reaction

before and after curing were measured. **Table 2** shows these densities and the calculated global shrinkage. The values of pure DGEBA were added in the table in order to compare the effect of the addition of both lactones. As we can see, the addition of lactone leads to a reduction of the shrinkage, which is more important with MDM, which could be attributed to the higher chemical incorporation of lactone by forming linear ester. These results put again into evidence the expandable character

of Meldrum acid derivatives, irrespective to the mechanism (cationic or anionic) of copolymerization.

### 3.4. Study of the thermal degradability

To test if our modification procedure by copolymerization leads to more reworkable thermosets, the thermal degradability of the materials synthesized was analyzed by TGA measurements. **Figure 10** shows the thermogravi-

**Table 2.** Densities and shrinkage, themogravimetric and thermodynamomechanical parameters of the systems studied using DMAP as initiator

Entry	Formulation <sup>a</sup>	$\rho_{im}^b$ ( $\text{g}/\text{cm}^3$ )	$\rho_{fm}^b$ ( $\text{g}/\text{cm}^3$ )	Shrink- age (%)	T <sup>c</sup> (°C)	T <sub>max</sub> <sup>d</sup> (°C)	% Char (T <sup>e</sup> = 600°C)	Tan $\delta$ <sup>d</sup> (°C)	E' <sup>e</sup> (MPa)
1	DGEBA/DMAP 1:0.088	1.155	1.192	3.2	337	430	16	146	35.2
2	DGEBA/MCP/DMAP 3:1:0.308	1.169	1.195	2.2	335	428	14	111	16.8
3	DGEBA/MDM/DMAP 3:1:0.308	1.159	1.181	1.9	252	425	13	87	7.5

- a. The compositions of the formulation is given in molar ratios  
 b. Densities before ( $\rho_{im}$ ) and after ( $\rho_{fm}$ ) curing process  
 c. Temperature of a 2% of weight loss calculated by thermogravimetry  
 d. Temperature of the maximum degradation rate calculated by thermogravimetry  
 e. The storage modulus was calculated at  $\tan \delta + 50^\circ\text{C}$

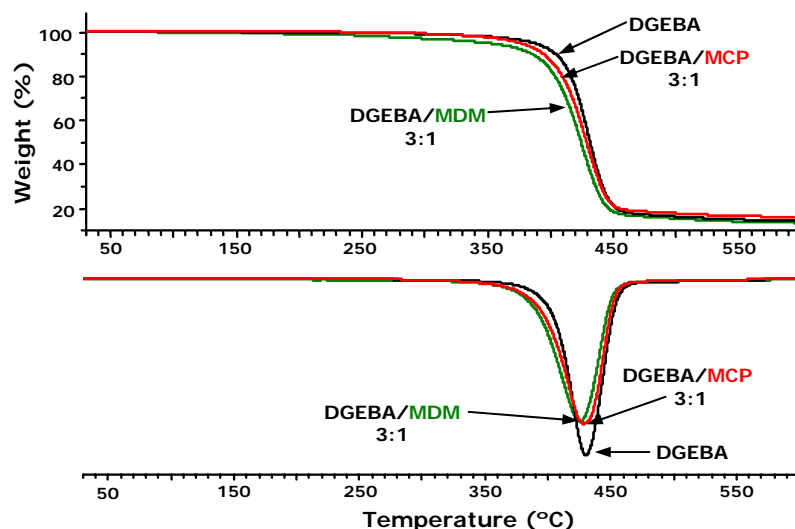


Figure 10. TGA and DTG curves at 10°C/min in a N<sub>2</sub> atmosphere of the crosslinked materials obtained

metric curves for the cured materials. In **Table 2** are collected the thermogravimetric parameters for the materials studied. The influence of the structure of the lactone in the degradability of the materials can be observed. The material obtained with MDM begin their degradation (2% weight loss) at much lower temperature than pure DGEBA, which can be attributed to the presence of tertiary ester linkages observed by FTIR, in the network. However, the addition of MCP does not produce any significant reduction. This is in accordance to the lower proportion of ester groups in the crosslinked structure. There are not many differences in the  $T_{max}$  and char yield on adding lactone, because of the absence of ester groups at this temperature and the low proportion of the aliphatic moieties introduced.

Comparing these values with those obtained from cationic crosslinked materials initiated by lanthanide triflates<sup>9,24</sup> we can conclude that the initial weight loss is related to the proportion of linear ester groups introduced in the network, whatever the initiator used, but the temperature of the maximum degradation rate is much lower for the lanthanide initiated materials, which can be attributed to the catalytic effect of these Lewis acids on the breakage of ether linkages.

### 3.5. Study of the thermomechanical properties

The copolymerization of epoxy resins with lactones, with a functionality of two, leads to less densely crosslinked networks with an increased distance between crosslinks and therefore, mechanical properties should experiment

some changes. The thermomechanical properties of these materials using DMTA were studied. **Figures 11 and 12** show the variations of the storage moduli ( $E'$ ) and  $\tan \delta$  change with the composition of the thermosets obtained. The characteristic parameters from these experiments are shown in **Table 2**. In **Figure 11** it can be seen how the storage moduli of the copolymers undergo relaxation at lower temperatures than DGEBA.

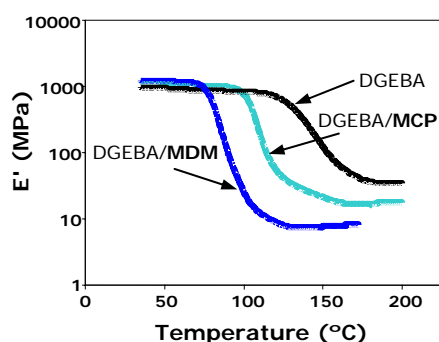


**Figure 11.** Storage modulus ( $E'$ ) against temperature for the materials obtained

The material with MDM relaxes at the lowest temperature and lead to the lowest relaxed modulus, which could be related to the higher proportion of linear ester introduced leading to a longer distance between crosslinks. **Figure 12** shows the values of  $\tan \delta$  against temperature, which confirm the flexibility introduced in the network by the chemically incorporated lactone. The height of the peak of  $\tan \delta$  is also an indicator of the significance of the relaxation of the material when it undergoes the glass transition. So, we can state that the addition of lactone diminishes the  $T_g$  value and increases

the flexibility of the network, which is more evident for the material obtained with MDM. The homogeneity of the copolymeric materials seems not to be lower than for the material obtained from pure DGEBA.

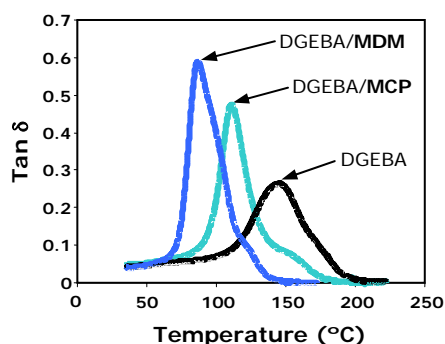


**Figure 12.**  $\tan \delta$  against temperature for the materials obtained

#### 4. CONCLUSIONS

The addition of MCP or MDM to DGEBA produced a decelerative effect in the curing process using DMAP as initiator.

The modification of DGEBA with MCP or MDM initiated by DMAP incorporated into the network, in addition to the expected tertiary ester moieties, other carbonylic groups, which were not formed under cationic conditions. The proportion of linear ester depends on the type of lactone used and is higher for MDM.

The materials obtained by copolymerization presented lower  $T_g$ ,  $\tan \delta$  and relaxed modulus than that obtained in absence of lactone, due to the increase of the flexibility when the lactones are incorporated into the network.

The incorporation of MCP or MDM to DGEBA epoxy resin increased slightly the thermal degradability of the final materials especially in that obtained with MDM due to the higher linear ester proportion.

The expandable character of Meldrum acid derivatives was demonstrated, because of the addition of MCP or MDM to the DGEBA reduces the global shrinkage on curing.

### Acknowledgements

*The authors from the Universitat Politècnica de Catalunya would like to thank CICYT and FEDER (MAT2004-04165-C02-02) for their financial support. The authors from the Rovira i Virgili University would like to thank the CICYT (Comisión Interministerial de Ciencia y Tecnología) and FEDER (Fondo Europeo de Desarrollo Regional) (MAT2005-01806).*

### 5. REFERENCES

1. Sathir RK and Luck MR Ed. "Expanding Monomers. Synthesis, Characterization and Applications" CRC Press, Boca Raton (1992).
2. Matejka L, Chabanne L, Tighzert L and Pascault JP, *J Polym Sci Part A: Polym Chem* 32: 1447-1458 (1994).
3. Fedtke M, Haufe J, Kahlert E and Müller G, *Angew Makromol Chem* 255: 53-59 (1998).
4. Mas C, Ramis X, Salla JM, Mantecón A and Serra A, *J Polym Sci Part A: Polym Chem* 41: 2794-2808 (2003).
5. Giménez R, Fernández-Francos X, Salla JM, Serra A, Mantecón A and Ramis X, *J Polym Sci Part A: Polym Chem* 46: 10637-10647 (2005).
6. Mas C, Ramis X, Salla JM, Mantecón A and Serra A, *J Polym Sci Part A: Polym Chem* 44: 1711-1721 (2006).
7. Canadell J, Mantecón A and Cádiz V, *J Polym Sci Part A: Polym Chem* 45: 4211-4224 (2007).
8. González L, Ramis X, Salla JM, Mantecón A and Serra A, *J Polym Sci Part A: Polym Chem* 44: 6869-6879 (2006).
9. González L, Ramis X, Salla JM, Mantecón A and Serra A, *J Appl Polym Sci*, 108, 1229-1237 (2008).
10. González L, Ramis X, Salla JM, Mantecón A and Serra A, *Eur Polym J*, *in press*.
11. Brady RF Jr and Simon FE, *J Polym Sci Part A: Polym Chem* 25: 231-239 (1987).
12. Sikes AM and Brady RF, *J Polym Sci Part A: Polym Chem* 28: 2533-2546 (1990).
13. Tadokoro A, Takata T and Endo T, *Macromolecules* 26: 2388-2389 (1993).
14. Chung K, Takata T and Endo T, *Macromolecules* 28: 1711-1713 (1995).
15. Mika T F and Bauer R S "Curing Agents and Modifiers," in *Epoxy Resins Chemistry and Technology*, May CA, editor, 2<sup>nd</sup> edition, Marcel Dekker, New York, p 465 (1998).
16. Pascault JP, Sautereau H, Verdu J and Williams RJJ "Thermosetting Polymers", Marcel Dekker, New York (2002).
17. Galià M, Serra A, Mantecón A and Cádiz V, *J Appl Polym Sci* 56: 193-200 (1995).
18. Ribera D, Mantecón A and Serra A, *J Polym Sci Part A: Polym Chem* 40: 3916-3926 (2002).



19. Fernández-Francos X, Salla JM, Mantecón A, Serra A and Ramis X, J Appl Polym Sci, in press.
20. Chen JS, Ober CK and Poliks MD, Polymer 43: 131-139 (2002).
21. Wang L, Li H and Wong CP, J Polym Sci Part A: Polym Chem 38: 3771-3782 (2000).
22. Li H and Wong CP IEEE Trans Adv Packaging 27: 165-172 (2004).
23. Chen JS, Ober CK, Poliks MD, Zhang Y, Wiesner U and Cohen C, Polymer 45: 1939-1950 (2004).
24. González L, Ramis X, Salla JM, Mantecón A and Serra A, Polym Degrad Stab 92: 596-604 (2007).
25. González L, Ramis X, Salla JM, Mantecón A and Serra A, Thermochim Acta 464: 35-41 (2007).
26. González S, Fernández-Francos X, Salla JM, Serra A, Mantecón A and Ramis X, J Appl Polym Sci 104: 3406-3416 (2007).
27. Coats AW and Redfern JP, Nature 201: 68-69 (1964).
28. Kissinger HE, Anal Chem 29: 1702-1706 (1957).
29. Criado JM, Thermochim Acta 24: 186-189 (1978).
30. Ramis X, Salla JM, Cadenato A and Morancho JM, J Therm Anal Calorim 72: 707-718 (2003).
31. Dell'Erba IE and Williams RJJ, Polym Eng Sci 46: 351-359 (2006).
32. Hall HK and Schneider AJ, J Am Chem Soc 80: 6409-6412 (1958).
33. Vyazovkin S and Linert W, J Solid State Chem 114: 392-398 (1995).
34. Cervellera R, Ramis X, Salla JM, Mantecón A and Serra A, J Polym Sci Part A: Polym Chem 44: 2873-2882 (2006).
35. Lee I, Han IS, Kim CK and Lee HW, Bull Korean Chem Soc 24: 1141-1149 (2003).
36. Chen BC, Heterocycles 32: 529-597 (1991).
37. McNab H, Chem Soc Rev 7: 345-358 (1978).
38. Singh RK and Danishefsky S, Organic Synthesis Coll. Vol VII, John Wiley & Sons, pp. 411-414, NY (1990).
39. Pretsch E, Clerc T, Seibl J and Simon W, "Tablas para la Determinación Estructural por Métodos Espectroscópicos" Springer Verlag Ibérica, Barcelona (1998).



*SÍNTESI D'UNA NOVA REÏNA EPOXI I  
COPOLIMERITZACIÓ CATIÒNICA  
AMB EL DGEBA*



5.1.



*INTRODUCCIÓ*

## 5. SÍNTESI D'UNA NOVA REÏNA EPOXI I COPOLIMERITZACIÓ CATIÒNICA AMB DGEBA

### 5.1. Introducció

Un cop realitzats els diferents estudis sobre les copolimeritzacions catiòniques de la reina epoxi de diglicidilèter de bisfenol A (DGEBA) amb les diferents lactones emprades (**MA**, **MDM**, **MCP** i **MCB**) ens vam proposar la síntesi d'un nou derivat de l'àcid de Meldrum que fos al mateix temps lactona i compost diepoxídric i que, per tant pogués homopolimeritzar o copolimeritzar amb el DGEBA.

Aquesta nova reina epoxi, el 5,5-(2,3-epoxipropil)-2,2-dimetil-4,6-dioxo-1,3-dioxà (**DGMA**) es representa a la **fig.5.1**.

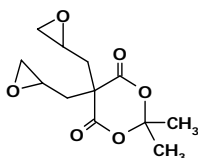


**Fig.5.1.** 5,5-(2,3-epoxipropil)-2,2-dimetil-4,6-dioxo-1,3-dioxà

La síntesi d'aquest compost es va realitzar en dues etapes. En primer lloc es va sintetitzar el 5,5-dial·lil-2,2-dimetil-4,6-dioxo-1,3-dioxà (**DAMA**) per reacció de l'àcid de Meldrum amb bromur d'al·lil en presència de carbonat de potassi anhidre i N,N-dimetilformamida<sup>118</sup> (**Fig.5.2**).

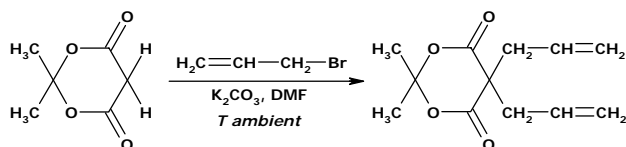


**Fig.5.2.** Obtenció del 5,5-dial·lil-2,2-dimetil-4,6-dioxo-1,3-dioxà (DAMA)

<sup>118</sup> D.G. Desai, R. B. Mane, Chem. Ind. (London) 809, 1982.

La segona etapa consisteix en l'epoxidació dels dobles enllaços amb l'àcid metacloroperbenzoic i diclorometà com a dissolvent<sup>119</sup> (**Fig.5.3**).

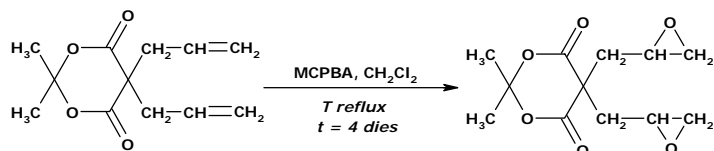


**Fig.5.3.** Epoxidació del 5,5-dial·lil-2,2-dimetil-4,6-dioxo-1,3-dioxà (DAMA)

Una vegada sintetitzada i caracteritzada aquesta nova reina es va estudiar el procés de curat catiònic de manera anàloga als anteriors treballs. Els iniciadors emprats van ser el Yb(OTf)<sub>3</sub> i el La(OTf)<sub>3</sub> en una proporció d'iniciador de 0.003 mols per equivalent reactiu de monòmer. El que pretenem és estudiar la influència d'aquesta nova lactona en el procés del curat, analitzar com es veuen afectades les propietats tèrmiques i l'estabilitat tèrmica dels materials resultants.

Els resultats d'aquests estudis estan reflectits en l'article:

**5.2.** "Synthesis of a New Diglycidyl Meldrum Acid Derivative and Study of the Curing with Lanthanide Triflates as Initiators".

L. González, J. Simokaitiene, X. Ramis, J.M. Salla, A. Mantecón, A. Serra.  
J. Polym. Sci. Part A. Polym. Chem. *En premsa*

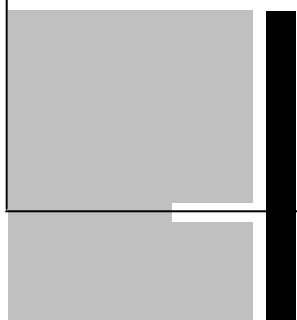
<sup>119</sup> A. Roig; M. Galià; V. Cádiz; A. Mantecón; A. Serra; Makromol Chem, **194**, 411-419 (1993).



## 5.2.



*SYNTHESIS OF A NEW DIGLYCIDYLIC MELDRUM ACID  
DERIVATIVE AND STUDY OF THE CURING WITH LANTHANIDE  
TRIFLATES AS INITIATORS*



## SYNTHESIS OF A NEW DIGLYCIDYLIC MELDRUM ACID DERIVATIVE AND STUDY OF THE CURING WITH LANTHANIDE TRIFLATES AS INITIATORS

Lidia González,<sup>1</sup> Jurate Simokaitiene,<sup>1\*</sup> Xavier Ramis,<sup>2</sup> Josep Maria Salla,<sup>2</sup>  
Ana Mantecón,<sup>1</sup> Angels Serra<sup>1</sup>

<sup>1</sup>Departament de Química Analítica i Química Orgànica. Universitat Rovira i Virgili. Marcel·lí Domingo s/n, 43007 Tarragona, Spain

<sup>2</sup>Laboratori de Termodinàmica, ETSEIB. Universitat Politècnica de Catalunya, Av. Diagonal 647, 08028 Barcelona, Spain

\*Permanent address: Department of Organic Technology, Kaunas University of Technology, Radvilenu Plentas 19, LT-50254 Kaunas, Lithuania.

---

### Abstract

A new epoxy resin derived from Meldrum acid (DGMA) was synthesized by a two steps synthetic procedure and structurally characterized by the usual spectroscopic techniques and elemental analysis. Ytterbium and lanthanum triflates were tested as cationic initiators to cure this resin and its mixtures with diglycidylether of bisphenol A (DGEBA) in several proportions. By ATR-FTIR spectroscopy the evolution of the groups which participate in the curing was followed.

The evolution of the curing and the Tg of the materials were studied by differential scanning calorimetry and the kinetic parameters were calculated applying isoconversional procedures. Ytterbium triflate led to a quicker curing than lanthanum.

The thermal stability of the materials obtained was evaluated by thermogravimetry and the higher thermal degradability of the materials containing DGMA was confirmed.

**Keywords:** Epoxy resins, lactones, cationic polymerization, crosslinking, thermosets

---

## 1. INTRODUCTION

Epoxy thermosets are one of the most applied materials in many industrial applications, such as the microelectronic industry. One of our research interests is the modification of the network structure to broaden the applicability of this type of materials and to reduce its limitations. In previous works<sup>1,2,3</sup> we used the strategy based on the copolymerization of commercially available epoxy resins, DGEBA, with Meldrum acid derivatives with the aim to improve the thermal degradability of the materials and reduce the shrinkage during curing. We could prove that Meldrum acid derivatives expand on copolymerizing with DGEBA and thus, the shrinkage during curing is lower than the experimented by curing pure DGEBA. Moreover, the thermosets obtained showed a higher thermal degradability, especially when they were obtained by using cationic initiators.

Another strategy to obtain epoxy thermosets with better characteristics is the synthesis of new epoxy monomers with an adequate designed chemical structure. For example, some authors introduced tertiary alkyl ester groups into the monomer structure, which are prone to be thermally broken. In this way, they obtained the so-called *reworkable epoxy thermosets*.<sup>4,5,6</sup> These thermosetting materials cannot be recycled but the network structure can be broken down under controlled conditions and therefore the materials can be removed from the substrate,

enabling the repairing or recycling of electronic devices assembled or coated with such materials.

In addition to the chemical structure of the monomers, it was recognized that the chemical nature of curing agents can also have a significant influence on the gel-time and the physical properties of the epoxy thermosets, because they can determine the morphology and the crosslinking density of the epoxy network. Lanthanide triflates are commercially available Lewis acids that maintain their catalytic activities in non-inert atmosphere,<sup>7,8</sup> and can act as cationic initiators in the curing of epoxy resins.<sup>9</sup> We applied them in the copolymerization of epoxides and Meldrum acid derivatives and we saw an increasing in the degradability of the thermosets,<sup>2</sup> a reduction of the shrinkage after gelation by the formation of intermediate spiroorthesters<sup>10</sup> and an improvement in the mechanical characteristics.<sup>11</sup>

In 1908 Meldrum reported the synthesis of 2,2-dimethyl-1,3-dioxane-4,6-dione, which was named Meldrum acid after him, from malonic acid and acetone in acetic anhydride containing a small amount of sulphuric acid.<sup>12</sup> The chemistry of this compound is determined by its acidity (pK 4.83). By the use of a base the correspondent anion in the methylene group can be formed and then it can react with alkyl halides, mainly to produce the dialkyl derivatives. Moreover, it can be attacked by nucleophiles in the carbonyl group.<sup>13</sup> We wanted to take advantage from both processes: a) preparing a new diepoxy monomer

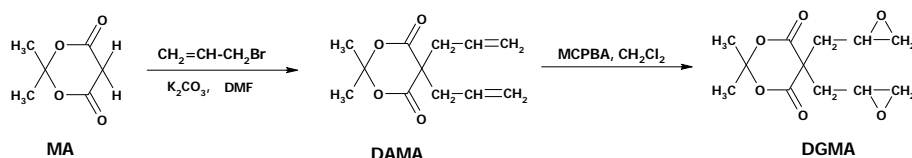


by dialkylation in the methylene group of the ring and b) forming a SOE intermediate by the nucleophilic attack of epoxide to the carbonyl groups. The SOEs formed can further polymerize to lead poly (ether-ester) thermosets. This article describes one of our current studies focusing in the preparation of degradable thermosets. We synthesized a new epoxy resin derived from Meldrum acid, 5,5-bis(diglycidyl)-2,2-dimethyl-4,6-dioxo-1,3-dioxane (DGMA) (**Scheme 1**), which have tertiary alkyl ester groups in its structure. Then, we studied by ATR/FTIR and differential scanning calorimetry (DSC) its homopolymerization and its copolymerization with a conventional epoxy resin, DGEBA, initiated by ytterbium and lanthanum triflates as cationic initiators. The influence of both lanthanide salts were evaluated from the point of view of the kinetics of curing and from the structural characteristics of the thermoset. The thermal degradability of the materials obtained was evaluated by thermogravimetry.

## 2. EXPERIMENTAL PART

### 2.1. Materials

Diglycidylether of bisphenol A (DGEBA) EPIKOTE RESIN 827 from Shell Chemicals (Epoxy Equiv. = 182.08g/eq);



**Scheme 1**

2,2-dimethyl -4,6-dioxo- 1,3-dioxane (Meldrum acid, Aldrich); 3-chloroperbenzoic acid (MCPBA, ~70%; Fluka) were used as received. Allyl bromide (Probus) was distilled over  $\text{CaCl}_2$  before use.

Lanthanum (III) and ytterbium (III) trifluoromethanesulfonates (Aldrich) were used without purification.

Organic solvents were purified by standard methods.

### 2.2. Synthesis of 5,5-diallyl-2,2-dimethyl-4,6-dioxo-1,3-dioxane (DAMA)<sup>14</sup>

20g (0.14mol) of Meldrum acid were added in a single portion to a stirred suspension of 28.76g (0.21mol) of anhydrous potassium carbonate in 70mL of N,N-dimethylformamide under magnetic stirring. After 15min at room temperature, 35.25g (0.3mol) of allyl bromide was added and the reaction mixture was maintained with stirring overnight. Then, the reaction mixture was poured into cold water (100-150mL) and the product extracted with methylene chloride. The dried organic solvent was eliminated by distillation under vacuum and a yellow viscous liquid was obtained. Yield 8.6g (56%).

$^1\text{H}$  NMR ( $\text{CDCl}_3$ ,  $\delta$  (ppm)): 1.68 (s, 6H,  $\text{CH}_3$ -); 2.74 (d, 4H,  $-\text{CH}_2-$ ); 5.2 (m, 2H,  $-\text{CH}=\text{}$ ); 5.57(m, 4H,  $\text{CH}_2=\text{}$ ).

$^{13}\text{C}$  NMR ( $\text{CDCl}_3$ ,  $\delta$  (ppm)): 30.11; 42.99; 55.68; 106.04; 112.57; 131.09; 168.93.

### 2.3. Synthesis of 5,5-bis(diglycidyl)-2,2-dimethyl-4,6-dioxo-1,3-dioxane (DGMA)

8.61g (0.04 mol) of 5,5-diallyl-2,2-dimethyl-4,6-dioxo-1,3-dioxane and 16.57g (0.1mol) of MCPBA were dissolved in 100mL of methylene chloride and stirred at reflux temperature for 4 days. Then, the solution was treated with 5 wt % sodium disulfite ( $\text{Na}_2\text{S}_2\text{O}_5$ ) solution and further with a saturated solution of sodium bicarbonate ( $\text{NaHCO}_3$ ) in a separator funnel in order to eliminate the m-chlorobenzoic acid formed. After drying with  $\text{MgSO}_4$  the solvent was evaporated and the oil obtained was left in the refrigerator. White crystals were obtained after one week. Yield 6.4g (65%). M.p. 48-50 °C.

$^1\text{H}$  NMR ( $\text{CDCl}_3$ ,  $\delta$  (ppm)): 1.80-1.81 (ds, 6H,  $\text{CH}_3$ -); 2.10-2.38 (m, 4H,  $-\text{CH}_2$ -); 2.51-2.78 (m, 2H,  $-\text{CH}$ -); 2.93-2.99 (m, 4H,  $\text{O}-\text{CH}_2$ ).

$^{13}\text{C}$  NMR ( $\text{CDCl}_3$ ,  $\delta$  (ppm)): 29.20; 41.13; 47.81; 48.22; 50.25; 107.05; 168.35.

FTIR/ATR ( $\text{cm}^{-1}$ ): 1768, 1731, 1437, 1416, 1392, 1378, 1348, 1267, 1205, 1175, 1139, 1116, 1076, 1016, 951, 917, 865.

Elemental analysis Calc. for  $\text{C}_{12}\text{H}_{16}\text{O}_6$ : C, 56.24%; H, 6.29%. Found: C, 56.13%; H, 6.35%.

### 2.4. Preparation of the curing mixtures

The samples were prepared by mixing the selected quantity initiator in the corresponding amount of resin (DGMA or DGMA/DGEBA) with manual stirring. The

prepared mixtures were kept at  $-18^\circ\text{C}$  before use. Their compositions are given in **Table 1**. Lanthanide triflates were added in a molar ratio of 0.006 mol per mol of DGEBA or mol of DGMA.

### 2.5. Characterization and measurements

Calorimetric studies were carried out on a Mettler DSC-821e thermal analyzer in covered Al pans under  $\text{N}_2$  at  $10^\circ\text{C}/\text{min}$ . The calorimeter was calibrated using an indium standard (heat flow calibration) and an indium-lead-zinc standard (temperature calibration). The samples weighed approximately 7-9mg. In the dynamic curing process the degree of conversion by DSC ( $\alpha_{\text{DSC}}$ ) was calculated as follows:

$$\alpha_{\text{DSC}} = \frac{\Delta H_T}{\Delta H_{\text{dyn}}} \quad (1)$$

where  $\Delta H_T$  is the heat released up to a temperature  $T$ , obtained by integration of the calorimetric signal up to this temperature, and  $\Delta H_{\text{dyn}}$  is the total reaction heat associated with the complete conversion of all reactive groups. The glass transition temperature for each material ( $T_g$ ) was calculated after complete curing, by means of a second scan, as the temperature of the half-way point of the jump in the heat capacity when the material changed from the glassy to the rubbery state.

The isothermal curing process at  $150^\circ\text{C}$  was monitored with a FTIR spectrophotometer FTIR-680PLUS from JASCO with a reso-

lution of  $4\text{cm}^{-1}$  in the absorbance mode. An attenuated-total-reflection accessory with thermal control and a diamond crystal (Golden Gate heated single-reflection diamond ATR, Specac-Teknokroma) was used to determine FTIR spectra. The conversions of the reactive groups were determined from the normalized changes in the absorbance by the Lambert-Beer law, as we explained previously.<sup>15</sup> After isothermal curing in the ATR-FTIR device, a dynamic scan by DSC was always carried out to prove that the curing was complete.

Thermogravimetric analyses (TGAs) were carried out with a Mettler TGA/SDTA 851e thermobalance. Cured samples with an approximate mass of 7mg were degraded between 30 and 600°C at a heating rate of 10°C/min in  $\text{N}_2$  (200  $\text{cm}^3/\text{min}$ ) measured in normal conditions.

## 2.6. Kinetic Analysis

Integral non-isothermal kinetic analysis was used to determine the kinetic triplet ( $A$  pre-exponential factor,  $E$  activation energy and  $g(\alpha)$  integral function of degree of conversion).

Nonisothermal kinetic analysis may start with the kinetic equation:

$$\beta \frac{d\alpha}{dT} = A \exp\left(\frac{-E}{RT}\right) f(\alpha) \quad (2)$$

where  $\beta$  is the heating rate,  $\alpha$  is the conversion,  $R$  is the universal gas constant,  $T$  is the temperature and  $f(\alpha)$  is the differential conversion function.

By using the Coats-Redfern<sup>16</sup> approximation to resolve the so-called temperature integral and considering that  $2RT/E$  is much lower than 1, the Kissinger-Akahira-Sunose (KAS) equation may be written as:<sup>17</sup>

$$\ln \frac{\beta}{T^2} = \ln \left[ \frac{AR}{g(\alpha)E} \right] - \frac{E}{RT} \quad (3)$$

For each conversion degree, the linear representation of  $\ln[\beta/T^2]$  versus  $T^{-1}$  enables  $E$  and  $\ln[AR/g(\alpha)E]$  to be determined from the slope and the ordinate in the origin. If the reaction model,  $g(\alpha)$ , is known, for each conversion the corresponding pre-exponential factor can be calculated for every activation energy. In this paper, to assign a reaction model to the systems studied, we used the Criado's reduced master curves procedure,<sup>18</sup> which is described elsewhere.<sup>19</sup>

Different kinetic models have been studied: diffusion ( $D_1$ ,  $D_2$ ,  $D_3$  and  $D_4$ ), Avrami-Erofeev ( $A_2$ ,  $A_3$  y  $A_4$ ), power law, phase-boundary-controlled reaction ( $R_2$  and  $R_3$ ), autocatalytic ( $n+m=2$  and  $3$ ) and  $n$  order ( $n=1, 2$  and  $3$ ).<sup>18</sup> We found that the curing of the systems studied follows a kinetic model of the surface-controlled reaction type  $R_3$ , with  $g(\alpha)=[1-(1-\alpha)^{1/3}]$ . The rate constants,  $k$ , were calculated with  $E$  and  $A$  determined at  $\alpha=0.5$ , using the Arrhenius equation.

## 3. RESULTS AND DISCUSSION

**Scheme 1** outlines the synthetic method and structures of

the monomers studied in this article. The two-step method of synthesis consists of a nucleophilic substitution initiated by the anion from Meldrum acid generated by potassium carbonate on the allyl bromide substrate and further epoxidation using *m*-chloroperbenzoic acid. A previous attempt to prepare this compound using epichlorohydrin and the anion generated from MA to introduce directly

glycidic groups did not produce the desired epoxy resin (DGMA) and only a viscous complex mixture was obtained.

The spectra of DGMA confirmed the structure of this product and its purity was confirmed by both NMR spectra and especially with elemental analysis. **Figures 1 and 2** show the  $^{13}\text{C}$  and  $^1\text{H}$  NMR spectra of this compound respectively.

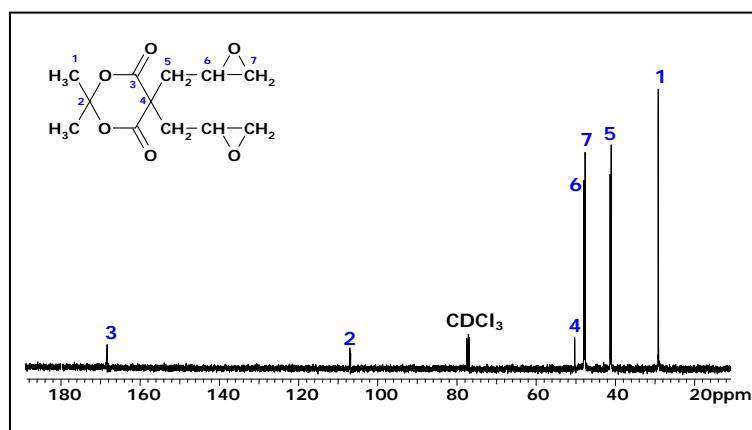


Figure 1.  $^{13}\text{C}$ -NMR spectrum (400MHz) in  $\text{CDCl}_3$  of 5,5-bis(diglycidyl)-2,2-dimethyl-4,6-dioxo-1,3-dioxane (DGMA)

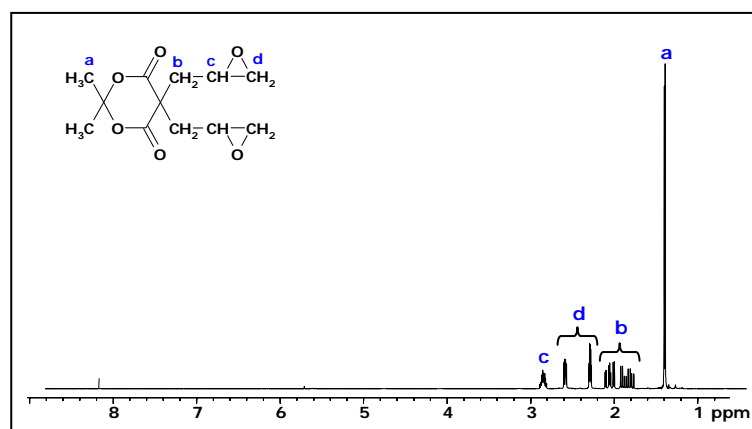
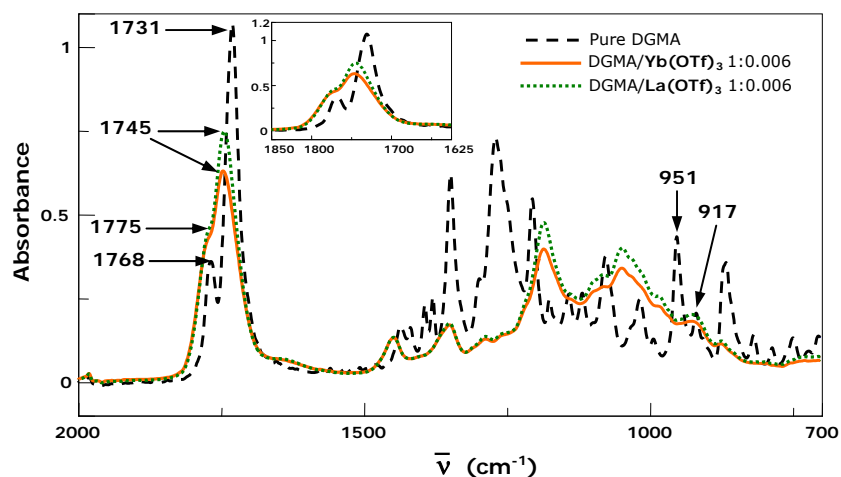


Figure 2.  $^1\text{H}$ -NMR spectrum (100MHz) in  $\text{CDCl}_3$  of 5,5-bis(diglycidyl)-2,2-dimethyl-4,6-dioxo-1,3-dioxane (DGMA)

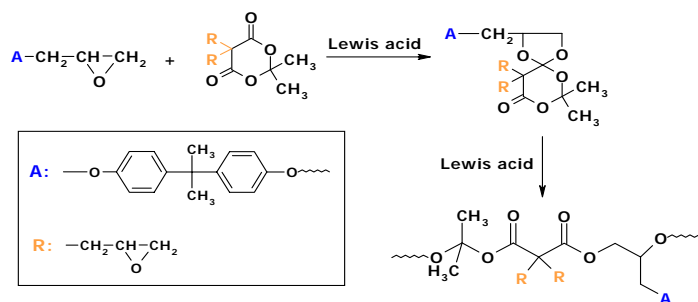
The cyclic structure of the Meldrum acid leads to the unequivalence of both glycidic groups because they can be in quasi-axial or equatorial positions. This is clearly observed in the splitting of signals 5 in **Figure 1**. The signal due to the carbon 6 appears very close to carbon 7. In **Figure 2** it can be seen that each glycidic group has five unequivalent protons due to the presence of a chiral carbon. Thus, coupling between methylene

and vicinal protons are expected leading to a complex coupling pattern, because of the highest shift difference among them.

FTIR spectrum of DGMA (**Figure 3**) shows the typical bands expected: 1768 and 1731  $\text{cm}^{-1}$  corresponding to the stretching of carbonyl esters, the band at 951  $\text{cm}^{-1}$  attributed to the deformation of the lactone ring and the band at 917  $\text{cm}^{-1}$  due to the epoxy group.



**Figure 3.** ATR/FTIR spectra of pure DGMA and the materials obtained by curing DGMA with  $\text{Yb}(\text{OTf})_3$  or  $\text{La}(\text{OTf})_3$  dynamically at a heating rate of  $10^\circ\text{C}/\text{min}$  in the DSC



**Scheme 2**

Once synthesized and characterized the curing reaction of DGMA using lanthanide triflates as initiators was studied. It is to note that the functionality of this resin in cationic systems can be four or six, depending if only both epoxy groups react or even the cyclic lactone structure opens, such as we observed in other non-glycidyl

cationically homopolymerize or copolymerize with epoxides to form poly(ether-ester) structures. **Scheme 2** depicts the formation of SOE and the chemical structure expected for the final material.

**Figure 4 (a and b)** shows the calorimetric curves recorded at 10°C/min. In the same figures are included the calorimetric curves of

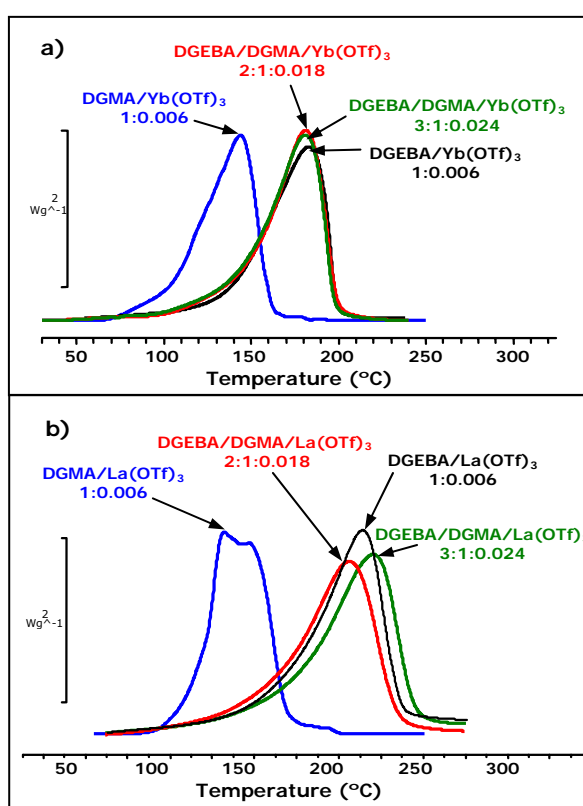


**Figure 4.** DSC scanning curves of DGEBA, DGMA and DGEBA/DGMA in different molar ratios initiated by  $Yb(OTf)_3$  or  $La(OTf)_3$  at a heating rate of 10°C/min

Meldrum acid derivatives.<sup>1,3,10</sup> In the presence of a Lewis acid, lactones react with epoxide to form a spiroorthoester (SOE) which can

pure DGEBA with the same initiators. We can see the higher reactivity of DGMA in comparison to DGEBA systems that allow perfor-

ming the cure at lower temperatures for the new synthesized resin. The shape of the calorimetric curves is different for ytterbium and lanthanum initiated DGMA curing. Whereas the former is practically unimodal the latter shows a splitting, which could indicate the existence of more than one curing mechanism. When these curves were recorded at lower heating rates, the curves got wider and some splitting occurred. Thus, we could not perform the kinetic study of the curing of DGMA. **Table 1** collects some calorimetric data of the curing process. The Tgs of the cured materials are significantly lower than those reached in the curing of DGEBA, with no big differences when the initiator was changed. The enthalpy per epoxy equivalent was lower than expected, which could indicate an uncomplete curing, which can be attributed to the low distance between epoxy rings that could lead to the topological impossibility to react.

To confirm if the complete disappearance of epoxy groups took place we recorded the FTIR spectrum of the cured materials, which are included in **Figure 3**. Looking at the spectra before and after curing we can see very big differences. The band at  $951\text{cm}^{-1}$  in the initial spectrum completely disappears, indicating the opening of the lactone ring. The opening of the lactone structure also leads to the disappearance or the shift of some C-O-C st. bands at 1348, 1269 and  $1204\text{cm}^{-1}$ . The deformation of the epoxy ring at  $917\text{cm}^{-1}$  decreases, but does not completely disappear, which proved that the curing was not complete. The ester

absorptions shifted to 1775 and  $1745\text{cm}^{-1}$  after curing. The presence of absorptions in this zone confirms the presence of ester groups in the final material. Although in the figure the carbonyl absorption seems to be higher for the lanthanum initiated material, these spectra are not quantitatively comparable because the absence of any reference band. The shifts of the carbonylic bands take place in the contrary sense to the observed in the copolymerization of DGEBA with other Meldrum acid derivatives<sup>1,3,10</sup> in which the epoxy groups were not directly attached to the Meldrum acid structure. The proximity of epoxy and lactone ring in DGMA can lead to unexpected structures, but the insolubility of these materials did not allow performing an NMR structural study.

Due to the uncomplete curing observed and the low Tgs obtained we decided to copolymerize this resin with commercial DGEBA using the same initiators. In **Figure 4** the calorimetric curves for different formulations are included. We can see that the mixtures lead to unimodal curves, but no significant shift to lower temperatures on increasing the proportion of DGMA was observed. Ytterbium triflate led to curves at lower temperatures than the lanthanum salt, which can be related to its highest Lewis acidity.<sup>20</sup> In **Table 1** some calorimetric data of these systems are collected. The Tgs of the cured materials (entries 3, 4, 7 and 8) are lower than that of pure cured DGEBA but higher than that of pure DGMA materials and decrease on increasing the proportion of DGMA in the reactive mixture. In

reference to the enthalpy per epoxy equivalent they are also comprised between those of pure DGEBA and DGMA mixtures and decreased when the proportion of DGMA increases, indicating that some epoxy from the new synthesized resin remains unreacted.

The dependence of the apparent activation energy on the degree of conversion calculated using the isoconversional method (Equation 3)<sup>21</sup> is represented in **Figure 5** for the curing of mixtures DGEBA/DGMA initiated by yttrium (**a**) and lanthanum triflates (**b**).

To calculate the frequency factors from the activation energies we determined the kinetic model which better fits with the experimental results. We used the reduced master curves procedure<sup>18</sup> that consists in comparing the experimental curves with the theoretical calculated for the different models mentioned in the experimental part. The kinetic parameters at a conversion of 0.5 given in **Table 1** were calculated with the selected  $R_3$  model.

Known the activation energy, the kinetic parameter  $\ln[(AR/g(\alpha)E)]$  and the kinetic model and using the equation 3,

**Table 1.** Calorimetric data and kinetic parameters of the system studied initiated by Lanthanide Triflates

Entry	Formulation <sup>a</sup>	T <sub>g</sub> <sup>c</sup> (°C)	ΔH <sup>d</sup> (J/g)	ΔH <sup>e</sup> (kJ/ee)	T <sub>max</sub> <sup>f</sup> (°C)	E <sub>a</sub> <sup>g</sup> (kJ/mol)	ln A <sup>h</sup> (s <sup>-1</sup> )	k <sub>150°C</sub> · 10 <sup>3</sup> (s <sup>-1</sup> )
1	DGEBA/Yb(OTf) <sub>3</sub> 1:0.006	135	519.7	95.6	184	90.7	18.09	0.45
2	DGMA/Yb(OTf) <sub>3</sub> 1:0.006	62	521.4	67.8	144	-	-	-
3	DGEBA/DGMA/Yb(OTf) <sub>3</sub> 3:1:0.024	108	507.8	86.3	182	76.5	14.16	0.50
4	DGEBA/DGMA/Yb(OTf) <sub>3</sub> 2:1:0.018	104	506.8	84.1	182	83.3	16.06	0.51
5	DGEBA/La(OTf) <sub>3</sub> 1:0.006	127	513.5	94.4	192	79.8	14.59	0.30
6	DGMA/La(OTf) <sub>3</sub> 1:0.006	60	496.8	64.6	125-140	-	-	-
7	DGEBA/DGMA/La(OTf) <sub>3</sub> 3:1:0.024	107	499.1	85.0	196	87.5	16.47	0.22
8	DGEBA/DGMA/La(OTf) <sub>3</sub> 2:1:0.018	103	498.8	82.7	185	82.0	15.47	0.40

a. The composition of the formulations is given in molar ratios

b. Glass transition temperatures obtained by DSC in the second scan after dynamic curing

c. Enthalpy per gram of mixture

d. Enthalpy per equivalent of epoxy group

e. Temperature of the maximum of the curing exotherm

f. Values of activation energies were evaluated by the isoconversional integral method (Eq.(3)) applied at conversion of 0.5

g. The values of pre-exponential factor for kinetic model with  $R_3$  kinetic model  $g(\alpha)=[1-(1-\alpha)^{1/3}]$

h. The values of the rate constants at 150°C were calculated using the Arrhenius equation  $\ln k = \ln A - \frac{E}{RT}$

The plots decrease until about 25% of conversion and then they remain practically horizontal. The relative high values in the initial stage can be attributed to the formation of initiating active species.

we can obtain the frequency factor  $A\alpha$  for each conversion. To obtain the rate constant we used the Arrhenius equation.

The activation energy values are not significant and do not



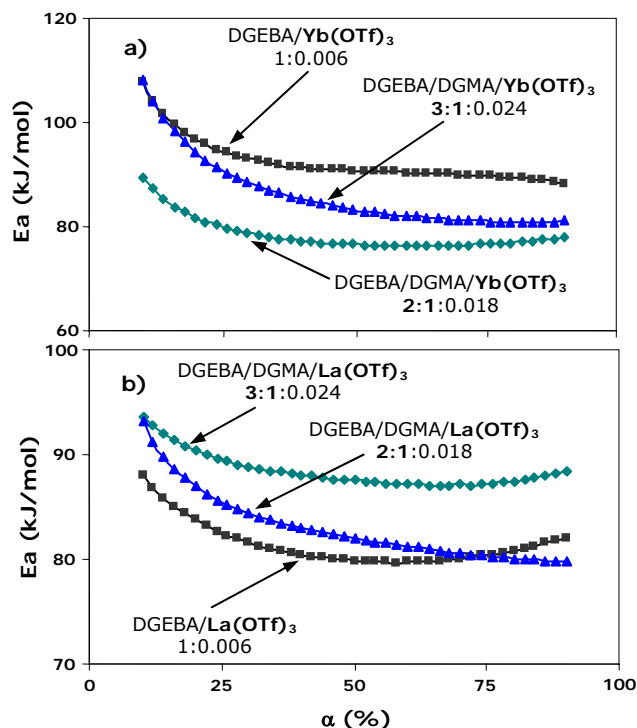


**Figure 5.** Dependence of the activation energy on the degree of conversion for the curing of DGEBA and DGEBA/DGMA formulations initiated by  $\text{Yb}(\text{OTf})_3$  and  $\text{La}(\text{OTf})_3$ .

show the effect of the mixture composition due to the compensation effect between the activation energy and the pre-exponential factor.<sup>19</sup> However, the calculated constant rates clearly show the order of reactivity observed by DSC. The rate constants show the accelerative effect of ytterbium triflate in comparison to lanthanum triflate. There is only a slight effect when DGMA is added to DGEBA.

To study the evolution of the reactive species during curing at 150°C we registered ATR/FTIR spectra at several times. As an example, **Figure 6** shows the spectra before and after curing of a mixture DGEBA/DGMA 2:1 (mol/

mol) initiated by  $\text{Yb}(\text{OTf})_3$ , where the change in the carbonyl region can be clearly observed. The carbonyl region got much wider and the maximum of the absorption is shifted from 1741 to 1762  $\text{cm}^{-1}$ . This is in accordance with the disappearance of the initial lactone structure. However, in this mixture the band at 965  $\text{cm}^{-1}$  assigned to the deformation of the ring give us no information, because of it is hidden in the broaden absorptions in this zone. The epoxy band at 912  $\text{cm}^{-1}$  decreases, but we can not assure its total disappearance. The lower enthalpy released per epoxy equivalent on curing could be due to an incomplete reaction of epoxy groups.

**Figure 7** shows the final FTIR spectra of the materials obtained from DGEBA/DGMA 2:1 (mol/mol) mixtures cured with ytterbium and lanthanum triflate at 150°C in the ATR. The main difference is the slightly greater ester incorporation in the thermoset when the initiator was ytterbium triflate. In this case, the absorption at 1650 cm<sup>-1</sup> due to the aromatic

group was used as a reference and therefore the intensities of the carbonyl ester absorptions can be compared. Another little difference is observed in the band at 1040 cm<sup>-1</sup>, which was attributed to the SOE group, which is slightly higher for La(OTf)<sub>3</sub> initiated curing. These differences were also observed in previous studies.<sup>1,22</sup> They could be attributed to the fact that

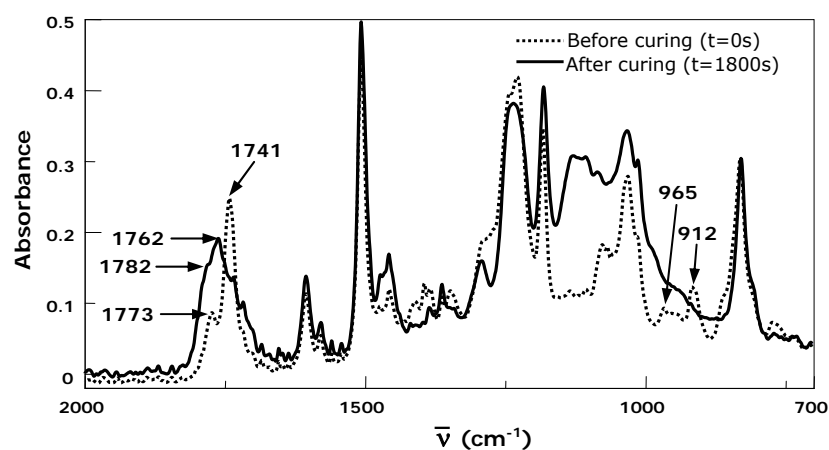


**Figure 6.** ATR/FTIR spectra of a mixture of DGEBA/DGMA 2:1 (mol/mol) formulation initiated by 0.018 mol of Yb(OTf)<sub>3</sub> before and after curing at 150°C

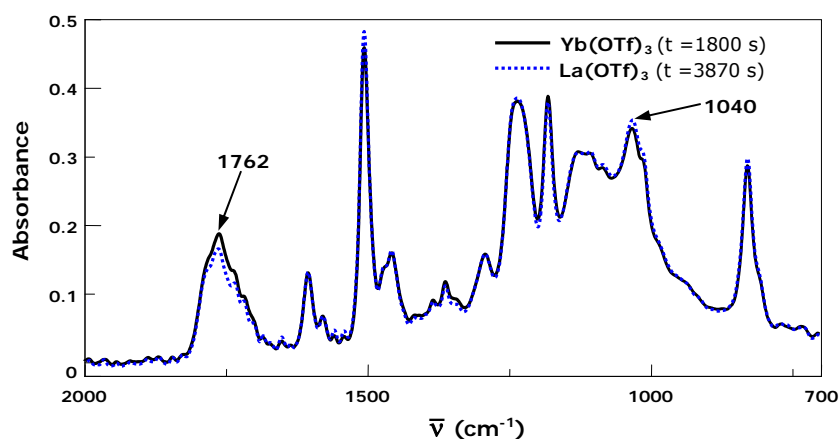


**Figure 7.** ATR/FTIR spectra of the materials obtained by curing at 150°C from DGEBA/DGMA mixtures 2:1 (mol/mol) formulation with 0.018 mol of ytterbium or lanthanum triflates

lanthanum initiator favors the formation of SOE groups but no their homo- and copolymerization with epoxides<sup>23</sup> (*Scheme 2*). This behavior is related to the different affinity of ytterbium and lanthanum cations to the different oxygens in the DGMA structure.<sup>24</sup>

In previous works we studied the curing of mixtures of DGEBA epoxy resin with several Meldrum acid derivatives using lanthanide triflates as initiators.<sup>2,3,10</sup> The thermosets obtained, with tertiary ester groups in their structure, showed an improved thermal degradability in reference

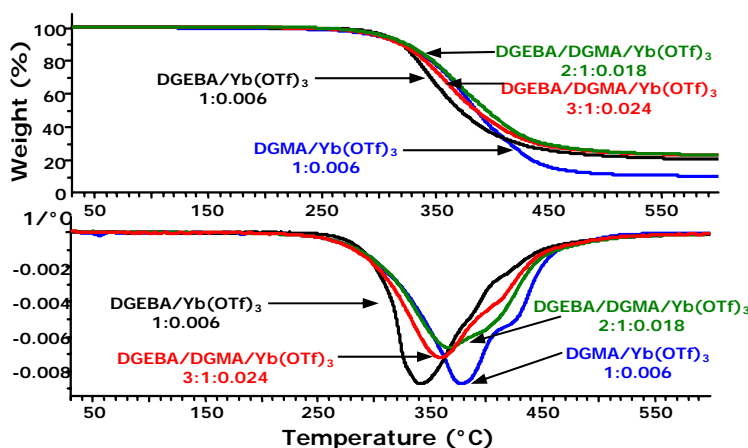


Figure 8. TGA and DTG curves recorded at 10°C/min in  $\text{N}_2$  atmosphere of the materials obtained from different formulations of DGEBA, DGMA and DGEBA/DGMA initiated by  $\text{Yb}(\text{OTf})_3$

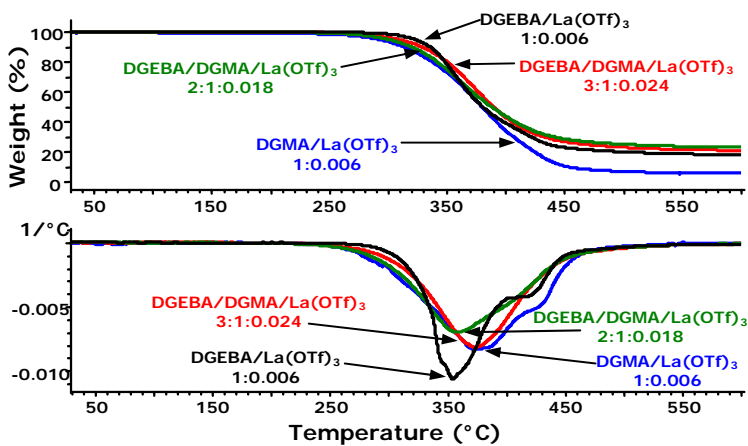


Figure 9. TGA and DTG curves recorded at 10°C/min in  $\text{N}_2$  atmosphere of the materials obtained from different formulations of DGEBA, DGMA and DGEBA/DGMA initiated by  $\text{La}(\text{OTf})_3$

to pure DGEBA materials, which lend a reworkable character to these materials.

**Figures 8 and 9** show the TGA and DTG curves for the degradation of the materials obtained from all the formulations studied initiated by ytterbium and lanthanum triflates, respectively. The broadness and shape of the DTG curves indicates the complexity of the degradative processes for the materials obtained. The use of ytterbium triflate as curing agent shifts to higher temperatures the maximum of the peak on increasing the proportion of DGMA. However, lanthanum cured materials does not show a regular trend. The main thermogravimetric data are collected in **Table 2**. From the point of view of the recovery of electronic devices coated with thermosets, the most important thermal parameter is the temperature at which the more labile linkages begin to break, which transform the insoluble three-dimensional network to fragments

that can be removed. As we can see, the temperatures of the 2% of weight loss of materials decrease on adding DGMA. Moreover, in a previous study<sup>2</sup> we could prove that the degradation of the materials obtained by initiation with lanthanides triflates was greater than the analogous materials obtained by conventional boron trifluoride complexes. The enhanced thermal degradability was attributed to the presence of lanthanide triflates in the network that catalyzes the rupture of both, ester and ether linkages, due to their coordination ability to oxygen atoms. Both the higher acidity of ytterbium triflate and the higher proportion of ester groups in the materials contribute to a higher thermal degradability.<sup>2</sup> However, the material obtained from pure DGMA is slightly more degradable when it was cured in the presence of lanthanum triflate (**Table 2**), probably due to the lower cross-linking density reached in this case.

**Table 2.** Thermogravimetric data of all cured materials

Entry	Formulation <sup>a</sup>	T <sup>b</sup> (°C)	T <sub>max</sub> (°C)	% Char Yield <sup>c</sup>
1	DGEBA/Yb(OTf) <sub>3</sub> 1:0.006	287	345	20
2	DGMA/Yb(OTf) <sub>3</sub> 1:0.006	261	377	10
3	DGEBA/DGMA/Yb(OTf) <sub>3</sub> 3:1:0.024	277	360	23
4	DGEBA/DGMA/Yb(OTf) <sub>3</sub> 2:1:0.018	271	367	23
5	DGEBA/La(OTf) <sub>3</sub> 1:0.006	303	354	19
6	DGMA/La(OTf) <sub>3</sub> 1:0.006	259	373	6
7	DGEBA/DGMA/La(OTf) <sub>3</sub> 3:1:0.024	281	364	21
8	DGEBA/DGMA/La(OTf) <sub>3</sub> 2:1:0.018	273	358	23

a. The composition of the formulations is given in molar ratios  
b. Temperature of a 2% of weight loss calculated by thermogravimetry  
c. Char yield at 600°C

#### 4. CONCLUSIONS

A new epoxy resin, DGMA, has been synthesized by a two-step procedure from commercial Meldrum acid and its structure was confirmed by elemental analysis and FTIR and NMR spectroscopy.

The homopolymerization of DGMA and the copolymerization of DGMA with DGEBA in different proportions have been studied using lanthanum and ytterbium triflates as initiators. In all cases, the ring opening polymerization of the lactone moiety of DGMA was demonstrated.

Although the curing of pure DGMA occurs at lower temperature than the cure of pure DGEBA, the addition of DGMA to DGEBA does not produce any significant reduction of the curing temperature.

The T<sub>g</sub>s of the materials obtained from pure DGMA with the two initiators are lower than those of its copolymers with DGEBA.

The materials containing DGMA showed a better thermal degradability at lower temperatures than pure DGEBA cured materials and therefore showed an increased reworkability.

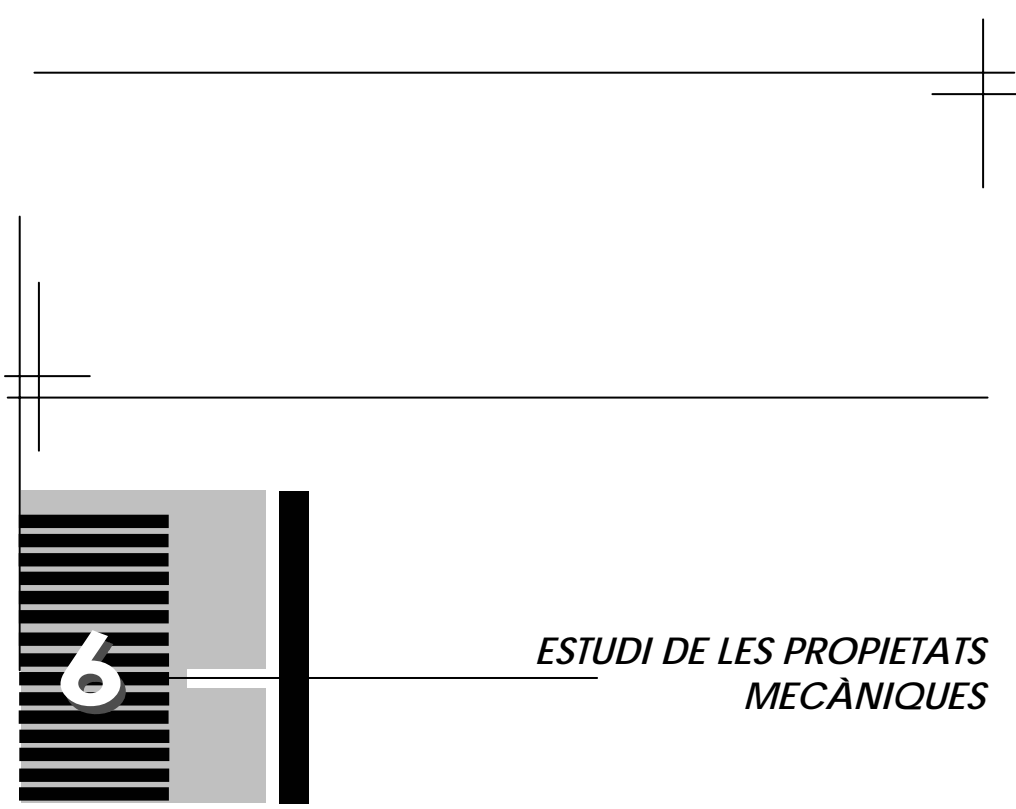
#### Acknowledgements

*The authors from the Universitat Politècnica de Catalunya would like to thank CICYT and FEDER (MAT2004-04165-C02-02) for their financial support. The authors from the Rovira i Virgili University would like to thank the CICYT (Comisión Interministerial de Ciencia y Tecnología) and FEDER (Fondo Europeo de Desarrollo Regional) (MAT2005-01806)*

#### 5. REFERENCES

1. González, L.; Ramis, X.; Salla, J.M.; Mantecón, A.; Serra, A. *J Polym Sci Part A: Polym Chem* 2006, 44, 6969-6979.
2. González, L.; Ramis, X.; Salla, J.M.; Mantecón, A.; Serra, A. *Polym Degrad Stab* 2007, 92, 596-604.
3. González, L.; Ramis, X.; Salla, J.M.; Mantecón, A.; Serra, A. *J Polym Sci Part A: Polym Chem* 2008, 46, 1229-1239.
4. Chen, J-S.; Ober, C.K.; Poliks, M.D.; Zhang, Y.; Wiesner, U.; Cohen, C.; *Polymer* 2004, 45, 1939-1950.
5. Wang, L.; Li, H.; Wong, C.P. *J Polym Sci Part A: Polym Chem* 2000, 38, 3771-3782.
6. Chen, J.S.; Ober, C.K.; Poliks, M.D. *Polymer* 2002, 43, 131-139.
7. Kobayashi, S., Ed. *"Lanthanides: Chemistry and Use in Organic Synthesis"* Topics in Organometallic Chemistry, Springer Verlag, Berlin, 1999.
8. Kobayashi, S.; Sugiura, M.; Kitagawa, H.; Lam, W.W.L. *Chem Rev* 2002, 102, 2227-2302.
9. Castell P.; Galià, M.; Serra, A; Salla, J.M.; Ramis, X. *Polymer* 2000, 41, 8465-8474.
10. González, L.; Ramis, X.; Salla, J.M.; Mantecón, A.; Serra, A. *J Appl Polym Sci* 2008, 108, 1229-1237.
11. Garcia, S.J. ; Serra, A. ; Suay, J. *J Polym Sci Part A: Polym Chem* 2007; 45: 2316-2327.
12. Meldrum, A.N. *J Chem Soc* 1908, 93, 598.
13. McNab, H. *Chem Soc Rev* 1978, 7, 345-358.

14. Desai, D.G.; Mane, R. B. Chem Ind (London) 1982, 20, 809.
15. Mas, C.; Ramis, X.; Salla, J.M.; Mantecón, A.; Serra, A. J Polym Sci Part A: Polym Chem 2003, 41, 2794-2808.
16. Coats, A.W.; Redfern, J.P. Nature 1964, 201, 68-69.
17. Kissinger, H.E. Anal Chem 1957, 29, 1702-1706.
18. Criado, J.M. Thermochim Acta 1978, 24, 186-189.
19. Ramis, X.; Salla J.M.; Cadenato, A.; Morancho, J.M. J Therm Anal Cal 2003, 72, 707-718.
20. Luo, S.; Zhu, L.; Talukdar, A.; Zhang, G.; Mi, X.; Cheng, J.P.; Wang, P.G. Mini-Rev Org. Chem. 2005, 2, 546-564.
21. Vyazovkin, S.; Linert, W. J Solid State Chem 1995, 114, 392-398.
22. Arasa, M.; Ramis, X.; Salla, J.M.; Mantecón, A.; Serra, A. J Polym Sci Part A: Polym Chem 2007, 45, 2129-2141.
23. Mas, C.; Mantecón, A.; Serra, A.; Ramis, X.; Salla, J.M. J Polym Sci Part A: Polym Chem 2004, 42, 3782-3791.
24. Pearson, R.G. J Am Chem Soc 1963, 85, 3533-3539.



*ESTUDI DE LES PROPIETATS  
MECÀNIQUES*

## 6. ESTUDI DE LES PROPIETATS MECÀNIQUES

### 6.1. Introducció

Aquest capítol està centrat en l'estudi de les propietats mecàniques dels diferents materials termoestables obtinguts per copolimerització catiònica o aniònica de la reina epoxi de diglicidilèter de bisfenol A (DGEBA) amb l'àcid de Meldrum (**MA**) o diferents derivats de l'àcid de Meldrum, el **MCP** (6,6-dimetil-5,7-dioxaspiro[2.5]octan-4,8-diona), el **MDM** (2,2,5,5-tetrametil-4,6-dioxo-1,3-dioxà) i el **MCB** (7,7-dimetil-6,8-dioxaspiro[3.5]nonan-5,9-diona) (**Fig.6.1**).

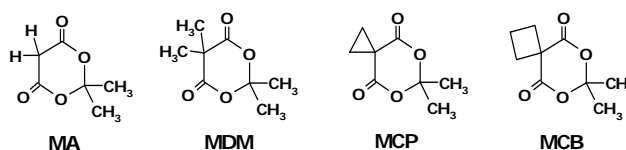


**Fig.6.1.** Lactones utilitzades en la copolimerització amb la reina epoxi de DGEBA

Per estudiar les propietats mecàniques dels materials, vam utilitzar dues tècniques:

- *Anàlisi termodinamomecànica mitjançant DMTA.*
- *Estudi de la microduresa*

### 6.2. Anàlisi termodinamomecànica (DMTA)

La tècnica de DMTA és de les més emprades per caracteritzar les propietats mecàniques de les reines epoxi i ens permet obtenir informació sobre les seves transicions tèrmiques, de primer i segon ordre, que no sempre són detectables per altres mètodes d'anàlisi tèrmica. Les propietats mecàniques d'un polímer entrecruat depenen de la temperatura d'assaig. En funció d'aquest paràmetre es poden considerar tres intervals de comportament, que s'anomenen regions viscoelàstiques (**Fig.6.2**).



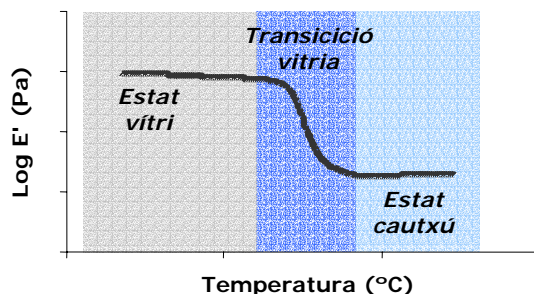


Fig.6.2. Regions viscoelàstiques d'un polímer entrecreuat

Al gràfic es representa la variació del mòdul d'emmagatzematge ( $E'$ ) front la temperatura, on es pot observar el diferent comportament d'un polímer en aquestes tres regions:

- **Estat vítri:** En aquesta primera regió el polímer es caracteritza pel seu estat sòlid amb una certa duresa i rigidesa.
- **Transició vítria o regió viscoelàstica:** En aquesta zona el material passa de trobar-se en un estat vítri a un estat cautxú de forma que la seva rigidesa es veu disminuïda ràpidament.
- **Estat cautxú:** En aquesta regió el material es molt més elàstic i presenta valors del mòdul baixos.

L'última regió es manté constant pels polímers entrecreuat, inclòs a temperatures elevades, arribant fins i tot a la degradació del polímer sense l'aparició de fenòmens de fluïdesa. El mòdul d'emmagatzematge ( $E'$ ) a la zona elàstica depèn de la densitat d'entrecreuament. Si un material presenta una densitat d'entrecreuament elevada, la deformació que experimenta front una força externa serà inferior que la d'un material que estigui menys entrecreuat.

El principi de la tècnica de l'anàlisi termodinamomecànica (DMTA) es fonamenta en l'aplicació d'una força sinusoidal al material avaluant-se la resposta que dona aquest. Els primers assaigs en estudis oscil·latoris van ser realitzats per Poynting en 1909.<sup>120</sup>

Al 1961 Ferry va escriure un estudi sobre propietats viscoelàstiques de polímers<sup>121</sup> incloent mesures dinàmiques com part integral del seu estudi. McCrum i col. van recopilar en el seu llibre de text les teories sobre anàlisi dinamomecànica i dielèctrica<sup>122</sup>. Els instruments disponibles en aquesta etapa eren difícils d'utilitzar, lents, limitats i amb baixa resolució. Al 1978 es van

<sup>120</sup> J. H. Poynting, Proc. Royal Soc., Series A, **82**, 546-559 (1909).

<sup>121</sup> J. Ferry, "Viscoelastic Properties of Polymers", 3rd Edition, John Wiley and Sons, New York, 1980.

<sup>122</sup> N. McCrum, G. Williams, B. Read, "Anelastic and Dielectric Effects in Polymeric Solids", Wiley, New York, 1967.

desenvolupar d'altres experiments portats a terme per Nijenhuis.<sup>123</sup> *Perkin Elmer* va ser una de les primeres companyies en desenvolupar un equip d'anàlisi de tensió controlada, basant-se en un equip previ d'anàlisi termomecànica (TMA).

Els experiments es poden realitzar en condicions isotèrmiques, és a dir a una temperatura prefixada, o bé en condicions dinàmiques, és a dir en un interval de temperatura. La resposta que ens proporciona el material ens ofereix informació sobre la seva estructura tant a nivell local com a nivell global. Com que els materials no són completament elàstics, la deformació que experimenten no és instantània i la resposta presenta un desfasament respecte la força aplicada, ja que les cadenes del polímer no tenen temps suficient per relaxar-se. La deformació variable amb el temps es tradueix en moviments moleculars de les cadenes polimèriques, les quals modifiquen la seva conformació per adaptar-se a la força aplicada.<sup>124</sup>

La força aplicada és de tipus sinusoidal i ve definida per la següent equació:

$$F = F_0 \sin(\omega t)$$

Aquesta força provoca a la proveta de tracció una tensió uniforme:

$$\sigma = \sigma_0 \sin(\omega t)$$

on  $\sigma$  és la tensió a un temps determinat,  $\sigma_0$  és l'amplitud de la tensió aplicada i  $\omega$  és la pulsació d'oscil·lació aplicada. Aquesta tensió provoca una deformació de tipus sinusoidal del material seguint l'expressió següent:

$$\varepsilon = \frac{\sigma_0}{E} \sin(\omega t) + \delta$$

on  $\varepsilon$  és la deformació en funció del temps,  $E$  el mòdul del material i  $\delta$  l'angle de desfasament entre la tensió aplicada i la deformació. Donada la dependència lineal amb la deformació, aquesta expressió es pot escriure com:

$$\varepsilon = \varepsilon_0 \sin(\omega t) + \delta$$

on  $\varepsilon_0$  representa la màxima deformació que assolix la mostra.

A la **fig. 6.3** es representa esquemàticament la tensió generada i la deformació que sofreix la mostra així com el desfasament que hi ha entre les dues magnituds degut al temps de resposta del material.

<sup>123</sup> K. te Nijenhuis, "Rheology" G. Astarita et al., Eds., Plenum Press, New York, 263, 1980.

<sup>124</sup> I. Katime, C. Cesteros, "Química física macromolecular II. Disoluciones y estado sólido" Servicio Editorial, Bilbao, 2002.

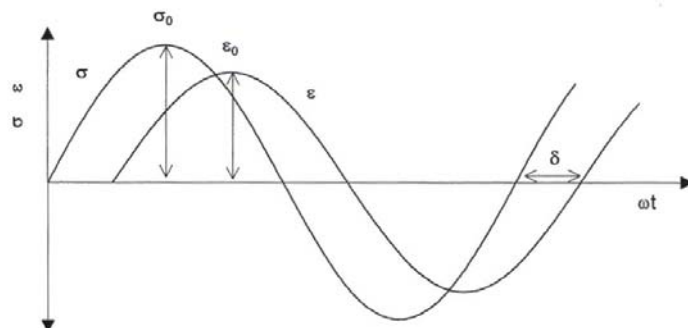


**Fig. 6.3.** Representació de la tensió generada sobre una mostra i la deformació que experimenta en DMTA

L'expressió de la resposta del material es pot escriure com:

$$\varepsilon = \varepsilon_0 [\sin(\omega t) \cos \delta + \cos(\omega t) \sin \delta]$$

Els mòduls ( $E'$  i  $E''$ ) permeten una millor caracterització del material ja que amb ells es pot examinar la capacitat de la mostra per a emmagatzemar energia ( $E'$ ), per dissipar energia ( $E''$ ) i la relació entre aquests dos paràmetres, coneguda com a tangent de pèrdues ( $\tan \delta$ ).

$$E'' = E * \sin \delta \quad E' = E * \cos \delta$$

La suma d'aquests dos mòduls ens dóna el mòdul d'elasticitat complex ( $E^*$ ) de la mostra, el qual es representa molts cops en forma de números complexos. La seva relació es troba representada a la **fig. 6.4**. Sovint es designa com  $E^*$  el mòdul d'elasticitat dinàmic obtingut mitjançant assaigs de tracció.

$$E^* = E' + iE''$$

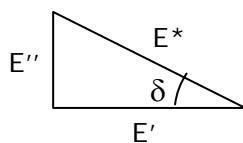


**Fig. 6.4.** Relació dels diferents mòduls obtinguts per DMTA

El mòdul d'emmagatzematge ( $E'$ ) és un paràmetre important ja que ens dóna idea de la resistència a la deformació. Representa la part de l'energia que el material absorbeix en cada cicle de deformació i que després pot retornar al sistema com a energia de recuperació, associant-se d'aquesta manera a la part del material que es comporta de forma elàstica i per tant donant una resposta elàstica.

El mòdul de pèrdues ( $E''$ ) representa la part de l'energia que no es recupera i que es dissipa en forma de calor degut a la fricció interna de les molècules. S'associa a la part viscosa del material.

La relació entre aquests dos paràmetres es denomina tangent de pèrdues ( $\tan \delta$ ) o factor de dissipació i representa el desfasatge entre la força aplicada i la resposta del material<sup>125</sup> i ve definida per la següent expressió:

$$\tan \delta = \frac{E''}{E'}$$

La tangent de pèrdues és un paràmetre molt sensible als canvis de mobilitat segmental i local que es donen en els polímers. La sensibilitat del DMTA és molt superior a la de la calorimetria diferencial d'escombrat (DSC), ja que sovint, quan el material presenta una densitat d'entrecreuament elevada, l'increment de la capacitat calorífica implicada en el pas de l'estat vítri a l'estat cautxú no és molt rellevant, de forma que la determinació precisa de la temperatura de transició vítria ( $T_g$ ) es converteix en una tasca bastant difícil.

Com s'ha comentat anteriorment, quan s'aplica una força a un material que posseeix propietats viscoelàstiques, les cadenes o els segments que el formen necessiten un cert temps per a reordenar-se. Aquest és el temps de relaxació. D'aquesta manera, en els experiments dinàmics, les propietats viscoelàstiques depenen de la pulsació ( $\omega$ ) de tal forma que si la freqüència ( $f$ ) varia, es veuran modificades les propietats dinamomecàniques per a un material determinat. Es defineix la freqüència com  $f = \omega/2\pi$

En un experiment dinamomecànic es sol treballar a una freqüència fixa i es pren la temperatura com a paràmetre variable. Mitjançant aquest procediment es poden observar diferents transicions tèrmiques designades per lletres gregues ( $\alpha, \beta$  i  $\gamma$ ), que estan relacionades amb diferents moviments interns del material. D'aquestes transicions, la més important és la transició  $\alpha$ , associada a la transició vítria. Així, la transició  $\alpha$ , igual que la  $T_g$ , es veu influenciada per diferents factors, la naturalesa del material, les condicions de curat, la densitat d'entrecreuament i interaccions físiques, entre d'altres.

<sup>125</sup> L. E. Nielsen, R. F. Landel, "Mechanical Properties of Copolymer and Composites", 2nd ed. New York, 1994.

Dependent de la temperatura a la que es realitzi la mesura s'obtidran uns valors o uns altres:

- **$T < T_g$ :** la tangent de pèrdues presenta valors baixos ja que la freqüència fixa és molt més gran que la velocitat a la que el material tendeix a l'equilibri, és a dir que el temps de relaxació es molt elevat. L'estructura es comporta de forma rígida i elàstica i s'obtenen valors de  $\tan \delta$  baixos i  $E'$  elevats.
- **$T > T_g$ :** el sistema adquireix l'estat d'equilibri de forma molt més ràpida que la que regeix la freqüència de l'experiment i per tant el temps de relaxació és molt més baix obtenint-se així valors baixos tant de  $\tan \delta$  com de  $E'$ .
- **$T$  a la zona de la transició vítria:** A mesura que augmenta la temperatura s'activa el moviment dels segments o de les molècules de la cadena que es troben involucrats en la transició. Aquest fet implica un augment del fregament i per tant de l'energia dissipada, traduïent-se així, en un augment del valor de  $E''$ . Aquesta situació és manté fins que la freqüència imposada coincideix amb la tendència del propi sistema a adquirir la conformació d'equilibri, punt on  $E''$  presenta un màxim, que correspon al màxim d'energia que el sistema dissipa degut al fregament. Una vegada superat aquest màxim, l'estructura que posseeix ara una major mobilitat, tendeix a la posició d'equilibri amb més facilitat i d'una forma més ràpida, que la que imposa la freqüència de deformació fixada, dissipant-se així menys energia i presentant valors de  $E''$  cada cop inferiors.

La variació del mòdul d'emmagatzematge ( $E'$ ) en funció de la temperatura ens proporciona informació sobre les condicions límit d'ús dels materials termoestables. Quan el material és sotmès a temperatures pròximes a la  $T_g$ , les seves propietats mecàniques disminueixen bruscament. Per aquest motiu, a nivell tecnològic i industrial, és de gran interès conèixer el valor d'aquest paràmetre.

Segons la *teoria molecular de l'elasticitat del cautxú* i mitjançant la mesura del mòdul d'emmagatzematge ( $E'$ ) a temperatures superiors a la  $T_g$ , on el mòdul és constant, podem avaluar la densitat d'entrecruament que presenta un material termoestable.

Aplicant aquesta teoria es calcula el pes molecular promig entre dos punts d'entrecruament ( $\overline{Mc}$ ) a la xarxa polimèrica, segons la següent expressió:<sup>126</sup>

$$\overline{Mc} = \frac{3\phi\rho RT}{E_r}$$

<sup>126</sup> L.R.G. Treolar "The Physics of Rubber Elasticity" Oxford Univ. Press, Oxford, 2<sup>a</sup> ed, 1958.

on  $\phi$  rep el nom de "front factor" i es considera normalment amb valor 1,<sup>127,128</sup>  $\rho$  és la densitat del polímer en (g/cm<sup>3</sup>),  $R$  és la constant universal dels gasos (J/mol·K),  $T$  la temperatura (Kelvin) i  $E'_r$  és el mòdul d'emmagatzematge del material a la zona cautxú expressat en (MPa).

En estudis realitzats en el nostre grup de recerca es va observar que en augmentar la proporció d'una lactona de cinc baules<sup>129</sup>, o carbonats de sis baules<sup>130</sup> a la mescla inicial de la reina epoxi de DGEBA, es produïa una disminució dels valors del mòdul d'emmagatzematge a la zona cautxú i un augment de la distància entre nusos. A més, també s'observà una disminució de la temperatura del màxim de la  $\tan \delta$  indicant una major flexibilitat de la xarxa polimèrica.

A la **fig. 6.5** es comparen els mòduls d'emmagatzematge en escala logarítmica, en funció de la temperatura, dels materials obtinguts a partir de DGEBA pur i de mescles de DGEBA/MA en les diferents proporcions molars estudiades amb  $Yb(OTf)_3$  i  $La(OTf)_3$ .

Es pot observar, pels dos iniciadors, que l'addició de MA al DGEBA redueix el mòdul d'emmagatzematge a la zona cautxú i la temperatura a on es dona la transició vítria. La variació de la composició de la barreja DGEBA/MA solament porta a diferències petites en la temperatura de la zona vítria i especialment en el valor del mòdul d'emmagatzematge en la zona cautxú.

A l'estat vítri, la rigidesa del material es relaciona amb els canvis de l'energia elàstica emmagatzemada en sotmetre el material a petites deformacions a causa de la resistència al moviment de segments moleculars. El material obtingut del curat del DGEBA amb el MA, sembla que ofereix més resistència als moviments segmentals i per tant és capaç d'emmagatzemar l'energia en l'estat vítri. En general, es relacionen els valors elevats d'aquest paràmetre amb una elevada densitat d'entrecruament, encara que alguns autors<sup>131-133</sup> proposen que aquesta densitat d'entrecruament exerceix poca influència en la rigidesa del material en l'estat vítri, i que depèn més del volum lliure, la interacció entre cadenes i l'empaquetament molecular.

<sup>127</sup> A. V. Tobolsky, J. Am. Chem. Soc. **80**, 5927-5929 (1958).

<sup>128</sup> W. W. Graessley, Adv. Polym. Sci. **16**, 1-179 (1974).

<sup>129</sup> C. Mas, A. Mantecón, A. Serra, X. Ramis, J. M. Salla, J. Polym. Sci. Part A: Polym. Chem. **44**, 1711-1721 (2006).

<sup>130</sup> R. Cervellera, A. Mantecón, A. Serra, X. Ramis, J. M. Salla, J. Polym. Sci. Part A: Polym. Chem. **44**, 2873-2882 (2006).

<sup>131</sup> V. B. Grupta, L. T. Drzal, D. Y. Lee, Polym. Eng. Sci., **25**, 812-823 (1985).

<sup>132</sup> E. Morel, V. Bellenger, M. Bocquet, J. Verdu, J. Mat. Sci., **24**, 69-75 (1989).

<sup>133</sup> N. Amdouni, H. Sautereau, J.-F. Gerard, Polymer, **31**, 1245-1253 (1990).

El mòdul d'emmagatzematge a la zona vítria es veu afectat per factors com la història tèrmica del material, i pel fet que el material no es trobi en el seu estat d'equilibri. Per això, el seu valor en aquesta zona no és utilitzable en l'estudi de la densitat de reticulació, sinó que s'ha d'avaluar a partir del mòdul d'emmagatzematge a la zona cautxú.

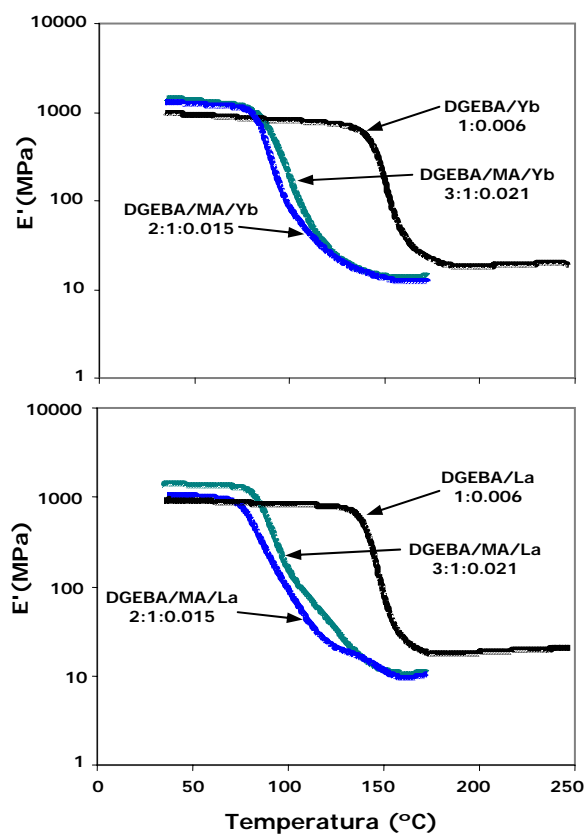


**Fig.6.5.** Mòdul d'emmagatzematge ( $E'$ ) en funció de la temperatura dels materials obtinguts pel curat de mesclades de DGEBA i DGEBA/MA (mol/mol) amb triflats d'iterbi i lantà

A la **fig.6.6** es representa la tangent de pèrdues front a la temperatura pels mateixos materials.

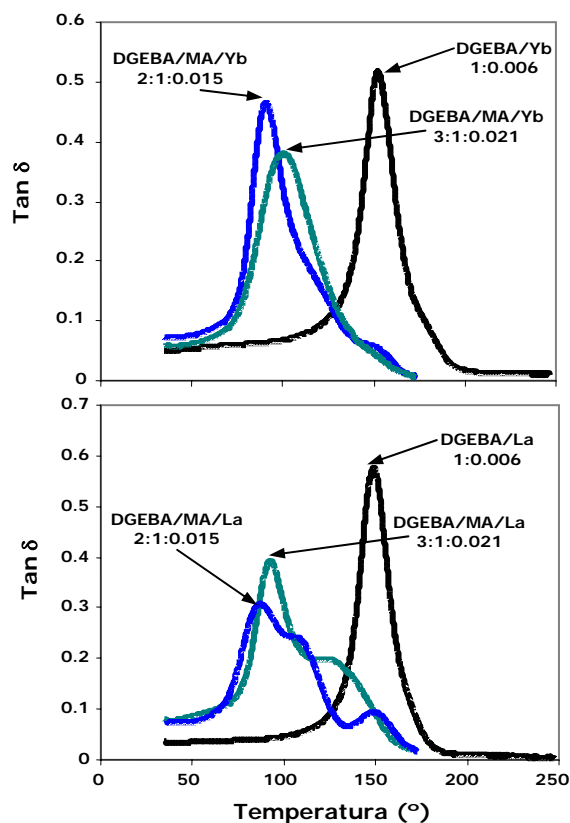


**Fig.6.6.** Tangent de pèrdues ( $\tan \delta$ ) en funció de la temperatura dels materials obtinguts a partir de DGEBA i mescles DGEBA/MA utilitzant triflats de lantànid

Com podem veure, al utilitzar  $\text{Yb}(\text{OTf})_3$ , part superior de la figura, l'addició d'àcid de Meldrum al DGEBA, disminueix de forma notable la temperatura del màxim de la  $\tan \delta$ . Tanmateix, no hi ha una gran diferència per a les diferents proporcions emprades. De la forma unimodal dels pics es pot deduir que els materials obtinguts amb  $\text{Yb}(\text{OTf})_3$  (part superior de la figura) són més homogenis front els obtinguts amb  $\text{La}(\text{OTf})_3$ , els quals no són unimodals. S'observa que un augment de la proporció d'àcid de Meldrum a les mostres produeix l'aparició d'una espatlla, a temperatures més elevades per a la proporció 3:1, i una espatlla addicional per a la proporció 2:1. Aquest fet ens indicaria que els sistemes no són homogenis, el que podria atribuir-se a una major homopolimerització de l'epòxid, el que ja es veia reflectit en els assaigs fets per ATR-FTIR.



A la **taula 6.1** es troben recollits els valors de la tangent de pèrdues, del mòdul d'emmagatzematge a la zona cautxú i del pes molecular promig entre nusos calculats pels diferents sistemes estudiats.

**Taula 6.1.** Tangent de pèrdues, mòdul d'emmagatzematge a la zona cautxú i la distància entre nusos pels sistemes estudiats iniciats amb  $\text{Yb}(\text{OTf})_3$  i  $\text{La}(\text{OTf})_3$

Mostra	Formulació	Tan $\delta$ (°C)	$E'$ (MPa)	$\overline{M}_c$ (g/mol)
1	DGEBA/ $\text{Yb}(\text{OTf})_3$ 1:0.006	152	22.7	556
2	DGEBA/MA/ $\text{Yb}(\text{OTf})_3$ 3:1:0.021	100	14.0	797
3	DGEBA/MA/ $\text{Yb}(\text{OTf})_3$ 2:1:0.015	93	13.4	815
4	DGEBA/ $\text{La}(\text{OTf})_3$ 1:0.006	149	20.5	611
5	DGEBA/MA/ $\text{La}(\text{OTf})_3$ 3:1:0.021	93	11.5	955
6	DGEBA/MA/ $\text{La}(\text{OTf})_3$ 2:1:0.015	87	10.2	1063

Podem observar al comparar els iniciadors que amb el  $\text{Yb}(\text{OTf})_3$  els materials van presentar valors de  $\tan \delta$  superiors al dels materials obtinguts amb  $\text{La}(\text{OTf})_3$  i també valors lleugerament superiors de  $E'$  a la zona cautxú. Pel que fa als valors de les  $\tan \delta$  podem apreciar que en tots dos casos segueixen la tendència esperada, ja que una major proporció de MA a la mostra condueix a un descens d'aquest valor. Respecte al pes molecular promig entre nusos, s'observa que augmenta amb la proporció de MA i que és superior pels materials obtinguts amb la sal de lantà.

A la **fig.6.7** es comparen els mòduls d'emmagatzematge en escala logarítmica en funció de la temperatura dels materials obtinguts a partir del DGEBA pur i de mescles de DGEBA/MCP en les diferents proporcions molars estudiades iniciades amb  $\text{Yb}(\text{OTf})_3$ ,  $\text{La}(\text{OTf})_3$  i  $\text{BF}_3 \cdot \text{MEA}$ .

Pels tres iniciadors, es pot observar que una menor quantitat de lactona a la mostra fa que la transició de l'estat vitri a l'estat cautxú dels materials es doni a temperatures més elevades.

En quant al mòdul  $E'$  a la zona cautxú es pot apreciar, pel cas dels triflats de lantànid, que aquest és lleugerament més baix en augmentar la proporció de MCP en el material. En canvi, aquest valor no mostra diferències significatives en augmentar la proporció de MCP en la mostra en el cas dels materials obtinguts amb  $\text{BF}_3 \cdot \text{MEA}$ .

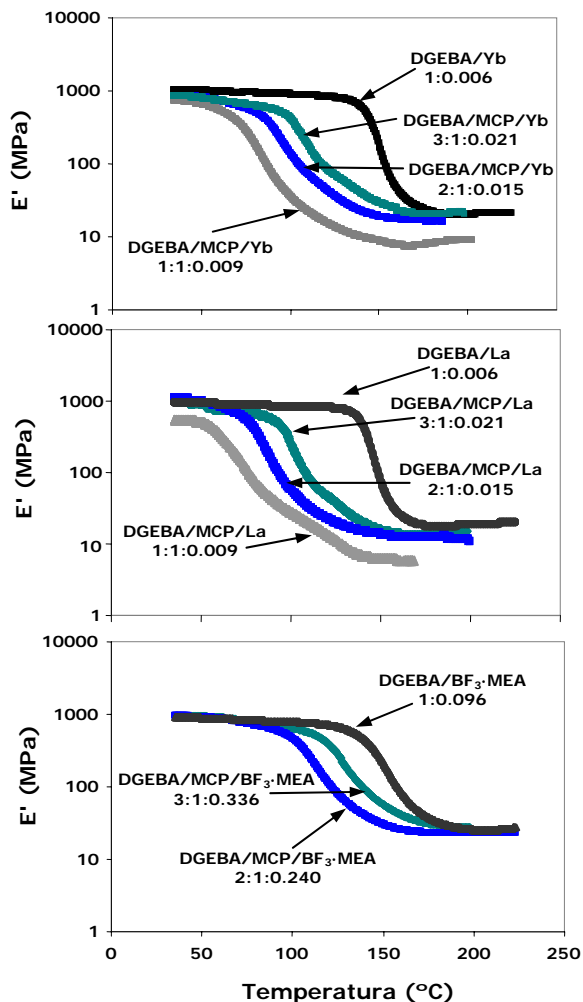


**Fig.6.7.** Mòdul d'emmagatzematge ( $E'$ ) en funció de la temperatura, dels materials obtinguts pel curat de mesclades de DGEBA i DGEBA/MCP (mol/mol) emprant diversos àcids de Lewis

A la **fig.6.8** es representa la tangent de pèrdues front la temperatura pels mateixos sistemes.

Com podem observar en els tres gràfics, una major proporció de MCP a la mescla porta a una disminució de la temperatura del màxim de la  $\tan \delta$ . De la forma, generalment unimodal dels pics, es pot deduir que els materials són suficientment homogenis.

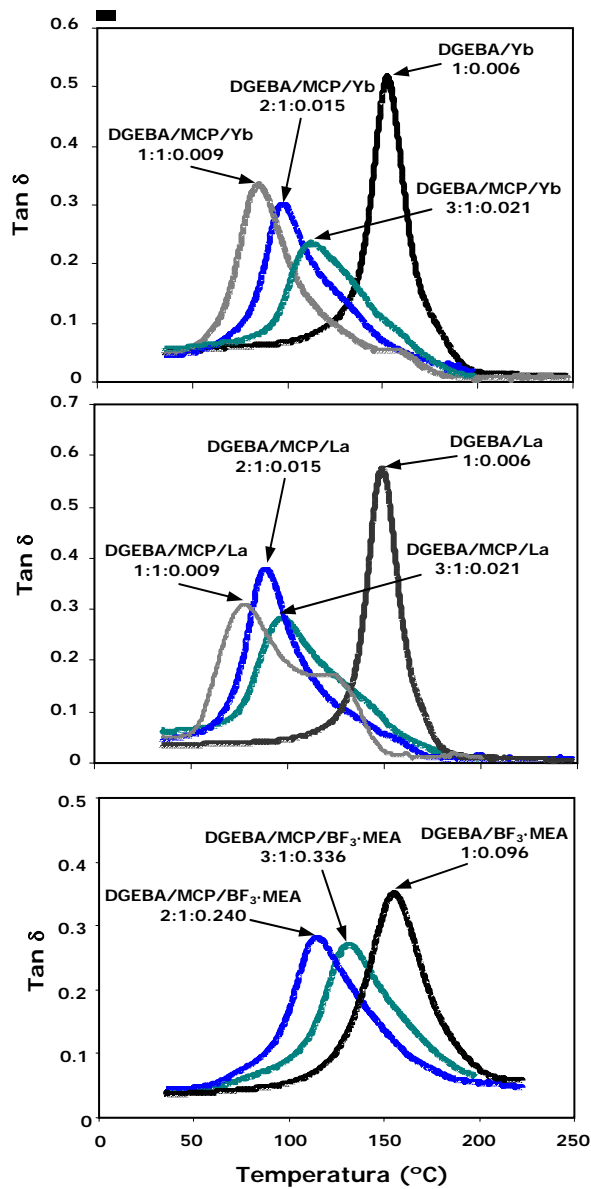


**Fig.6.8.** Tangent de pèrdues (tan  $\delta$ ), en funció de la temperatura, dels materials obtinguts pel curat de mescles de DGEBA i DGEBA/MCP (mol/mol) utilitzant diversos àcids de Lewis

A la **taula 6.2** es troben els paràmetres termodinamomecànics per a aquests materials.

**Taula 6.2.** Tangent de pèrdues, mòdul d'emmagatzematge a la zona cautxú i distància entre nusos pels sistemes estudiats iniciats amb diferents àcids de Lewis

Mostra	Formulació	Tan $\delta$ (°C)	E' (MPa)	$\bar{M}_c$ (g/mol)
1	DGEBA/Yb(OTf) <sub>3</sub> 1:0.006	152	22.7	556
2	DGEBA/MCP/Yb(OTf) <sub>3</sub> 3:1:0.021	112	20.5	560
3	DGEBA/MCP/Yb(OTf) <sub>3</sub> 2:1:0.015	100	14.1	790
4	DGEBA/La(OTf) <sub>3</sub> 1:0.006	149	20.5	611
5	DGEBA/MCP/La(OTf) <sub>3</sub> 3:1:0.021	97	14.7	753
6	DGEBA/MCP/La(OTf) <sub>3</sub> 2:1:0.015	90	10.6	1029
7	DGEBA/BF <sub>3</sub> ·MEA 1:0.096	155	25.5	499
8	DGEBA/MCP/BF <sub>3</sub> ·MEA 3:1:0.336	131	24.1	502
9	DGEBA/MCP/BF <sub>3</sub> ·MEA 2:1:0.240	115	23.0	503

Pel que fa referència a la distància entre nusos, s'observa que amb els triflats de lantànid augmenta al haver una major proporció de MCP, donat que s'introdueix l'estructura lineal procedent de la lactona entre els punts d'entrecruament. Tanmateix, amb el BF<sub>3</sub>·MEA aquest augment no és gens significatiu, el que estaria d'acord amb la baixa proporció d'ester lineal incorporat a la xarxa quan s'empra aquest iniciador i amb la baixa reducció del mòdul a la zona cautxú.

A la **fig.6.9** i **6.10** es comparen els mòduls d'emmagatzematge i l'evolució de la tangent de pèrdues amb la temperatura pels materials obtinguts a partir de mesclades de DGEBA/MDM en les diferents proporcions molars estudiades i iniciades amb els triflats de lantànid.

Al igual que succeïa amb el MCP, pels dos iniciadors, una menor quantitat de MDM a la mostra fa que la transició de l'estat vitri a l'estat cautxú dels materials es doni a temperatures més elevades. En quant al mòdul a la zona cautxú es pot apreciar que aquest és lleugerament més baix conforme augmenta la proporció de MDM incorporat al material.

D'altra banda, s'observa una disminució de la temperatura del màxim de la *tan  $\delta$*  al augmentar la proporció de MDM a la mescla. La forma pràcticament unimodal dels pics indica que els materials són relativament homogenis.

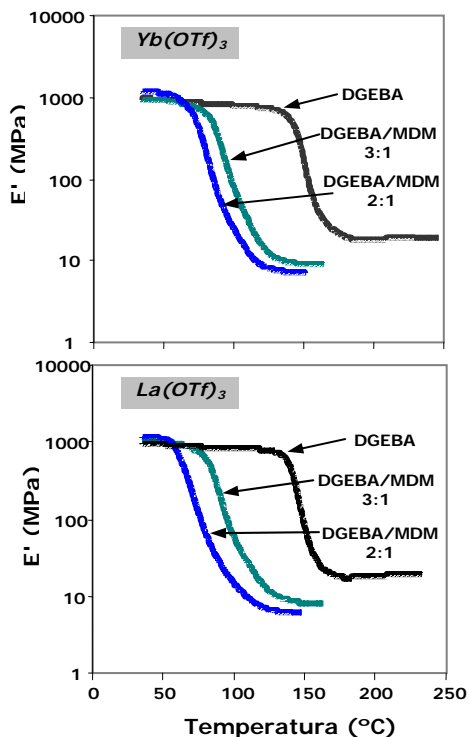


Fig.6.9. Mòdul d'emmagatzematge ( $E'$ ) en funció de la temperatura dels materials obtinguts pel curat de mescles de DGEBA i DGEBA/MDM (mol/mol) emprant  $Yb(OTf)_3$  i  $La(OTf)_3$

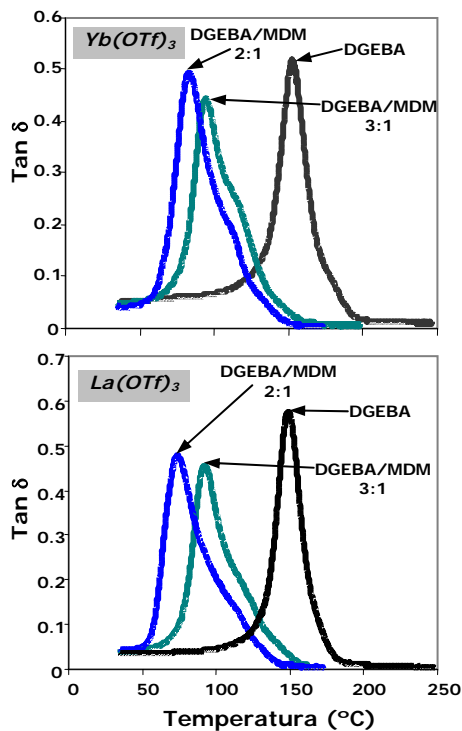


Fig.6.10. Tangent de pèrdues ( $\tan \delta$ ) en funció de la temperatura dels materials obtinguts pel curat de mescles de DGEBA i DGEBA/MDM (mol/mol) utilitzant  $Yb(OTf)_3$  i  $La(OTf)_3$

A la **taula 6.3** es recullen els valors obtinguts pels materials amb MDM. Comparant els dos iniciadors, podem observar que les mostres curades amb  $Yb(OTf)_3$  tenen valors de mòdul relaxat i valors de  $\tan \delta$  lleugerament més elevats front les mostres amb les mateixes proporcions curades amb  $La(OTf)_3$ . Pel que fa referència a la distància entre nusos, es pot veure que augmenta amb una major proporció de MDM i que és major en els materials iniciats amb lantà. Tots aquest valors permeten concloure, que el  $Yb(OTf)_3$  porta a un grau de curat superior, com ja s'havia observat a l'estudi calorimètric.

**Taula 6.3.** Tangent de pèrdues, mòdul d'emmagatzematge a la zona cautxú i distància entre nusos pels sistemes estudiats iniciats amb els triflats de lantànid

Mostra	Formulació	Tan $\delta$ (°C)	E' (MPa)	$\bar{M}_c$ (g/mol)
1	DGEBA/Yb 1:0.006	152	22.7	556
2	DGEBA/MDM/Yb 3:1:0.021	95	9.1	1208
3	DGEBA/MDM/Yb 2:1:0.015	85	7.2	1472
4	DGEBA/La 1:0.006	149	20.5	611
5	DGEBA/MDM/La 3:1:0.021	92	8.4	1300
6	DGEBA/MDM/La 2:1:0.015	75	6.2	1662

A la **fig.6.11** es comparen els mòduls d'emmagatzematge en escala logarítmica i la tangent de pèrdues ( $\tan \delta$ ), en funció de la temperatura del DGEBA pur i de mescles de DGEBA/lactona 2:1 (mol/mol) iniciades amb 0.015 mols de  $Yb(OTf)_3$ .

Podem observar que tots els mòduls d'emmagatzematge ( $E'$ ), a la zona elàstica, dels materials que incorporen les lactones són inferiors al de la reina epoxi pura, essent el més baix pel MDM i el més alt pel MCP. Els valors de la tangent de  $\delta$  són molt inferiors al de la reina pura, però bastant similars entre sí. El material que incorpora MCP, presenta un pic més ample i baix, el que indicaria la seva menor homogeneïtat.

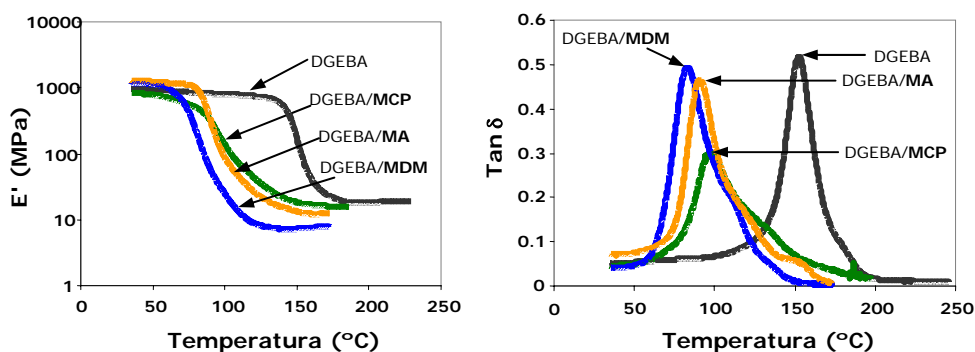


**Fig.6.11.** Mòdul d'emmagatzematge ( $E'$ ) en escala logarítmica i tangent de pèrdues ( $\tan \delta$ ) en funció de la temperatura de materials obtinguts per curat de DGEBA i mesclures de DGEBA/lactona 2:1 (mol/mol) amb  $Yb(OTf)_3$

A la **taula 6.4** es recullen els valors numèrics de les tangents de pèrdues, dels mòduls d'emmagatzematge a la zona cautxú i dels pesos moleculars promig entre nusos d'entrecruament pels diferents sistemes de DGEBA/lactona amb proporcions 2:1 entre comonòmers i curats amb  $\text{Yb}(\text{OTf})_3$  i  $\text{La}(\text{OTf})_3$ .

**Taula 6.4.** Tangent de pèrdues, mòdul d'emmagatzematge a la zona cautxú i distància entre nusos dels diferents sistemes estudiats

Mostra	Formulació <sup>a</sup>	Tan $\delta$ (°C)	E' <sup>b</sup> (MPa)	$\bar{M}_c$ (g/mol)
1	DGEBA/ $\text{Yb}(\text{OTf})_3$ 1:0.006	152	22.7	556
2	DGEBA/ <b>MCP</b> / $\text{Yb}(\text{OTf})_3$ 2:1:0.015	100	14.1	790
3	DGEBA/ <b>MA</b> / $\text{Yb}(\text{OTf})_3$ 2:1:0.015	93	13.4	815
4	DGEBA/ <b>MDM</b> / $\text{Yb}(\text{OTf})_3$ 2:1:0.015	85	7.2	1472
5	DGEBA/ $\text{La}(\text{OTf})_3$ 1:0.006	149	20.5	611
6	DGEBA/ <b>MCP</b> / $\text{La}(\text{OTf})_3$ 2:1:0.015	90	10.6	1029
7	DGEBA/ <b>MA</b> / $\text{La}(\text{OTf})_3$ 2:1:0.015	87	10.2	1063
8	DGEBA/ <b>MDM</b> / $\text{La}(\text{OTf})_3$ 2:1:0.015	75	6.2	1662

a. La composició de les formulacions ve expressada en relacions molars

b. Mòdul d'emmagatzematge calculat a  $\tan \delta + 50^\circ\text{C}$

Podem veure que les mostres curades amb  $\text{Yb}(\text{OTf})_3$  presenten valors de  $\tan \delta$  lleugerament majors front les curades amb  $\text{La}(\text{OTf})_3$  i a més, valors de mòdul relaxat superiors. En el valor dels paràmetres termodinamomècanics influeixen principalment dos factors. D'una banda el grau d'entrecruament assolit i per l'altra la proporció d'ester lineal introduït entre nusos. Com podem veure, en el curat del DGEBA pur, el triflat d'iterbi porta a un grau d'entrecruament superior. Quan se li addiciona la lactona la proporció d'ester lineal és més elevada amb triflat d'iterbi i això porta a una reducció de la  $\tan \delta$  i el  $E'$ . Aquests dos factors actuen de forma contrària amb aquests dos iniciadors i semblar ser que el primer factor és predominant pel  $\text{Yb}(\text{OTf})_3$ .

En quant a la polimerització aniónica, a la **fig. 6.12** es comparen els mòduls d'emmagatzematge en escala logarítmica en funció de la temperatura dels materials obtinguts a partir de DGEBA pur i mescles de DGEBA/lactona/DMAP 3:1:0.308 (mol/mol). Com en els casos anteriors, la incorporació de lactona a la reïna epoxi fa que la transició de l'estat vitri a l'estat cautxú del material es doni a temperatures inferiors. El valor del mòdul relaxat és superior pel material que incorpora el MCP, el que pot ésser atribuït a la menor incorporació d'ester lineal a la xarxa.

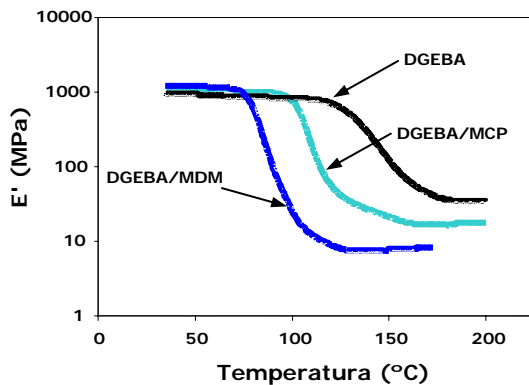


**Fig.6.12.** Mòdul d'emmagatzematge ( $E'$ ) en funció de la temperatura dels materials obtinguts per curat aniónic de mescles de DGEBA i DGEBA/lactona 3:1 (mol/mol) emprant DMAP

A la **fig.6.13** es representa la tangent de pèrdues front la temperatura pels mateixos materials. Com podem veure, la incorporació del MDM a la mescla porta a una major disminució de la temperatura del màxim de la  $\tan \delta$ . A més, podem observar que l'alçada del pic de la tangent de pèrdues del material que incorpora MDM és superior. Aquest fet podria explicar-se per la incorporació d'una major proporció d'ester lineal a la xarxa. A més, podem dir que els materials són bastant homogenis.

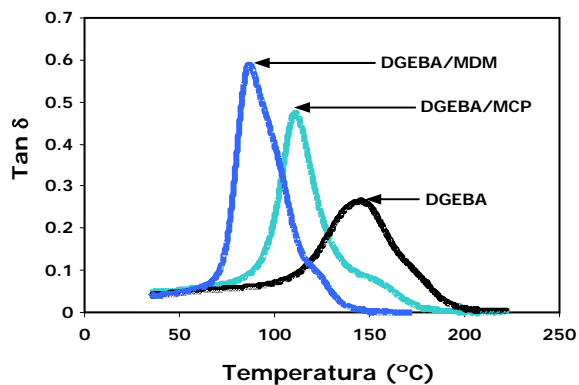


**Fig.6.13.** Tangent de pèrdues ( $\tan \delta$ ) en funció de la temperatura dels materials obtinguts pel curat aniónic de mescles de DGEBA i DGEBA/lactona 3:1 (mol/mol)



A la **taula 6.5** es mostren els valors de la tangent de pèrdues, del mòdul relaxat i del pes molecular promig entre nusos pels diferents materials estudiats. El valor del pes molecular promig entre nusos confirma la major incorporació d'unitats lineals a la xarxa per el MDM.

**Taula 6.5.** Tangent de pèrdues, mòdul d'emmagatzematge a la zona cautxú i distància entre nusos pels materials obtinguts amb DMAP

Mostra	Formulació	Tan $\delta$ (°C)	E' (MPa)	$\bar{M}_c$ (g/mol)
1	DGEBA/DMAP 1:0.088	146	35.2	355
2	DGEBA/MCP/DMAP 3:1:0.308	111	16.8	683
3	DGEBA/MDM/DMAP 3:1:0.308	87	7.5	1418

### 6.3. Estudi de la microduresa

La tècnica de determinació de la *microduresa superficial* o *microindentació* s'utilitza en el món industrial degut a que és un bon mètode per caracteritzar les propietats mecàniques que tenen a veure amb la resistència i la duresa d'un material. Es mesura l'aptitud dels materials per a resistir càrregues estàtiques o aplicades a baixa velocitat.

Un assaig de *microduresa* consisteix en generar una empremta molt petita per mesurar la duresa puntual. S'apliquen càrregues molt petites i els assaigs són de precisió. S'utilitza en metal·lúrgia per avaluar la duresa entre fases diferents o per analitzar la duresa d'un recobriments (com els galvanitzats). També s'utilitza per assajar materials ceràmics, que presenten una elevada fragilitat.

En els tests de microduresa<sup>134</sup> s'aplica un indentador de diamant contra la superfície del recobriments amb una força fixa. L'empremta resultant es mesura. Quan més gran sigui l'empremta més tou serà el material. La força aplicada ha de ser la mínima per tal que el indentador no penetri completament en el material i poder mesurar la mida de l'empremta. Els tests de microduresa han estat àmpliament utilitzats en el camp dels metalls<sup>135</sup> i també per a recobriments òptics o dielèctrics.<sup>136-138</sup> Aquests tests són utilitzats habitualment per avaluar les propietats físiques dels compostos i també com a mètode indirecte d'avaluació del grau de polimerització relatiu.<sup>139-141</sup> Mitjançant aquesta tècnica s'ha trobat una elevada dispersió en

<sup>134</sup> V. E. Lysaght, Met. Prog. **78**, 93-97 (1960).

<sup>135</sup> L. S. Palatnik and N. F. Gladkikh, Zavod. Lab. **30**, 1097 (1964).

<sup>136</sup> N. Nishibori and K. Kinoshita, Thin Solid Films **48**, 325-331 (1978).

<sup>137</sup> M. Laugier, Thin Solid Films **76**, 289-294 (1981).

<sup>138</sup> D. S. Whitnell and R. Williamson, Thin Solid Films **35**, 255-261 (1976).

<sup>139</sup> M. Helvatjoglou-Antoniadi, Y. Papadogianis, E. Koliniotou-Kubia, S. Kubias, J. Prosthet. Dent., **65**, 215-220 (1991).

les mesures de microdureza, superior al 20%,<sup>142,143</sup> quan els materials compostos estan formats per una matriu dúctil i partícules dures que tenen la funció de reforçant.

La escala de Mohs classifica els minerals per la resistència a ratllar-se uns als altres. S'utilitza com a referència de la duresa d'una substància. Va ser proposada pel geòleg *Friedrich Mohs* i es basa en el principi que una substància més dura pot ratllar a una més tova, però sent impossible el contrari. *Mohs* va escollir deu minerals als quals els hi va atribuir un determinat grau de duresa en la seva escala. Va començar amb el talc que, va rebre el número 1 i va acabar amb el diamant, assignant-li el número 10.

Existeixen diversos mètodes de mesura de la duresa:

- **Rockwell:** És un mètode per determinar la resistència d'un material a ser penetrat. En aquest test es mesura el grau de penetració causat en un material per un indentador de bola esfèric d'acer o de punta cònica de diamant. És una tècnica dissenyada per a materials com les ceràmiques i plàstics "durs" com per exemple el niló, els policarbonats i el poliestirè. Es sol considerar un assaig no destructiu per la petita mida de l'empremta.
- **Shore:** Consisteix en una prova de duresa dissenyada per a mesurar en termes d'elasticitat la duresa de materials com per exemple els hules. Al provador Shore se li anomena també *durómetro*.
- **Brinell:** És el mètode de duresa més antic i va ser proposat per l'enginyer suec *Johan August Brinell* al 1900. S'utilitza en materials tous i mostres primes, i consisteix en mesurar el diàmetre d'un cercle format per la penetració d'una bola d'acer templat o carbur de tungstè de 10mm sota una pressió de càrrega fixa. Estima la resistència a tracció.
- **Vickers:** Aquest assaig, anomenat *l'assaig universal*, va ser ideat per *Vickers i col.* al 1920 i consisteix en una prova de duresa on s'usa un indentador de diamant de base piramidal quadrangular que es forçat contra el material per tal de crear una indentació en un temps d'espera estàndard. La mida de la indentació determina el valor de duresa.
- **Knoop:** En aquesta prova s'utilitza, a diferència del *Vickers*, un indentador de diamant de base piramidal romboïdal i càrregues relativament lleugeres entre 10gf i 1kgf. El indentador Knoop té una diagonal gran que és perpendicular i 7 vegades la longitud de la diagonal petita. S'aplica a materials orgànics, com pintures assecades, vernissos i recobriments aplicats a superfícies planes i rígides com per exemple el metall o el vidre.

<sup>140</sup> D. C. Watts, O.M. Amer, E.C. Combe, Dent. Mater., **3**, 265–269, (1987).

<sup>141</sup> A.U. Yap, K.E. Wee, S.H. Teoh. Oper. Dent., **27** 25–29, (2002).

<sup>142</sup> M. R. Rosenberger, E. Forlerer, C. E. Schvezov, Wear **259**, 590-601 (2005).

<sup>143</sup> J. Zhang, A. T. Alpas, Mat. Sci. Eng. A. **160**, 25-35 (1993).

La caracterització dels nostres materials ha estat realitzada mitjançant el *test Knoop* ja que és un bon mètode per a molts materials durs i fràgils, i que presenten seccions molt primes com els recobriments orgànics. A més, presenta una major sensibilitat superficial front el *Vickers*. Aquest test va ser desenvolupat el 1939 per *F. Knoop i col.* a l'Institut Nacional d'Estàndards i Tecnologia (NIST) del Departament de Comerç dels Estats Units d'Amèrica i ve definit per la normativa ASTM D-1474.

La deformació produïda es mesura mitjançant un microscopi òptic i el numero de duresa Knoop (KHN) ve definit per la següent expressió:

$$KHN = L/l^2 \cdot C_p = 0.025/l^2 C_p$$

on  $L$  és la càrrega aplicada expressa en kilogram-força (*kgf*) i que és igual a 0.025,  $l$  és la diagonal gran de la marca piramidal realitzada sobre el material expressada en (*mm*) i  $C_p$  és la constant del indentador ( $7.028 \cdot 10^{-2}$ ). D'aquesta manera, la unitat del numero de duresa Knoop és *kgf/mm<sup>2</sup>*.

Per avaluar els resultats obtinguts s'ha de considerar la *precisió*<sup>144</sup> dels mateixos. En el nostre cas vam considerar una  $n$  petita igual a 6 rèpliques amb un interval de confiança del 95 per cent i 5 graus de llibertat. De tal forma que en tots els casos, els resultats es mostraran de la següent manera:

$$\bar{x} \pm 2.56 \sigma_m$$

on  $\sigma_m$  és la desviació estàndard de la mitjana i  $\sigma_s$  és la desviació estàndard de la mostra:

$$\sigma_m = \frac{\sigma_s}{\sqrt{n}} \quad \sigma_s = \sqrt{\frac{\sum (x_i - \bar{x})^2}{n - 1}}$$

A la **fig.6.15** es representa un diagrama de barres amb la microduresa determinada pels diferents materials que incorporen l'àcid de *Meldrum*, en funció de la composició i utilitzant com a iniciadors el  $\text{Yb}(\text{OTf})_3$  i el  $\text{La}(\text{OTf})_3$  respectivament.

<sup>144</sup> H. E. Davis, G. E. Troxell and G. F. W. Hauck, "The Testing of Engineering Materials" 4th. Edition McGraw-Hill Inc., New York, 1-55 (1982).

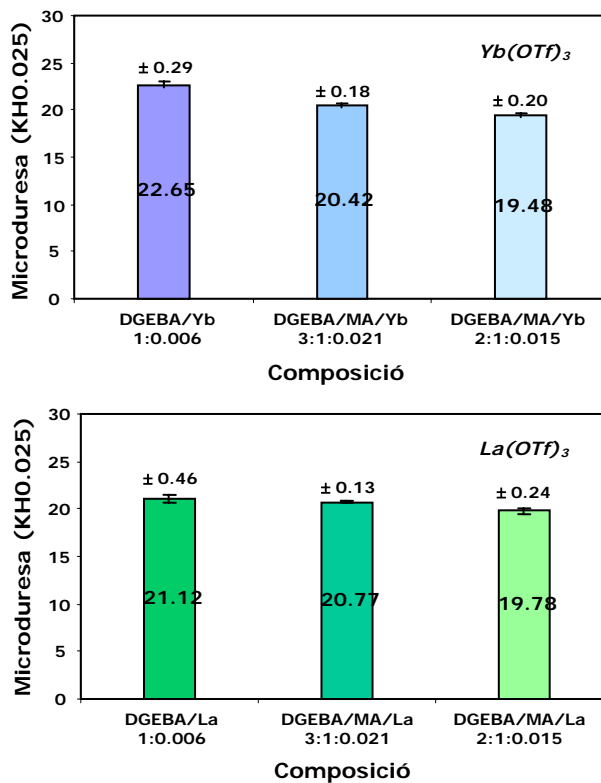


Fig.6.15. Microduresa Knoop front la composició de materials que incorporen àcid de Meldrum

Com podem observar, la incorporació d'àcid de Meldrum a la reïna epoxídica produeix una lleugera disminució de la microduresa dels materials obtinguts tant amb triflat d'iterbi com el de lantà, com a conseqüència d'un augment en la flexibilitat de la cadena polimèrica. Com a resultat presenten una resistència lleugerament menor. Tanmateix, es produeix una disminució molt lleu d'aquesta microduresa en augmentar la proporció d'àcid de Meldrum. Comparant els dos iniciadors en el curat de la reïna pura podem veure una major duresa pel triflat d'iterbi. Ara bé, donat que el triflat d'iterbi incorpora una major proporció d'ester lineal a la xarxa, la davallada de la microduresa és quelcom superior al afegir MA als materials preparats amb aquest iniciador.

A la **fig.6.16** podem veure representada la microduresa en funció de la composició dels materials obtinguts per addició de *MCP*, utilitzant com a iniciadors el  $\text{Yb}(\text{OTf})_3$ , el  $\text{La}(\text{OTf})_3$  i el  $\text{BF}_3 \cdot \text{MEA}$ .

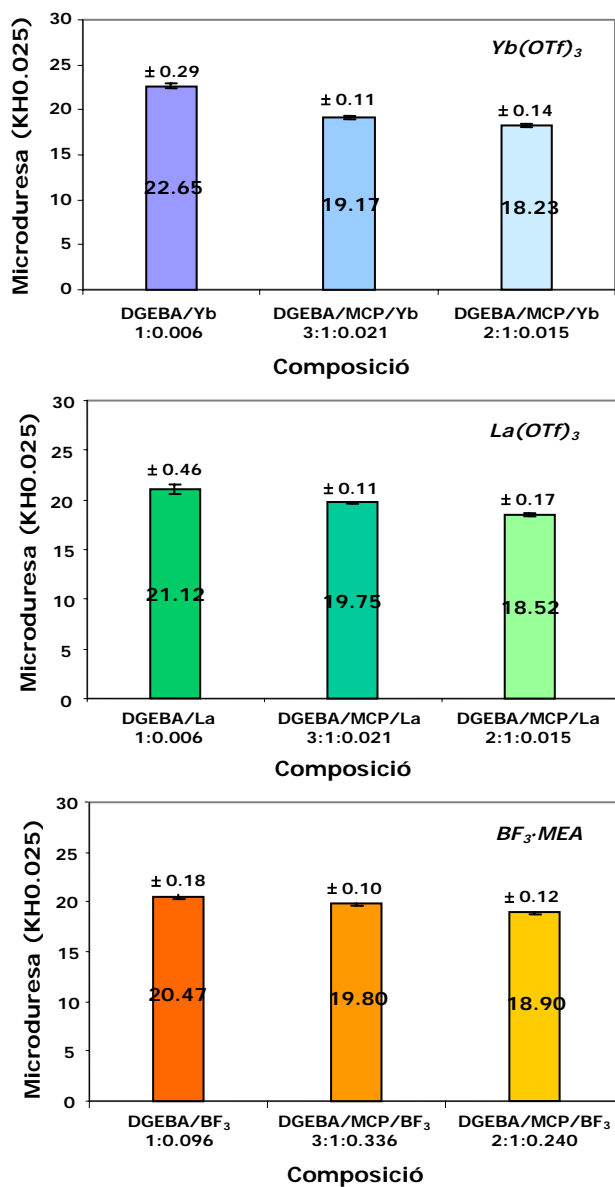


Fig.6.16. Microdureza Knoop front la composició de materials que incorporen MCP

Com es pot observar en els tres casos, una major proporció de MCP a la xarxa polimèrica condueix a l'obtenció de materials amb una

microdureza menor a la de la reïna epoxi pura. L'iniciador que incorpora una major proporció d'ester lineal a la xarxa polimèrica, el  $\text{Yb}(\text{OTf})_3$ , porta a una davallada lleugerament superior de la microdureza mentre que el  $\text{BF}_3 \cdot \text{MEA}$ , que incorpora una menor proporció d'ester, porta a un valor de microdureza més elevat degut a la menor flexibilitat de la xarxa polimèrica.

Posteriorment es va realitzar el mateix estudi però amb mostres que incorporaven *MDM* com a lactona i que van ser curades catiònicament amb  $\text{Yb}(\text{OTf})_3$  i  $\text{La}(\text{OTf})_3$ . A la **fig.6.17** es representa la microdureza dels diferents materials front la composició.

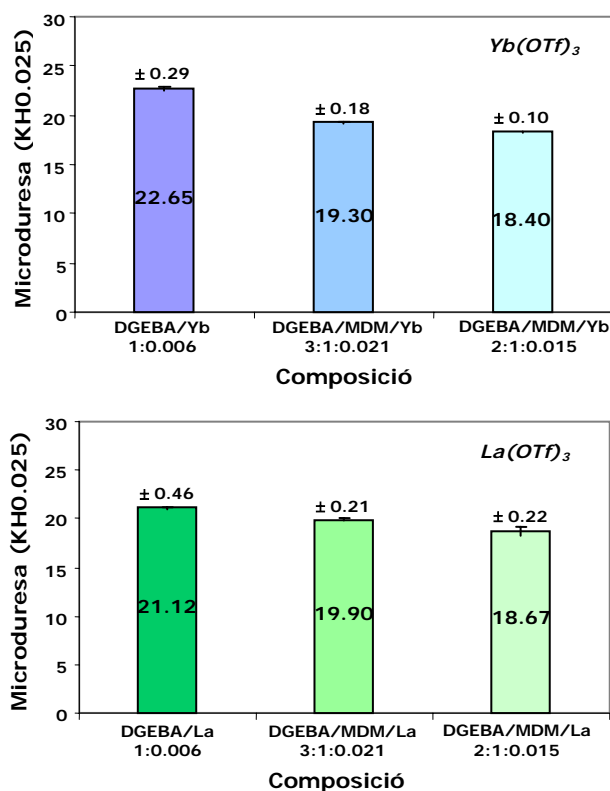
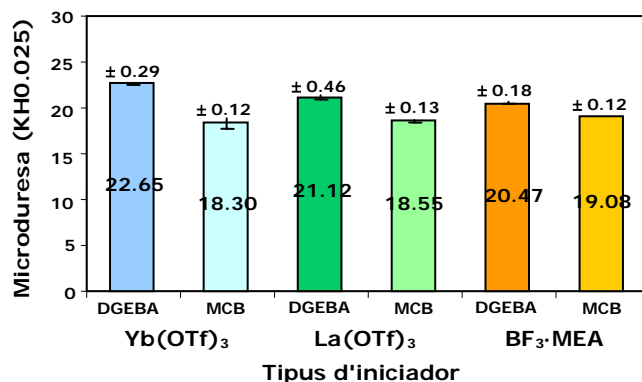


Fig.6.17. Microdureza Knoop front la composició de materials que incorporen MDM

Al igual que en els casos anteriors podem veure que l'addició de MDM a la reïna produeix una disminució de la microdureza dels materials obtinguts tant amb triflat d'iterbi com amb triflat de lantà, i que a en augmentar la proporció de MDM s'obtenen valors de microdureza lleugerament inferiors.

A la **fig.6.18**, es mostren els resultats obtinguts de mostres de DGEBA/MCB 2:1 (mol/mol) curades amb  $\text{Yb}(\text{OTf})_3$ ,  $\text{La}(\text{OTf})_3$  i  $\text{BF}_3\cdot\text{MEA}$ .



**Fig.6.18.** Microdureza Knoop front el tipus d'iniciador catiònic emprat de mostres de DGEBA/MCB 2:1 (mol/mol)

Com podem veure, en els tres casos, la incorporació de MCB a la reïna epoxi pura produeix una disminució de la microdureza dels materials. A més, podem apreciar que amb els triflats de lantànid aquesta és més acusada que en el cas d'utilitzar  $\text{BF}_3\cdot\text{MEA}$ , el qual estaria relacionat amb la major proporció d'unitats d'ester lineal flexibles que introdueixen els triflats de lantànid a la xarxa tridimensional.

A les **fig.6.19** i **6.20** es representen els valors de microdureza en funció de la lactona emprada, utilitzant com a iniciadors  $\text{Yb}(\text{OTf})_3$  i  $\text{La}(\text{OTf})_3$ . La composició dels materials DGEBA/lactona/iniciador és 2:1:0.015.

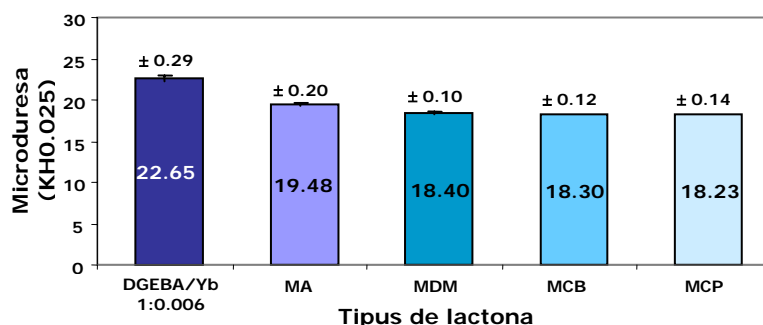


**Fig.6.19.** Microdureza Knoop dels diferents materials obtinguts amb  $\text{Yb}(\text{OTf})_3$

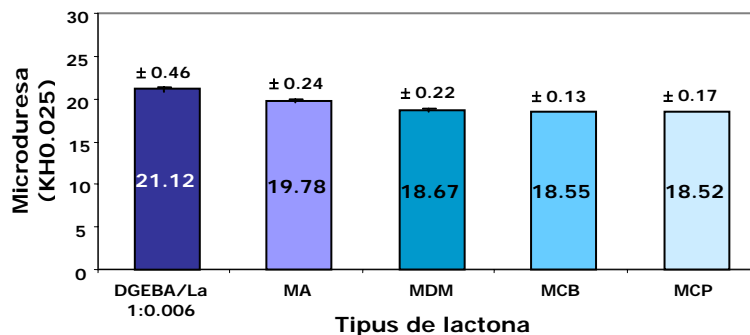


Fig.6.20. Microduresa Knoop dels diferents materials obtinguts amb  $La(OTf)_3$

Com es pot veure, l'estructura del derivat de l'àcid de Meldrum no afecta significativament a la microduresa dels materials. Tanmateix, és quelcom més alta amb l'àcid de Meldrum. Els materials que incorporen lactona presenten microdureses quelcom més baixes al utilitzar  $Yb(OTf)_3$  com a iniciador.

També es va assajar la microduresa dels materials obtinguts per copolimerització anònica del DGEBA amb MCP o MDM amb DMAP. A la **fig.6.21** es mostren els resultats obtinguts.

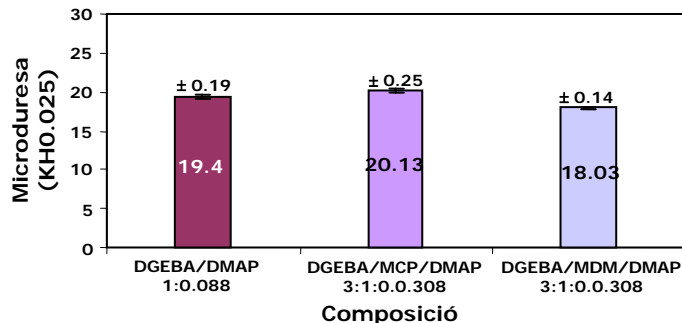
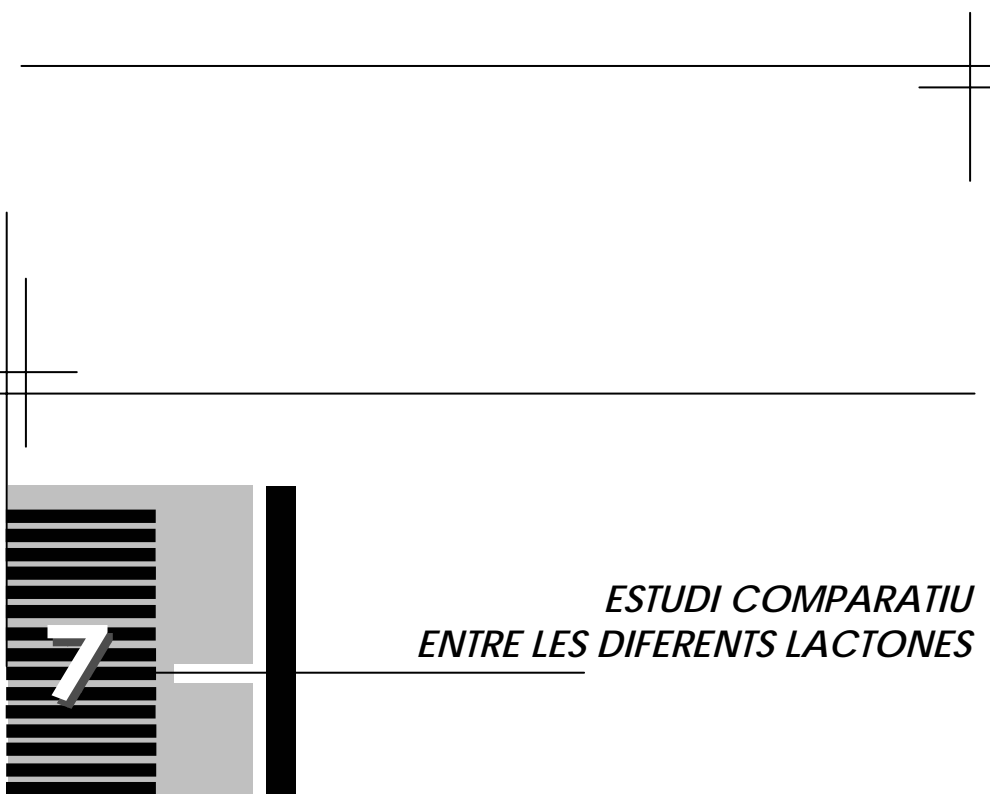


Fig.6.21. Microduresa Knoop front la composició de materials obtinguts amb **DMAP**

En aquest cas l'addició de MDM al DGEBA porta a una disminució de la microduresa, de forma anàloga a l'observat en els sistemes catiónics. Tanmateix, quan s'addiciona MCP al DGEBA puja lleugerament la microduresa. Aquest fet podria relacionar-se amb un major grau d'entrecreuament degut a l'obertura de l'anell de tres baules, que portaria a una major funcionalitat de la lactona. Aquesta obertura no va poder ésser confirmada espectroscòpicament en el curat de les barreges DGEBA/MCP, però si ho va ser en l'homopolimerització del MCP amb DMAP.





*ESTUDI COMPARATIU  
ENTRE LES DIFERENTS LACTONES*

## 7. ESTUDI COMPARATIU ENTRE LES DIFERENTS LACTONES

### 7.1. Introducció

La idea d'aquest capítol és reflectir mitjançant un estudi comparatiu entre les diferents lactones emprades en aquest treball (**Fig. 7.1**), la seva influència en el procés de curat i en les propietats dels materials termoestables obtinguts per copolimerització catiònica o aniónica amb la reina epoxi de diglicidilèter de bisfenol A (DGEBA) i emprant els diferents iniciadors. Entre els iniciadors catiònics, ens centrarem amb els *triflats d'iterbi i de lantà*, ja que han estat emprats amb totes les lactones. S'han considerat tan sols les mescles formades per *DGEBA/lactona/iniciador 2:1:0.015*, ja que ha resultat ser la proporció més idònia.

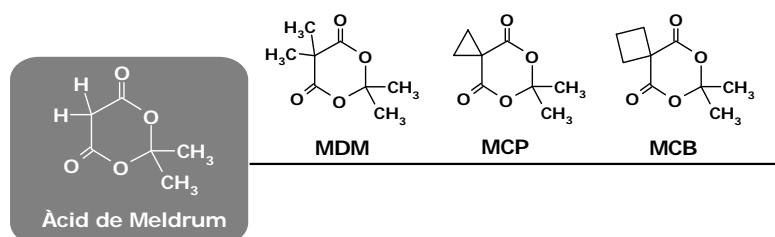


**Fig.7.1.** Lactones utilitzades en la copolimerització catiònica o aniónica amb la reina epoxi de DGEBA

### 7.2. Estudi per calorimetria diferencial d'escombrat (DSC)

A les **fig.7.2** i **7.3** es mostren les corbes calorimètriques i les de conversió front la temperatura pel curat de les mescles de DGEBA amb les diferents lactones emprant  $Yb(OTf)_3$  i  $La(OTf)_3$ . S'observa a les dues figures que l'addició de la lactona desplaça el màxim de l'exoterma cap a temperatures més baixes. Amb l'àcid de Meldrum aquest desplaçament es major i a més, s'observa una lleugera modificació de la forma de la corba, indicant la complexitat del procés de curat. Aquest fet podria atribuir-se a l'acidesa de l'àcid de Meldrum, que podria afavorir el mecanisme de

propagació "monòmer actiu (AM)" de la polimerització. Les corbes de conversió mostren que l'addició de lactona produeix un increment de la conversió per a una temperatura determinada. Aquest fet podria ésser degut al paper que juga la lactona en la formació de l'espècie iniciadora.<sup>145</sup>

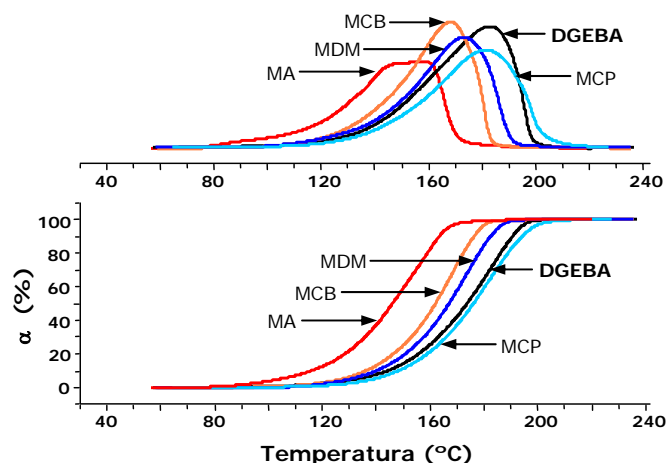


**Fig.7.2.** Corbes calorimètriques i grau de conversió vers la temperatura del curat de DGEBA i de mescles DGEBA/lactona 2:1 (mol/mol) emprant  $\text{Yb}(\text{OTf})_3$  com a iniciador obtingudes a una velocitat d'escalfament de  $10^\circ\text{C}/\text{min}$

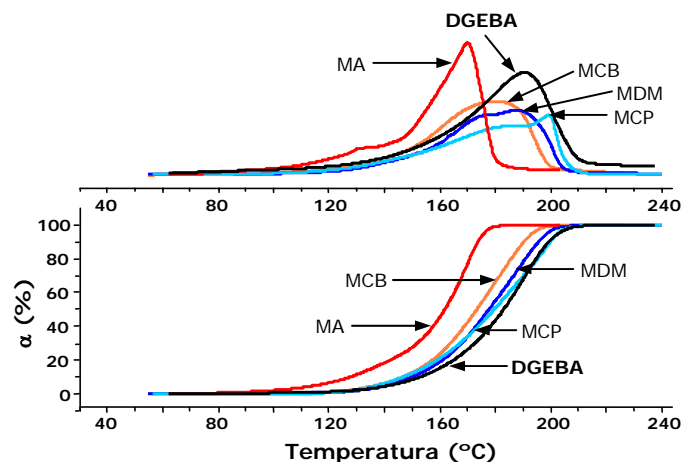


**Fig.7.3.** Corbes calorimètriques i grau de conversió vers la temperatura de curat de DGEBA i de mescles DGEBA/lactona 2:1 (mol/mol) emprant  $\text{La}(\text{OTf})_3$  com a iniciador obtingudes a una velocitat d'escalfament de  $10^\circ\text{C}/\text{min}$

<sup>145</sup> C. Mas, X. Ramis, J. M. Salla, A. Mantecón, A. Serra, J. Polym. Sci.: Part A: Polym. Chem. **41**, 2794-2808 (2003).

A les **taules 7.1 i 7.2**, es troben recollides les dades calorimètriques de tots els processos de curat.

**Taula 7.1** Dades calorimètriques i paràmetres cinètics dels diferents sistemes estudiats iniciats amb **Yb(OTf)<sub>3</sub>**

Mostra	Formulació <sup>a</sup>	T <sub>g</sub> <sup>b</sup> (°C)	ΔH <sup>c</sup> (J/g)	ΔH <sup>d</sup> (kJ/ee)	T <sub>max</sub> <sup>e</sup> (°C)	E <sub>a</sub> (kJ/mol)	ln A <sup>f</sup> (s <sup>-1</sup> )	k <sub>150°C</sub> · 10 <sup>3 g</sup> (s <sup>-1</sup> )
1	DGEBA/Yb(OTf) <sub>3</sub> 1:0.006	135	519.7	95.6	184	90.7	18.09	0.45
2	DGEBA/MA/Yb(OTf) <sub>3</sub> 2:1:0.015	118	415.0	91.3	160	73.2	14.24	1.39
3	DGEBA/MCP/Yb(OTf) <sub>3</sub> 2:1:0.015	110	388.0	88.2	177	-	-	-
4	DGEBA/MDM/Yb(OTf) <sub>3</sub> 2:1:0.015	107	396.5	90.1	174	87.9	17.74	0.71
5	DGEBA/MCB/Yb(OTf) <sub>3</sub> 2:1:0.015	104	433.4	99.8	170	81.8	16.31	0.96

- a. La composició de les formulacions ve expressada en relacions molars  
 b. Temperatura de transició vítria obtinguda per DSC en el segon scan després d'un curat dinàmic  
 c. Entalpia per gram de mescla  
 d. Entalpia per equivalent de grups epoxi  
 e. Temperatura del màxim de l'exoterma  
 f. Factor pre-exponencial considerant el model cinètic R<sub>3</sub> ( $g(\alpha)=1-(1-\alpha)^{1/3}$ ) per  $\alpha=50\%$   
 g. Constant de velocitat a 150°C obtinguda a partir de l'equació d'Arrhenius  $\ln k = \ln A - \frac{E}{RT}$

**Taula 7.2** Dades calorimètriques i paràmetres cinètics dels diferents sistemes estudiats iniciats amb **La(OTf)<sub>3</sub>**

Mostra	Formulació <sup>a</sup>	T <sub>g</sub> <sup>b</sup> (°C)	ΔH <sup>c</sup> (J/g)	ΔH <sup>d</sup> (kJ/ee)	T <sub>max</sub> <sup>e</sup> (°C)	E <sub>a</sub> (kJ/mol)	ln A <sup>f</sup> (s <sup>-1</sup> )	k <sub>150°C</sub> · 10 <sup>3 g</sup> (s <sup>-1</sup> )
1	DGEBA/La(OTf) <sub>3</sub> 1:0.006	127	513.5	94.4	192	79.8	14.59	0.30
2	DGEBA/MA/La(OTf) <sub>3</sub> 2:1:0.015	109	410.0	90.3	173	68.5	12.45	0.90
3	DGEBA/MCP/La(OTf) <sub>3</sub> 2:1:0.015	100	386.8	87.7	200	-	-	-
4	DGEBA/MDM/La(OTf) <sub>3</sub> 2:1:0.015	105	394.1	89.6	188	80.4	15.15	0.44
5	DGEBA/MCB/La(OTf) <sub>3</sub> 2:1:0.015	90	430.1	98.7	181	82.9	16.03	0.54

- a. La composició de les formulacions ve expressada en relacions molars  
 b. Temperatura de transició vítria obtinguda per DSC en el segon scan després d'un curat dinàmic  
 c. Entalpia per gram de mescla  
 d. Entalpia per equivalent de grups epoxi  
 e. Temperatura del màxim de l'exoterma  
 f. Factor pre-exponencial considerant el model cinètic R<sub>3</sub> ( $g(\alpha)=1-(1-\alpha)^{1/3}$ ) per  $\alpha=50\%$   
 g. Constant de velocitat a 150°C obtinguda a partir de l'equació d'Arrhenius  $\ln k = \ln A - \frac{E}{RT}$

Tal i com es pot observar pels dos iniciadors, l'addició de les diferents lactones a la mescla produeix una disminució de la Tg del material. A més, els valors de les Tg són majors pels materials obtinguts amb triflat d'iterbi. Els materials obtinguts a partir d'àcid de Meldrum tenen els valors més alts de tots els copolímers, mentre que aquells que tenen MCB tenen els valors més baixos. Aquesta diferència pot ésser atribuïda al volum del substituent a la posició 5 de l'anell de lactona, que dificulta l'empaquetament de les cadenes.

Malgrat que l'entalpia per equivalent epoxi de les mostres és diferent al canviar la lactona, tots els valors indiquen un alt grau d'entrecruament. En general, en les mescles amb lactona aquest valor és lleugerament inferior a l'entalpia per equivalent epòxid de la reina pura, excepte pel cas del derivat ciclobutenílic que és lleugerament major.

La comparació de les constants de velocitat pels sistemes que podien ajustar-se al mateix model cinètic R<sub>3</sub> permet observar el major efecte acceleratriu de l'àcid de Meldrum. Tanmateix, l'addició de qualsevol de les lactones assajades accelera el procés de curat. Les reaccions iniciades per Yb(OTf)<sub>3</sub> són més ràpides que les iniciades amb La(OTf)<sub>3</sub>. L'efecte accelerant superior de l'àcid de Meldrum podria explicar-se per la intervenció dels protons metilènics.

A la **Taula 7.3** es comparen les dades calorimètriques obtingudes dinàmicament en el curat de mescles *DGEBA/lactona 3:1 (mol/mol)*, ja que la polimerització aniònica només es va estudiar amb aquesta relació molar entre comonòmers. Cal esmentar que per aconseguir un curat aniònic complet, la proporció d'iniciador ha de ser superior que amb triflats de lantànid.

**Taula 7.3.** Dades calorimètriques i paràmetres cinètics dels diferents sistemes estudiats iniciats catiònicament o aniònicament

Mostra	Formulació <sup>a</sup>	T <sub>g</sub> <sup>b</sup> (°C)	ΔH <sup>c</sup> (J/g)	ΔH <sup>d</sup> (kJ/ee)	T <sub>max</sub> <sup>e</sup> (°C)	E <sub>a</sub> (kJ/mol)
1	DGEBA/MCP/Yb(OTf) <sub>3</sub> 3:1:0.021	117	430.3	91.5	177	75.8
2	DGEBA/MDM/Yb(OTf) <sub>3</sub> 3:1:0.021	111	427.6	91.1	175	86.5
3	DGEBA/MCP/La(OTf) <sub>3</sub> 3:1:0.021	105	418.6	89.1	199	89.0
4	DGEBA/MDM/La(OTf) <sub>3</sub> 3:1:0.021	110	422.1	89.8	190	81.6
5	DGEBA/MCP/DMAP 3:1:0.308	116	427.3	92.5	175	67.3
6	DGEBA/MDM/DMAP 3:1:0.308	97	423.1	91.8	141	59.6

- a. La composició de les formulacions ve expressada en relacions molars  
b. Temperatura de transició vítria obtinguda per DSC en el segon scan després d'un curat dinàmic  
c. Entalpia per gram de mescla  
d. Entalpia per equivalent de grups epoxi  
e. Temperatura del màxim de l'exoterma

La  $T_g$  dels materials que incorporen MCP són bastant similars tant amb iniciadors catiònics com amb l'aniónic. D'altra banda, el material amb MDM curat aniónicament té una  $T_g$  lleugerament inferior a la dels materials curats catiònicament. La proporció tan alta d'iniciador porta a molts grups terminals, que haurien de baixar aquest paràmetre. La presència d'un grup ciclopropenil en la MCP, que pot ésser atacat nucleofilicament pot explicar la major  $T_g$  observada per aquest material.

La diferència en el model cinètic seguit en els curats d'aquestes mostres no permeten comparar les constants de velocitat. A la **fig. 7.4** es mostren les corbes calorimètriques i les corbes de conversió calculades pel curat de les dues lactones. Com es pot veure, mentre que per les mescles de MCP els sistemes aniónic porten a un curat més ràpid, pel MDM no hi massa diferència entre la iniciació amb DMAP i amb  $\text{Yb}(\text{OTf})_3$ .

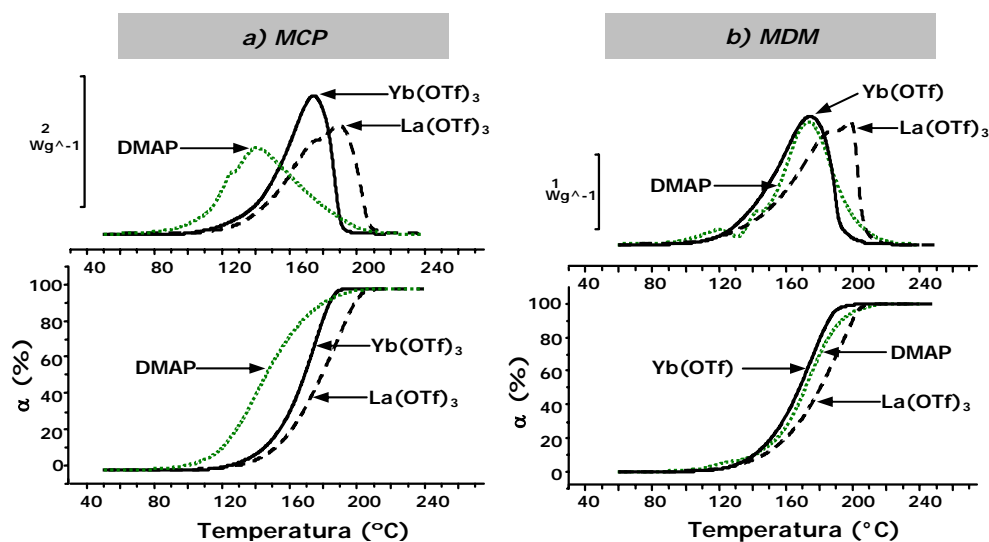


**Figura 7.4.** Corbes calorimètriques i grau de conversió vers la temperatura del curat de mescles de (a) DGEBA/MCP 3:1 (mol/mol) i (b) DGEBA/MDM 3:1 (mol/mol) emprant  $\text{Yb}(\text{OTf})_3$ ,  $\text{La}(\text{OTf})_3$  i DMAP com a iniciadors obtingudes a una velocitat d'escalfament de  $10^{\circ}\text{C}/\text{min}$

### 7.3. Estudi per espectroscòpia d'infraroig (ATR-FTIR)

A les **fig. 7.5**, **7.6**, **7.7** i **7.8** es mostren solapats els espectres de ATR-FTIR després del curat de les mostres de la reina epoxi amb les diferents lactones, emprant els triflats d'iterbi i lantà com iniciadors, curades a la temperatura de  $150^{\circ}\text{C}$ .

La comparació de l'àrea de la banda al voltant de  $1734\text{ cm}^{-1}$ , corresponent a les vibracions de tensió del grup carbonil del poli(èter-ester) lineal, permet avaluar quantitativament la proporció de lactona químicament incorporada a la xarxa polimèrica.

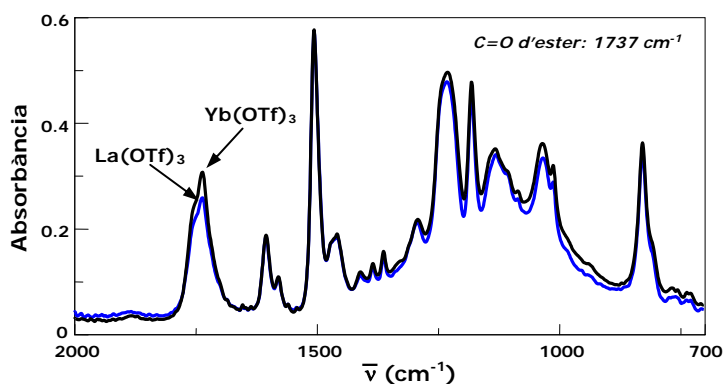


Fig.7.5. Espectres de ATR-FTIR dels materials obtinguts a 150°C de mescles DGEBA/MA 2:1 (mol/mol) amb 0.015 mols de triflats de lantànid

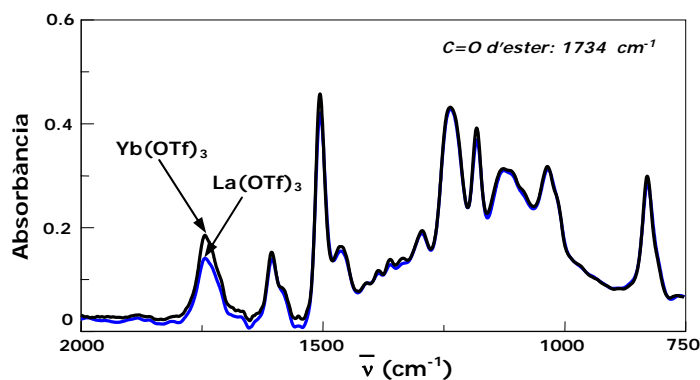


Fig.7.6. Espectres de ATR-FTIR dels materials obtinguts a 150°C de mescles DGEBA/MCP 2:1 (mol/mol) amb 0.015 mols de triflats de lantànid

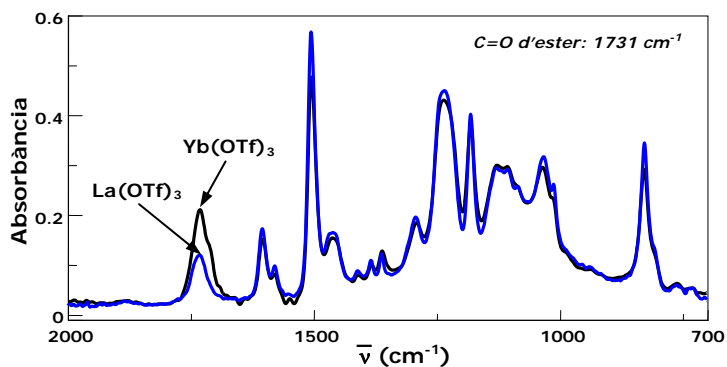
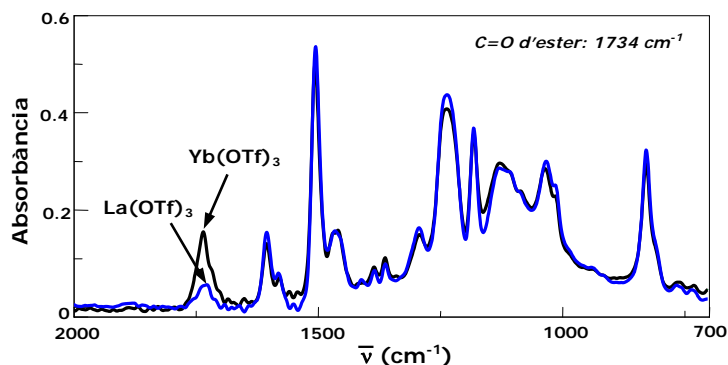


Fig.7.7. Espectres de ATR-FTIR dels materials obtinguts a 150°C de mescles DGEBA/MCB 2:1 (mol/mol) amb 0.015 mols de triflats de lantànid



**Fig. 7.8.** Espectres de ATR-FTIR dels materials obtinguts a 150°C de mesclades DGEBA/MDM 2:1 (mol/mol) amb 0.015 mols de triflats de lantànid

Com es pot observar en els quatre casos, es produeix una major incorporació de grups ester a la xarxa polimèrica emprant triflat d'iterbi com a iniciador degut a que una major proporció de grups SOE ha polimeritzat.

Per tal de conèixer quina de les lactones incorporava un major nombre de grups ester a la matriu polimèrica, es va integrar la banda al voltant de 1734  $\text{cm}^{-1}$  corresponent a l'ester lineal i es va normalitzar amb una banda de referència (1605  $\text{cm}^{-1}$ ) corresponent a l'anell aromàtic de DGEBA. A partir del quocient d'absorbàncies s'ha calculat el percentatge d'ester lineal, donant el valor 1 a la mostra 1 que donava el quocient més gran.

A la **taula 7.4** es mostren els resultats obtinguts pels diferents sistemes. Els temps de curat de la taula s'han calculat a partir dels experiments d'infrarroig.

**Taula 7.4.** Proporció d'ester lineal a la xarxa polimèrica dels diferents sistemes de DGEBA/lactona 2:1 (mol/mol) amb 0.015 mols de  $\text{Yb}(\text{OTf})_3$  o  $\text{La}(\text{OTf})_3$  calculats a partir d'experiments de ATR-FTIR

Mostra	Formulació	Iniciador	$A_{1734}/A_{1605}$	Ester Lineal	Temps de reacció (s)
1	DGEBA/MA	$\text{Yb}(\text{OTf})_3$	3.4	1	480
2	DGEBA/MCP	$\text{Yb}(\text{OTf})_3$	2.1	0.62	6285
3	DGEBA/MCB	$\text{Yb}(\text{OTf})_3$	1.9	0.56	1990
4	DGEBA/MDM	$\text{Yb}(\text{OTf})_3$	1.7	0.50	2370
5	DGEBA/MA	$\text{La}(\text{OTf})_3$	3.0	0.88	885
6	DGEBA/MCP	$\text{La}(\text{OTf})_3$	1.5	0.44	7370
7	DGEBA/MCB	$\text{La}(\text{OTf})_3$	1.1	0.32	2180
8	DGEBA/MDM	$\text{La}(\text{OTf})_3$	0.5	0.15	2970



Com es pot observar hi ha una major proporció de grups ester a la matriu polimèrica quan la mescla conté l'àcid de Meldrum no modificat, a més que porta a un temps de curat menor. Dels diferents derivats de l'àcid de Meldrum, el MCP produeix una major proporció de grups ester a la xarxa però en un temps de curat superior.

A les **fig.7.9** i **7.10** es mostren solapats els espectres dels materials obtinguts a partir de mescles amb MCP o MDM curades amb  $\text{Yb}(\text{OTf})_3$  o DMAP a  $150^\circ\text{C}$ . En aquest cas no és possible avaluar la proporció de lactona incorporada a la xarxa polimèrica en el curat aniònic, ja que la banda a  $1734\text{ cm}^{-1}$  associada a les vibracions de tensió del grup carbonil del poli(èter-ester) lineal està parcialment solapada amb altres grups carbonílics que es formen. Tanmateix, la mescla amb MDM sembla portar a una major proporció d'ester lineal amb DMAP que la mescla que conté el MCP.

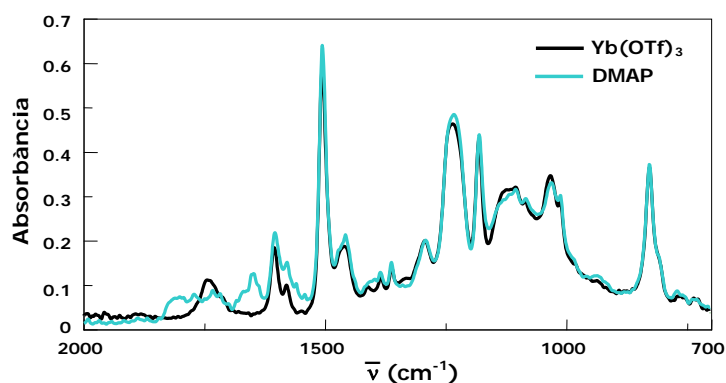


**Fig.7.9.** Espectres de ATR-FTIR de materials obtinguts per curat a  $150^\circ\text{C}$  de mescles DGEBA/MCP 3:1 (mol/mol) utilitzant  $\text{Yb}(\text{OTf})_3$  i DMAP com a iniciadors

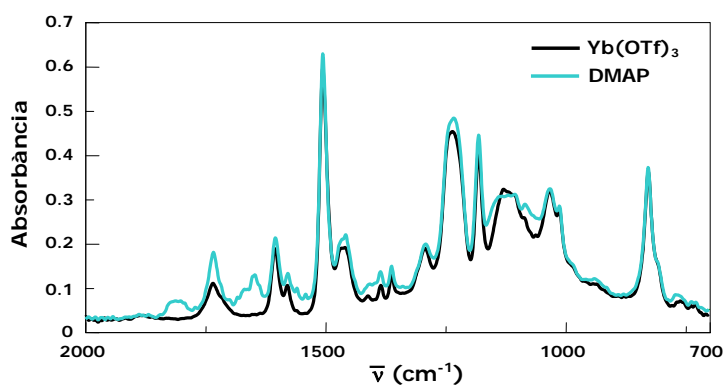


**Fig.7.10.** Espectres de ATR-FTIR de materials obtinguts per curat a  $150^\circ\text{C}$  de mescles DGEBA/MDM 3:1 (mol/mol) utilitzant  $\text{Yb}(\text{OTf})_3$  i DMAP com a iniciadors

#### 7.4. Estudi de l'estabilitat tèrmica mitjançant TGA

A les **fig.7.11** i **7.12** es mostren les corbes termogravimètriques i les primeres derivades obtingudes pels diferents materials curats dinàmicament al DSC. Com es pot observar, tant emprant  $\text{Yb}(\text{OTf})_3$  com  $\text{La}(\text{OTf})_3$ , els materials que contenen lactones van resultar lleugerament més degradables degut a la incorporació química de grups ester a la xarxa polimèrica. Si comparem les DTG de les dues figures es pot observar que amb triflat de lantà la degradació del materials és més complexa.

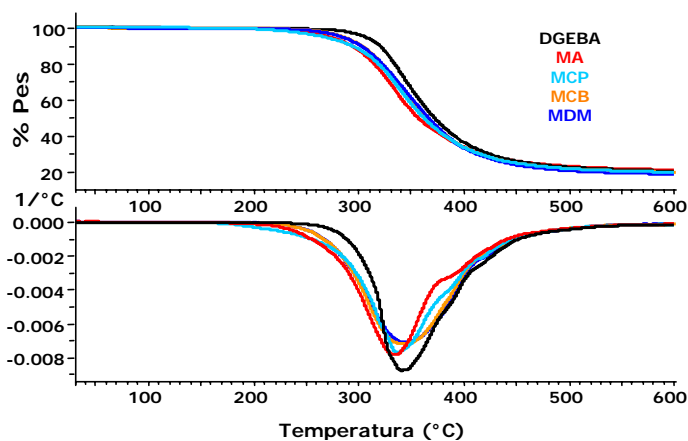


**Fig.7.11.** Corbes TGA i DTG a 10°C/min en atmosfera de  $\text{N}_2$  dels diferents materials termoestables obtinguts per curat dinàmic de mescleres de DGEBA/lactona 2:1 (mol/mol) amb  $\text{Yb}(\text{OTf})_3$

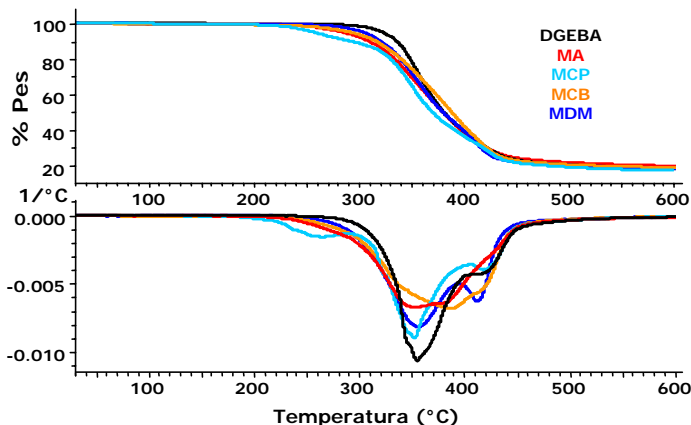


**Fig.7.12.** Corbes TGA i DTG a 10°C/min en atmosfera de  $\text{N}_2$  dels diferents materials termoestables obtinguts per curat dinàmic de mescleres de DGEBA/lactona 2:1 (mol/mol) amb  $\text{La}(\text{OTf})_3$

A les **taules 7.5 i 7.6** es troben recollides les dades termogravimètriques dels materials obtinguts.

**Taula 7.5.** Dades termogravimètriques obtingudes per TGA a una velocitat d'escalfament de 10°C/min i en atmosfera de N<sub>2</sub> dels diferents materials curats amb **Yb(OTf)<sub>3</sub>**

Mostra	Formulació <sup>a</sup>	T <sub>2%</sub> <sup>b</sup> (°C)	T <sub>max</sub> (°C)	Residu <sup>c</sup> (%)
1	DGEBA/La(OTf) <sub>3</sub> 1:0.006	303	354	19
2	DGEBA/MA/La(OTf) <sub>3</sub> 2:1:0.015	256	352	21
3	DGEBA/MCP/La(OTf) <sub>3</sub> 2:1:0.015	233	348	17
4	DGEBA/MDM/La(OTf) <sub>3</sub> 2:1:0.015	282	355	18
5	DGEBA/MCB/La(OTf) <sub>3</sub> 2:1:0.015	262	386	19

a. La composició de les formulacions ve expressada en relacions molars  
b. Temperatura del 2% de pèrdua de pes calculada per anàlisi termogravimètric  
c. Residu a una temperatura 600°C

**Taula 7.6.** Dades termogravimètriques obtingudes per TGA a una velocitat d'escalfament de 10°C/min i en atmosfera de N<sub>2</sub> dels diferents materials curats amb **La(OTf)<sub>3</sub>**

Mostra	Formulació <sup>a</sup>	T <sub>2%</sub> <sup>b</sup> (°C)	T <sub>max</sub> (°C)	Residu <sup>c</sup> (%)
1	DGEBA/Yb(OTf) <sub>3</sub> 1:0.006	287	345	20
2	DGEBA/MA/Yb(OTf) <sub>3</sub> 2:1:0.015	244	337	21
3	DGEBA/MCP/Yb(OTf) <sub>3</sub> 2:1:0.015	230	332	19
4	DGEBA/MDM/Yb(OTf) <sub>3</sub> 2:1:0.015	262	340	18
5	DGEBA/MCB/Yb(OTf) <sub>3</sub> 2:1:0.015	258	342	20

a. La composició de les formulacions ve expressada en relacions molars  
b. Temperatura del 2% de pèrdua de pes calculada per anàlisi termogravimètric  
c. Residu a una temperatura 600°C

Tal i com podem veure a les taules els materials obtinguts amb les diferents lactones i emprant Yb(OTf)<sub>3</sub> com a iniciador van començar la pèrdua de pes a temperatures lleugerament més baixes que els obtinguts amb La(OTf)<sub>3</sub>, el que els fa més degradables des del punt de vista de l'eliminació del recobriments. Els materials que incorporen MCP van presentar un millor degradabilitat tèrmica. Aquest resultat no es correlaciona amb la proporció d'ester lineal a la xarxa, que és major en el cas del MA. Tanmateix, la Tg dels materials que incorporen MA i les seves entalpies de curat són majors, el qual indica un major grau d'entrecruament per aquests materials, dificultant la degradació i posterior pèrdua de pes. Això indica que a més de la proporció

de grups ester, la topologia del material també juga un paper en la degradabilitat tèrmica. La degradació pirolítica d'esters requereix l'adopció d'una geometria adient, que un alt grau d'entrecruament i menor mobilitat podria impedir.

A la **taula 7.7** es recullen els resultats termogravimètrics obtinguts de mostres de DGEBA/MCP i DGEBA/MDM curades catiònica o aniònica. El material obtingut per iniciació aniònica de DGEBA pur inicia la seva pèrdua de pes a temperatura més baixa i té una temperatura de màxima velocitat de degradació molt més alta, el que confirma l'efecte catalític dels triflats de lantànid en la ruptura d'èters, ja que a la temperatura de màxima velocitat de degradació els enllaços que es trenquen són principalment èters. Els materials obtinguts amb lactones per iniciació amb les sals de lantànid presenten valors significativament més baixos d'aquest paràmetre. En quant a l'inici de la degradació, té més a veure amb la presència d'una alta proporció de grups ester a la xarxa o amb una topologia més oberta. D'acord amb això, dels materials obtinguts aniònicament, el que conté MDM amb una Tg de 97°C i una major proporció d'esters lineals inicia la degradació a una temperatura inferior que el material amb MCP, que té una Tg de 116°C i una baixa proporció d'ester lineal.

**Taula 7.7.** Dades termogravimètriques obtingudes a una velocitat d'escalfament de 10°C/min i en atmosfera de N<sub>2</sub> de materials curats amb triflats de lantànid i DMAP

Mostra	Formulació <sup>a</sup>	T <sup>b</sup> (°C)	T <sub>màx</sub> (°C)	Residu <sup>c</sup> (%)
1	DGEBA/Yb(OTf) <sub>3</sub> 1:0.006	287	345	20
2	DGEBA/La(OTf) <sub>3</sub> 1:0.006	303	354	19
3	DGEBA/DMAP 1:0.088	337	430	16
4	DGEBA/MCP/Yb(OTf) <sub>3</sub> 3:1:0.021	241	335	19
5	DGEBA/MCP/La(OTf) <sub>3</sub> 3:1:0.021	250	350	18
6	DGEBA/MCP/DMAP 3:1:0.308	335	428	14
7	DGEBA/MDM/Yb(OTf) <sub>3</sub> 3:1:0.021	265	337	19
8	DGEBA/MDM/La(OTf) <sub>3</sub> 3:1:0.021	286	361	18
9	DGEBA/MDM/DMAP 3:1:0.308	252	425	13

a. La composició de les formulacions ve expressada en relacions molars  
b. Temperatura del 2% de pèrdua de pes calculada per anàlisi termogravimètric  
c. Residu a una temperatura 600°C

### 7.5. Estudi de la contracció

A les **taules 7.8** i **7.9** es troben recollits els resultats dels diferents sistemes catiónics estudiats.

**Taula 7.8.** Densitats i encongiment dels materials curats amb  $Yb(OTf)_3$

Mostra	Formulació <sup>a</sup>	$\delta_{mi}^b$ (g/cm <sup>3</sup> )	$\delta_{mf}^b$ (g/cm <sup>3</sup> )	Encongiment (%)
1	DGEBA/Yb(OTf) <sub>3</sub> 1:0.006	1.158	1.192	2.9
2	DGEBA/MA/Yb(OTf) <sub>3</sub> 2:1:0.015	1.183	1.198	1.3
3	DGEBA/MCP/Yb(OTf) <sub>3</sub> 2:1:0.015	1.176	1.193	1.5
4	DGEBA/MCB/Yb(OTf) <sub>3</sub> 2:1:0.015	1.171	1.191	1.7
5	DGEBA/MDM/Yb(OTf) <sub>3</sub> 2:1:0.015	1.167	1.190	2.0

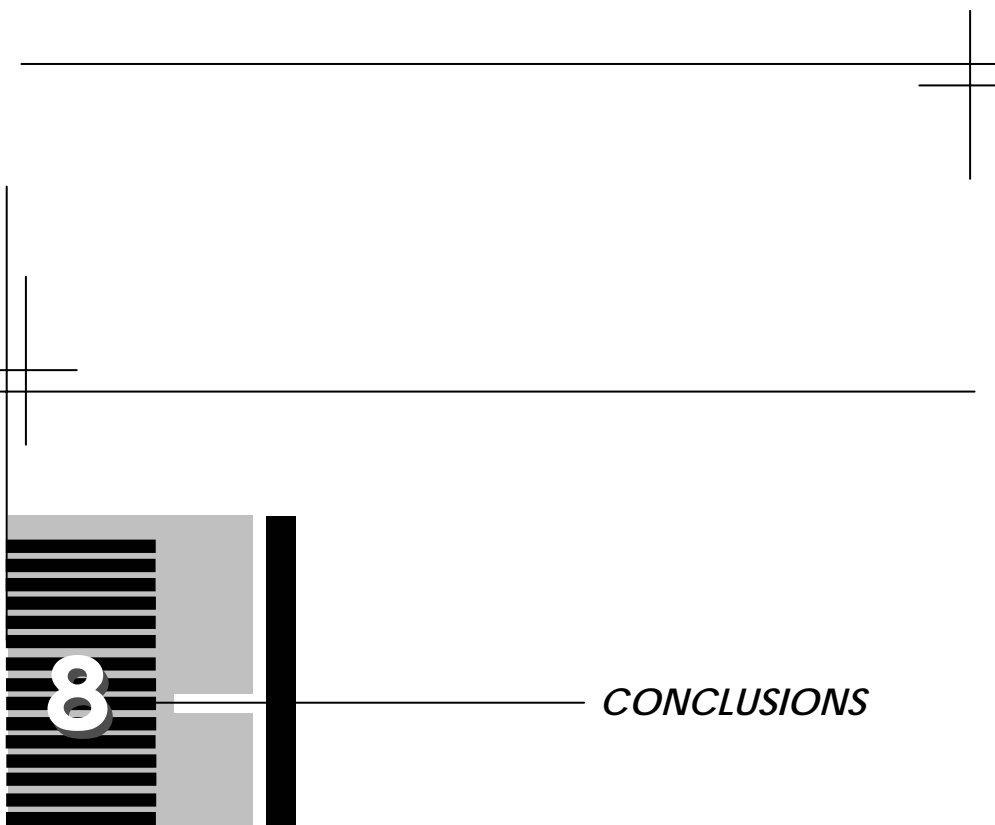
a. La composició de les formulacions ve expressada en relacions molar  
b. Densitats abans ( $\delta_{mi}$ ) i després ( $\delta_{mf}$ ) del procés de curat

**Taula 7.9.** Densitats i encongiment dels materials curats amb  $La(OTf)_3$

Mostra	Formulació <sup>a</sup>	$\delta_{mi}^b$ (g/cm <sup>3</sup> )	$\delta_{mf}^b$ (g/cm <sup>3</sup> )	Encongiment (%)
1	DGEBA/La(OTf) <sub>3</sub> 1:0.006	1.158	1.193	3.0
2	DGEBA/MA/La(OTf) <sub>3</sub> 2:1:0.015	1.184	1.202	1.5
3	DGEBA/MCP/La(OTf) <sub>3</sub> 2:1:0.015	1.175	1.200	2.1
4	DGEBA/MCB/La(OTf) <sub>3</sub> 2:1:0.015	1.168	1.195	2.3
5	DGEBA/MDM/La(OTf) <sub>3</sub> 2:1:0.015	1.164	1.193	2.5

a. La composició de les formulacions ve expressada en relacions molar  
b. Densitats abans ( $\delta_{mi}$ ) i després ( $\delta_{mf}$ ) del procés de curat

Com es pot observar a les taules la incorporació de les diferents lactones a la xarxa polimèrica va permetre en tots els casos una reducció de la contracció durant el curat front aquells materials obtinguts a partir de la reïna epoxi pura. La contracció és menor pels curats duts a terme amb  $Yb(OTf)_3$  i disminueix al augmentar la proporció d'ester lineal incorporat a la xarxa. Això confirma que la reducció de l'encongiment dels materials està directament relacionada amb el procés de polimerització dels grups SOEs intermedis degut al seu caràcter expansible.

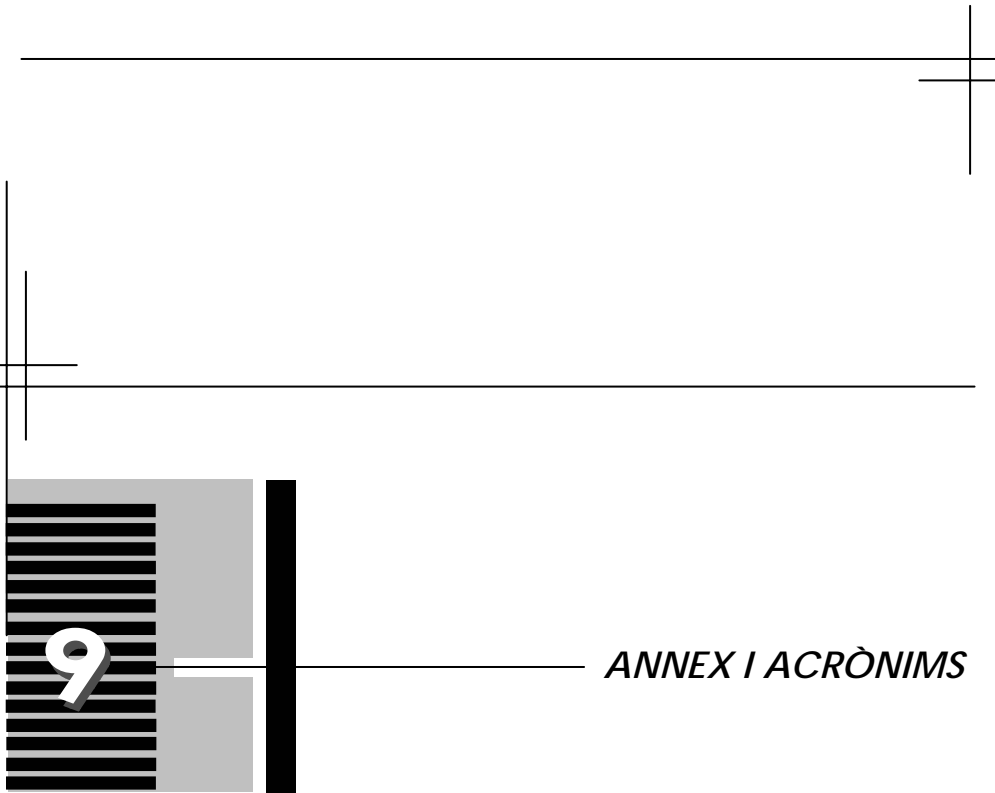


***CONCLUSIONS***

1. La modificació de DGEBA per copolimerització catiònica amb l'àcid de Meldrum i els seus derivats utilitzant els triflats de terres rares com iniciadors porta a una xarxa tridimensional amb estructures de poli(èter-ester). La major proporció d'ester lineal s'ha aconseguit emprant triflat d'iterbi. La utilització del iniciador catiònic convencional  $\text{BF}_3 \cdot \text{MEA}$  porta a materials amb la menor proporció d'ester incorporat a la xarxa.
2. La copolimerització aniònica, iniciada amb DMAP, del DGEBA amb MCP o MDM porta a una xarxa polimèrica que, a més dels grups ester terciaris esperats, presenta altres grups carbonílics, com esters vinílics i anhídrids. La proporció d'ester lineal depèn del tipus de lactona emprada i és més elevada pel MDM.
3. En general l'addició d'àcid de Meldrum i derivats al DGEBA accelera el procés de curat en sistemes catiònics, mentre que l'addició de derivats d'àcid de Meldrum produeix l'efecte contrari quan s'utilitza DMAP com a iniciador aniònic.
4. Dels iniciadors catiònics assajats el  $\text{Yb}(\text{OTf})_3$  és el que accelera més el procés de curat i el que permet dur a terme el curat isotèrmic a temperatures més baixes, el que es pot atribuir a la seva major acidesa de Lewis.
5. L'addició de les lactones estudiades a la reina de DGEBA porta a una reducció de la  $T_g$  dels materials curats amb tots els iniciadors assajats. Aquesta reducció augmenta amb la proporció de lactona a la mescla reactiva.
6. Un augment de la proporció d'iniciador comporta un lleuger increment de la  $T_g$  dels materials. En tots els casos, el  $\text{Yb}(\text{OTf})_3$  porta a materials amb valors de  $T_g$  superiors als obtinguts amb el  $\text{La}(\text{OTf})_3$ .
7. L'addició de les lactones a la mescla reactiva porta a una menor contracció durant el curat que la mesurada en el curat de la reina epoxi pura, tant en curats catiònics com aniònics. Aquesta reducció és proporcional a la quantitat de lactona afegida, el que indica el caràcter expansible de l'anell d'àcid de Meldrum.
8. La degradabilitat tèrmica dels nous materials obtinguts augmenta respecte als termoestables de DGEBA pur. La temperatura inicial de degradació disminueix al augmentar la proporció d'ester lineal a la xarxa. S'ha comprovat l'efecte catalític dels triflats de terres rares en el procés degradatiu, especialment en la ruptura d'enllaços èter. El  $\text{Yb}(\text{OTf})_3$  porta a materials tèrmicament més degradables.

9. S'ha sintetitzat un nova reina epoxi, la DGMA, a partir de l'àcid de Meldrum mitjançant una reacció de dues etapes. S'ha confirmat la seva estructura per anàlisi elemental i espectroscòpia de FTIR i RMN.
10. La homopolimerització de DGMA i la seva copolimerització amb DGEBA amb diferents proporcions amb triflats de lantànid com a iniciador porta a termoestables amb estructura de poli(èter-ester), el que confirma l'obertura tant de l'epòxid com de l'anell de lactona.
11. L'addició de DGMA al DGEBA no produeix cap disminució significativa de la temperatura del curat, malgrat que el DGMA pur pot ésser curat a temperatura més baixa que el DGEBA pur.
12. Els materials que contenen DGMA mostren una  $T_g$  inferior i una major degradabilitat tèrmica que els obtinguts a partir del DGEBA pur.
13. La copolimerització del DGEBA amb àcid de Meldrum o derivats porta a una flexibilització del material i a una baixa reducció de la microduresa.





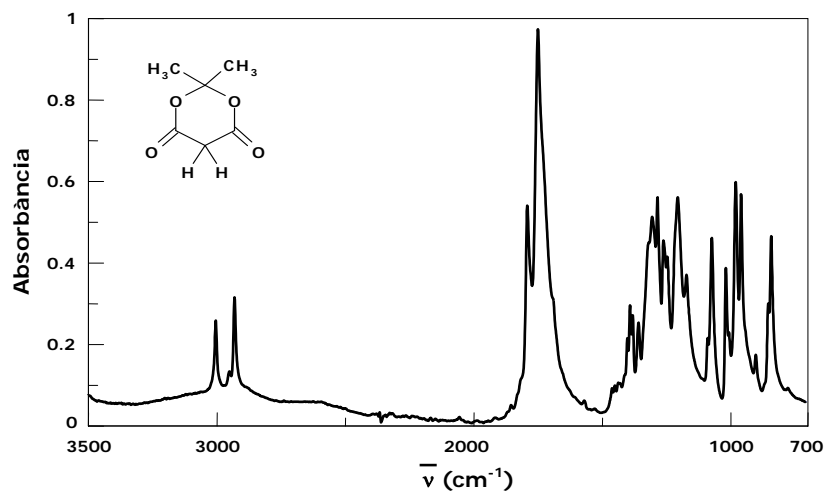
*ANNEX I ACRÒNIMS*

## 9.1. MODELS CINÈTICS

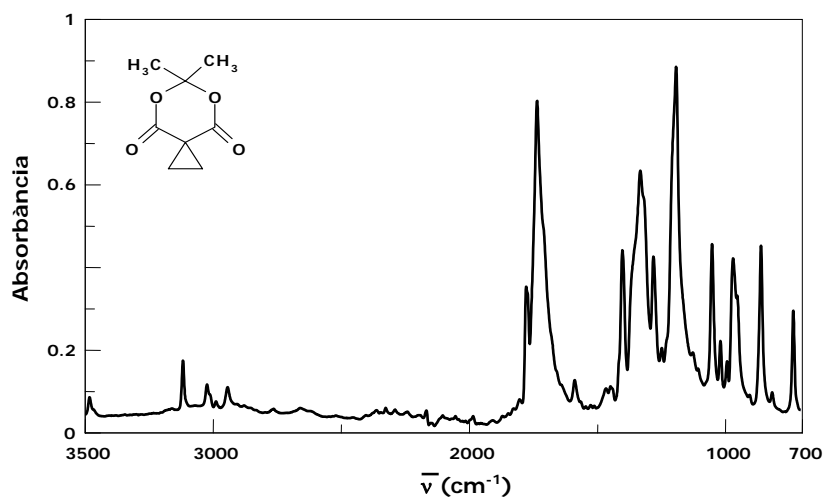
**Taula 1.1.** Expressions algebraiques de  $f(\alpha)$  i  $g(\alpha)$  pels diferents models cinètics usats

<b>Model cinètic</b>	<b><math>f(\alpha)</math></b>	<b><math>g(\alpha)</math></b>
<b><math>A_2</math></b>	$2(1-\alpha)[- \ln(1-\alpha)]^{1/2}$	$[- \ln(1-\alpha)]^{1/2}$
<b><math>A_3</math></b>	$3(1-\alpha)[- \ln(1-\alpha)]^{2/3}$	$[- \ln(1-\alpha)]^{1/3}$
<b><math>A_{3/2}</math></b>	$3/2(1-\alpha)[- \ln(1-\alpha)]^{1/3}$	$[- \ln(1-\alpha)]^{2/3}$
<b><math>A_4</math></b>	$4(1-\alpha)[- \ln(1-\alpha)]^{3/4}$	$[- \ln(1-\alpha)]^{1/4}$
<b><math>D_1</math></b>	$1/2(1-\alpha)^{-1}$	$\alpha^2$
<b><math>D_2</math></b>	$-\ln(1-\alpha)$	$(1-\alpha)\ln(1-\alpha) + \alpha$
<b><math>D_3</math></b>	$3/2(1-\alpha)^{2/3}[1-(1-\alpha)]^{-1/3}$	$[1-(1-\alpha)^{1/3}]^2$
<b><math>D_4</math></b>	$3/2(1-\alpha)^{1/3}[1-(1-\alpha)]^{-1/3}$	$(1-2/3\alpha)(1-\alpha)^{2/3}$
<b><math>F_1</math></b>	$(1-\alpha)$	$-\ln(1-\alpha)$
<b><math>R_2</math></b>	$2(1-\alpha)^{1/2}$	$[1-(1-\alpha)^{1/2}]$
<b><math>R_3</math></b>	$3(1-\alpha)^{2/3}$	$[1-(1-\alpha)^{1/3}]$
<b>Power</b>	$2\alpha^{1/2}$	$\alpha^{1/2}$
<b><math>n=2</math></b>	$(1-\alpha)^2$	$-1+(1-\alpha)^{-1}$
<b><math>n=3</math></b>	$(1-\alpha)^3$	$2^{-1}[-1+(1-\alpha)^{-2}]$
<b><math>n=1.5 ; m=0.5</math></b>	$\alpha^{0.5}(1-\alpha)^{1.5}$	$[(1-\alpha)\alpha^{-1}]^{-0.5}(0.5)^{-1}$
<b><math>n=1.5</math></b>	$(1-\alpha)^{1.5}$	$[1-(1-\alpha)^{-0.5}](-0.5)^{-1}$
<b><math>n=1.0 ; m=0.1</math></b>	$\alpha^{0.1}(1-\alpha)^{1.9}$	$[(1-\alpha)\alpha^{-1}]^{-0.9}(0.9)^{-1}$

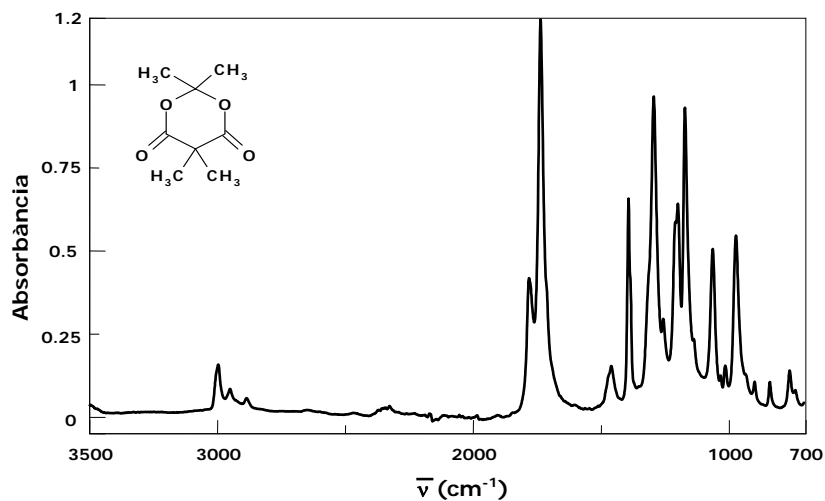
## 9.2. ESPECTRES DE ATR-FTIR



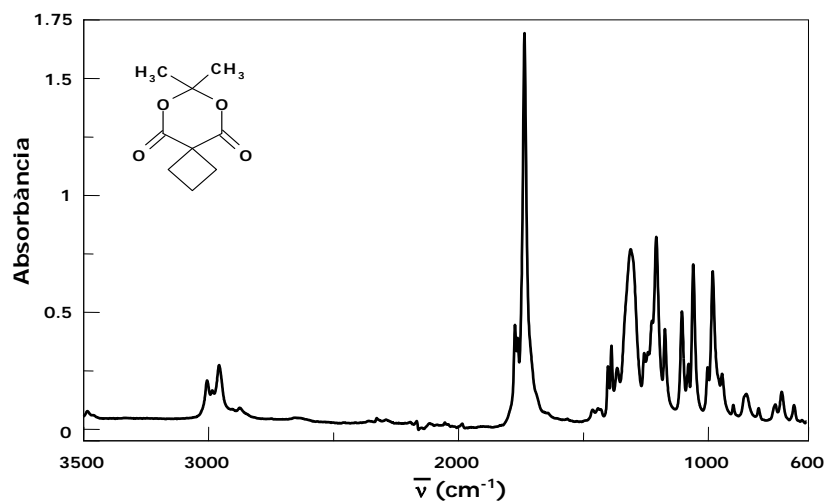
**ATR-FTIR (cm<sup>-1</sup>) de l'àcid de Meldrum (MA) :** 3003, 2929, 1788, 1746, 1388, 1354, 1300, 1280, 1257, 1201, 1167, 1067, 1013, 975, 954, 836.



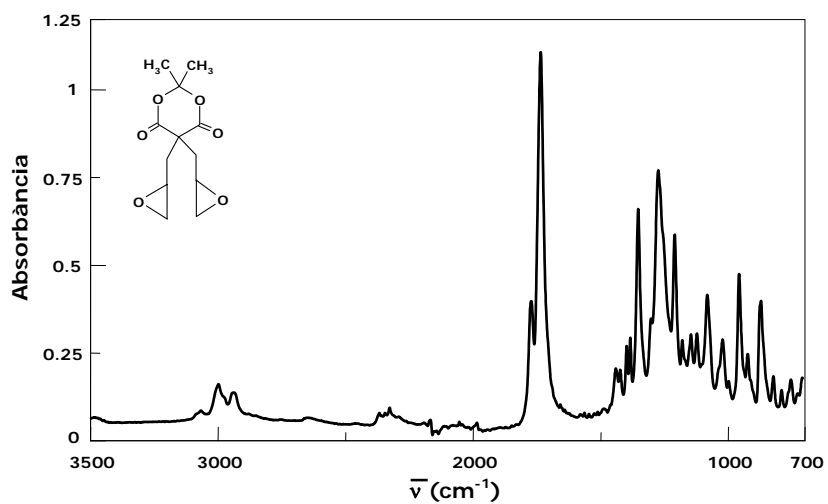
**ATR-FTIR (cm<sup>-1</sup>) de MCP:** 3315, 3019, 2943, 1772, 1732, 1397, 1328, 1276, 1188, 1046, 1012, 964, 947, 853, 729.



**ATR-FTIR (cm<sup>-1</sup>) de MDM:** 2995, 1778, 1733, 1455, 1387, 1288, 1193, 1166, 1058, 1008, 966.



**ATR-FTIR (cm<sup>-1</sup>) de MCB:** 3004, 2955, 1769, 1731, 1396, 1383, 1360, 1306, 1202, 1168, 1099, 1073, 1054, 997, 976, 938, 842.



**ATR-FTIR ( $\text{cm}^{-1}$ ) de DGMA:** 2997, 2938, 1768, 1731, 1437, 1416, 1392, 1378, 1348, 1267, 1205, 1175, 1139, 1116, 1076, 1016, 951, 917, 865.

### 9.3. ESPECTRES DE RMN

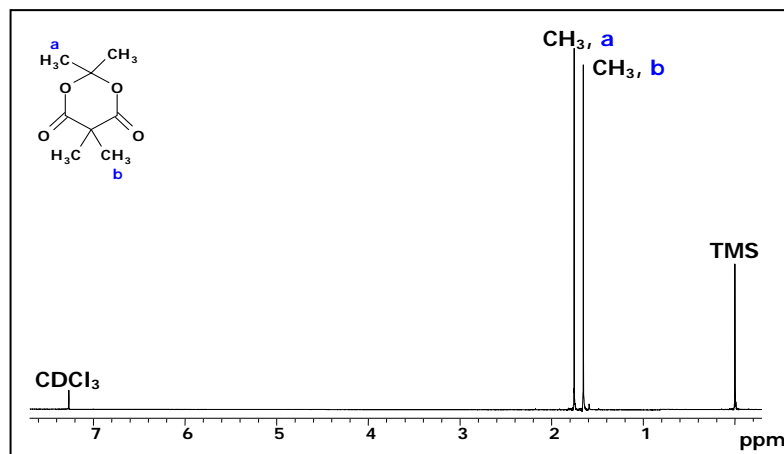


Figura 1. Espectre de RMN de  $^1\text{H}$  (400 MHz) en  $\text{CDCl}_3$  de 2,2,5,5-tetrametil-4,6-dioxo-1,3-dioxà (*MDM*)

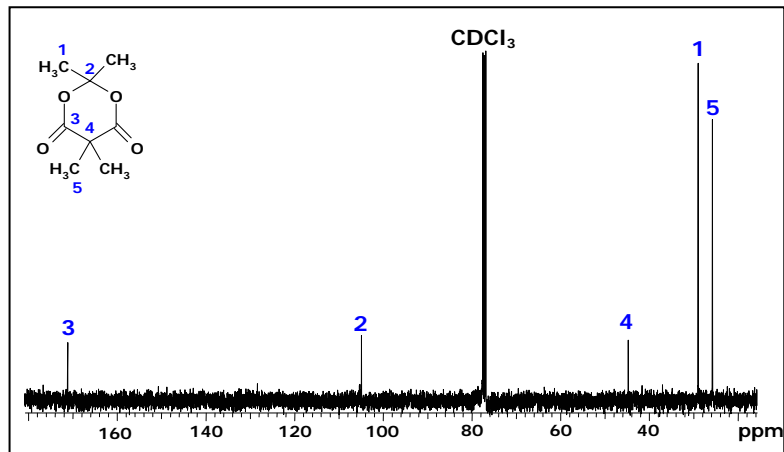


Figura 2. Espectre de RMN de  $^{13}\text{C}$  (100 MHz) en  $\text{CDCl}_3$  de 2,2,5,5-tetrametil-4,6-dioxo-1,3-dioxà (*MDM*)

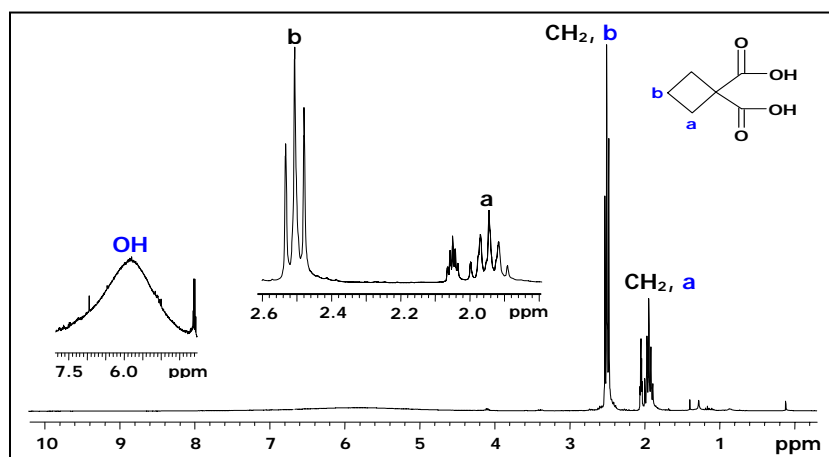


Figura 3. Espectre de RMN de  $^1\text{H}$  (300 MHz) de l'àcid 1,1-ciclobutandicarboxílic

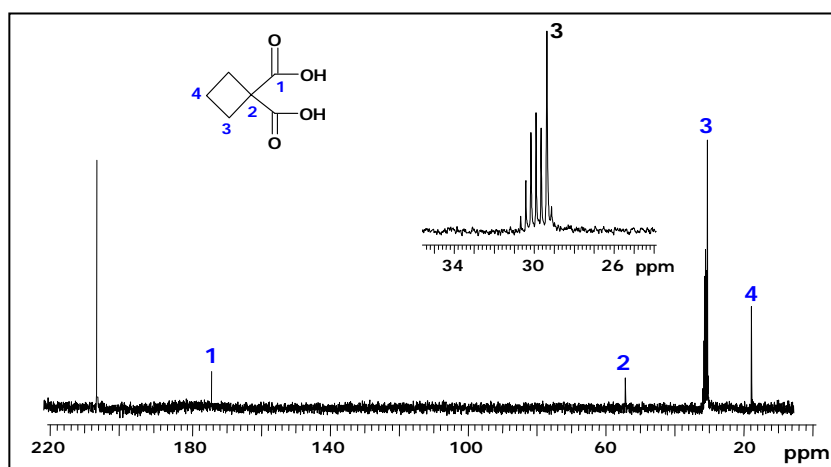


Figura 4. Espectre de RMN de  $^{13}\text{C}$  (75.4 MHz) de l'àcid 1,1-ciclobutandicarboxílic

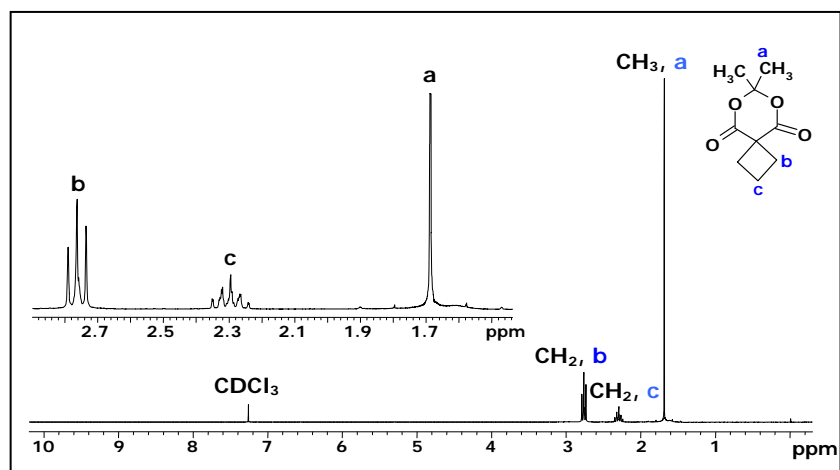


Figura 5. Espectre de RMN de  $^1\text{H}$  (300MHz) en  $\text{CDCl}_3$  7,7-dimetil-6,8-dioxaspiro[3.5]nonà-5,9-diona (*MCB*)

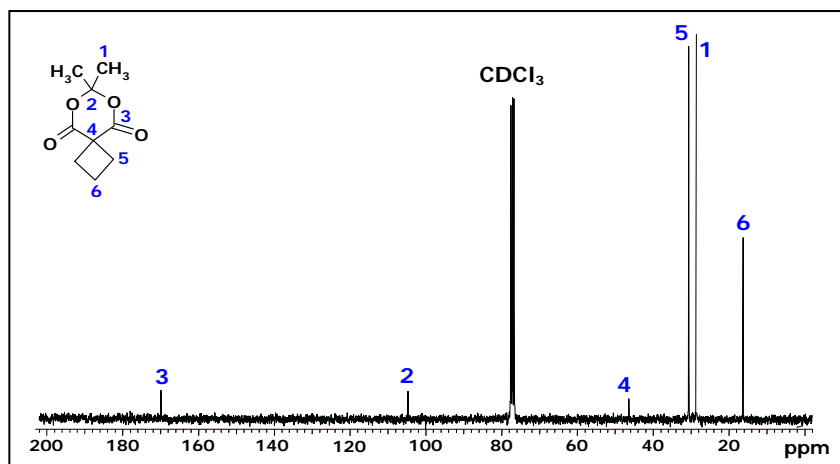


Figura 6. Espectre de RMN de  $^{13}\text{C}$  (75.4MHz) en  $\text{CDCl}_3$  7,7-dimetil-6,8-dioxaspiro[3.5]nonà-5,9-diona (*MCB*)



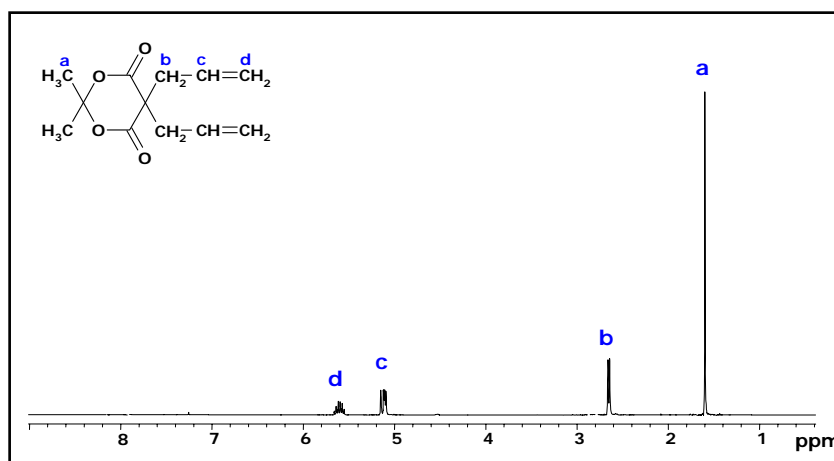


Figure 7. Espectre de RMN de <sup>1</sup>H (400 MHz) en CDCl<sub>3</sub> de 5,5-dial·lil-2,2-dimetil-4,6-dioxo-1,3-dioxà (*DAMA*)

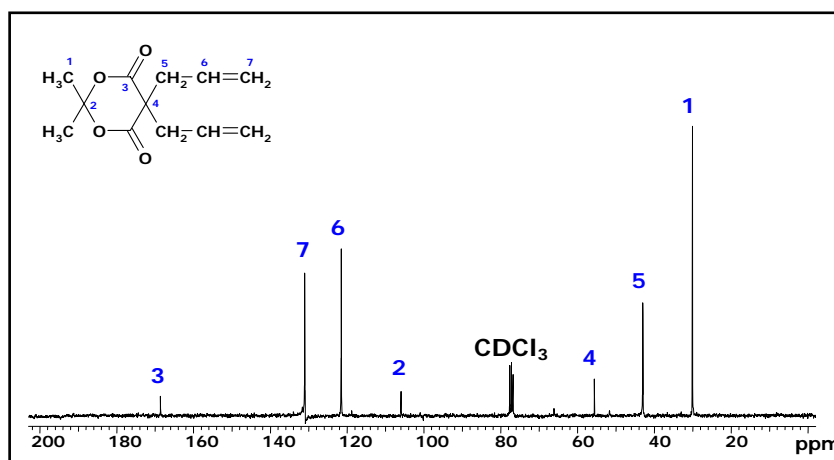


Figure 7. Espectre de RMN de <sup>13</sup>C (100 MHz) en CDCl<sub>3</sub> de 5,5-dial·lil-2,2-dimetil-4,6-dioxo-1,3-dioxà (*DAMA*)

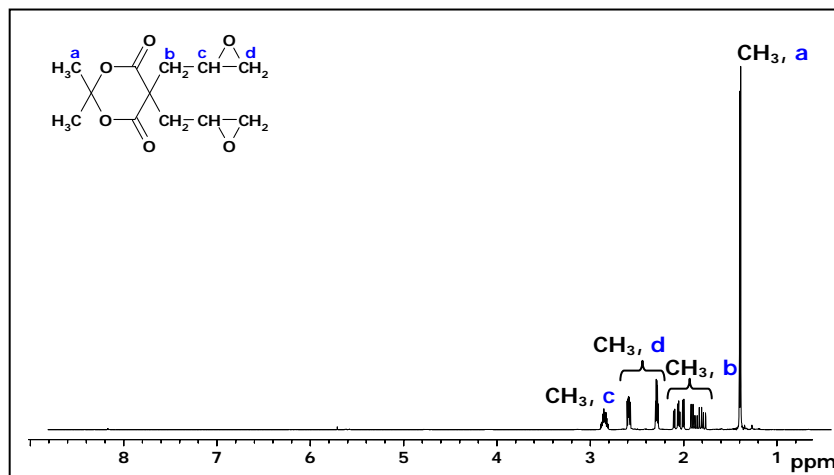


Figura 9. Espectre de RMN de <sup>1</sup>H (400 MHz) en CDCl<sub>3</sub> de 5,5-(2,3-epoxipropil)-2,2-dimetil-4,6-dioxo-1,3-dioxà (*DGMA*)

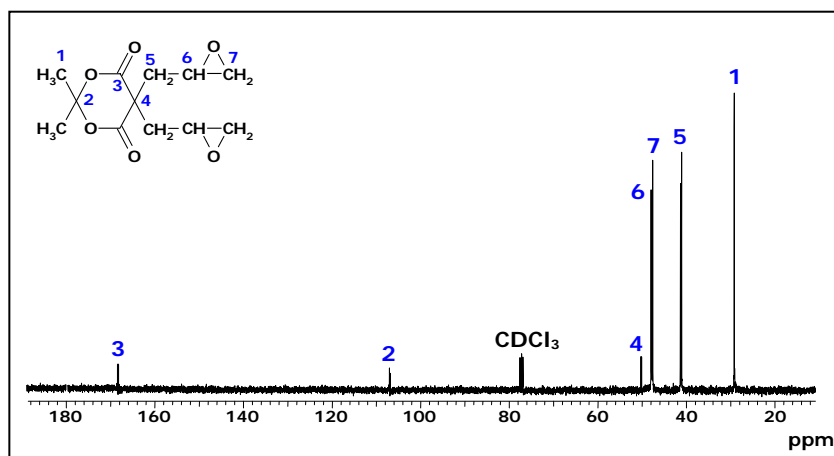
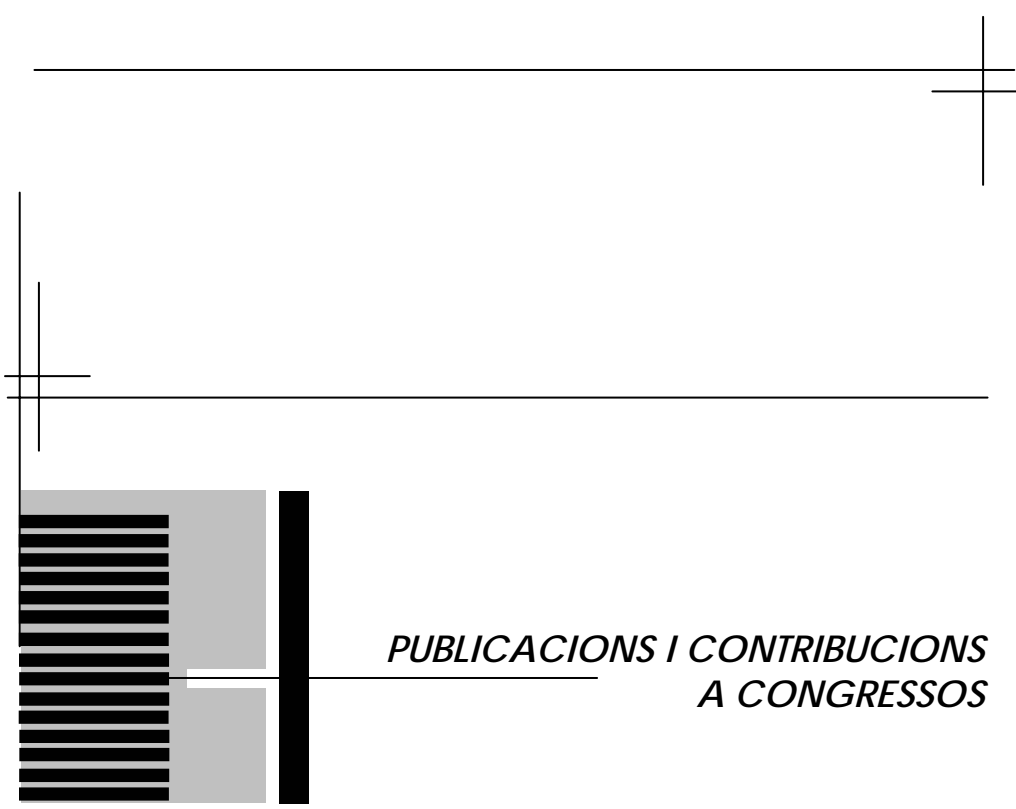


Figura 10. Espectre de RMN de <sup>13</sup>C (100 MHz) en CDCl<sub>3</sub> de 5,5-(2,3-epoxipropil)-2,2-dimetil-4,6-dioxo-1,3-dioxà (*DGMA*)

## ACRÒNIMS

<b><math>\gamma</math>-BL</b>	$\gamma$ -Butirolactona
<b>BOE</b>	Bicicloortoester
<b>DAMA</b>	5,5-dial·lil-2,2-dimetil-4,6-dioxo-1,3-dioxà
<b>DABCO</b>	1,4-diazabicyclo[2.2.2]octà
<b>DBN</b>	1,5-diazabicyclo[4.3.0]-5-nonè
<b>DBU</b>	1,8-diazabicyclo[5.4.0]-7-undecè
<b>DFT</b>	3,3'-Diftalida
<b>DGEBA</b>	Diglicidil èter de bisfenol A
<b>DGMA</b>	5,5-(2,3-epoxipropil)-2,2-dimetil-4,6-dioxo-1,3-dioxà
<b>DMF</b>	N,N-dimetilformamida
<b>DMAP</b>	4-N,N-dimetilaminopiridina
<b>DMTA</b>	Anàlisi termodinamomecànica
<b>DSC</b>	Calorimetria diferència d'escombrat
<b>ECH</b>	3,4-epoxiciclohexancarboxilat de 3,4-epoxiciclohexilmetil
<b>FT</b>	Ftalida
<b>FTIR-ATR:</b>	Infraroig amb Transformada de Fourier- Reflectança Atenuada Total
<b>KHN</b>	Numero de duresa Knoop
<b>MA</b>	Àcid de Meldrum; (2,2-dimetil-4,6-dioxo-1,3-dioxà)
<b>MCB</b>	7,7-dimetil-6,8-dioxaspiro[3.5]nonan-5,9-diona
<b>MDM</b>	2,2,5,5-tetrametil-4,6-dioxo-1,3-dioxà
<b>MCP</b>	6,6-dimetil-5,7-dioxaspiro[2.5]octan-4,8-diona
<b>PGE</b>	Fenilglicidil èter (1,2-epoxi-3-fenoxipropà)
<b>phr</b>	parts d'iniciador per cent parts de mescla de monòmers
<b>SOE</b>	Espiroortoester
<b>SOC</b>	Espiroortocarbonat
<b>TGA</b>	Anàlisi termogravimètrica
<b>Tg</b>	Temperatura de transició vitria
<b>TMS</b>	Tetrametilsilà



*PUBLICACIONES I CONTRIBUCIONS  
A CONGRESSOS*

**Publicacions:**

**2006**

- "Reduction of the Shrinkage of Thermosets by Cationic Curing of Mixtures of Diglycidyl Ether of Bisphenol A and 6,6-Dimethyl-(4,8-dioxaspiro[2.5]octane-5,7-dione)". L. González, X. Ramis, J. M. Salla, A. Mantecón, A. Serra, *Journal of Polymer Science: Part A: Polymer Chemistry*, **44**, 6869-6879.

**2007**

- "The Degradation of New Thermally Degradable Thermosets Obtained by Cationic Curing of Mixtures of DGEBA and 6,6-Dimethyl-(4,8-dioxaspiro[2.5]octane-5,7-dione)". L. González, X. Ramis, J. M. Salla, A. Mantecón, A. Serra, *Polymer Degradation and Stability*, **92**, 596-604.
- "Kinetic Analysis by DSC of the Cationic Curing of Mixtures of DGEBA and 6,6-Dimethyl-(4,8-dioxaspiro[2.5]octane-5,7-dione)". L. González, X. Ramis, J. M. Salla, A. Mantecón, A. Serra, *Thermochimica Acta*, **464**, 35-41.

**2008**

- "Study of the Cationic Curing of DGEBA and 2,2,5,5-Tetramethyl-4,6-dioxo-1,3-dioxane and the Degradation of the Thermosets Obtained". L. González, X. Ramis, J. M. Salla, A. Mantecón, A. Serra, *Journal of Applied Polymer Science*, **108**, 1229-1237.
- "New Poly(ether-ester) Thermosets Obtained by Cationic Curing of DGEBA and 7,7-Dimethyl-6,8-dioxaspiro[3.5]nonane-5,9-dione with Several Lewis Acids as Initiators". L. González, X. Ramis, J. M. Salla, A. Mantecón, A. Serra, *Journal of Polymer Science: Part A: Polymer Chemistry*, **46**, 1229-1239.
- "New Thermosets Obtained from DGEBA and Meldrum Acid with Lanthanum and Ytterbium Triflates as Cationic Initiators". L. González, X. Ramis, J. M. Salla, A. Mantecón, A. Serra, *European Polymer Journal*, *en premsa*.
- "Anionic Copolymerization of Diglycidyl Ether of Bisphenol A with Two Meldrum Acid Derivatives Initiated by 4-(N,N-Dimethylamino) Pyridine". L. González, X. Ramis, J. M. Salla, A. Mantecón, A. Serra, *Journal of Applied Polymer Science*, *revisió menor*.
- "Synthesis of a New Diglycidyl Meldrum Acid Derivative and Study of the Curing with Lanthanide Triflates as Initiators". L. González, J. Simokaitiene, X. Ramis, J. M. Salla, A. Mantecón, A. Serra, *Journal of Polymer Science: Part A: Polymer Chemistry*, *en premsa*.

**Comunicacions escrites:**

**2005**

- “Nuevos materiales termoestables degradables a partir de DGEBA y Ácido de Meldrum y derivados”. L. González, X. Ramis, J. M. Salla, A. Mantecón, A. Serra, *IX Reunión del Grupo Especializado de Polímeros (GEP)* de las Reales Sociedades Españolas de Química y Física (RSEQ, RSEF), (11-15 Setembre, Jaca, Spain).
- “New degradable thermosets obtained by copolymerization of DGEBA with 2,2,5,5-tetramethyl-4,6-dioxo-1,3-dioxane”. J. Simokaitiene, L. González, A. Mantecón, A. Serra, *Baltic Polymer Symposium* (19-21 Octubre, Tallin, Estonia).

**2006**

- “Study on the thermal degradation of new thermosets obtained by copolymerization of DGEBA with 6,6-dimethyl-(4,8-dioxaspiro[2.5]octane-5,7-dione)”. L. González, X. Ramis, J. M. Salla, A. Mantecón, A. Serra, *4th International Conference on Polymer Modification, Degradation and Stabilisation (MODEST)* (10-14 Setembre, San Sebastián, Spain).

**Comunicacions orals:**

**2006**

- “Nuevos materiales termoestables obtenidos por copolimerización de resinas epoxi y 6,6-dimetil-(4,8-dioxaspiro[2.5]octano-5,7-diona)”. L. González, X. Ramis, J. M. Salla, A. Mantecón, A. Serra, *3er Congreso Nacional de Jóvenes Investigadores en Polímeros (JIP)* (4-8 Juny, El Ferrol, Spain).

**2007**

- “Mejora de las propiedades de las resinas epoxi mediante copolimerización catiónica por apertura de anillo con derivados de ácido de Meldrum”. L. González, F. Ferrando, X. Ramis, J. M. Salla, A. Mantecón, A. Serra, *X Reunión del Grupo Especializado de Polímeros (GEP)* de las Reales Sociedades Españolas de Química y Física (RSEQ, RSEF), (16-22 Setembre, Sevilla, Spain).

UNIVERSITAT ROVIRA I VIRGILI  
COPOLIMERITZACIÓ DE DGEBA AMB ÀCID DE MELDRUM I DERIVATS  
Lidia González Búrdalo  
ISBN:978-84-691-9759-2/T-1252-2008